UNIVERSITY OF BIRMINGHAM

Metabolism and Transport of Complex Metabolites of Mycobacteria

by

CRISTIAN HERNAN VARELA RAMIREZ

A thesis submitted to the

UNIVERSITY OF BIRMINGHAM

for the degree of

DOCTOR OF PHILOSOPHY

School of Biosciences
College of Life and Environmental Sciences
The University of Birmingham

September 2013

DECLARATION

The work presented in this thesis was carried out in the School of Biosciences at The University of Birmingham, U.K., B15 2TT during the period September 2009 to October 2012. The work in this thesis is original except where acknowledged by references.

No part of the work is being, or has been submitted for a degree, diploma or any other qualification at any other University.

ABSTRACT

Mycobacterium tuberculosis, the causative agent of the infectious disease Tuberculosis, is one of the most successful human pathogen. The disease remains a global health priority due to the spread of HIV and multidrug resistant strains. Therefore, there is a need to extend the understanding of the physiology and pathogenicity of *M. tuberculosis* in order to develop new therapies, antimicrobial drugs and vaccines.

Mycobacterium possesses a unique cell envelope responsible for the reduced susceptibility to antibiotics and pathogenicity due to the high lipid content. It is composed by the plasma membrane, an unusual lipid-rich cell wall and an outermost layer known as the capsule. Moreover, other complex metabolites play a role in *M. tuberculosis* virulence such as inorganic polyphosphate, a polymer involved in stringent response and long term survival. In this study, a transposon mutant library was generated in order to identify new genetic determinants related to cell envelope; furthermore, specific mutants strains were generated to investigate the role of MmpL factors in mycolic acids transport, to test the role of a group of ABC-transporters in capsule biosynthesis and also to assess the function of exopolyphosphatases in survival under stress and nutrient limitation condition.

This thesis is dedicated to my grandfather

ACKNOWLEDGEMENTS

In first place, I would like to express my sincere gratitude to my supervisor, Dr Apoorva Bhatt, for granting me the opportunity to carry out this project with him, for sharing his knowledge and expertise during all this time, for supporting me unconditionally with the problems I faced, and for his friendship and noble human qualities. I would also like to thank Professor Besra, for the opportunity he gave me to be part of his amazing research group. I am grateful to the Darwin Trust of Edinburgh for funding my studies and also to The University of Birmingham for the PhD position granted.

I need to thank the Besra-Lab Crew for making every day so special with loads of food, fun conversations and nice atmosphere; everyone I have met here has now a special place in my heart. Special thanks to A. Singh, for his invaluable help at any time with my experiments and day to day problems.

I want to acknowledge this country and this city, for becoming my house far away from home, for all the amazing people I have had the opportunity to meet here and the awesome experience I had the chance to live.

Thanks to Carlos and the EuroChara for the new opportunity showing me how amazing you guys are, thanks for your support, patience, help, companionship and also for making me feel I had a piece of "home" close to me at any time.

I would also like to say thanks to Lenny and Karen for being my family all this time, for all your support, love and friendship, you guys are simply amazing. Finally, I would like to thank Nadine, for your support, help, time and for being such an awesome person.

TABLE OF CONTENTS

LIST OF FIGURES

Chapter 1

Chapter 2

Chapter 3

Chapter 4

Chapter 5

LIST OF TABLES

LIST OF ABBREVIATIONS

2D-TLC	two-dimensional thin layer chromatography
ABC	ATP-binding-cassette
ACP	acyl carrier protein
AG	arabinogalactan
ATP	adenosine triphosphate
BCG	Bacille Calmette-Guerin
BHI	brain heart infusion
BLAST	basic local alignment search tool
BN-PAGE	blue native polyacrilamide gel electrophoresis
CESTET	conditional expression–specialized transduction essentiality test
CD	cluster of differentiation
CDP	cytidine diphosphate
CLR	C-type lectin receptor
cpm	counts per minute
CR	complement receptors
CTP	cytidine triphosphate
CXCR3	CXC-chemokine receptor 3
DAPI	4’,6-diamidino-2-phenylindole
DAT	diacyl trehalose
DC	dendritic cells
DC-SIGN	dendritic cell-specific intercellular adhesion molecule-3-grabbing non-integrin
DNA	deoxyribonucleic acid
EMB	ethambutol
ESX	ESAT-6 Secretion System
FAMES	fatty acid methyl esters
Fas	apoptosis-stimulating fragment
FAS	fatty acid synthetase
FATP	fatty acyl-tetrapeptide
GITC	guanidinium thiocyanate
GlcNAc	*N*-acetylglucosamine
GMM	glucose monomycolate
GPL	glycopeptidolipids
GTP	guanosine triphosphate
HIV	human immunodeficiency virus
HPA	hydroxyphthioceranates
Icl	isocitrate lyase
IFN	interferon
IL	interleukin
iNOS	inducible nitric oxide synthase
INH	isoniazid
LAM	lipoarabinomannan
LB	Luria-Bertani
LM	lipomannan
LOS	lipooligosaccharides

LPS	lipopolysaccharide
LT	lymphotoxin
LTB	leukotriene B
LXA	lipoxin A
MA	mycolic acids
MAC	*Mycobacterium avium* complex
mAGP	mycolyl-arabinogalactan-peptidoglycan
MAMES	mycolic acid methyl esters
MDR-TB	multidrug-resistant strains
MFS	major facilitator superfamily
MGLP	methylglucose lipopolysaccharide
MIC	minimum inhibitory concentration
MIP	major intrinsic protein family
MMG	glycerol monomycolate
MmpL	mycobacterial membrane protein large
MmpS	mycobacterial membrane protein smalle
MOI	multiplicity of infection
MR	mannose receptor
MurNAc	*N*-acetylmuramic acid
MTBC	*Mycobacterium tuberculosis* complex
MycPL	6-O-mycolyl-β-D-mannopyranosyl-monophospho-heptaprenol
NADPH	nicotinamide adenine dinucleotide phosphate
NAG	N-acetylglucosamine
NAM	N-acetylmuramic acid
NDK	nucleoside diphosphate kinase
NK	natural killer
NOX	NADPH oxidase
OADC	oleic acid-albumin-dextrose catalase
PA	phthioceranate
PAT	polyacyltrehaloses
PBS	phosphate-buffered saline
PCR	polymerase chain reaction
PDIM	Phthiocerol dimycocerosates
PG	peptidoglycan
PGE	prostaglandin
PGL	phenolic glycolipids
PFU	plaque forming units
Pks	polyketide synthases
p-HBADs	*p*-hydroxybenzoic acid derivatives
Pi	orthophosphate
PILAM	inositol phosphate-capped LAM
PIM	phosphatidylinositol mannan
PM	plasma membrane
polyP	inorganic polyphosphate
Ppk	polyphosphate kinase
Ppx	exopolyphosphatase
PTS	phosphotransferase system
RD9	region of difference 9

Rif	rifampicin
RND	resistance, nodulation, and division
RNS	reactive nitrogen species
ROS	reactive oxigen species
Rpf	resuscitation-promoting factor
SLs	sulfolipids
SNPs	single nucleotide polymorphisms
RNA	ribonucleic acid
SpA-R	surfactant protein A receptor
TAT	triacyltrehaloses
TB	tuberculosis
TbD	*M. tuberculosis* specific deletion
TCA	tricarboxylic acid
TDCM	trehalose dicorynomycolates
TDM	trehalose dimycolate
TDP	thymidine diphosphate
TLR	Toll-like receptor
TM	transmembrane
TMCM	trehalose monocorynomycolates
TMM	trehalose monomycolate
Tn	transposon
TNF	tumour necrosis factor
TSB	tryptic soy broth
XDR-TB	extensively drug-resistant TB
WHO	world health organisation

PUBLISHED WORK ASSOCIATED WITH THIS THESIS

Chemistry and Biology (2012)
19(4):498-506

MmpL genes are associated with mycolic acid metabolism in mycobacteria and corynebacteria

Varela C, Rittmann D, Singh A, Krumbach K, Bhatt K, Eggeling L, Besra GS, Bhatt A.

CHAPTER 1

GENERAL INTRODUCTION

1.1 OVERVIEW

Tuberculosis (TB) is an infectious disease that afflicts human and is caused by the bacterium *Mycobacterium tuberculosis*. It can develop as a pulmonary and extrapulmonary disease; the first one corresponds to the most common type which affects the lungs, whilst the second one can target several other organs and tissues. The transmission of the disease occurs by direct contact from person to person, via bacilli expelled through the air.

The problem of TB as global health crisis was highlighted in 2011 by the World Health Organisation (WHO), who placed it as the second causal agent of death by infection, only surpassed by the human immunodeficiency virus (HIV), with 1.4 million TB deaths reported (430,000 HIV-associated TB deaths). The statistics also showed 9 million new cases (Fig. 1.1) and an estimated prevalence of 12 million cases. Geographically, the estimated number of cases occurred mainly in Asia (59%) and Africa (26%), with some cases in the Eastern Mediterranean region (7.7%) and a few in Europe (4.3%) and the Americas (3%). While 3.7% of new TB patients in the world have been diagnosed with multidrug-resistant strains (MDR-TB), the levels are much higher in individuals previously treated (20%). Moreover, extensively drug-resistant TB (XDR-TB) represents 9% of MDR-TB cases and it has been identified in 84 countries (WHO, 2012).

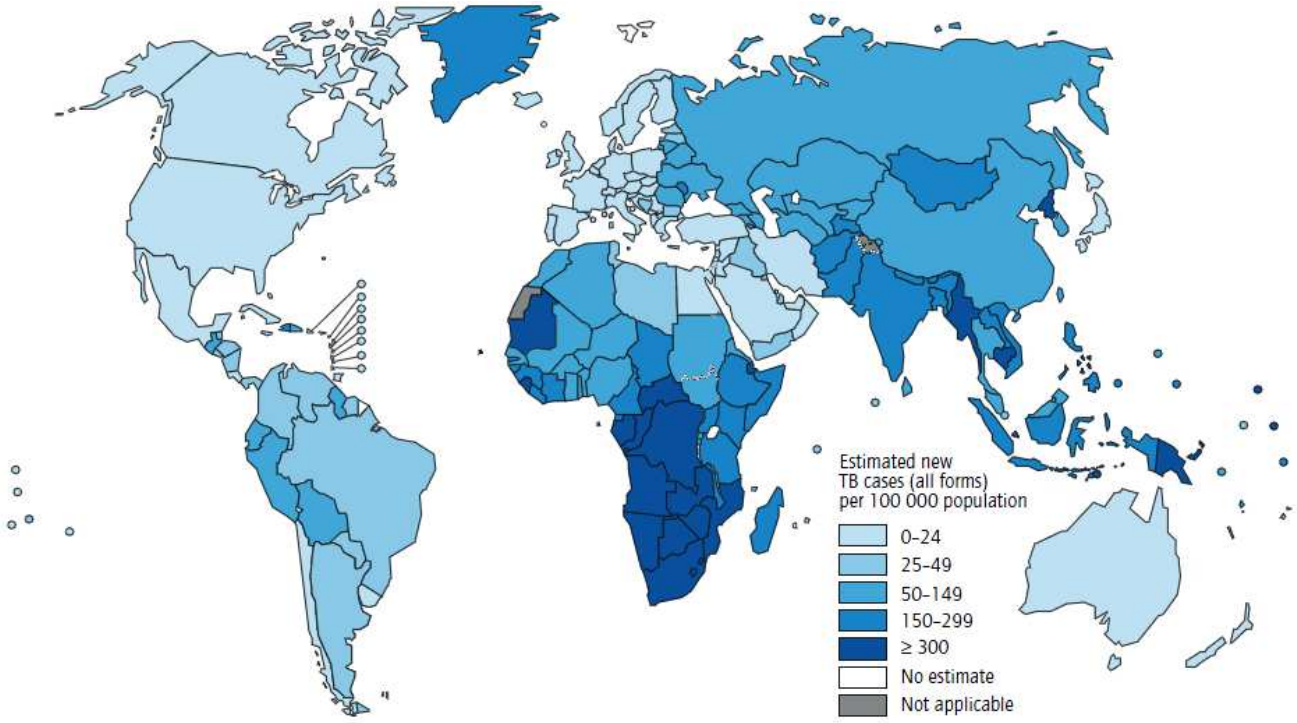

Figure 1.1: Estimated number of new TB cases in the year 2011 (used with permission from WHO, 2012).

1.2 HISTORY OF TB

The genus *Mycobacterium* is estimated to have appeared more than 150 million years ago. An ancestral strain of *M. tuberculosis* was proposed to have been present in East Africa 3 million years ago suggesting that early hominids may have been a host. Written texts have been found describing TB in India as early as 3,300 years ago and in China 2,300 years ago (Gutiérrez *et al*., 2005; Daniel, 2006); moreover, typical skeletal abnormalities of TB in ancient Egyptian mummies together with molecular evidence indicate the disease has been a burden throughout the whole human era as well (Nerlich *et al*., 1997; Crubézy *et al*., 1998). The first documented account of TB emerged around 460

BC, it was called “phthisis” by ancient Greeks and considered the most widespread disease of the times by Hippocrates who described tuberculosis and understood its clinical features (Coar, 1982). Between the 17th and 19th centuries became the principal cause of death in Europe reaching the highest mortality rates and even though pulmonary form of the TB was established as pathology with several symptoms by R. Morton in 1689, although it was not clasiffied and described as a disease until 1810 by G.L. Bayle. The disease was not named tuberculosis until 1839 by J.L. Schönlein (Bayle, 1810; Schönlein, 1839; Daniel, 2006). Finally, in 1882, Hermann Heinrich Robert Koch identified the tubercle bacillus demonstrating it was the causative factor of the disease. For this work, he was awarded the Nobel Prize in Medicine or Physiology in 1905 (Koch, 1882; Daniel, 2005).

Although several therapies and techniques were attempted to prevent TB over the years, it was not until 1921 when Albert Calmette and Camille Guerin accomplished a successful attenuation of the aetiological agent of bovine form of TB, *Mycobacterium bovis*. They developed a vaccine called Bacille Calmette-Guerin (BCG) that was used in humans (Calmette, 1928) and remains the only vaccine in use today regardless its partial efficacy. This changed drastically with the introduction of chemotherapy, the discovery of paraaminosalicylic acid and thiosemicarbazone during the Second World War resulted the first agents with bacteriostatic effects for treating TB patients. After its isolation in 1944, streptomycin was used as the first bactericidal drug against the bacteria (Schatz *et al*., 1944; Hinshaw and Feldman, 1945) followed by the first oral drugs, isoniazid and rifamycins in 1952 and 1957, respectively. Together, these drugs accomplished effective public health measures against the disease and including curing latent tuberculosis infected patients (Daniel, 2006). Nowadays, access to TB care has expanded substantially since the mid-1990s, when the World Health Organisation launched a new global strategy and began

systematically monitoring the progress of the disease together with the development of new drugs and new vaccines. However, the global burden of TB remains enormous and the response to MDR-TB and XDR-TB is still slow (WHO, 2012).

1.3 ORIGINS AND EVOLUTION OF *Mycobacterium tuberculosis*

Mycobacterium is a genus of the *Actinobacteria* phylum, which contains around 120 described species, the majority of which are saprophytic soil species. Within the genus *Mycobacterium*, there is a small and closely related group known as the *Mycobacterium tuberculosis* complex (MTBC), which includes seven species and subspecies of both human and veterinary significance because they cause similar pathologies in various mammalian hosts, i.e., *Mycobacterium canettii*, *Mycobacterium africanum*, *Mycobacterium pinnipedii*, *Mycobacterium microti*, *M. bovis* (Brosch *et al*., 2002; Smith *et al*., 2006a; Ventura *et al*., 2007). Typical MTBC members, show more than 99.9% sequence similitude at nucleotide level, virtually identical 16S rRNA sequences and a strict clonal population structure, with little or no evidence suggesting exchange of chromosomal DNA (Smith *et al*., 2006b).

M. tuberculosis is a Gram-positive bacterium which possesses a cell wall with high amount of lipids which is distinctive of some members of the order *Actinomycetes* such as *Corynebacterium*, *Mycobacterium*, *Nocardia* and *Rhodococcus*, all of which containing characteristically high proportions of guanine and cytosine in their genomes (Woese, 1987; Brennan and Nikaido, 1995). Despite its classification as a Gram-positive, the cell wall of

M. tuberculosis is impervious to Gram-staining reagents. Instead, more abrasive "acid-fast" detection techniques are used to stain mycobacteria (Minnikin, 1982).

As mentioned before, members of MTBC show poor genetic and allelic variation, therefore the general consensus indicates that the modern members of the complex would have a single African ancestor that resulted from a so-called "evolutionary bottleneck" that evolved in a clonal fashion around 35,000 years ago (Sreevatsan *et al*., 1997; Brosch *et al* 2002; Gutiérrez *et al*., 2005). Nevertheless, genomic analysis of the group reveals that previous horizontal gene transfer events originated the arrangement of *M. tuberculosis* genome and also the existence, approximately 3 million years ago, of an ancient wider group of species from where MTBC evolved (Gutiérrez *et al*., 2005; Smith *et al*., 2009).

Existing strains of *M. tuberculosis* can be clustered in six major lineages geographically distributed and whose diversity, calculated using the mutation rate, should have been developed 250 to 1000 years before (Hirsh *et al*., 2004; Gagneux *et al*., 2006). Despite the similarities, it is yet possible to differentiate amongst members of the MTBC, discriminating by deletions, single nucleotide polymorphisms (SNPs), the distribution of variable regions or mutations (Mostowy *et al*., 2002; Tsolaki *et al*., 2004). Moreover, these molecular peculiarities can be used to elucidate the evolutionary scenario faced by the members of the genus, for instance, while the deletion of chromosomal region of difference 9 (RD9) allows to classify strains as animal-adapted, the *M. tuberculosis* deletion TbD1 defines the modern strains and both support the idea that *M. tuberculosis* likely evolved to *M. bovis* (Brosch *et al*., 2002). The idea that TB evolved as a zoonosis comes from work done on now extinct animals: mycobacterial lipid biomarkers have been detected in 17,000 years old bone samples from an extinct bison, which is much older than

the oldest human remains (9,000 years old) shown to contain traces of the TB bacillus (Lee *et al*., 2012).

1.4 BIOLOGY AND PATHOGENESIS OF *Mycobacterium tuberculosis*

As an airborne disease, the bacterium is transmitted through aerosols, by which *M. tuberculosis* bacilli are inhaled and penetrate the lungs. Even though TB targets any tissue or organ, the respiratory tract corresponds to the main site of entry and, therefore, the most important place of disease appearance, since extra pulmonary TB accounts for not more than 10% of all cases (Kaufmann, 2001; Smith *et al*., 2009).

Inhaled *M. tuberculosis* faces a very special immunological unit formed by both the respiratory tract and the bronchoalveolar spaces. In this compartment, tissue-specific cells and interactions form the first-line defence, where humoral factors (surfactant proteins A–D) and other effectors activate alveolar macrophages. Moreover, a local immune response takes place under the control of dendritic cells (DC) and macrophages (Kaufmann, 2001; Holt *et al*., 2008; Schwander and Dheda, 2011). Normally, most of people succeed controlling the primary infection via a cell-mediated immune response; although 5-10% of the cases develop the disease (Stewart *et al*., 2003).

1.4.1 Binding of *M. tuberculosis* to alveolar macrophages

Intimate pathogen–macrophage contacts occur inside the alveoli by specific receptor-ligand interactions as part of the innate immunity, where *M. tuberculosis* components, such as polysaccharides and glycolipids, are recognised by the receptor of the

host. On the other hand, *in vitro* analysis have demonstrated that *M. tuberculosis* binds to mononuclear phagocytes opsonically via the receptors, CR1, CR3, CR4 and the surfactant protein A receptor (SpA-R), and also non-opsonically to the miceoglial mannose receptor (MR) and CD14, and possibly to macrophage scavenger receptors. The list of diverse ligands that the pathogen displays on its surface, including β-glucans, mannose, fucose, mannan, lipoarabinomannan (LAM) or Man-LAM, engage multiple receptors on the host simultaneously (Ehlers and Daffé, 1998; Ernst, 1998), such as Toll-like receptors, group that sense a wide diversity of molecule like lipoprotein, phosphatidylinositol mannans (PIMs) and lipomannan (LM) in the case of TLR2, or foreign DNA in the case of TLR9 (Bafica *et al*., 2005), the receptor repertoire also includes C-type lectin receptors (CLR) (Tanne *et al*., 2009), dectin 1 (Rothfuchs *et al*., 2007), the mannose receptor (Court *et al*., 2010) and mincle (Schoenen *et al*., 2010), playing an major role in the production of cytokines and in the inflammatory response (Dorhoi *et al*., 2010; Ernst, 2012) (Fig. 1.2).

1.4.2 Innate immune response following infection of macrophages

Once infected, alveolar macrophages release a set of antimicrobial molecules such as pro-inflammatory cytokines, which activate both local and systemic responses in different ways; for instance, while the production of tumour necrosis factor (TNF), lymphotoxin (LT) promotes the expression of chemokines recruiting inflammatory cells to the lung (Fig. 1.2) (Cooper *et al*., 2011), the production of vimentin mediates lysis of infected cells by NK cells (Garg *et al*., 2006). These factors govern innate immune responses and provide the basis for the specific immunity by inducing activation of antimicrobial activity in macrophages, the migration of activated phagocytes to the lymph nodes, the recruitment and maturation of DCs and finally the arrival of antigen-specific T

lymphocytes to the site of infection (Stenger, 2005; Cooper, 2009). In the case of infection involving *M. tuberculosis* the adaptive immune response is crucial due to the delayed innate immune response produced by the pathogen (Ernst, 2012).

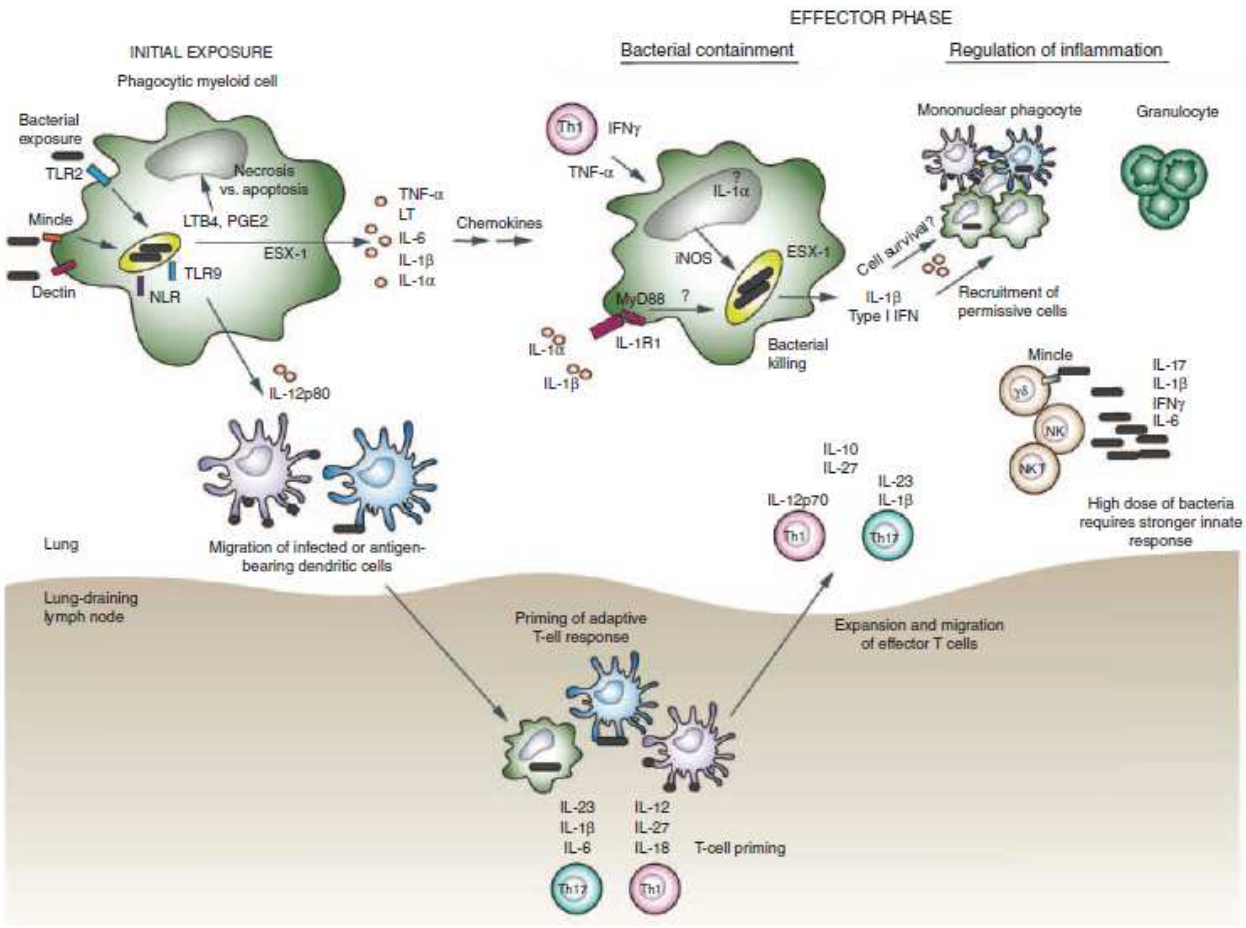

Figure 1.2: Molecular and cellular bases of immune response against *M. tuberculosis*. The diagram shows innate cytokines production by infected cells and immune system cells acting during initiation, expansion and chronic stages of TB. At the infection site the antimicrobial activity is carried out by the phagocytes producing IFN-γ, TNF, LT and IL-1R1, while IL-12p80 promotes migration of activated DCs to the lymph node, to start the adaptive immune response. In the lymph node, the type of cytokine determine the function of the T cell. IL regulate protective and inflammatory responses at different stages. IFN- γ, interferon-γ; IL, interleukin; LT, lymphotoxin; TNF, tumor necrosis factor. (Adapted with permission from Cooper *et al*., 2011. Confirmation Nº 11128980)

In mice infected with *M. tuberculosis*, antigen-specific T cell response can be observed 11–14 days post-infection. Initially, the activated DCs migrate from the infection place to the lymph node to start the acquired immune process by presenting the antigen to the naive T cells (Tailleux *et al.*, 2003). The activation of T cells and the initiation of the acquired immune response to *M. tuberculosis* is delayed, likely due to the impaired migration of infected DCs (Wolf *et al*., 2008; Blomgran and Ernst, 2011).

Contradictorily, the first steps of the general response against mycobacteria infection seem to provide favourable cellular conditions to the bacillus, as once engulfed, the pathogen can regulate both trafficking and maturation of phagosomes, evading the lysosomally mediated antimicrobial mechanisms. Furthermore, no anti-mycobacterial activity has been detected in CD4+ T cells on the first 7 days of infection. In this scenario, the role of the innate immune response to the *M. tuberculosis* infection seems more to set up favourable conditions to the adaptive T cell response rather than a prompt antimicrobial reaction (Gallegos *et al*., 2008; Ernst, 2012).

1.4.3 Adaptive immune response to *M. tuberculosis*

The survival to mycobacterial infection strictly depends on the development of an efficient adaptive immune response. Regardless the correct activation of the immune system, *M. tuberculosis* is still able to overcome the defensive mechanisms, since the bacillus limits both phagocytes and macrophage action (Cooper, 2009).

The role of CD4 and CD8 T lymphocytes in the control of *M. tuberculosis* dissemination in the lung has been demonstrated; the bacterium induces a broad immune response that requires the participation of unconventional T cells as well as conventional T cells (Kaufmann, 2001). Both CD4+ and CD8+ T cells have shown a role in fighting *M.*

tuberculosis infection due to their cytotoxic ability (Tan *et al*., 1997). Mycobacteria-specific CD4+ T cells are typically of the Th1 type, which is a potent producer of IL-12 and IFN-γ, both of which are critical in actimicrobial-mycobacterial activities of macrophages (Cooper *et al.*, 1997a; Cooper *et al*., 2011), while Th2 cytokines, such as interleukin IL-4 and IL-10 are scarce, though not fully absent (Lin *et al*., 1996). On the other hand, CD8+ T cells, which can also produce IFN-γ, play an essential role killing *M. tuberculosis*-infected cells (Serbina and Flynn, 2001). The lymphocyte-mediated cytotocixity has been described to occur via two mechanisms. First, by exocytosis of cytotoxic granules such as perforin or granzyme, and secondly,and second by the CD95 (Fas) apoptotic pathway (Nagata, 1999; Cooper *et al*., 1997b). During *M. tuberculosis* infection, the lysis of infected macrophages by CD8+ T cells takes place using both mechanisms (Canaday *et al*., 2001; Lazarevic and Flynn, 2002; Carranza *et al*., 2006; Woodworth *et al*., 2008).

The desire effects of developing an adaptive immune response during the *M. tuberculosis* infection are the control of the bacterial growth and the eradication of the pathogen. Although, after an infectious episode, commonly the humans become asymptomatic but develop a latent infection (Ernst, 2012).

1.4.4 Granuloma and persistent bacteria

As the bacterial load increases, T cells first migrate to the site of infection where they attract and activate more macrophages in an attempt to eradicate the pathogen and leading to the formation of a granulomatous lesion. A chronic inflammatory tissue response is causative of the granuloma and is initiated by either an infectious agent or a non-infectious factor. Aggregates of host cells such as macrophages, DCs as well as

lymphocytes B and T (at later stages of formation) all contribute to the granuloma structure (Kaufmann, 2001; Ernst, 2012).

The chronic *M. tuberculosis* infection implies that the bacterium overcomes the immune response. *M. tuberculosis* has developed several systems to avoid the antibacterial features of the macrophages, allowing it to live and replicate in a protected intracellular environment where controlling the macrophage death pathway constitutes one of the pathogen survival mechanisms (Behar *et al*., 2010). An interesting strategy shown by virulent *M. tuberculosis* strains is the prevention of apoptosis while inducing the necrotic death of infected cells. Several studies has partially described how the pathogen accomplishes that task, but the mechanisms are still not totally clear; for instance, the bacteria suppresses TNF and induces the production of both lipoxin A_4 (LXA_4) (Chen *et al*., 2008) and leukotriene B_4 (LTB_4) (Fig. 1.2) modulating the response of phagocytes and eliminating their protective action (Wada *et al*., 2006; Cooper *et al*., 2011). Additionally, ESX1 also recruits new macrophages and contributes to the development of the granulomas (Davis and Ramakrishnan, 2009) unlike it happens during a normal infection, where the macrophages undergo apoptosis mediated by TNF in vitro (Keane *et al*., 1997). In terms of the structure, *M. tuberculosis* is shielded by a singular lipid-rich cell wall that is composed of long chain fatty acids and glycolipids which contribute to its capacity to survive in host phagocytes, and that also provide the source of glycolipid antigens for a specialized population of T-cells (Daffé and Draper, 1998).

An effective control of the *M. tuberculosis* infection requires a continuous supply of immune effectors to granulomas, it has been demonstrated that defective trafficking of monocytes and DCs cells is related to a poor control of the infection, allowing granuloma formation and TB reactivation (Scott and Flynn, 2002). Therefore, an enhancement in the

cell migration confers more resistance to the infection and also control of the chronic disease, as it occurs in CXC-chemokine receptor 3 (CXCR3)-deficient mice (Chakravarty *et al*., 2007). In the case of humans, both active infection and the reactivation of the disease have been associated to polymorphisms in genes encoding chemokines and their receptors, indicating that the proper traffic of effectors is crucial for the control of the disease (Flores-Villanueva *et al*., 2002; Ernst, 2012).

The immune response against different mycobacterial species infection shows different features compared to *M. tuberculosis*, this fact also occurs between different strains. The genetic variability of the pathogen allows the strains to show several mechanisms of action in order to control immunity differentially, including the dissemination by using the inflammatory response (Cooper, 2009). Following phagocytosis, the environment and immune state of the host determine how the infection progresses under mechanisms yet to be determined. The granuloma consists in an important structural unit since it is there where the transition, from a disease with latent and subclinical characteristics into an active infection, occurs; at this stage sequestration takes place, the bacterium induces an alteration of host lipids biosynthesis, and the elimination of the non-replicating bacilli does not take place. Moreover, the pro-inflammatory response induces a macrophages and mononuclear cells recruitment into the infected tissue, that later will form a stratified structure composed by foamy macrophages and phagocytes inside a fibrous cuff surrounded by lymphocytes (Russell, 2007; Russell *et al*., 2009). The features presented by granuloma during latency are different depending on the phase of the infection, and three major types can be described: solid granuloma containing bacilli and necrotic granuloma observed on early phases of active disease and

caseous granuloma observed at later phases or during severe infection (Fig. 1.3) (Reece and Kaufmann, 2011; Gengenbacher and Kaufmann, 2012).

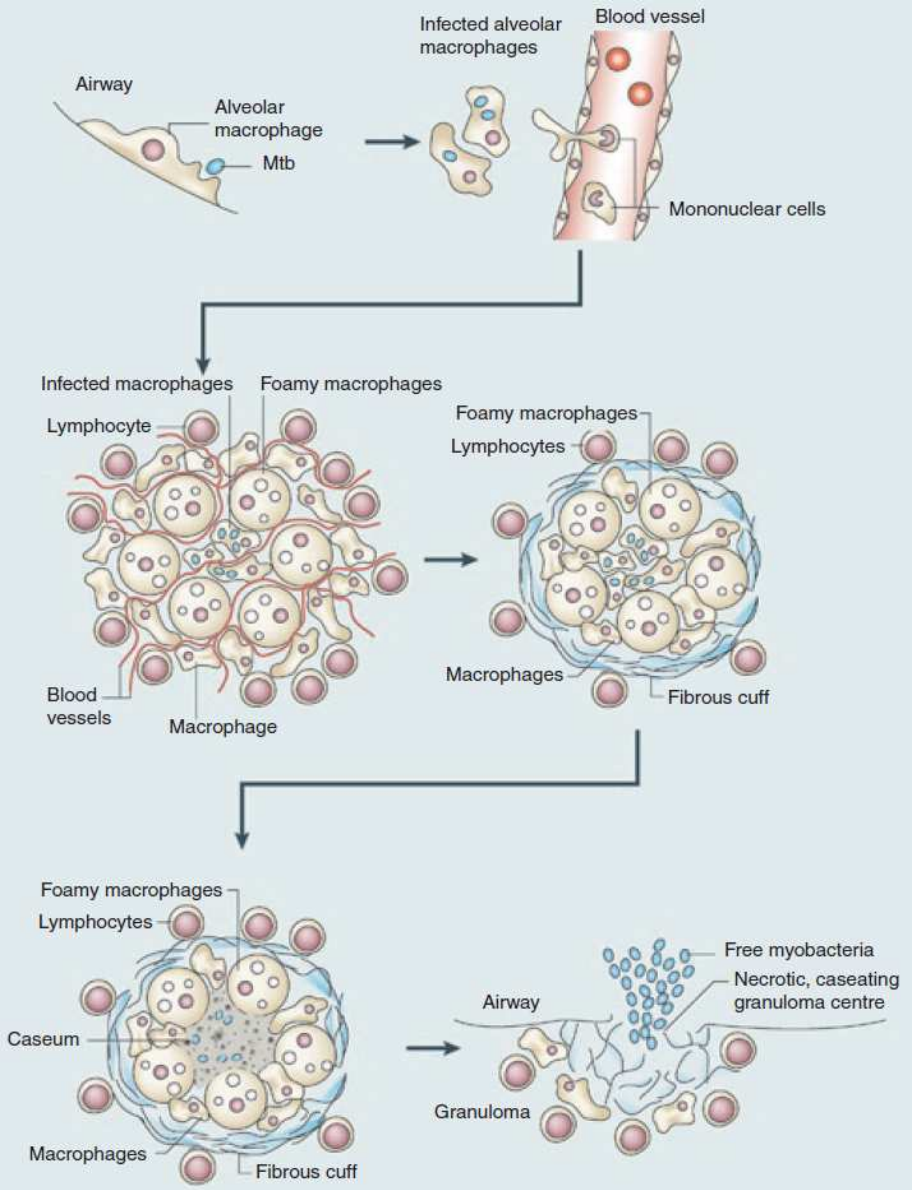

Figure 1.3: Progression of the human tuberculosis granuloma. Diagram showing the stages of formation of granuloma in the lung. Phagocystosis of bacilli in the alveoli induces a pro-inflammatory response which triggers the recruitment of macrophages and mononuclear cells to the site of infection which form the early phase of granuloma together with foamy macrophages that will finally end up covered by a fibrous capsule surrounded by lymphocytes. Latter stages of granuloma upon an active infection will exhibit caseous and necrotic tissue (Adapted with permission from Russell *et al*., 2009. Confirmation Nº 11128999).

Upon an active infection, latter stages of granuloma exhibit accumulation of caseous tissue that develops to necrosis and finally ends up in the collapse and rupture of the granuloma, releasing virulent bacteria and disseminating the disease (Fig. 1.4) (Kaplan *et al*., 2003; Schreiber *et al*., 2010).

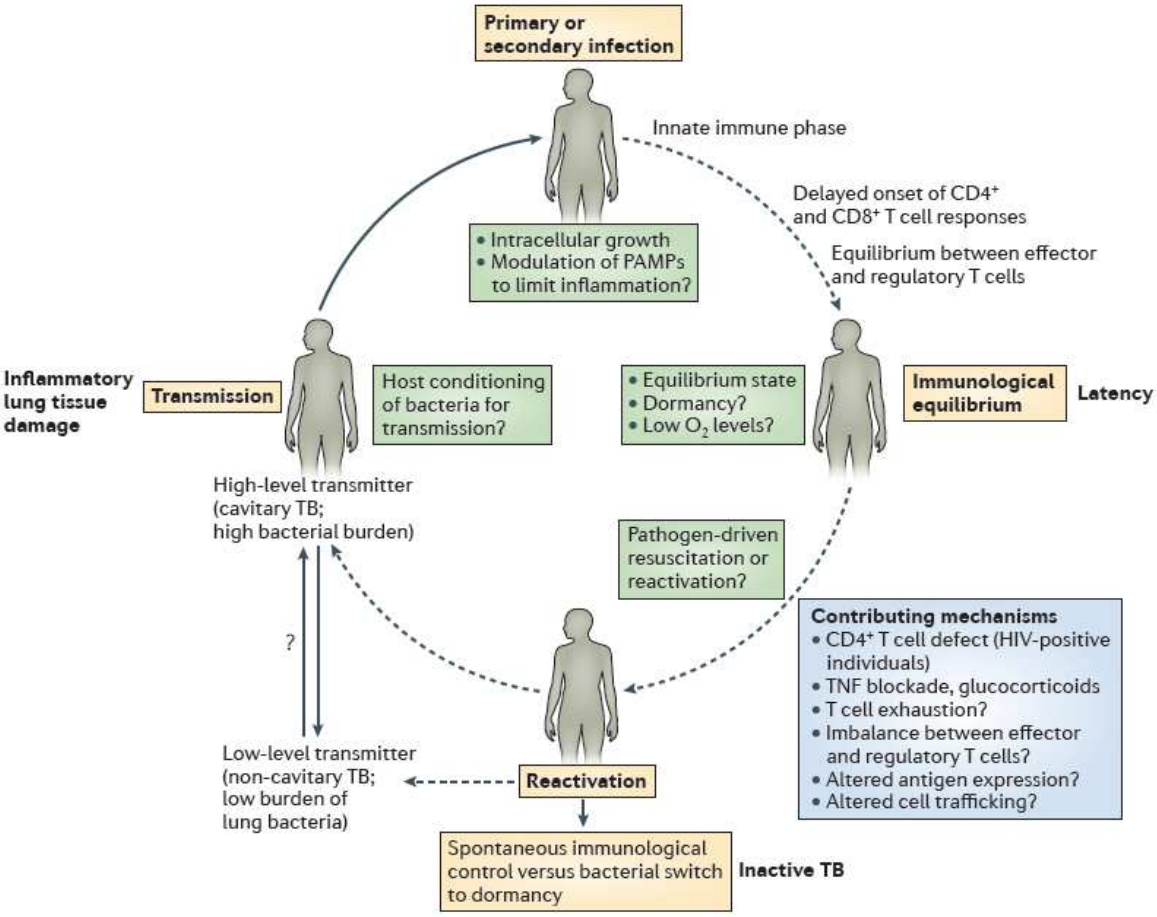

Figure 1.4: Phases of *M. tuberculosis* infection. Diagram showing the cycle of TB infection in humans and indicating immunological, clinical and epidemiological distinctive features of each stage of the disease. PAMP: pathogen associated molecular pattern; TNF: tumor necrosis factor. (Adapted with permission from Ernst, 2012. Confirmation Nº 11129016).

1.4.5 Adaptation of *M. tuberculosis* to the intracellular environment

In addition to the mechanisms previously stated, the success as a pathogen exhibited by *M. tuberculosis* lies in the ability to shut down its metabolism and vital functions during the intracellular life, where host-pathogen interactions are still not well understood. The dormancy state developed confers an extremely high capacity to resist the defensive mechanisms of the host and also drug treatments, key factors in the survival and persistence shown by *M. tuberculosis* (Gengenbacher and Kaufmann, 2012).

The progression of a primary infection can lead to three different pathways: active disease, latent infection or eradication. The resultant situation depends on the response of the host at cellular level, where the pathogen faces a variety of drastic conditions that are usually impaired in immunocompromised individuals, in whom the risk of active disease is highly increased (Barry *et al*., 2009).

The phagosomal conditions faced by *M. tuberculosis* after phagocytosis corresponds to a nitrosative, oxidative, hypoxic and poor in nutrients environment, where bacteria modifies its metabolism in order to survive (Schnappinger *et al*., 2003). The adaptive repertoire includes the modification of pathways and also the utilisation of host-derived molecules, with crucial roles in virulence. In the first case, for instance, there have been reported the upregulation of lipid metabolism genes (Brzostek *et al*., 2007), the utilisation of lipids via glyoxylate cycle (McKinney *et al.*, 2000), carbon dioxide fixation via anaplerotic reactions (Beste *et al*., 2011) and the critical role of gluconeogenesis in dormancy (Marrero *et al*., 2010); on the other hand, *M. tuberculosis* has been shown to utilise host molecules as nutrients, such as cholesterol that is crucial in the maintenance of chronic infection (Pandey and Sassetti, 2008) and also triacylglycerol (Daniel *et al*., 2011).

To tolerate the acidic environment within the phagolysosome, *M. tuberculosis* has has developed several mechanisms, such as excluding the host proton ATPase or by secreting urease (Reyrat *et al*., 1995; Sturgill-Koszycki *et al*., 1994). Moreover, the cell wall integrity is crucial in the survival under this harsh condition, since it has been demonstrated that resistance to elevated acidic stress is a desirable feature in order to succeed as a pathogen inside the late phagolysosome (Vandal *et al*., 2008; 2009).

The defensive mechanisms against *M. tuberculosis* displayed inside the phagosome also includes the production of both oxygen and nitrogen reactive species (ROS and RNS, respectively). Two crucial enzymes have been described related to these functions, namely phagocyte oxidase (NOX2) which produces hydroxyl radicals (Bedard and Krause, 2007) and the inducible nitric oxide synthase (iNOS), which produces nitrate and nitrite (Nathan and Shiloh, 2000). In order to avoid the toxic effect caused by ROS and NOS, two mechanisms have been described, namely detoxification and damage repair. In the first case, involving enzymes such as catalase peroxidase, superoxide dismutases, NADPH-dependent peroxidases or peroxynitrite reductase; while in the second mechanism the strategy consists in the substitution of molecules by synthesis *de novo* and the degradation via proteosome (Gengenbacher and Kaufmann, 2012).

During the last few years, a new adaptive mechanism to intracellular life has been described in *M. tuberculosis* consisting in a metal detoxification system used by the bacilli to counteract the zinc poisoning response developed by macrophages. The gene *ctpC* encodes for a putative zinc efflux pump and it has been characterized as crucial microbial virulence determinant, since its absence produces hypersensitivity to zinc poisoning (Botella *et al*., 2011; 2012).

It is likely that unfavourable conditions inside the granuloma induce the metabolic downshift that leads *M. tuberculosis* into the dormancy state, nutrient starvation models have shown an arrested growing-machinery along with decreased respiration rates, low intracellular ATP levels and increased resistance to isoniazid, metronidazole and rifampicin (Betts *et al*., 2002), moreover, as it occurs with LuxR family transcription factor gene, a deletion reported to be involved in recovery from dormancy state during anaerobiosis have shown not to be related to bacterial growth and long term survival under aerobiosis (Fang *et al*., 2013), During oxygen starvation, the upregulation of lipid metabolism genes occurs as well, hypoxic non-replicating BCG cells have shown to accumulate triacylglycerol forming intracellular droplets that are required for reactivation (Low *et al*., 2009). The adaption during the hypoxic state is carried out by the DosS/DosT-DosR regulation complex, shifting the bacteria metabolically from the aerobic to the anaerobic status, controlling the reverse process and responding to NO and CO as well (Kumar *et al*., 2007). Therefore, active growth and persistent states are seemingly disengaged processes, supporting the fact that TB drugs targeting active growth normally fail to eradicate non-growing *M. tuberculosis* (Gengenbacher and Kaufmann, 2012).

Studies have shown that the growth of *M. tuberculosis* is also restricted under phosphate limitation but, interestingly, the genes encoding for polyphosphate kinase and ppGpp synthetase, *ppk1* and *relA* respectively, have been found to be upregulated during phosphate starvation, along with inorganic polyphosphate accumulation and triggering the stringent response (Rifat *et al*., 2009). Due to the phosphate-limited environment inside the macrophage phagosomes, it can envisage that polyphosphate plays an important role in persistence by acting as a phosphate store and source of phosphate molecule when studying *M. tuberculosis* persistence.

The infection with *M. tuberculosis* in dormant stage produces a disease without clinical manifestation, the reactivation occurs by the re-establishing of both metabolic and replicative machinery. A few factors regarding regrowth have been described, such as resuscitation-promoting factor (Rpf) which has shown to have lysozyme activity in *Micrococcus luteus* (Cohen-Gonsaud *et al*., 2005) and implicated in resuscitation from dormancy in *M. tuberculosis* (Kana *et al*., 2008), as well as factors related to degradation of the cell wall and peptidoglycan in *Bacillus* species (Shah *et al*., 2008; Giebel *et al*., 2009). A model has been hypothesised where an equilibrium between dormant and replicating populations of bacteria exists during the progression from latent to active infection, and the resuscitation would occur by either stochastic events or mediated by signals; nevertheless, the mechanisms at molecular level remain far unknown (Gengenbacher and Kaufmann, 2012).

1.4.6 Vaccines, drugs and treatment

In spite of numerous researches and the use of chemotherapy, current rates of TB prevalence are higher than in the past, claiming a life every ten seconds with increasing global mortality rates. As described above, *M. tuberculosis* utilises different ways to survive and evade the immune system. Persistence along with the emergence of MDR and XDR strains makes the development and synthesis of novel drugs and therapies a priority in order to achieve effective control.

Due to little concrete information on the cellular or metabolic status of persistent mycobacteria, drug treatments available are extended and current antibiotics require long periods of time to cure patients and preventing relapse. Moreover, drug resistance due to genetic mutations has resulted into loss of susceptibility to antibiotics, therefore, during the

past decade, the efforts in order to develop new diagnostics, drugs and vaccines against TB have been intensified. The most effective regimen requires a combination of at least three drugs and lasts for six months, with an initial phase of two months where isoniazid, a rifamycin, pyrazinamide and ethambutol are administrated, and later, a phase of four months using isoniazid and rifampycin. The long therapy generates natural resistance in the pathogen and lack of motivation on patients (Sacchettini *et al.*, 2008; Koul *et al.*, 2011; WHO, 2012). Table 1.1 shows the current first and second-line drugs, their most common mutations and also their respective mechanisms of action.

According to the resistance pattern, the WHO classifies the strains as follows:

- MDR-TB: strain who display resistance to the first-line drugs isoniazid and rifampicin. Individuals are either infected primarily with drug-resistant bacteria, or drug resistance can appear during the treatment under non-optimal conditions. The success of the treatment against infection by MDR-TB is achieved only in 50% to 70% of the cases.
- XDR-TB: a highly lethal strain who shows resistance to isoniazid, rifampicin and fluoroquinolones. Additionally, the strain presents resistance to any of the second-line drugs such as amikacin, capreomycin or kanamycin.

Table 1.1: Commonly used TB drugs

(Adapted with permission from Sacchettini *et al.*, 2008. Confirmation Nº 11129031)

first-line antituberculosis agents

Antibiotic	Chemical structure	Mechanism and target	Mutations associated with resistance
Isoniazid		Inhibits mycolic acid synthesis; primary target is InhA and secondary targets are KasA and DfrA	*katG* (required for drug activation); *inhA* (promoter mutations); and others
Rifampicin	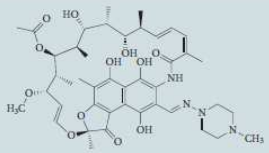	Inhibits transcription; RNA polymerase β-subunit	*rpoB*
Ethambutol	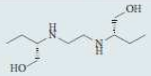	Inhibits arabinogalactan synthesis; possibly EmbB	*embB*
Pyrazinamide		Unknown (possibly inhibits FAS-I or alters membrane energetics)	*pncA* (required for drug activation)
Streptomycin	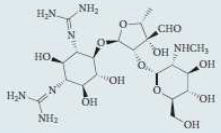	Inhibits protein synthesis; 30S ribosomal subunit	*rpsL* and *rrs*

second-line antituberculosis agents

Antibiotic	Chemical structure	Mechanism and target	Mutations associated with resistance
Fluoroquinolones	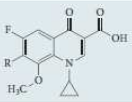	Inhibits DNA gyrase	*gyrB*
Ethionamide		Inhibits mycolic acid synthesis; InhA	*ethA* (required for drug activation) and *inhA* (promoter mutations)
Cycloserine		Inhibits peptidoglycan synthesis by blocking the synthesis and use of D-alanine (Ala); Ala racemase and D-Ala-D-Ala ligase	*alr* (overproduction) and *ddl* (overproduction)
Para-aminosalicylic acid		Inhibits folate metabolism; possibly dihydropteroate synthase	*thyA*
Capreomycin	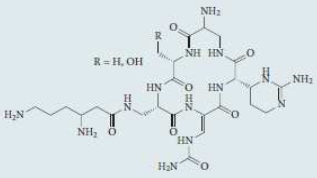	Inhibits protein synthesis; methylated nucleotides in both ribosomal subunits	*tlyA and rrs*
Kanamycin	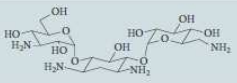	Inhibits protein synthesis	*rrs*
Amikacin	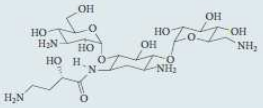	Inhibits protein synthesis	*rrs*

Therefore, in order to succeed in the global control of TB, exists an urgent need for new TB drugs that could shorten treatments duration, target MDR or XDR strains and simplify the treatments (Koul *et al*., 2011). New TB drugs have been discovered and can be found in different clinical trials phase already. i.e., Fluoroquinolones, Rifampicin analogues, Rifalazil, SQ109, TMC207, Sudoterb, Nitroimidazoles, OPC‑67683 (Sacchettini *et al*., 2008).

In the case of the vaccines, the BCG vaccine for the prevention of TB is almost 100 years old, protecting with an effectiveness of approximately 75% against the severe forms of TB such as tuberculous meningitis or miliary tuberculosis (Trunz *et al.*, 2006), unfortunately, its efficacy in preventing pulmonary TB in adults is highly variable since the range of protection showed is between 0 to 80% with an average of 50% (Brewer, 2000). The use of BCG is not recommended in children infected with HIV, due to the risk of dissemination of BCG disease (WHO, 2009).

Currently, the clinical trials for new vaccines include eleven candidates for prevention of TB and one immunotherapeutic vaccine. Some of them are AERAS-402/Crucell Ad35 (adeno-vectored vaccine), M72 and Hybrid-1 (protein subunit vaccines), VPM 1002 (live recombinant vaccine), RUTI (non-live vaccine, based on fragmented bacteria). The expectations indicate that one or two vaccines in Phase II should enter to Phase III within the next 2–3 years, perhaps licensing one new vaccine in 7 years time (Brennan *et al*., 2012; WHO, 2012). Unfortunately, in the case of former promising MVA85A (attenuated vaccinia-vectored vaccine), the last phase IIb trials have revealed that it did not induce a good cell-mediated immune response, either showed the desired effects against the infection in children (Pathan *et al*., 2012; Tameris *et al*., 2013).

1.5 MYCOBACTERIAL CELL WALL

Mycobacteria have a distinct lipid-rich cell wall which is associated with pathogenicity (Takayama *et al*., 2005; Kaur *et al*., 2009). The structure possesses an unusual low permeability that contributes to the resistance of mycobacteria to therapeutic agents, provides a physical protection against hostile environmental conditions such as inside macrophages (Brennan and Nikaido, 1995; Wang *et al.*, 2000), it is involved in the interaction with the host cell, the immunomodulation and virulence as well (Cox *et al.*, 1999; Kan-Sutton *et al.*, 2009). The mycobacterial cell wall is formed of mycolyl-arabinogalactan-peptidoglycan (mAGP) complex found on the inner side of the outer membrane (Azuma and Yamamoto. 1963; Lederer *et al*., 1975; Daffé *et al.*, 1990; Besra *et al.*, 1995; Brennan, 2003; Takayama *et al*., 2005) and additional lipids such as phthiocerol dimycocerosates, phenolic glycolipids, glycopeptidolipids, menaquinones and trehalose-based lipooligosaccharides forming the outer region of the cell wall (Fig. 1.5) (Yassin *et al*., 1988; Brennan and Nikaido, 1995; Brennan and Crick, 2007). The arrangement of the hydrocarbon chains of the lipids forms a thick asymmetric bilayer, the structure and the composition suggest that the fluidity gradually increases from the innermost part toward the outer surface, may affect permeability of the bilayer and also explain the different sensitivity levels to lipophilic inhibitors of different mycobacterial species (Brennan and Nikaido, 1995).

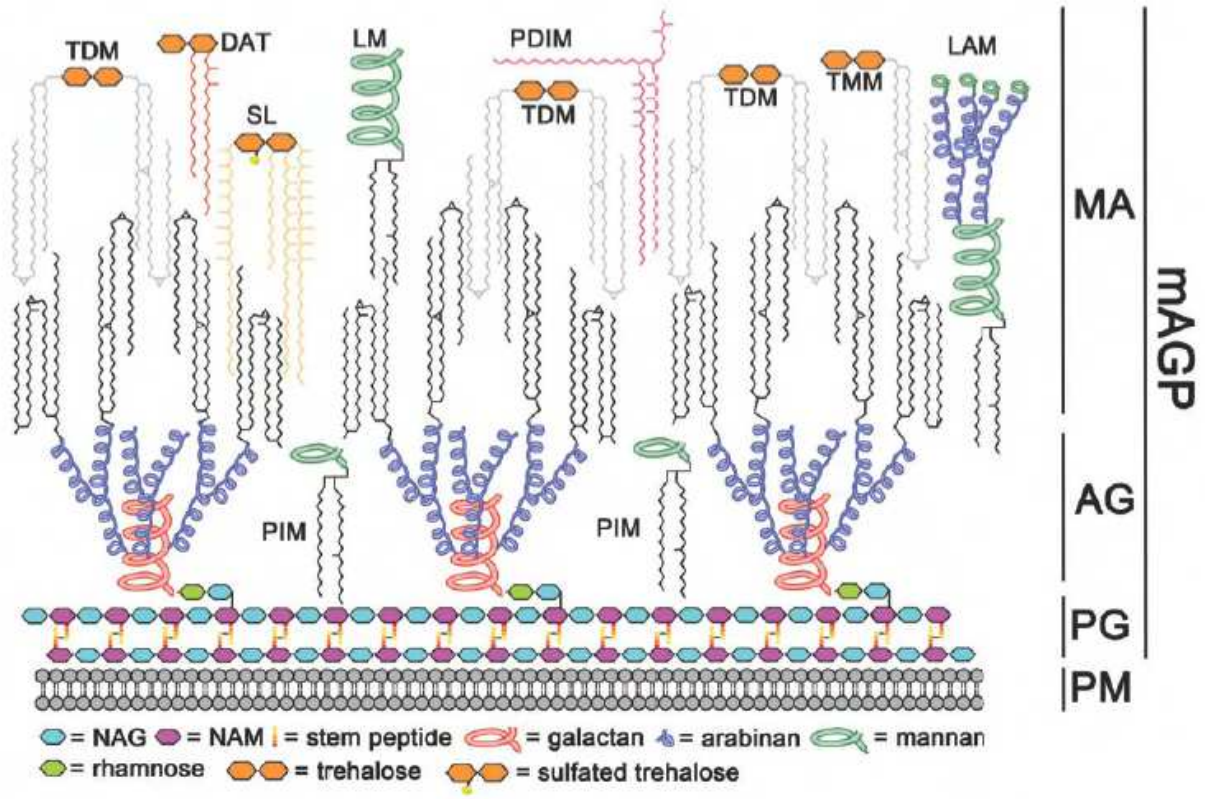

Figure 1.5: Arrangement of structural components in the mycobacterial cell wall. Mycolyl arabinogalactan (mAG) is linked to peptidoglycan (PG) by a phosphoryl part. The diagram shows the interactions between the methyl-branched long-chain components and the mycolic acid matrix. Arabinogalactan (AG), diacyl trehalose (DAT), lipoarabinomannan (LAM), mycolyl-arabinogalactan-peptidoglycan (mAGP), Nacetylglucosamine (NAG), N-acetylmuramic acid (NAM), penta-acyl trehalose (PAT), phthiocerol dimycocerosates (PDIM), peptidoglycan (PG), plasma membrane (PM), sulfated tetra-acyl trehalose (SL), trehalose monomycolate (TMM), trehalose dimycolate (TDM). Model as proposed by Dmitriev *et al*., 2000 and Minnikin *et al*., 2002. Dr L. Alderwick, personal communication.

1.5.1 Structure of mAGP

The insoluble cell wall matrix is located beyond the membrane and it is composed by a cross-linked peptidoglycan (PG) bound to arabinogalactan (AG), which is esterified by the mycolic acids (MA).

1.5.1.1 Peptidoglycan

Peptidoglycan is a macromolecular structure localised on the external side of the bacterial cell membrane of the majority of eubacteria (Schleifer and Kandler, 1972). It preserves cell structure by maintaining the osmotic pressure, the cell form and it plays a crucial role in cell division as well (Nanninga, 1998).

The structure of bacterial peptidoglycan is composed by linear glycan chains linked by a peptide linkage which binds peptide subunits of two chains or a bridge formed by two peptide subunits. The glycan chains are formed by units of *N*-acetylglucosamine (GlcNAc) and *N*-acetylmuramic acid (MurNAc) linked by β1→4 bonds. The carboxyl group of the *N*-acetylmuramic acid residue is replaced by a peptide subunit, normally is L-alanyl-γ-D-glutamyl-diaminopimelyl (or L-lysyl)-D-alanyl-D-alanine in the growing peptidoglycan, without one or both of the D-alanine residues in the mature version of peptidoglycan (Adam *et al*., 1969; Petit *et al.*, 1969). The biosynthesis of PG involves glycosyltransferases for the linear glycan chains and transpeptidases for peptide cross-bridges, including two mechanisms: septation and elongation (van Heijenoort, 2001). The PG structure of *Mycobacterium* contains unusual features: it is N-glycolylated, in addition to N-acetylated, muramic acid units; it exhibits direct cross-linkage between *meso*-diaminopimelic acid components and also the replacement of L-alanine by glycine in the peptide chains of *M. tuberculosis* and *M. smegmatis*. However, in *M. leprae* the muramic acid units are exclusively N-acetylated (due to the non-functional *namH* gene) and the uncross-linked peptide side chains consist of tri- and tetrapeptides, containing additional glycine residues (Mahapatra *et al*., 2008).

1.5.1.2 Arabinogalactan

AG, a branched polymer of galactose and arabinose, is the most important cell wall polysaccharide of mycobacteria located immediately outside the PG. The function has been proposed to produce a viscous hydrophilic region between the PG and MA layers. A structural model indicates that AG contains 125 glycosyl units, composed by: a galactan domain of 30 Gal*f* residues, three arabinan domains of 31 Ara*f* units each and a specific linker unit that binds it covalently to PG composed by a rhamnosyl residue attached to a *N*-acetylglucosaminosyl-1-phosphate unit (Bhamidi *et al.*, 2008). The galactan unit is made of a disaccharide repeating unit: $[\rightarrow$6-D-Gal*f*β1$\rightarrow$5-D-Gal*f*β$]_{15}$ while arabinan chains are attached to *O*-5 of Gal*f* residues 8, 10 and 12 of galactan. The arabin domain contains a non-reducing extreme of an Ara6 motif, Ara*f*β1 → 2Ara*f*α1 → 5(Ara*f*β1 → 2Ara*f*α1 → 3)-Ara*f*α1 → 5Ara*f*α1 →, whose position 5 of both the terminal β-Ara*f* and the penultimate 2-α-Ara*f* are the attachment sites for the mycolic acids. Under physiological conditions, approximately two-thirds of the Ara6 motifs are mycolylated (McNeil *et al.*, 1990; 1991).

The arabinan domain is formed by a central structure made up of linear α–1,5-linked Ara*f* units and branches to form a α–3,5-branch site (Lee *et al.*, 2006; Alderwick *et al.*, 2007; Bhamidi *et al.*, 2008, Kaur *et al.*, 2009).

1.5.1.3 Mycolic Acids

Mycolic acids (MA) are β-hydroxy fatty acids with a long α-alkyl side chain, they can be represented by the formula shown in Fig. 1.6 (Asselineau and Lederer, 1950). The mycolic unit is formed by the long alkyl chain along with the meromycolate chain which normally incorporates up to two functional groups. The merochain exhibits different modifications, including double bonds, keto or methoxy functional groups, *cis- or trans-*

cyclopropanations and epoxidations as well, which vary depending on the species (Barry *et al.*, 1998).

MA are usually bound to the cell wall by esters formed between the acid and an alcohol of a sugar, often as pentaarabinose tetramycolates. They can also be found as non-bound esters, such as glucose monomycolate (GMM), glycerol monomycolate (MMG), trehalose mono- and dimycolates (TMM and TDM), and as free MA (Takayama *et al*., 2005; Andersen *et al*., 2009; Verschoor *et al*., 2012). MA ccur in a specific group of Gram-positive bacteria such as *Corynebacterineae*, including the genera *Mycobacterium*, *Nocardia*, *Rhodococcus* and *Corynebacterium*. In *Corynebacterium* the MA are smallest (C28–C40) and not essential (Gebhardt *et al*., 2007), unlike in *Mycobacterium* species where they have been found to be essential for growth and survival *in vitro* and *in vivo*, with length between C60–C90 (Vilchèze *et al*., 2000; Portevin *et al*., 2004). *Rhodococcus* has MA in the range of C30–C54 and *Nocardia* in the range of C42–C66, in both cases the mero-chain does not exhibit functional groups other than one or more double bonds (Sutcliffe, 1998; Nishiuchi *et al*., 1999; Verschoor *et al*., 2012).

In *M. tuberculosis*, MA are composed by highly hydrophobic fatty acids with α-side chains of three different types found, namely α- (the most abundant form, accounting for >70%), methoxy- and keto-mycolic acids (Fig. 1.6) (Qureshi *et al*., 1978; Takayama *et al*., 2005).

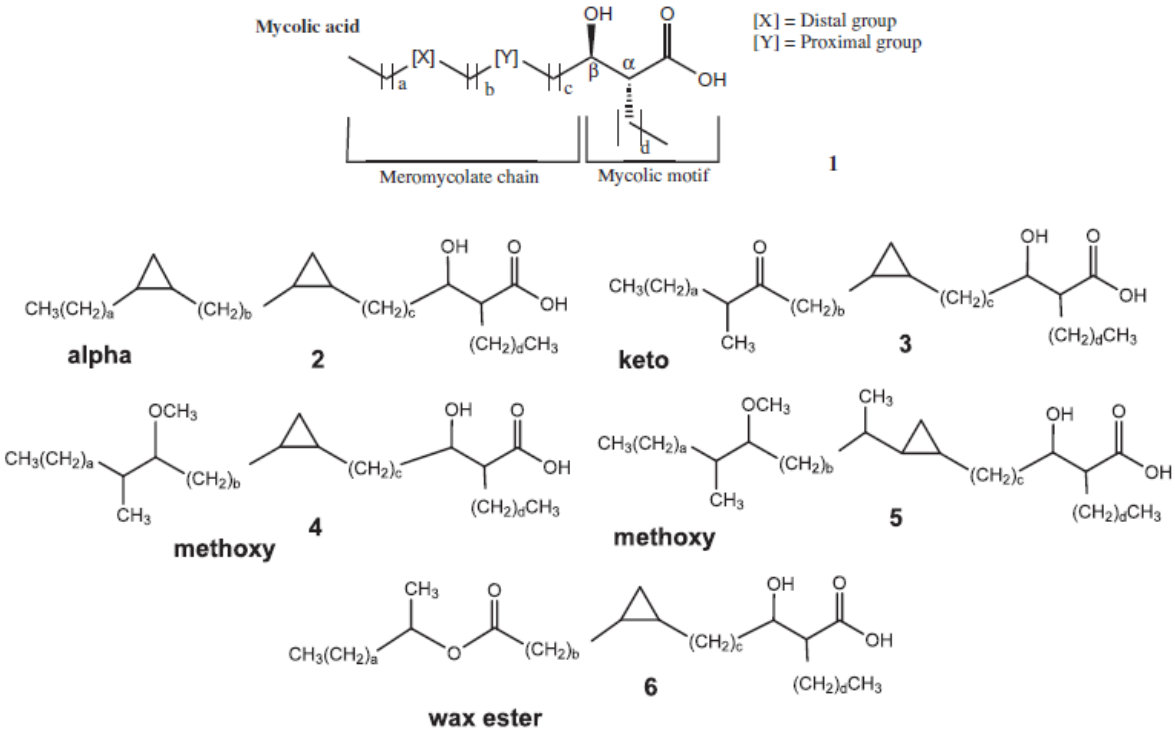

Figure 1.6: Mycolic acid structure. 1: general formula, a–d: varying lengths of methylene chains. 2-5: major types of mycolic acid from MTBC according to the functional groups; 6: a related wax ester from *M. paratuberculosis*. (Adapted with permission from Verschoor *et al*., 2012. License Nº 3244830256376).

1.5.2 Noncovalently bound glycoconjugates: free lipids of *M. tuberculosis*

The glycoconjugates of the outer membrane correspond to a group of lipids noncovalently bound to the cell wall, they are intercalated within the lipids region formed by the MA of the mAGP complex, this group includes: Phthiocerol dimycocerosate (DIM/PDIMs), phenolic glycolipids (PGLs), acyltrehaloses (TMM, TDM and GMM), sulfolipids (SLs), phosphatidyl-*myo*inositolmannosides (PIMs), lipomannan (LM) and lipoarabinomannan (LAM), etc (Kaur *et al*. 2009; Pitarque *et al*., 2008).

1.5.2.1 Acyltrehaloses

These are an important group of virulence factors in the envelope of mycobacteria, formed by trehalose-containing glycolipids (Fig. 1.7). Trehalose is a non-reducing disaccharide of glucose (α-D-Glc*p*-(1<->1)-α-D-Glc*p*) and it is found in organisms such as bacteria, yeast, fungi, plants and invertebrates, but it is absent in mammals. In mycobacteria, it can be found free in the cytoplasm or esterified to a different fatty acyl groups in the cell envelope. The free version of trehalose could be a storage carbohydrate as well as a stress protectant, while the acyltrehaloses found in the cell envelope of *M. tuberculosis* include diacyltrehaloses (DAT), polyacyltrehaloses (PAT), sulfatides (SL), triacyltrehaloses (TAT), trehalose dimycolates (TDM), trehalose monomycolate (TMM) and polar species-specific lipooligosaccharides (LOS) (Kaur *et al.*, 2009). Trehalose dimycolate (TDM), known as cord factor, accumulates in a cord-like fashion outside the cells (Noll and Bloch, 1955; Noll *et al*., 1956), has a toxic effect in mice (Goren and Brennan, 1980).

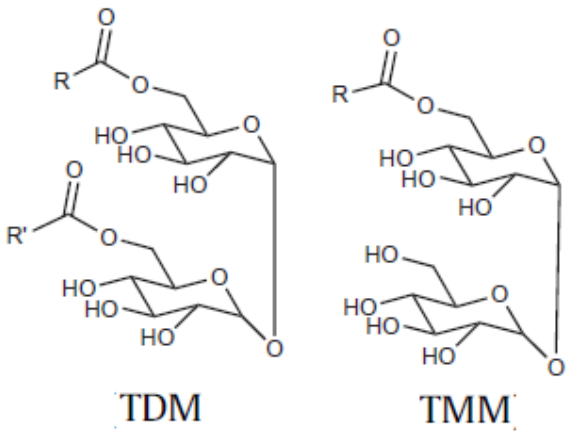

Figure 1.7: Acyltrehaloses. Structures of trehalose dimycolate (TDM) and monomycolate (TMM); RCOOH, R'COOH: mycolic acid. Adapted with permission from Verschoor *et al*., 2012. License Nº 3244830256376

1.5.2.2 Sulfolipids

Several slowly growing mycobacteria contain an array of waxes so called sulfolipids, they are formed by multi-acylated varieties of trehalose sulfate differing by the amount, composition and location of the acyl units (Goren *et al.*, 1971). The major sulfolipid, SL-I, is characterized as a tetraacyl-trehalose-2-sulfate, acylated by two hydroxyphthioceranates (HPA), one phthioceranate (PA), and one palmitate (C16) or stearate (C18). They have been implicated in the pathogenesis of tuberculosis, but the function still remains unclear (Brennan and Nikaido, 1995; Converse *et al.*, 2003; Layre *et al.*, 2011).

1.5.2.3 Phthiocerol dimycocerosate

PDIM, is a major lipid of *M. tuberculosis* and is related to its virulence ability. It is composed by 35 carbons as methyl or methylene groups and two hydroxy groups esterified with two mycocerosic acids (Goren and Brennan, 1980; Brennan, 2003). PDIM is also related to other lipids and methyl branched fatty acids, such sulfolipids where phthioceranic or hydroxy-phthioceranic acids are the major acyl constituents (Sirakova *et al.*, 2001).

Recent studies in *M. marinum* have shown another structurally related group of molecules called phenolic glycolipids (PGLs). The structure of the carbohydrate domain of these compounds is highly variable and the genetic bases for these variations remain unknown. PGLs are, together with PDIMs, required for virulence and the lack of genes related to their biosynthetic pathways produces hypersensitive to antibiotics and negative effects in the cell wall such as higher permeability. It has been demonstrated that PGLs play a major role in the virulence of some strains of *M. tuberculosis* complex and in *M.*

leprae (Málaga *et al*., 2008; Yu *et al*., 2012). Although most of the strains of *M. tuberculosis* do not produce PGLs due to a mutation in the polyketide synthase *pks15/1*, they still retain the ability to produce and secrete *p*-hydroxybenzoic acid derivatives (*p*-HBADs) glycoconjugates which share with PGLs the same glycosylated aromatic nucleus (Constant *et al.*, 2002).

1.5.2.4 PIMs, LM, and LAM

Mycobacterial cell envelope contains high amounts of mannosylated molecules. These are ubiquitous mannosyl-phosphatidyl-*myo*-inositol based glycolipids and are metabolically-related lipoglycans, comprising PIMs, LM and LAM. These are non-covalently anchored to the cell envelope through their phosphatidyl-*myo*-inositol (PI) moiety (Besra *et al.*, 1997; Hunter and Brennan, 1990; Pitarque *et al.*, 2008). They promote the entry of *M. tuberculosis* inside phagocytic cells through mannose-specific C-type lectins, regulate phagosome maturation and modulate the host immune response (Briken *et al.*, 2004; Kaur *et al*., 2009).

Structurally PIMs, LM and LAM are formed by a conserved PI backbone with mannosylation branch at the C-6 position of the *myo*-inositol. The backbone is heterogeneous and the differences are based on the amount, position and type of the fatty acids. The PIMs include PI-dimannosides (Ac1PIM2 and Ac2PIM2) and PI-hexamannosides (Ac1PIM6 and Ac2PIM6): Ac1PIM2 and Ac1PIM6 contain one fatty acid bound to the Man*p* attached to position 2 of *myo*-Ins in addition to a diacylglycerol moiety; on the other hand, Ac2PIM2 and Ac2PIM6 contain a fourth fatty acyl chain linked to position 3 of *myo*-Ins. LM and LAM are formed by a mannan core of approximately 20-25 α(1→6)-linked Man*p* residues, sometimes showing substitution at C-2 by single Man*p*

units in all mycobacterial species investigated, except in *M. chelonae* where the branching occurs at C-3 (Guérardel *et al.*, 2002; Kordulakova *et al.*, 2003; Briken *et al.*, 2004; Hsu *et al.*, 2007; Kaur *et al.*, 2009). The mannan core of LM varies in length and degree of branching depending on the species, the type of motifs capping the non-reducing extremes of the arabinan domain of LAM differs among mycobacterial species, finding mannose-, inositol phosphate-, phosphate- and non- capped LAM (Nigou *et al.*, 2003). This feature is crucial since alterations in the lipoglycan composition and structure can be recognised differentially by the cells of the immune system, having an important effect on the resulting adaptive immune response (Mishra *et al.*, 2012). Moreover, non-pathogenic species as *M.smegmatis* appears to be permissive to a variety of mutations affecting PIM, LM and LAM synthesis, the inability to generate mutants of *M. tuberculosis* deficient in the acylation of PIMs or LAM synthesis (Goude *et al.*, 2008) indicates that these molecules probably play a more crucial role in the physiology pathogen rather than in the non-pathogenic strain (Kaur *et al.*, 2009).

1.5.2.5 Glycopeptidolipids

GPLs are main constituent of the external layer of the cell wall, involved in different roles such as morphology of the cells, motility, biofilm development, immune response trigger and pathogenesis. They can be found in different non-tuberculosis-causing species of the *Mycobacterium* group, such as the saprophytic *M. smegmatis* and the opportunistic species of the *Mycobacterium avium* complex (MAC), such as *M. avium* and *M. intracellulare*. One specific feature of this group is the production of highly antigenic, typeable serovar-specific GPLs (ssGPLs) (Schorey and Sweet, 2008). GPLs are composed

of a glycosylated lipopeptide core and the type of glycosylations differs between infective and non-infective species (Chatterjee and Khoo, 2001; Patterson *et al.*, 2000).

1.5.2.6 Lipooligosaccharides

Lipooligosaccharides (LOSs) are a type of antigenic glycolipids present in some species of *Mycobacterium* such as *M. canetti*. LOSs compounds contain a α,α′-trehalose unit that is acylated and further glycosylated in a species-specific manner. Structural analyses demonstrated that LOS-I, -II, -III, and -IV share the same glycan core of acylated trehalose substituted by two β-D-Glcp residues and one 3-O-methylated α-L-Rhap (Rombouts *et al*., 2011). Studies using *M. marinum* have shown that LOSs are associated to functions such as motility, biofilm development and infection of macrophages (Ren *et al*., 2007).

1.6 AIMS AND OBJECTIVES

The broad aim of this work is to identify components of metabolic pathways with potential role in the virulence of *M. tuberculosis*. In this research I plan to study both cell and non-cell envelope components by the use of genetic mutants, determining the effects of their respective deletions. While a vast majority of this work will be focused on cell envelope elements, part of the project also involves studies on intracellular metabolites as polyphosphate. Due to the fact that the study of *M. tuberculosis* constitutes a major technical challenge, the fast-growing and non-pathogenic organisms *M. smegmatis* mc^2155 and *C. glutamicum* ATCC13032 will be used in this work instead, as surrogate models.

They have been chosen because both share similar genomic organization and cell wall biosynthetic machinery than *M. tuberculosis*. Moreover, they can stand deletion of several genes that are essential in that pathogen.

In order to study cell envelope biosynthesis in mycobacteria, mutants will be generated, selected and used according to the criteria specified in each chapter. Summarising the approaches, the study will go as follows:

1) Firstly, a strategy based on random transposon mutagenesis will be used to generate a *M. smegmatis* transposon-mutant library. The strains displaying altered colony morphology and increased sensitivity to the lipophilic drug rifampicin will be selected for further analysis as potential cell-envelope defective strains, trying to look for a link between the gene disrupted and the phenotype shown.

2) Secondly, using bioinformatics tools, a group of genes will be selected in order to identify components involved in capsule and cell-wall biosynthesis in mycobacteria. Specifically, based on the homology to carbohydrate ABC-transporters, a list of putative genes involved in the transport of capsule components will be selected to construct knockout strains. On the other hand, the role of large membrane proteins encoded by *mmpL* genes in mycolic acid biosynthesis will be investigated using *M. smegmatis* specific mutant strains. Respectively, the strains will be analysed and tested for: a) changes in the capsule main component production and the effects of the deletion of the genes; b) effects of the deletion in biosynthesis and transport of the mycolic acids and the other “free lipids” of the mycobacterial cell wall mycolic acid biosynthesis. Additionally, *C. glutamicum* will be used as a model system of mycolic acid biosynthesis as well.

3) Finally, in order to address the role of polyphosphate in the metabolism during phosphate-starvation condition in mycobacteria, knockouts strains will be generated for the

exopolyphosphatases homologs in *M. smegmatis*. Polyphosphate consumption will be measured and effect in growth will be monitored in every strain.

The final objective of this study is to highlight the role of several genes involved in cell envelope metabolism and the response under limiting conditions. Therefore, identify them as potential new targets for anti-TB drug development.

CHAPTER 2

SCREENING OF TRANSPOSON LIBRARIES OF *Mycobacterium smegmatis* FOR MUTANTS WITH CELL WALL ALTERATIONS

2.1 INTRODUCTION

As highlighted in the introduction chapter, mycobacteria produce lipid-rich cell walls that have low permeability and high hydrophobicity. This distinct structure contributes to their pathogenicity and resistance to both therapeutic agents and host defence mechanisms (Brennan and Nikaido, 1995; Barry *et al*., 1998; Daffé and Draper, 1998; Cox *et al.*, 1999). It is composed of two segments, lower and upper. The lower consists on the cell wall core, located beyond the membrane, where the peptidoglycan (PG) covalently attached to arabinogalactan (AG), which is in turn esterified to the mycolic acids forming the mycolyl-arabinogalactan-peptidoglycan (mAGP) complex. This structure provides the template for insertion, in an interspersed way, of products such as cell-wall proteins and a number of free complex lipids: phthiocerol-containing lipids, trehalose mycolates, phosphatidylinositol mannans (PIMs) and glycosylated derivatives lipomannan (LM) and lipoarabinomannan (LAM) (Kaur *et al*., 2009; Pitarque *et al*., 2008). The upper segment is composed of free lipids, namely trehalose-based lipooligosaccharides (LOSs), phenolic glycolipids (PGLs) and also glycopeptidolipids (GPLs) with both short and long fatty acids. This unique arrangement produces an asymmetric bilayer of exceptional viscosity and width where fluidity and permeability are potentially low in the internal part of the bilayer and increased on the external face. Due to such a lipid rich structure, it can be envisaged that even lipophilic substances may face an exceptional barrier whereas the hydrophilic nutrients and inhibitors pass through channels like porins (Engelhardt *et al*., 2002; Brennan, 2003; Rodrigues *et al*., 2011).

A number of studies in the past have reported functional and structural changes in mycobacteria as a consequence of alterations in cell wall composition. Therefore, the

integrity of morphological and structural features like biofilm pellicle or cording is the result of right interactions of the correct cell surface components and also between the healthy cells. A seemingly minor alteration as a reduction in the length of the mycolate chain by deleting *kasB* produces a drastic alterations in the morphology, loss of acid fastness and virulence of *Mycobacterium tuberculosis* (Bhatt *et al.*, 2007). Glickman *et al*. also observed that the classic cord formation displayed in cultures of *M. tuberculosis* and *Mycobacterium bovis* was disrupted by the loss of proximal cyclopropane ring of the major mycolic acid (Glickman *et al*., 2000). On the other hand, the loss of a reductase in the non-virulent *Mycobacterium smegmatis* leads to the presence of a β-oxo rather than a β-hydroxyl group in the mycolate unit that alters the morphology of the mutant and sensitivity to antibiotics, likely caused by the changes produced to the hydrophobic properties of the outermost part of the cells (Bhatt *et al*., 2008). Moreover, in the same species, the loss of GPLs and defects in LAM biosynthesis lead to important changes in both morphology, biofilm formation and structure of the colony (Billman-Jacobe *et al*., 1999; Recht and Kolter, 2001; Kovacevic *et al*., 2006), altered growth and modulated immunology response when the deletion of the arabinofuranosyltransferase C (*aftC*) occurs due to the absence of AG alpha (1-->3)-linked arabinofuranosyl (Araf) residues (Birch *et al*., 2008; 2010). In the case of *Mycobacterium marinum* (a fish and amphibian pathogen) lipooligosaccharides play an important role in infection of host macrophages, biofilm formation and sliding motility an virulence (Ren *et al*., 2007), as well as it occurs in *Mycobacterium avium* when the glycopeptidolipids GPLs are loss (Miyamoto *et al*., 2008; Schorey and Sweet, 2008).

Therefore, alterations in its composition may affect the properties of the bilayer and could also be responsible for colony morphology changes, susceptibility to the host

immune response, phage resistance of different mycobacterial species, biofilm formation, loss of cording formation and the increased sensitivity to lipophilic inhibitors, which have demonstrated to be good indicators of cell wall disruption (Brennan and Nikaido, 1995; Gao *et al*., 2003a; Chen *et al*., 2009; Deshayes *et al*., 2010).

In the study of tuberculosis, the use of *M. smegmatis* as an experimental model has generated controversy and discussion (Reyrat and Kahn, 2001; Barry, 2001a; Tyagi and Sharma, 2002), due to its low pathogenicity as it survives poorly in macrophages (Anes *et al*., 2006; Jordao *et al*., 2008) and also because it exhibits no detectable virulence in mice (Bange *et al*, 1999). The composition of the *M. tuberculosis* cell wall presents a high level of similarity compared to *M. smegmatis*, in fact, in both organisms the synthesis of mycolic acids is carried out by the same set of enzymes namely FAS-I and –II systems, FabH, KasA, KasB, MabA and Pks13 (Takayama *et al*., 2005). Although, they exhibit different types of mycolic acids: while *M. tuberculosis* presents α-, methoxi- and keto- types, *M. smegmatis* shows α-, α'- and epoxy-. Another difference shown by *M. tuberculosis* cell wall compared to *M. smegmatis* corresponds to the nature of other lipids; for instance, its cell wall displays an unusual abundance of sulfolipids and produces LAM containing short mannose caps, unlike *M. smegmatis* (Brennan and Nikaido, 1995; Brennan, 2003; Mougous *et al*., 2004), these differences in the composition of the cell wall account for different metabolic and virulence features.

As a surrogate model, *M. smegmatis* is not as useful as *M. bovis* BCG when used in anti-tubercular drug discovery tests, since a significant percentage of *M. tuberculosis* targets are missing, making *M. bovis* BCG a more sensitive model in library screening for compounds active against *M. tuberculosis* (Altaf *et al*., 2010). The studies to determine its applicability in anti-tubercular drug discovery are rare and the reliability of *M. smegmatis*

as a model for the detection of inhibitors of *M. tuberculosis* could be controversial. Nevertheless, due to its shorter generation time, highly similar cell wall-lipids content compared to *M. tuberculosis* and the lack of complications on the handling, *M. smegmatis* has demonstrated to be useful as a surrogate model for study. For instance, this organism offers several advantages in order to decipher the structure and understanding how the biosynthesis of the cell wall occurs (Bhatt *et al*., 2005), as well as the cytoplasmic functioning and regulation (Zahrt *et al*., 2001; O'Toole *et al*., 2003) because it can easily be genetically manipulated, obtaining viable mutants without losing the advantages to tolerate mutation that would be lethal in *M. tuberculosis*, as it occurs with single gene deletions of *embA*, *embB* or *embC* (Amin *et al*., 2008; Goude *et al*., 2008). The *emb* genes encode for key proteins in AG biosynthesis and the corresponding knockouts in *M. smegmatis* resulted in AG with reduced amount of arabinose content together with an increased amount of galactose, although the effect was less dramatic with *embC* (Escuyer *et al*., 2001; Zhang *et al*., 2003; Alderwick *et al*., 2011).

M. smegmatis is also known for showing less sensitivity towards the two frontline anti-TB drugs isoniazid and rifampicin (Chung *et al*., 1995; Quan *et al*., 1997; Li *et al*., 2004), and its susceptibility is identical to that of MDR clinical isolates of *M. tuberculosis*. The stringency is not necessarily a disadvantage, since both drugs have shown a better activity against the pathogen not only *in vitro* but also *in vivo*, so in addition to their non-pathogenic and fast-growing conditions, it turns *M. smegmatis* into a good surrogate when testing sensitivity to lipophilic antibiotics (Chaturvedi *et al*., 2007). The reduced susceptibility to these antibiotics shown by *M. smegmatis* remains not totally clear; in mycobacteria, the role of efflux pumps in antibiotic resistance has already been probed but it does not necessarily explain the difference with *M. tuberculosis*, since most of the

homologous pumps are present in both organisms and, specifically in the case of the *efpA* mutant, the lack of the efflux-pump gene increases the resistance to rifamycins instead of reducing the susceptibility (Liu *et al*., 1996; Li *et al*., 2004). Perhaps, the difference in susceptibility is based on the fast-growing nature of *M. smegmatis* along with other unknown factors absent in *M. tuberculosis*, due to a greater genome with approximately 3,000 more genes.

In this chapter a random transposon mutant library of *M. smegmatis* has been generated in order to use it as a source of strains with altered cell wall. Transposon mutagenesis has been a powerful tool for the study of several biological aspects of *M. tuberculosis*, like genetic, pathogenesis and also to decipher metabolic pathways, discovering new virulence factors and essential genes (Guilhot *et al*., 1994; Barry, 2001b; Sassetti *et al*., 2001; McAdam *et al*., 2002; Gao *et al*., 2003a; Gao *et al*., 2003b; Lamichhane *et al*., 2003). It has been shown that target sites are preferably the regions of the chromosome where transcription is inactive at the moment of transduction (Manna *et al*., 2004).

A mariner-based transposon has been used for mutagenesis in mycobacteria offering the advantage of being non-indigenous and having a high transposition frequency since its efficiency has been improved using a temperature sensitive phage delivery system. The recombinant phage phAE181 was used in this study, which is derived from the mariner-based Tn*5371* and the lytic mycobacteriophage TM4 (Rubin *et al*., 1999 Kriakov *et al.*, 2003). The phage can infect several species of both slow and fast growing mycobacteria as *M. tuberculosis*, *M. smegmatis* or *M. marinum* and replicates inside a mycobacterial host at 30°C as part of its lytic cycle, but not at 37°C. The hygromycin resistance gene (*hyg*) is then inserted by infection of the host at 37°C to be used as a

selection marker, the cassette disrupts the ORF imparing the transcription of the gene (Bardarov *et al*., 1997; Rubin *et al*., 1999; Sassetti *et al*., 2001; Rybniker *et al*., 2003). In order to detect putative cell wall alterations, the phAE181 system was used to generate transposon mutant strains that were selected by visual criteria when loss of biofilm pellicle formation occurred (loss of the cell interface between the liquid media and the air, as shown in figure 2.1) and also by increased sensitivity to rifampicin, a lipophilic drug.

2.2 RESULTS

2.2.1 Isolation of *M. smegmatis* Tn-mutants with altered growth patterns and increased sensitivity to the lipophilic drug rifampicin

Following transposon mutagenesis using phAE181, a total of 1672 hyg^R transductants were obtained and inoculated into 96-well plates on duplicates. While a vast majority of strains showed normal growth patterns compared to the wild type control, some strains exhibited poor growth and/or alterations in the formation of pellicles on extended incubations (Fig. 2.1). These two types of strains amounted to a total of forty two Tn-mutants, each of which was then tested for i) colony morphology alterations on solid media; ii) increased rifampicin sensitivity on agar plates using concentrations of the antibiotic lower than the minimal inhibitory concentration (MIC) previously reported of 30 μg/ml (Chakravorty *et al*., 2008) and iii) cording in liquid media by optical microscopy. A total of fifteen strains displayed traits as small colony size, loss of cord formation, glossy texture or rifampicin sensitivity (Fig. 2.2). No spontaneous resistance was observed during the screening.

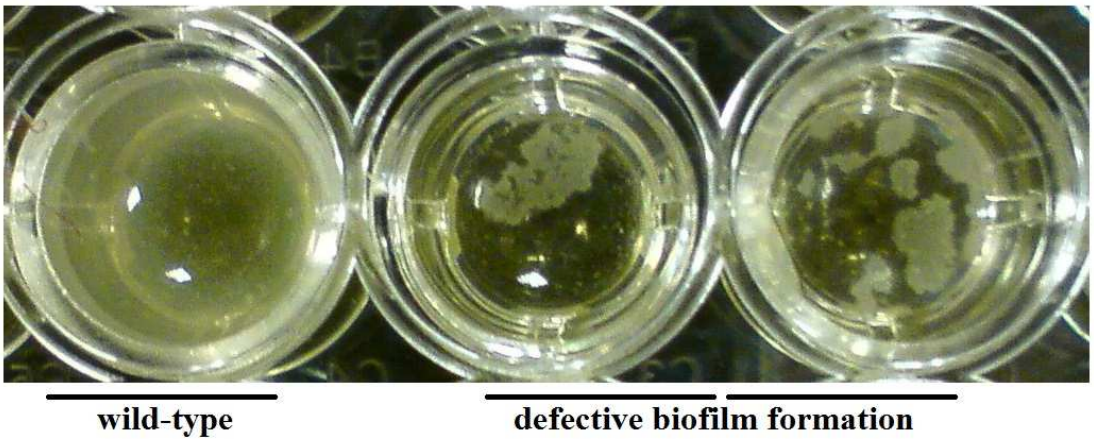

Figure 2.1: Pellicle formation assay of different *M. smegmatis* strains. Picture showing a top view of the biofilm pellicles formed on the surface of TSB-cultures incubated in 96-well plates at 37°C for 5 days without agitation. Left well shows wild-type pellicle pattern; center and right wells show defects in biofilm formation in two different Tn-mutants (Tn-mutagenesis using phAE181). The loss of the ability to form biofilm pellicle was used as one of the selection criteria.

2.2.2 Identification of Tn-insertion sites and disrupted genes

Since the mutant strains contain the Tn*5371* insertion, the transposon-disrupted genes were identified by DNA sequencing and the results obtained were analysed using the BLAST software (Altschul *et al.*, 1990) and the MycoDB database (http://xbase.bham.ac.uk/mycodb/). Interestingly, two categories of biological processes were mainly represented amongst the insertions sites. Whilst six genes encoded functions related to lipid metabolism, three were similar to genes involved in intermediate metabolism processes. Transposon insertions were also found in genes related to cell division, transporting and transcription regulation. Results are shown on Table 2.1.

Table 2.1
Transposon mutant library strains

Strain	Gene	Function	*M. tuberculosis* H37Rv homologs	Changes observed
1	*MSMEG_0472*	putative lipoprotein	No	Glossy, small, loss of cord formation (549587)
18A	*MSMEG_6387*	probable arabinosyltransferase A	*Rv3793* / *embC* *	Small, Rif^S, loss of cord formation (6444823)
23	*MSMEG_5041*	acyltransferase	*Rv1254* / acyltransferase ‡	Small colony, Rif^S, loss cord formation (5136306)
30A	*MSMEG_0147*	C-5 sterol desaturase	*Rv1814* / *erg3* †	Normal size, loss of cord formation (170248)
85B	*MSMEG_0408*	type I modular polyketide synthase	*Rv1661* / *pks7* ‡	Glossy, small, loss of cord formation (482115)
10F7B	*MSMEG_6599*	LuxR regulator	No	Glossy, small, loss of cord formation (6655089)
25B	*MSMEG_0157*	Oxalyl-CoA decarboxylase	*Rv0118c* / *oxcA* ‡	Glossy, small, loss of cord formation (180910)
143	*MSMEG_4269*	asparagine synthase (glutamine-hydrolyzing)	*Rv2201* / *asnB* ‡	Small size, Rif^S (4353015)
245	*MSMEG_3641*	conserved hypothetical protein	*Rv1836c* / hypothetical protein †	Rif^S (3705662)
43B	*MSMEG_3108*	ABC transporter, ATPase subunit	*Rv2832c* / *ugpC* ‡	Glossy, small, loss of cord formation (3183779)
55B	*MSMEG_2860*	virulence factor mce family protein	*Rv1971* / *mce3F* †	Glossy, small, loss of cord formation (2923473)
56B	*MSMEG_3743*	*Soj* - *Spo*OJ regulator protein	*Rv1708* / putative initiation inhibitor protein ‡	Glossy, small, loss of cord formation (3807758)
104B	*MSMEG_3926*	cation-transporting ATPase Pma1	*Rv1997* / *ctpF* †	Glossy, small, loss of cord formation (3995223)
208	*MSMEG_1930*	DEAD/DEAH box helicase	*Rv3211* / *rhlE* ††	Rif^S, loss of cord formation (2009180)
109A	*MSMEG_4751*	hypothetical protein	No	Normal size, loss of cord formation (4849186)

* Essential gene (Goude *et al*., 2008)
‡ In vitro essential gene (Sassetti *et al*., 2003)
† Non- essential gene (Sassetti *et al*., 2003)
†† Non-essential gene (Lemichhane *et al*., 2003)
( ) Position of the genome where the transposon insertion occurred (*M. smegmatis* mc^2155, GenBank CP000480.1)

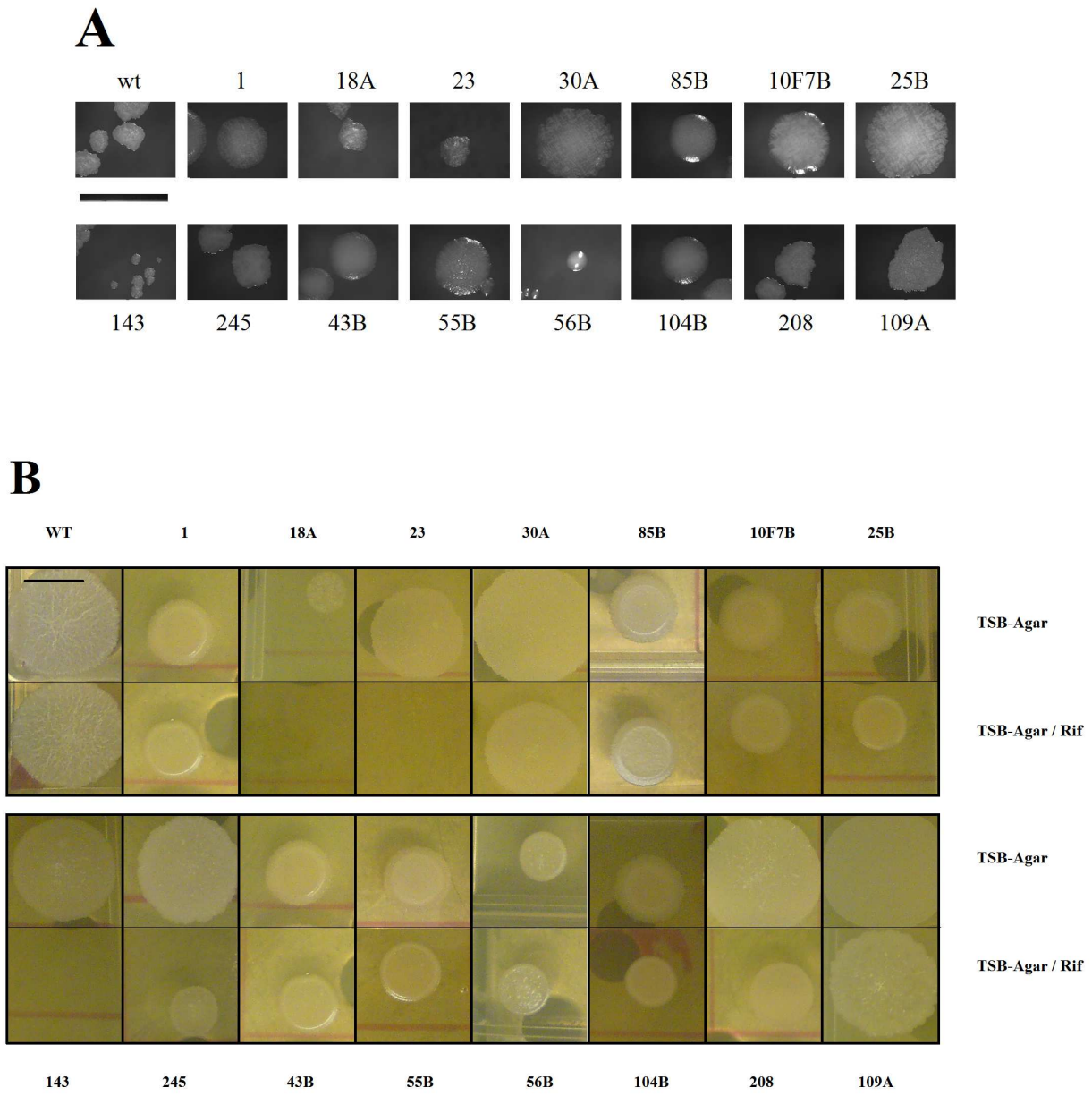

Figure 2.2: Morphology of *M.smegmatis* Tn-mutants. Cultures grown until late-log phase in TSB were plated out on: **(**A) TSB-agar plates to display single colony formation. (B) 10µl drops of 10^{-5} serial dilutions from stationary phase cultures were spotted on TSB-agar plates with and without rifampicin 5µg/ml in order to check antibiotic sensitivity as result of transposon gene disruption. Plates were incubated at 37ºC. Scale bars: 1 cm.

A set of the disrupted genes found in this library corresponded to genes previously described as involved in processes like biogenesis, structure or transport of cell wall components, validating the method and the selection criteria used. Among this group, the disrupted genes were: *MSMEG_6387* (arabinosyltransferase A) and *MSMEG_0408* (type-I modular polyketide synthase) which are involved in *M. tuberculosis* cell wall components biosynthesis; *MSMEG_0147* (C-5 sterol desaturase) that has been described playing a role in membrane permeability in yeasts; finally, *MSMEG_0157* (oxalyl-CoA decarboxylase) and *MSMEG_4269* (glutamine-hydrolyzing) have been previously described as related to energy metabolism and aminoacid biosynthesis with implications in structural development of the cell wall as well.

A complete analysis of non-polar (system A, B, C, D) and polar lipids (system D, E) of the Tn-mutant strains was carried out using a 2D-TLC system to visualise the samples (Dobson *et al*., 1985). Neither the cell wall associated lipids nor the free lipids were considerably altered in any of the mutants analysed compared to the wild type strain when growing in rich media (Fig. 2.3).

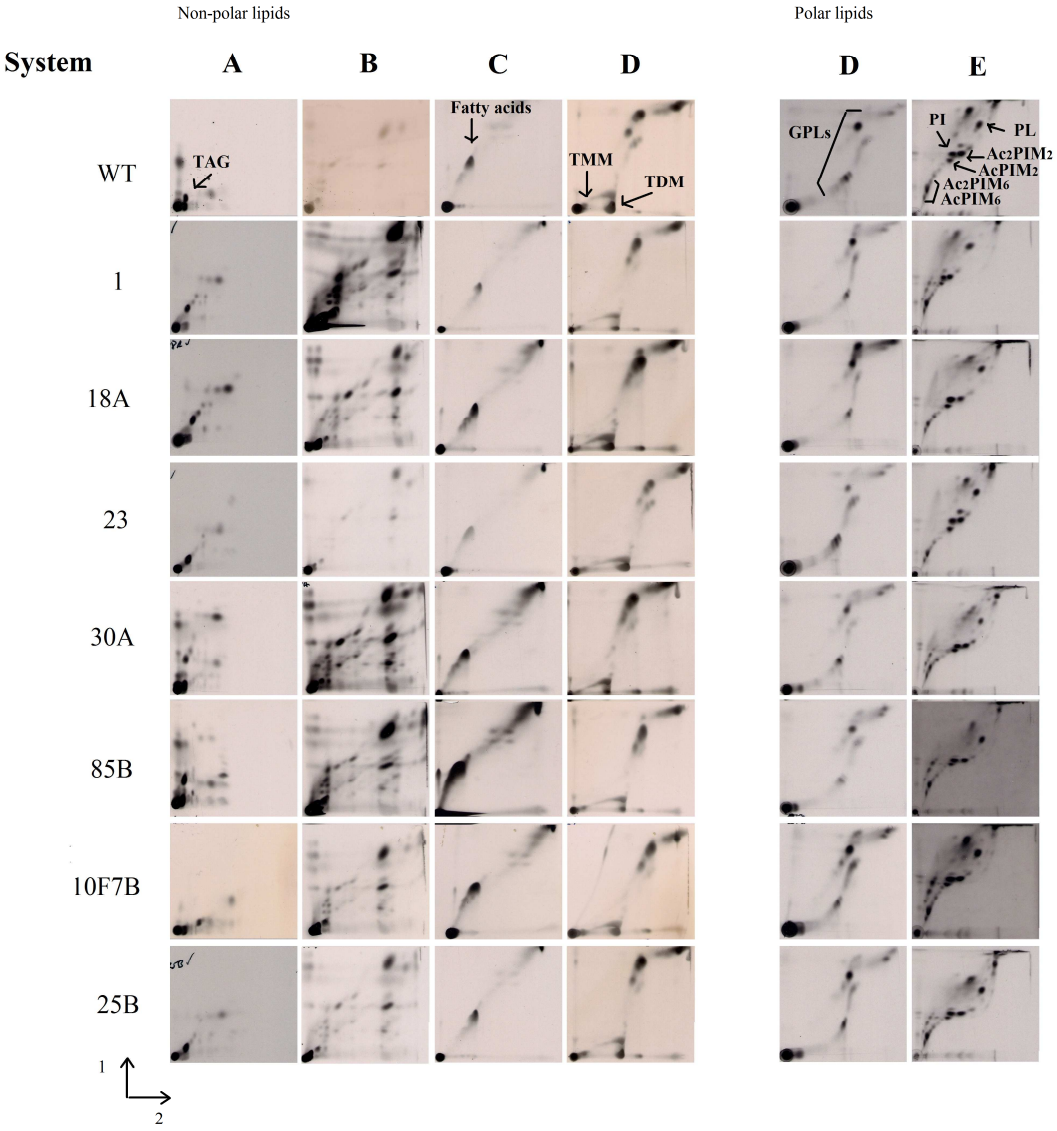
Non-polar lipids
Polar lipids
System
A
B
C
D
D
E
TAG
Fatty acids
TMM
TDM
GPLs
PI
PL
Ac2PIM2
AcPIM2
Ac2PIM6
AcPIM6
WT
1
18A
23
30A
85B
10F7B
25B
1
2

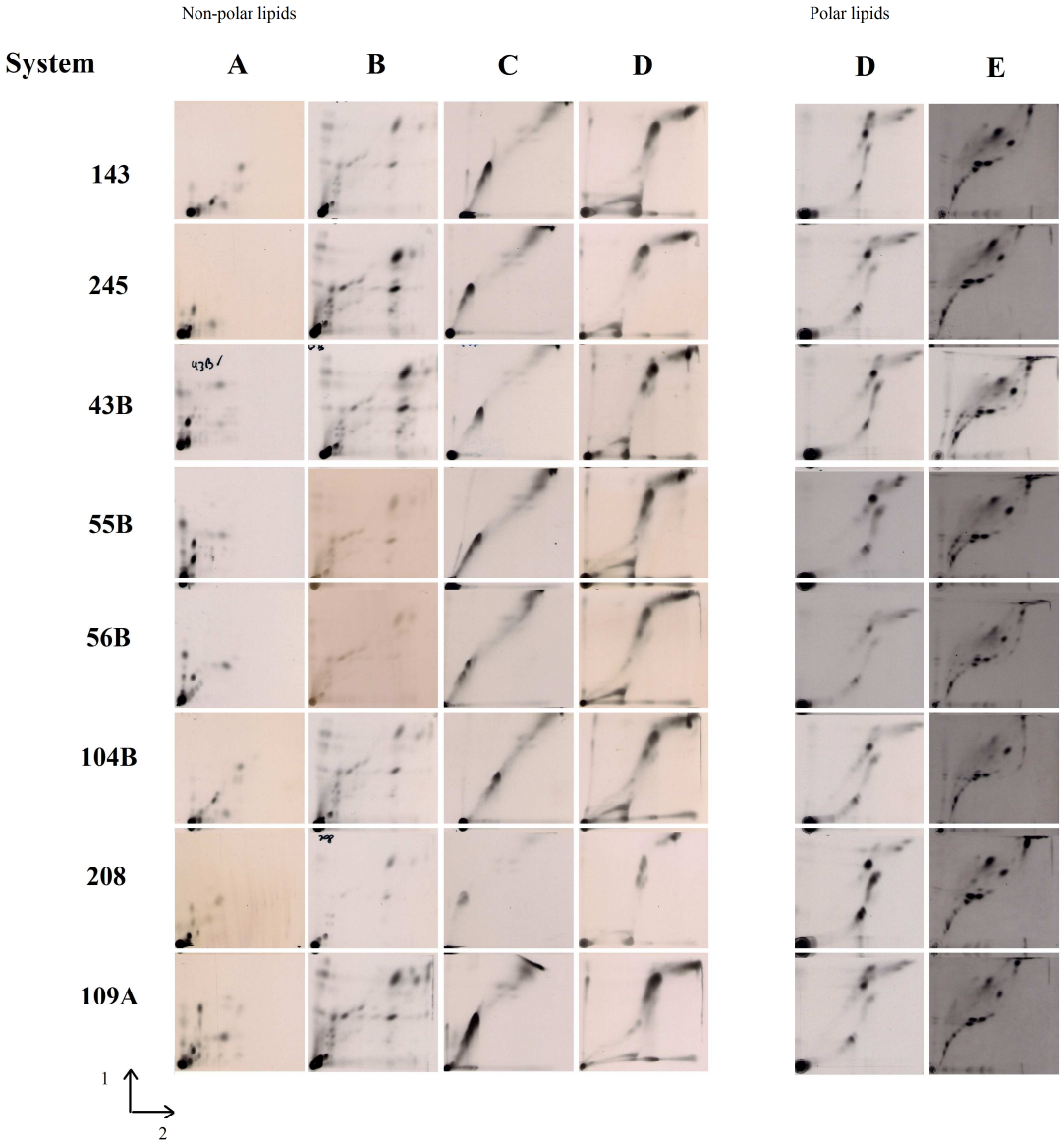

Figure 2.3: Lipid analysis of *M. smegmatis Tn*-mutants. Two dimensions-TLC analysis of [^{14}C]-labelled lipids from mutant strains grown in 10 ml of TSB culture, cells were labelled during mid-log phase. Extracted lipids were separated using different solvent systems by spotting 20,000 cpm of each lipid sample (see General Materials and Methods chapter). Positions of known lipids from the wild-type are indicated by arrows. 1 and 2 indicate first and second dimension, respectively. Ac2PIM2 di- and monoacyl phosphatidylinositol dimannosides, Ac2PIM6 and AcPIM6 di and monoacyl phosphatidylinositol hexamannosides; GPLs–glycopeptidolipids; PI–phosphatidyl inositol; PL–phospholipids; TAG–triacylglycerol; TMM–trehalose monomycolate; TDM–trehalose dimycolate.

2.2.3 Disruption of the *parA* homolog *MSMEG_3743* causes growth inhibition, impaired DNA segregation and delayed cell division of *M. smegmatis*

The *ΔMSMEG_3743* Tn-mutant strain showed a severe impairment in its growth, forming clumping aggregates and a small amount of cells yield in both solid and liquid media even after long periods of incubation. Growth rate analysis was attempted by measuring optical density and counting viable cells, but the results were not reliable due to the way the cells clumped each other. Fluorescence microscopy was performed for visualisation of septa/membrane and nucleoids by staining with FM4-64 and DAPI, respectively. The majority of the wild-type cells clearly showed the midcell septa with well-segregated nucleoids in both halves of the cell. On the other hand, the mutants contained an asymmetric distribution of the septum ("spots-like") along the cell surface and the DNA nucleoid distributed either as granules or multinucleoidal cells (Fig. 2.4).

2.3 DISCUSSION

Given the fact that *M. smegmatis* possesses ~6500 genes, approximately 25% of the genes were, supposedly, disrupted from a pool of approximately 70,000 possible mariner insertion sites in a typical mycobacterial chromosome (Gao *et al*., 2003a). The transposon insertion *M. smegmatis* mc^2155 mutant library had been successfully developed according to the aim previously established, since the method used biased the results towards the selection of mutants where the genes disrupted were involved in cell wall biosynthesis. The majority of the mutants showed loss of cord formation pattern when were grown on plates, revealing the lack of a normal structural organisation in the cell wall due to the gene disruption.

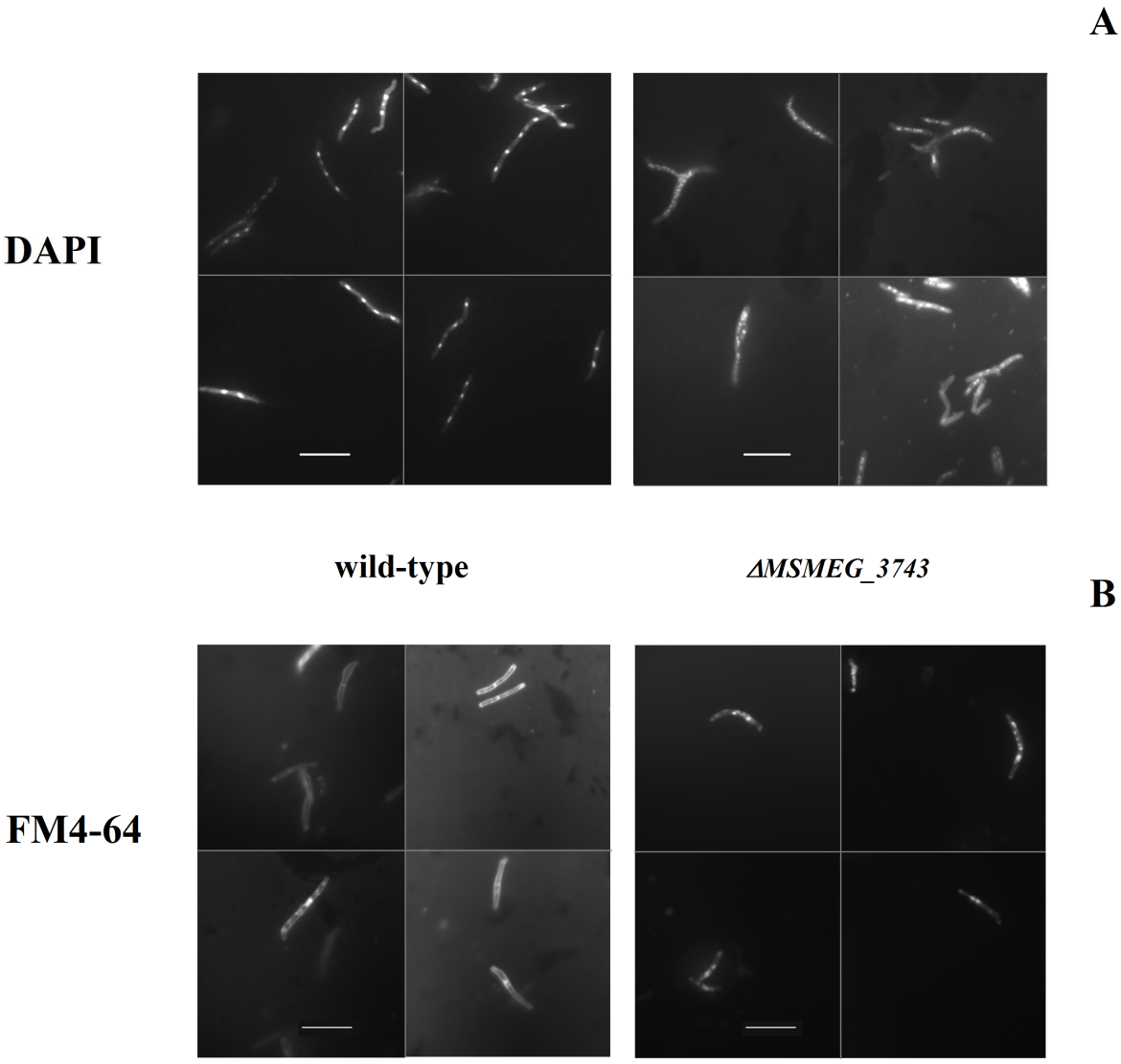

Figure 2.4: Fluorescence micrographs of *M. smegmatis* cells. Both wild-type and *ΔMSMEG_3743* strains were stained with (A) DAPI (DNA) and (B) FM4-64 (membrane). DAPI staining revealed aberrant DNA chromosome distribution and localisation in the mutant cytoplasm. Membrane staining showed an abnormal septa organisation (membrane aggregates) as result of the transposon disruption of *MSMEG_3743*, unlike the center-localised septa displayed by the wild-type cells. Scale bars: 2 μm.

Therefore, the selection of biofilm defective strains revealed colony morphology alterations and/or rifampicin sensitivity on plates, caused by the inactivation of genes mainly related to structural lipids metabolism and intermediate metabolism, but without changes in the lipid profile as it was expected from literature (Ojha *et al*., 2010) after losing the biofilm formation ability (*i.e*., loss of free mycolic acids or TDM pattern alteration). However, in the case of mutants who showed no alteration in lipids metabolism, changes could be related to slow growth or alterations in capsule or AG/LAM composition.

Fifteen Tn-mutant strains were identified and six out of them were annotated as genes related to cell wall biosynthesis or metabolism. Amongst them, *MSMEG_6387* encodes an arabinosyltransferase A termed *embC*, which along with its *M. tuberculosis* homolog *Rv3793*, have been extensively studied due to its role in the biosynthesis of the mycobacterial cell wall, since that it is essential for LAM synthesis and also as part of the *embCAB* operon whose the target of the ethambutol (EMB) (Telenti *et al*., 1997; Zhang *et al*., 2003; Alderwick *et al*., 2011). In contrast to the *Rv3793*, and as I have said in the introduction section, the Δ*MSMEG_6387* strain yields viable. Consistently with previous results (Escuyer *et al*., 2001) the changes in morphology and cell wall permeability were expected but not drastic, therefore the TLC lipid analysis of the mutant did not show differences compared to the wild-type strain since the gene is involved in LAM synthesis (Alderwick *et al*., 2011), whose disruption leads to a structural deficiency, altering colony morphology and also increasing permeability of the cell wall that could explain the sensitivity to rifampicin.

Another gene disrupted was *MSMEG_0408*, which encodes for a type-I polyketide synthase. A multi-domain fatty acid synthase-like enzyme that belongs to the polyketide

synthases (Pks) family, whose members are involved in complex fatty acyl components of the cell wall biosynthesis, such as glycopeptidolipids (GPL) in *Mycobacterium* genus (Tatham *et al*., 2012), surface-exposed lipooligosaccharides (LOS) in *M. smegmatis* (Etienne *et al*., 2005) or phthioceroldimycocerosates (PDIM) in *M. tuberculosis* (Jain and Cox, 2005). Therefore, polyketide synthases are related to virulence (Rousseau *et al*., 2003; Matsunaga *et al*., 2004; Astarie-Dequeker *et al*., 2009). It was not surprising that this mutant displayed the above-described characteristics as previous studies on *pks* genes have reported major alterations in the cell wall composition. The BLAST analysis of the protein sequence against the *M. tuberculosis* H37RV protein data base showed high scores for several polyketide synthases such as Pks7, Pks12 or Pks2, while the search for equivalent regions in both *M. smegmatis* and *M. tuberculosis* genomes did not show synteny. Moreover, TLC-analysis of the mutant strain did not reveal any detectable change in the lipid pattern compared to the wild-type strain. These apparently negative results are still consistent with previous reports, were the cell envelope of pks-mutant strain is similar to that of the wild-type strain, despite the altered phenotype displayed (Rousseau *et al*., 2003).

A group of genes related to lipid metabolism were disrupted. In first place, *MSMEG_0147* was found to have a potential link to the cell envelope. Its closest homolog has been described as a sterol desaturase related to membrane-sterols production in yeast, where the mutants showed increased permeability and sensitivity to antifungal drugs (Smith and Parks, 1993; Brumfield *et al*., 2010). Although no synteny with a *M. tuberculosis* cluster was found, the role of the *erg3* gene must be considered for further studies. Regarding the *ΔMSMEG_6599* mutant strain obtained, in *Mycobacterium avium*, a *luxR* gene have been described as regulator of several genes related to cell wall-associated

lipids, lipid metabolism and host cell invasion, thus controlling the envelope composition (Alonso-Hearn *et al*., 2010). In this case, the disrupted *luxR* gene contains a frame shift showing no *M. tuberculosis* homologous gene, then it is still possible to have a different biological effect over the same genes. On the other hand, even though *MSMEG_0472* has no homologs in *M. tuberculosis* and the cluster that belongs to showed no synteny, lipoproteins have shown to have a role in the composition and structure of the cell wall as well as in virulence (Crellin *et al*., 2008; Brülle *et al*., 2010). Finally, the acyltransferase gene is located downstream an ATP-dependent RNA-helicase of unknown function, more detailed study is necessary in order to elucidate the specific role it has, since rifampicin sensitivity was observed most likely as an increased permeability of the envelope.

Regarding the disrupted genes related to intermediary metabolism, previous screenings in *M. smegmatis* have shown that TCA cycle crucial enzymes are related to colony morphology alterations as a result of an impaired growth rate (Chen, 2010), and also crucial enzymes in glyoxylate metabolic pathway, both isocitrate lyase and malate synthase, have been previously reported as related in pathogenesis of *M. tuberculosis* (Muñoz-Elias and McKinney, 2005; Dunn *et al*., 2009; Quartararo and Blanchard, 2011). In this study, a transposon mutant strain was found carrying a disruption in the gene encoding for the oxalyl-CoA decarboxylase, an enzyme which is part of the glyoxylate cycle. Moreover, a disruption in *MSMEG_3641* was found, this gene encodes for a conserved hypothetical protein that is likely to be related to malate synthase expression. Then, further studies are necessary in order to elucidate the role of *MSMEG_3641* in the rifampicin sensitivity shown by the mutant and its link to the glyoxylate cycle.

The *MSMEG_4269* gene encondes for the AsnB protein that has been reported as protector factor against several antibiotics since the disruption of *asnB* gene increases the

sensitivity to drugs in *M. smegmatis*. The protein is the only putative asparagine synthetase present in the *Mycobacterium* genus, and yet the knockout strain does not seem to be an asparagine auxotroph (Ren and Liu, 2006). The *C. glutamicum* homolog *ltsA*, encodes a glutamine-dependent amidotransferase is related to the cell wall structure formation and in the L-glutamate production (Hirasawa, 2000). Interestingly, in this study, the colony morphology analysis also showed a change in the colony edges and rifampicin sensitivity when the strain was exposed to Tween. These facts, along with the high degree of synteny of the clusters found when compared with *M. tuberculosis*, suggest *asnB* gene as a good drug target. Due to the fact that the changes in the morphology can be the result of a slow growth rate instead of a structural or biochemical alteration in the cell wall, it was not surprising to have found no alterations in the lipid analysis. Nevertheless, AG, LAM and capsular components remained to be analysed.

The *ΔMSMEG_3743* mutant strain was chosen for further analysis due to the unique phenotype shown and the importance of the cell cycle control as a vital function, whose mechanisms still remain unknown. Normal wild-type strains of *M. smegmatis* stained to visualise the septum show a normal midcell septum with two segregated chromosomes (Errington *et al.*, 2003). In this study, the traits shown by the *MSMEG_3743* mutant indicated that the cell division process was severely delayed, since the strain exhibited an abnormal amount of nucleoids and also defective DNA segregation, suggesting a DNA structural scaffold role for the Soj- *Spo*OJ regulator protein protein, a ParA-like homologous (Jakimowicz *et al*., 2007; Maloney *et al*., 2009). The presence of multinucleoids or granules phenotypes could be just an effect of spotting cells at different cellular stages. The results showed that there is no functional redundancy between the *parA* homologous since the presence of two other ones does not rescue the cell from the altered

condition, this result was expected since the overexpression of each of them also produced DNA segregation defects and cell progression impairment, probably as the effect of the lack of an optimal ratio of ParB/ParA (Maloney *et al*., 2009). Nevertheless, recent studies have shown very similar segregation and DNA distribution patterns in *parA* knockout *M. smegmatis* cells, suggesting similar functions for both genes (Ginda *et al*., 2013). In this study, anucleate cells were not possible to be found in the mutant cells, as it could be expected from the literature (Bignell and Thomas, 2001). Complementation assay was attempted several times using the vector pMV261 without success, it is likely that the impaired partitioning function of the disrupted gene *MSMEG_3743* prevents the correct replication of the plasmid; therefore, I suggest performing the complementation assay using an integrative vector as pMV306 bearing the promoter of the gene in order to avoid the potential loss of the plasmid and to allow the transcription under native conditions.

The putative role in coordination and/or regulation of the cell cycle given to the ParA-like homolog shows it a potential candidate for drug target.

2.4 MATERIALS AND METHODS

2.4.1 Phages, bacterial strains and growth conditions

The bacterial strains, plasmids and bacteriophages used in this screening are listed in Table 2.2. *M. smegmatis* strain was grown in TSB liquid media containing, 0.05% Tween-80 (surfactant agent to avoid clumping effect of the lipid cell wall) and on TSB-1.5% agar plates at 37°C; *Escherichia coli* was grown in LB broth and on LB-1.5% agar plates at 37°C. Hygromycin B was added at concentrations of 50 or 100 μg/ml for *M. smegmatis* and 150 μg/ml for *E. coli*. The transposon is a mariner variant with a

hygromycin resistance cassette and carried an origin of replication in *E. coli* which allows the transposon along with the insertion site to be rescued from the genomic DNA, as a plasmid replicating in *E.coli C118* λpir, to be sequenced. High titre bacteriophage lysate was prepared as explained in the General Materials and Methods chapter (Larsen *et al*., 2007).

Table 2.2: Phages and bacterial strains used

Phage/ Bacteria	Genotype or description	Reference
Phage		
phAE181	Temperature-sensitive derivative of mycobacteriophage TM4 containing the Himar1-derived transposon Tn*5371*. Hyg^R	Rubin *et al*., 1999 Kriakov *et al*., 2003
Bacteria		
Escherichia coli CC118λpir	CC118 lysogenized with λpir phage	Manoil and Beckwith, 1985 Herrero *et al*., 1990
Mycobacterium smegmatis mc^2155	Parental strain, *ept-1* mutation conferring high efficiency of plasmid transformation	Snapper *et al*., 1990

2.4.2 Transposon mutagenesis and isolation of mutants

M. smegmatis culture was grown in 50 ml of TSB-0.05% Tween-80 to an OD_{600} value of 1. Tween is a non-ionic surfactant added as an emulsifier between the liquid media and the lipidic surface of the cells. The cells were harvested by centrifugation at room temperature, washed twice with 50 ml MP buffer (50 mM Tris/HCl pH 7.6, 150 mM NaCl, 10 mM MgCl2 and 2 mM CaCl2) and then resuspended in 1ml of MP buffer. An aliquote of 0.5 ml was mixed with high titre phage lysate 10^{10} to 10^{11} pfu/ml at a

multiplicity of infection (MOI) of 10, a control sample was prepared adding 0.5 ml of MP buffer instead. After incubation at 37°C for 3 hours without agitation, the cells were harvested and resuspended in 1 ml TSB plus 0.05% Tween-80. Cells were recovered at 37°C overnight, plated on TSB-Hyg_{50} agar and then incubated at 37°C for 4 to 5 days.

Hygromycin resistant strains were selected and inoculated in 96-well plates containing TSB-Hyg_{100} media without Tween-80 in order to allow the biofilm pellicle formation. Rifampicin increased sensitivity was tested by plating on TSB-agar plates with and without rifampicin by using a spike replicator from cultures grown in 96-well plates and incubated at 37°C for 4-5 days, the concentrations of antibiotic used were 5 and 7.5 μg/ml (from stock solutions 50 mg/ml dissolved in dimethyl sulfoxide) which were lower than the 30 μg/ml previously reported for *M. smegmatis* mc^2155 (Chakravorty *et al*., 2008), additionally, a MIC of 20 μg/ml was obtained for the wild type strain used in this study. The hygromycin resistant colonies showing loss of the biofilm pellicle formation in 96-well plates, defective colony morphology or rifampicin sensitivity were selected for sequencing and further analysis. Selected strains were grown until late-log phase in TSB-broth containing 0.05% Tween-80 in order to observe cording and colony morphology. For cording, 1 ml of culture was spun for 10 s to remove cell aggregates, 10 μl were loaded on microscope slides, air-dried out and observed at magnification 1000x using immersion oil; colony morphology was observed on TSB-agar plates plating 10 μl drops of serial dilutions (10^{-2} to 10^{-6}) and also streaking agar plates in order to obtain single colonies.

2.4.3 Isolation and sequencing of transposon insertion sites

Genomic DNA was extracted from the transposon mutant strains (see General Materials and Methods chapter), digested with *BssHII* and then ligated with T4 ligase. The

resulting ligated fragments were used to transform *E. coli* CC118λpir by heat shock procedure and selecting the self-ligated fragments that contained the Tn*5371* with the hygromycin cassette and the R6K ori. The colonies resistant to hygromycin were inoculated into LB broth with hygromycin to obtain plasmid DNA that was sequenced using the primers marinerKMN1 (Tn5371-L) 5'-AGTGCCACCTAAATTGTAAGC-3' and marinerHyg (Tn5371-R) 5'-TAGACAGATCGCTGAGATAGG-3' to obtain the sequences of the regions flanking the insertions. Since the disruption of the gene by the transposon includes the insertion of a hygromycin resistance cassette, the RNA transcription of the disrupted genes was not checked by RT-PCR or any other method. Downstream effects of the disruptions were expected for genes forming part of an operon.

2.4.4 Fluorescence microscopy

M. smegmatis mc^2155 10 ml culture was grown to stationary-phase in tryptic soy broth at 37ºC and agitation. The cells were collected by centrifugation. Prior to DAPI staining, the cells were permeabilized by exposure to toluene 0.3% for 20 min at 37ºC and then washed twice in phosphate-buffered saline PBS (10 mM sodium phosphate, 150 mM NaCl, 15 mM KCl, pH 7.4). Vectashield® containing DAPI 1.5 µg/ml was added and incubated for 20 min. For membrane visualisation, the cells were incubated with the membrane dye, FM4-64 at a final concentration of 0.5 µg/ml for 1h and 10 µl of sample were mounted on poly-L-lysine coated slides.

The cells were visualized by brightfield and fluorescence microscopy using a Nikon Eclipse TE-300 microscope, capture and image analysis was conducted using Analysis (Olympus) and a Nikon super high-pressure mercury lamp. A Nikon filter set

(Ex528-553/Em600-660) was used for FM4-64 stained cells and DAPI-stained cells were imaged with a standard DAPI filter set (Ex325-375/Em435-485).

CHAPTER 3

ADDRESSING THE ROLE OF MMPL GENES IN MYCOLIC ACID METABOLISM IN MYCOBACTERIA AND CORYNEBACTERIA

3.1 INTRODUCTION

Mycolic acids (MA) are major cell wall components of the genus *Mycobacterium* and are required for viability and virulence (Bhatt *et al*., 2005, 2007; Dubnau *et al*., 2000; Glickman *et al*., 2000; Vilchèze *et al*., 2000). As discussed in Chapter One, MA are very long chain α-alkyl, β-hydroxy fatty acids (C60 to C90) that can be found associated with the cell wall in two different ways: 1) Covalently attached to arabinogalactan (AG) which is also bound to the peptidoglycan of the cell wall by phosphodiester bond on the internal region of the outer membrane and 2) Present as a part of the interspersed glycolipids in the form of simple monomycolyl glycerol (MMG), glucose monomycolate (GMM), trehalose monomycolate (TMM) and trehalose dimycolate (TDM) (Besra *et al*. 1994; Andersen *et al*., 2009).

MA confer important features to mycobacteria, which include resistance to chemicals such as hydrophobic antibiotics and dryness, low permeability of the cell wall, the ability to stain acid-fast and form biofilms. In *Mycobacterium tuberculosis*, mycolates are also critical for virulence and the persistance inside the host (Daffé and Draper, 1998; Yuan *et al*., 1998; Dubnau *et al*., 2000; Glickman *et al*., 2000; Ojha *et al*., 2005; Bhatt *et al*., 2007). Moreover, chain modifications such as cyclopropane rings, keto and methoxy groups play an important role in immunomodulation since mutant strains that exhibit altered MA subtypes have shown hypersusceptibility to the host immune response, alterations in cell wall permeability and also resulted in virulence attenuation (Glickman *et al*., 2000; Rao *et al*., 2005, 2006; Bhatt *et al*., 2007).

In mycobacteria, the biosynthetic pathway of MA involves two enzymatic systems. The type-I fatty acid synthetase (FAS-I), a multidomain peptide found in eukaryotes

(mammals and fungi) and prokaryotes; and also the type-II fatty acid synthetase (FAS-II), which is found in plants and bacteria. The FAS-I synthase, who also provides the fatty acids for phospholipids, synthesises the precursors for MA elongating a growing fatty acid chain by two-carbon units, using acetyl-CoA and malonyl-CoA as substrates to produce C16 and C26 fatty acids. The C16 acyl-CoA is the precursor for the production of meromycolic acids via FAS-II elongations where a protein called FabH acts as the link between the two systems by catalysing the condensation of the FAS-I-derived acyl-CoAs with malonyl-acyl carrier protein (ACP) (Choi *et al*., 2000; Brown *et al*., 2005, 2007). The product of the condensation is then incorporated by FAS-II as a substrate for the synthesis of the very long mero chain of α-, methoxy- and keto- mycolic acids while the C26 fatty acid unit corresponds to the short α-branch of the resulting MA. The latter steps involve four enzymes that act successively elongating the fatty acid to meromycolates (C56), the condensing KasA and KasB, the keto-reductase MabA, the hydroxyacyl-dehydratase and the enoyl-reductase InhA. The final step is catalysed by the polyketide synthase Pks13, which condensates the α-branch and the meromycolate to produce MA (Quemard *et al*., 1995; Schaeffer *et al*., 2001; Kremer *et al*., 2002; Gande *et al*., 2004; Portevin *et al*., 2004; Takayama *et al*., 2005; Bhatt *et al*., 2007; Brown *et al*., 2007).

Although steps implicated in the biosynthesis of MA have been described, the components that are involved in mycolate transport and deposition in the cell wall still remain unidentified. A hypothetical pathway has been proposed that involves the transfer of a mature mycolate to an isoprenoid carrier, forming MycPL (6-O-mycolyl-β-D-mannopyranosyl-monophospho-heptaprenol) (Besra *et al*., 1994), and subsequently to trehalose inside the cell to yield TMM (Takayama *et al*., 2005). TMM is then proposed to be transported by a yet unknown mechanism outside the cell, where it is the substrate of

the mycolyltransferases of the Ag85 complex (Belisle *et al*., 1997; Puech *et al*., 2002), transfering the mycolate unit to either the AG complex, or to another TMM resulting in formation of TDM (Fig. 3.1). Alternatives to this hypothetical pathway may involve intracellular synthesis of TDM prior to transport, or the flipping of Myc-PL outside the cell to be used as substrate for extracellular formation of TMM.

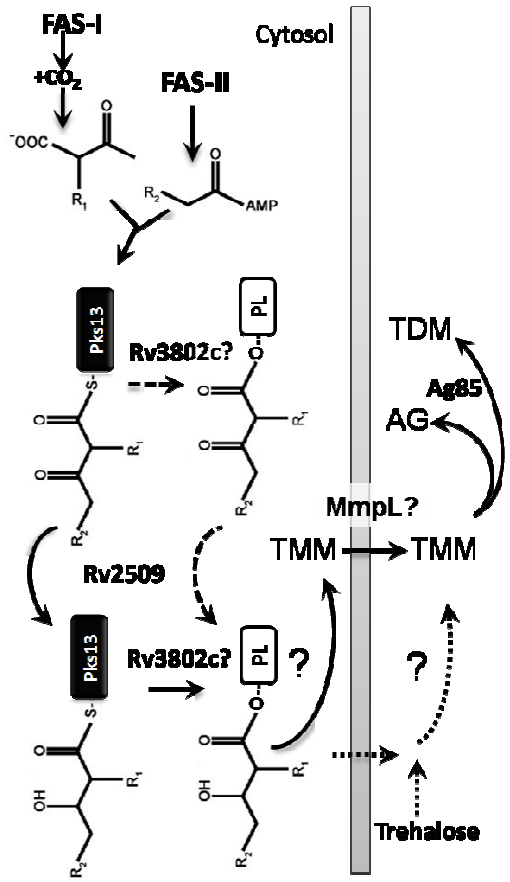

Figure 3.1: Schematic diagram of putative steps in MA biosynthesis and transport in *M. tuberculosis.* Hypothetical pathway proposed by Takayama *et al*., 2005. Inside the cell, a mature mycolate would be transferred to a carrier (PL: mannophospho-heptaprenol) and subsequently to trehalose to yield TMM, which would be transported outside by an unknown mechanism. Alternative steps are shown by hatched or dotted arrows and also genes involved are indicated; ?: unknown steps.

As it is clear from the literature already cited, the MA metabolism is critical for viability and virulence, therefore the understanding of MA transport will open new options for discovering targets and developing new drugs against it. In this chapter, I describe the potential role of a class of transmembrane (TM) proteins, designated MmpL (mycobacterial membrane protein large), as the transporter of MA in mycobacteria.

The genomes of *M. tuberculosis* H37Rv and other mycobacteria contain genes encoding proteins that belong to a family of multidrug resistance pumps called RND

proteins (resistance, nodulation, and division), normally contain 12 TM domains and two non-TM loops (Cole *et al*., 1998; Domenech *et al*., 2005). Due to the efflux pump nature of MmpL proteins, the genes encoding them have become of high interest to understand drug-resistance mechanisms; nevertheless, only MmpL5 has been hypothetically described as a drug-efflux system for azoles, clofazimine and bedaquiline, where a transcriptional regulator encoded by *Rv0678* has been shown to be implicated in resistance to the compounds via upregulation of *mmpL5* in *M. tuberculosis* (Milano *et al*., 2009; Hartkoorn *et al*., 2014). So far, none of the other mycobacterial MmpLs studied appears to play any role in drug resistance even though when some of them have shown to share transcriptional regulation systems with *mmpL5*, like in the case of *mmpL2* and *mmpL4* (Radhakrishnan *et al*., 2014). In fact, recently, *mmpL4* and *mmpL5* have been described as part of an novel siderophore export system which is essential in the virulence of *M. tuberculosis* (Wells *et al*., 2013). The gene *mmpL7* conferred resistance to isoniazid when overexpressed in *Mycobacterium smegmatis* but the *M. tuberculosis mmpL7* mutant did not display altered sensitivity to the drug (Pasca *et al*., 2005). Instead, many *mmpL* genes are associated with clusters involved in the biosynthesis of cell wall-associated glycolipids like sulfolipids, polyacylated trehalose (PAT), glycopeptidolipids, lipooligosaccharides and other complex lipids like phthiocerol dimycocerosate (PDIM) where they are required as scaffolds for the biosynthetic machinery, allowing localized synthesis of a cell wall associated lipid together with ABC-transporter or smaller MmpS protein to facilitate transport (Cole *et al*., 1998; Converse *et al*., 2003; Cox *et al*., 1999; Domenech *et al*., 2004, 2005; Sondén *et al*., 2005; Deshayes *et al*., 2010; Rombouts *et al*., 2011). In the case of PDIM biosynthesis, a two hybrid screening using the non-TM domains of the PDIM transporter MmpL7 revealed interactions with enzymes implicated in later stages of biosynthesis of the phthiocerol

moiety (Jain and Cox, 2005). On the other hand, MmpL8 has been found involved in sulfolipid SL-1 biosynthesis as part of a protein complex that translocates either the final lipid or an intermediate to the extracytoplasmic side (Converse *et al*., 2003; Domenech *et al*., 2004), as well as the case of MmpL10, whose function has been associated to diacyltrehalose/polyacyltrehalose (DAT/PAT) biosynthesis (Rodríguez *et al*., 2013).

Given that MmpLs proteins are predominantly involved in the transport of different glycolipids, it seemed likely that one of them could also be involved in the translocation of a mycolate-containing glycolipid such as TMM, TDM, or Myc-PL to the outside of the bacterial cell for subsequent use as a substrate for cell wall mycolylation.

Mycobacterium leprae, contains a high degree of genetic decay and has an intact cell wall containing MA, therefore, it is a valuable organism to use when considering essential candidate genes for functions related to the cell wall, like MA metabolism. Only five out of fourteen homologs of *mmpL* genes from *M. tuberculosis* are present in *M. leprae*, where only *mmpL3* was predicted to be an essential gene (Domenech *et al*., 2005). Due to the essentiality of MA for viability of mycobacteria (Vilchèze *et al*., 2000; Portevin *et al*., 2004; Bhatt *et al*., 2005; Parish *et al*., 2007), it was likely that *mmpL3* was involved in mycolate transport in *M. tuberculosis*.

In this study, I have investigated the role of *mmpL3* in MA transport and biosynthesis by generating and characterising a conditional mutant of *MSMEG_0250*, the homolog of the *M. tuberculosis mmpL3* (*Rv0206c*) in the fast growing and non-pathogenic *M. smegmatis*. In parallel, to overcome the complications of gene essentiality, I also compared and contrasted the potential role of *mmpL* genes in mycolate transport in *Corynebacterium glutamicum*. In this organism, the MA biosynthesis associated genes are not essential and thus viable mycolate-less mutants can be generated. Its cell wall is similar

to mycobacteria but with a less complex structure and composition level since corynebacteria only synthesises trehalose monocorynomycolates (TMCM) and trehalose dicorynomycolates (TDCM) as extractable lipids, apart from the membrane inserted lipoglycans. For instance, members of the genus *Corynebacterium* has been previously used as model for the study of MA metabolism and a mutant for an ABC-transporter produces altered mycolates as an indirect effect of an impaired lipoglycan biosynthesis (Mishra *et al*., 2008; Wang *et al*., 2006).

In this context, a complete characterisation of the strains was performed in order to probe the role of the *mmpL* genes in the MA biosynthesis.

3.2 RESULTS

3.2.1 *mmpL3* is an essential gene in mycobacteria

In *M. tuberculosis*, *mmpL3* was first proposed to be an essential gene by Domenech *et al*. (2005) on the basis of the inability to obtain an *mmpL3* knockout mutant. While the gene is not located near any known MA biosynthesis gene, the gene cluster surrounding *mmpL3* shows a high level of synteny with other mycobacterial species including *M. leprae*. This includes the presence of three putative membrane associated proteins and a second *mmpL* gene, *mmpL11*, situated downstream of *mmpL3* (Fig. 3.2), whose mutant strain have been reported as attenuated in the mouse model of infection by Domenech *et al*. (2005), on the other hand, the *M. smegmatis* mutant strain has shown reduced membrane permeability and also altered biofilm formation (Purdy *et al*., 2009; Pacheco *et al*., 2013).

A knockout phage was designed to delete *MSMEG_0250*, the *M. smegmatis* homolog of *mmpL3*, and consistently with findings from previous studies (Domenech *et al*., 2005) it was not possible to generate a null mutant.

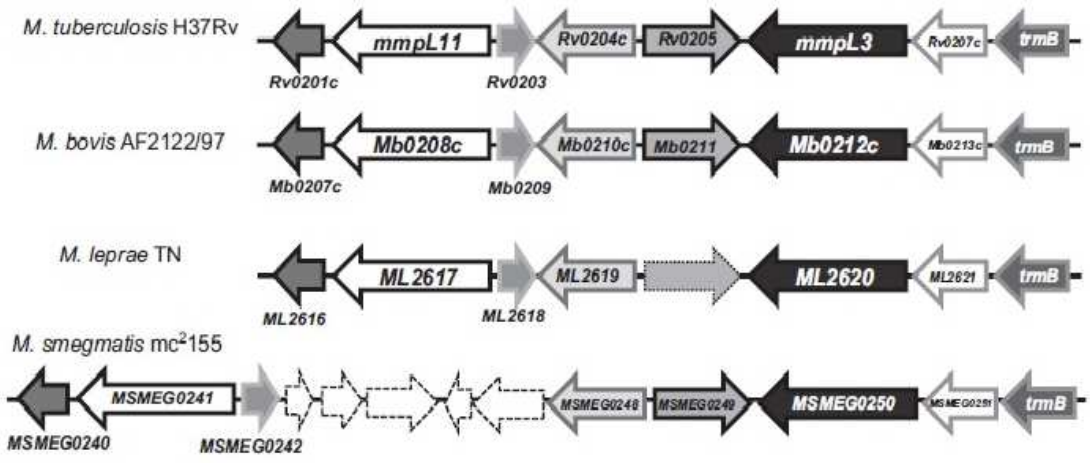

Figure 3.2: Map of the *mmpL3-mmpL11* region in different mycobacteria genomes. Homologous genes are indicated by similar arrows. Hatched borders indicate genes found exclusively in *M. smegmatis* and a pseudogene in *M. leprae* is depicted by a dotted border arrow (Varela *et al*., 2012. License Nº 3244880310622).

Subsequently, CESTET (Conditional expression–specialized transduction essentiality test), a tool designed to test gene essentiality in *M. smegmatis*, was used to obtain a conditional mutant of the gene *MSMEG_0250* (Fig. 3.3). The technique consists in the generation of a merodiploid strain carrying a second copy of a putative essential gene under the control of the acetamidase promoter, the replacement of the target gene with a selection marker using a phage that contains an allelic-exchange substrate and finally the growth of the strain in the presence or absence of acetamide (Bhatt *et al*., 2005; Bhatt and Jacobs, 2009).

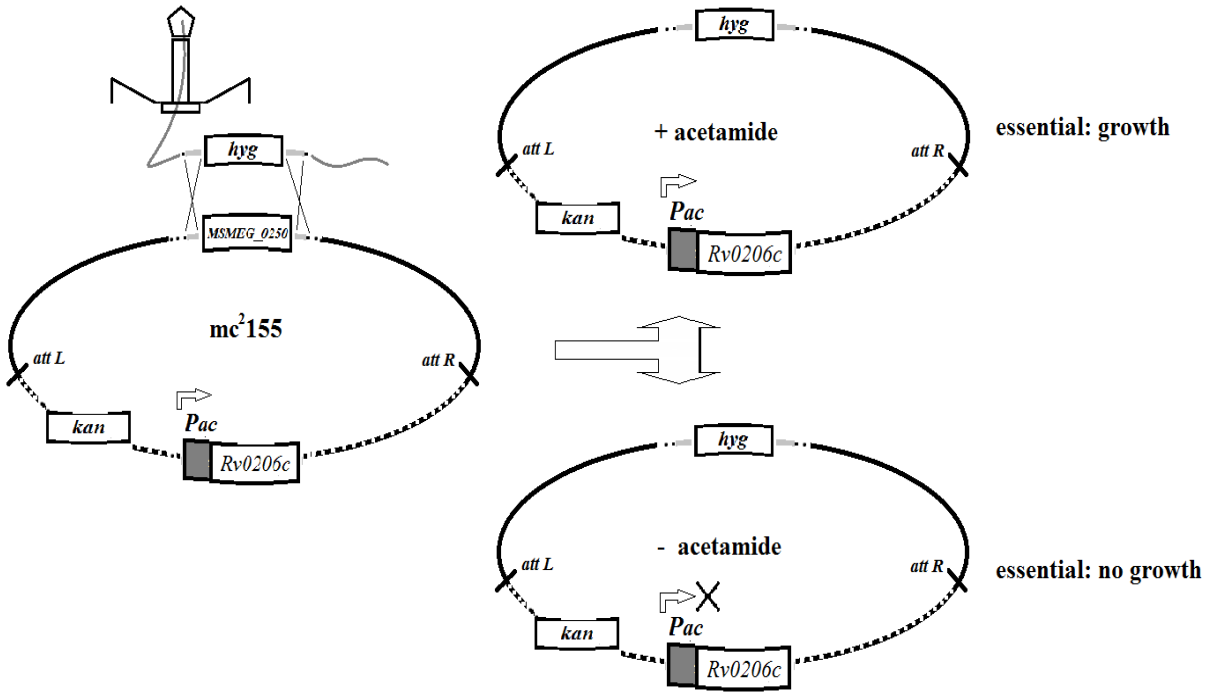

Figure 3.3: Schematic diagram of CESTET in *Mycobacterium smegmatis* mc²155. Left side: The recombinant phage is transduced into a merodiploid strain and homologous recombination produces allelic exchange deleting the native copy of the putative essential gene (*MSMEG_0250*). Right side: The transductants strains are selected on hygromycin-containing medium with or without acetamide. When the gene tested is essential the growth is only observed on plates containing acetamide. *kan* and *hyg* resistance cassettes; Pac, inducible acetamidase promoter; dotted and solid arcs represent the integrative vector and the mc²155 chromosome, respectively. Adapted from Bhatt and Jacobs, 2009.

In this study, the strain *ΔMSMEG_0250* was constructed containing a recombinant, integrated copy of *mmpL3* under the control of the inducible acetamidase promoter, while the native copy of the gene was replaced with a hygromycin resistance cassette, the strains generated were confirmed by Southern and used in the study. They were spotted in two different agar-plates with and without acetamide, showing that the viability of *ΔMSMEG_0250* was dependent on the addition of the inducer in the growth medium, confirming that *MSMEG_0250* was an essential gene (Fig. 3.4). Growth analysis in liquid

media was not performed since the conditional mutant lysis in absence of acetamide was clearly easy observed after the depletion of the remaining MmpL3 protein.

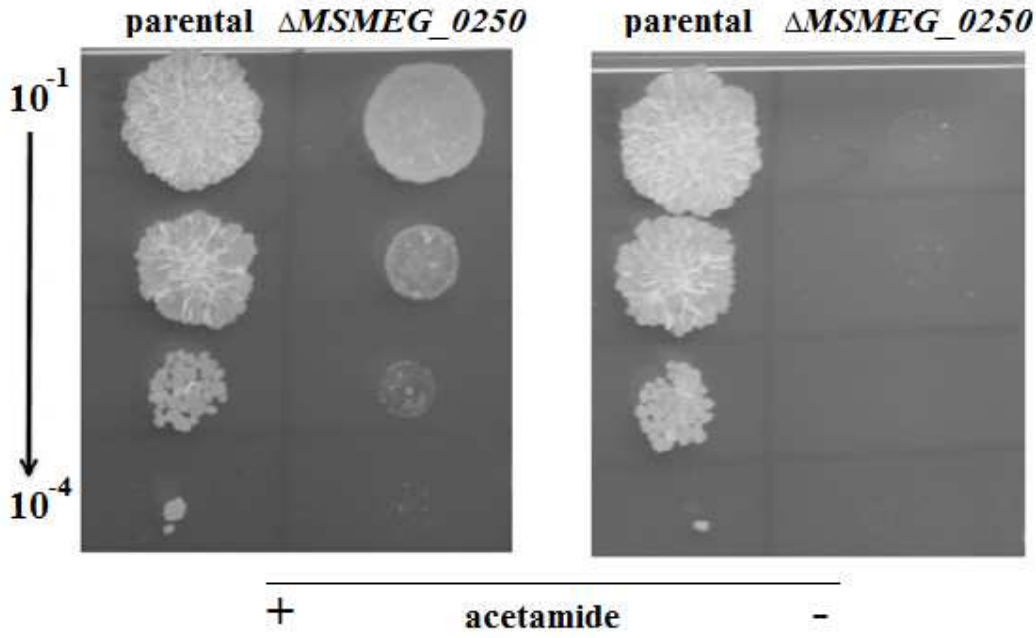

Figure 3.4: Essentiality of *MSMEG_0250* in *M. smegmatis* mc^{2}155. Growth of the conditional mutant Δ*MSMEG_0250* and parental merodiploid strain (mc^{2}155::pMV306-*mmpL3*) on TSB-agar with or without the inducer acetamide. 10 µl of 10-fold serial dilutions of cultures were spotted on the agar plates and incubated for 5 days at 37ºC. (Varela *et al*., 2012. License Nº 3244880310622).

3.2.2 MmpL3 is involved in mycolic acid transport in mycobacteria

In order to address the putative role of MmpL3 in MA transport, the effects of depletion of *MSMEG_0250* on lipid metabolism in the *M. smegmatis* conditional mutant were tested. Cultures of the Δ*MSMEG_0250* conditional mutant were grown in broth in the presence or absence of acetamide and labelled with [^{14}C]-acetate at different time points. Using a three stage extraction procedure the lipids were collected and analysed as follows: 1) Petroleum ether extraction of the cell pellet not affecting the integrity of the cells, but extracting the surface-exposed, noncovalently bound cell wall lipids; 2) Extraction of

apolar and polar lipids from the previously treated pellet; and 3) Extraction of AG-bound mycolic acids from the resultant delipidated cells. For cultures grown in the presence of acetamide, TMM was predominantly found in the apolar lipid extract from cell pellets and TDM in both the petroleum ether extract and in the apolar lipid extract. Nevertheless, an earlier examination performed using *M. smegmatis* cell pellets extracted with consecutive treatments of petroleum ether, indicated that no further TDM was extracted from cells after the third consecutive extraction. Each petroleum ether extract of the *ΔMSMEG_0250* conditional mutant represent a pool of five consecutive extractions of the same sample and thus the presence of TDM in the subsequently processed cell pellet was not due to insufficient petroleum ether extraction. The exact location of these cell-associated TDM molecules that resist petroleum ether extraction is unknown, but it is possible that they represent newly synthesized TDM that is closer to the inner membrane and thus inaccessible to petroleum ether extraction. In contrast to the cultures of the conditional mutant grown in the presence of acetamide, [^{14}C]-labeled cultures grown in the absence of acetamide showed an increasing amount of TMM in cell pellets, which was accompanied by decrease in TDM levels both in the petroleum ether extracts and in the apolar fraction from cells. Conditional depletion of *MSMEG_0250* also resulted in a decrease in mycolylation of AG. The accumulation of TMM in the cells over time following conditional depletion suggested that loss of *MSMEG_0250* function affected TMM transport either directly or indirectly (Fig. 3.5).

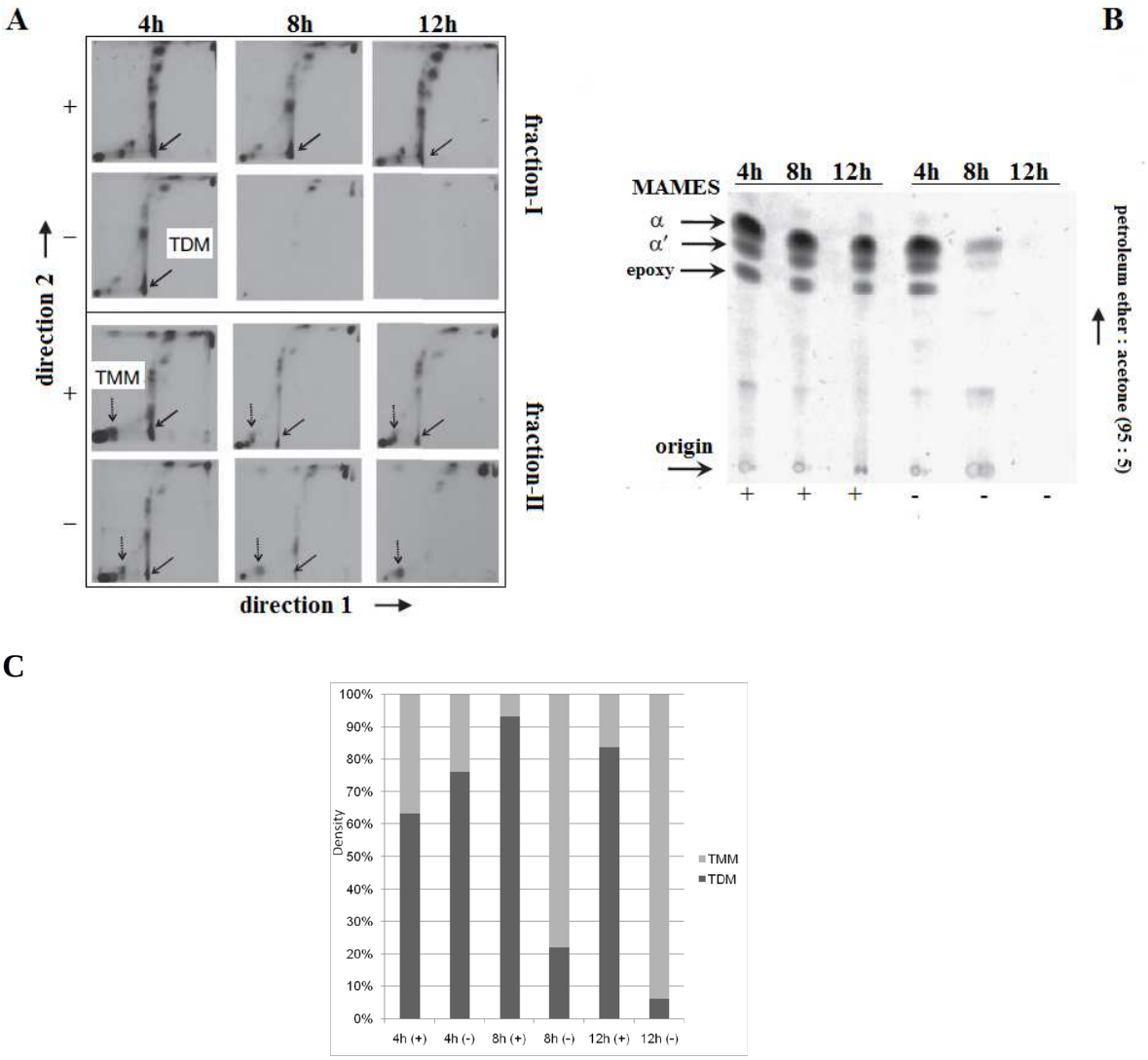

Figure 3.5: Lipid analysis of the *ΔMSMEG_0250* conditional mutant.
Cultures were grown and labeled in TSB, (–) or (+) acetamide and the samples were collected at the indicated times.
(A) 2D-TLC analysis of [^{14}C]-labelled lipids from *ΔMSMEG_0250* strain. Fraction-I: petroleum ether extracts; Fraction-II: intracellular apolar lipids. Fractions were separated in two directions, Direction 1 using chloroform:methanol:water (100:14:0.8) and Direction 2 using chloroform:acetone:methanol:water (50:60:2.5:3). TMM and TDM are indicated by dotted and solid arrows, respectively.
(B) TLC analysis of methyl esters of [^{14}C]-labelled cell wall bound mycolic acids. MAMES were separated using petroleum ether:acetone (95:5) as the solvent system. Methyl esters of the different subclasses of mycolic acids are indicated by arrows as well as the origin and the direction of the moving phase.
(C) TMM and TDM levels (%) from TLC (A) measured by densitometry. (-) and (+): acetamide (Figure by A. Singh).
(Varela *et al*., 2012. License Nº 3244880310622)

3.2.3 Bioinformatic analysis of potential *mmpL* genes in corynebacteria

As it was previously described, the cell wall of corynebacteria is similar to the cell wall of mycobacteria, containing TMCM and TDCM as the outer non-covalently bounds glycolipids. Due to the existing similarities, a parallel study in corynomycolate biosynthesis was conducted, also assuming that an MmpL-like protein was involved in its transport. Therefore, using the BLAST, a search in the *C. glutamicum* genome was carried out in order to find *mmpL* genes, with the amino acid sequence of the *M. tuberculosis*-MmpL3 protein as a query sequence. Additionally, a cluster analysis was performed, comparing the *C. glutamicum* genome with the *mmpL3-mmpL11* region from *M. tuberculosis* as query sequence using the MycoDB database.

The *C. glutamicum* ATCC13032 genome was found to contain four *mmpL*-like genes, including *NCgl0228, NCgl0599, NCgl0887 and NCgl2769*. BLAST results details were *NCgl0228*: Id 25%, E=5e-47; *NCgl0887*: Id 37% and 25% for the main alignment segments and E=4e-30 for the whole sequence; and *NCgl2769*: Id 43% E=8e-159. On the other hand, the search revealed that there is no corynebacterial region equivalent to the mycobacterial *mmpL3-mmpL11* cluster. Although, *NCgl0887* is situated in a cluster that contains *NCgl0885*, a putative trehalose corynomycolyl transferase; while *NCgl2769* is present downstream of the corynomycolate condensase gene, *pks13* (which encodes Pks13, the enzyme catalysing the condensation of the meromycolate and α-chains) and two putative esterases genes: *NCgl2777* and *NCgl2779* (Fig. 3.6). Given both, the genetic context of *NCgl0887* and *NCgl2769*, and the far lesser complexity of the cell wall of *C. glutamicum*, it was likely that any of these three *mmpL* genes were involved in TMCM/mycolate processing and transport. The gene *NCgl0599* has been previously found

related with a cluster of a carotenoid/lycopene pigment biosynthesis, thus was not consider for this study (Krubasik *et al*., 2001).

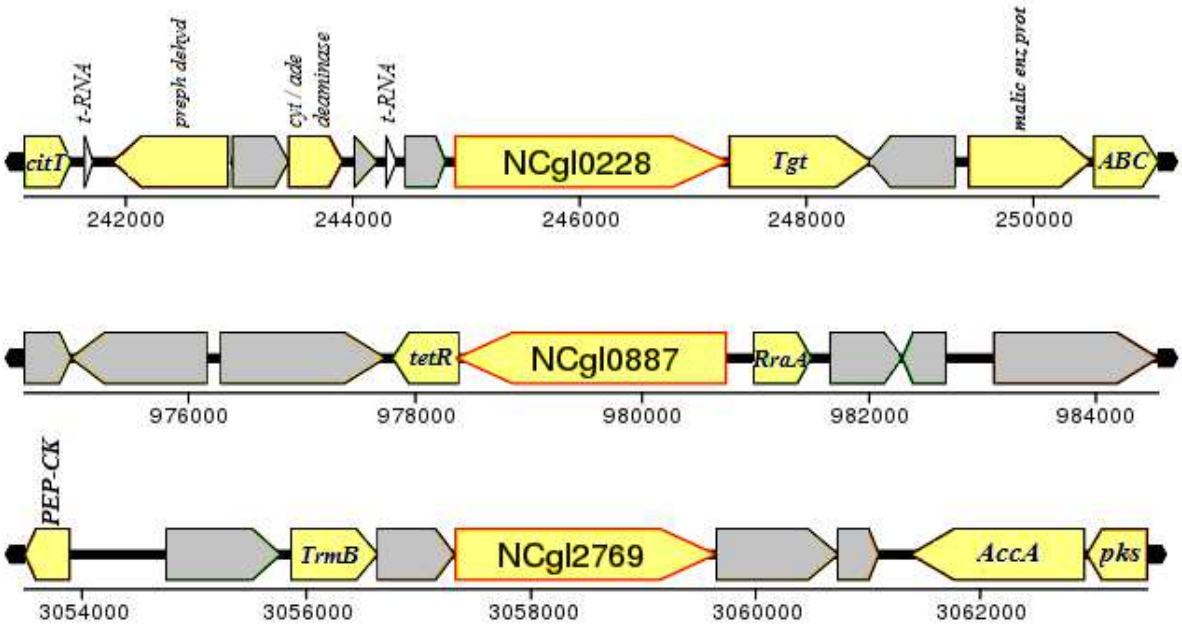

Figure 3.6: Diagrammatic representation of the genomic map of the putative *mmpL* genes of *Corynebacterium glutamicum* ATCC 13032. The regions surrounding the three RND superfamily drug-exporter genes do not show synteny unlike it was seen for the *Mycobacterium* genus region *mmpL3-mmpL11*. Grey boxes indicate genes encoding for hypothetical proteins. Fragment size: 10kb.

A topology prediction was carried out using the MmpL3 sequence showing that the protein contains 12 TM domains and 2 non-TM loops, named L1 and L2 of sizes 151 and 142 amino acids, respectively. On the other hand, *in silico* analysis of the MmpL3-like amino acid sequences showed a similar topology with both loops and TM-domains present as well. *NCgl0228* and *NCgl2769* amino acid sequences revealed predicted topologies similar to the *M. tuberculosis*-MmpL3 (12 TM domains and two non-TM loops), while *NCgl0887* predicted topology was 11 TM and the L1-loop facing the cytoplasm. The non-TM loops could be, potentially, involved in interactions with the mycolic acid biosynthesis machinery. (Fig. 3.7).

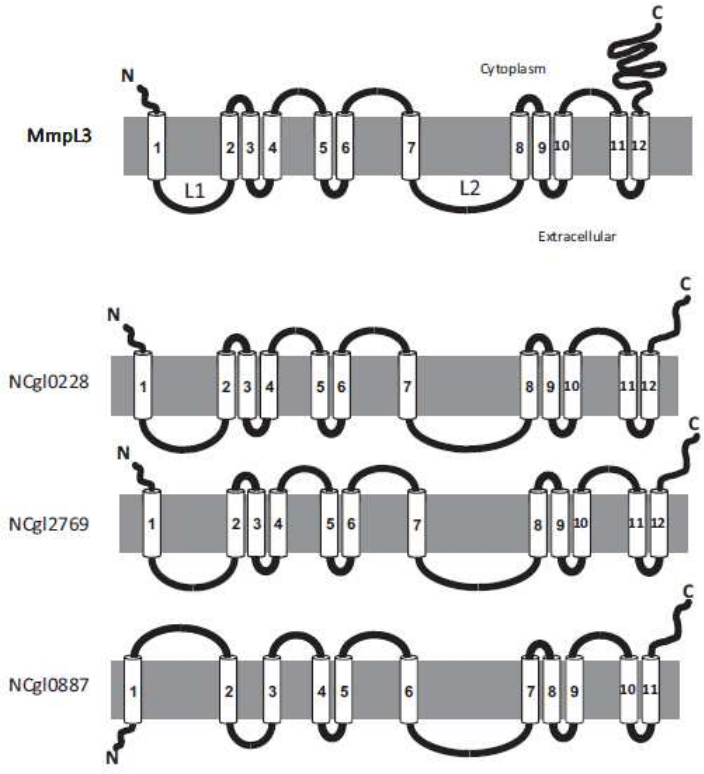

Figure 3.7: Predicted topology of MmpL3 and corynebacterial MmpLs. TM regions are indicated by cylinders and are numbered while the non-TM loops of MmpL3 are indicated as L1 and L2. The carboxy- and amino- termini are indicated by C and N, respectively. Topology predictions were done using the Mobyle@Pasteur server and the TopPredII tool. (Varela *et al*., 2012. License Nº 3244880310622).

3.2.4 Redundant *mmpL* functions in *Corynebacterium glutamicum*

As corynomycolic acid biosynthesis is a non-essential process, it is possible to generate viable mutants of corynebacteria that do not produce corynomycolates and the loss of corynomycolic acids from the cell envelope results in poor growth rates leading to smaller colonies (Gande *et al*., 2004). To probe the role of *mmpL*s in corynomycolate transport, individual in-frame deletion mutants were generated for the genes *NCgl0228*, *NCgl0887,* and *NCgl2769* from *C. glutamicum* ATCC13032. None of the three mutant strains Δ*NCgl0228,* Δ*NCgl0887,* and Δ*NCgl2769* showed any alterations in colony size or appearance. To investigate potential functional redundancies between the three *C. glutamicum mmpL* genes, double and triple mutant strains were constructed. While the

colony sizes and appearance of the double mutants, Δ*NCgl0228*-Δ*NCgl0887* and Δ*NCgl0887*-Δ*NCgl2769*, remained unaltered, the Δ*NCgl0228*-Δ*NCgl2769* mutant formed smaller colonies and showed clumpy pattern growth in broth. A similar growth defect was observed for the triple mutant Δ*NCgl0228*-Δ*NCgl0887*-Δ*NCgl2769*. Thus, while single deletions of *NCgl0228* or *NCgl2769* did not have any effect, the concurrent loss of *NCgl0228* and *NCgl2769* severely affected the growth patterns of the mutant strain, indicating potential alterations in the cell wall (Fig.3.8).

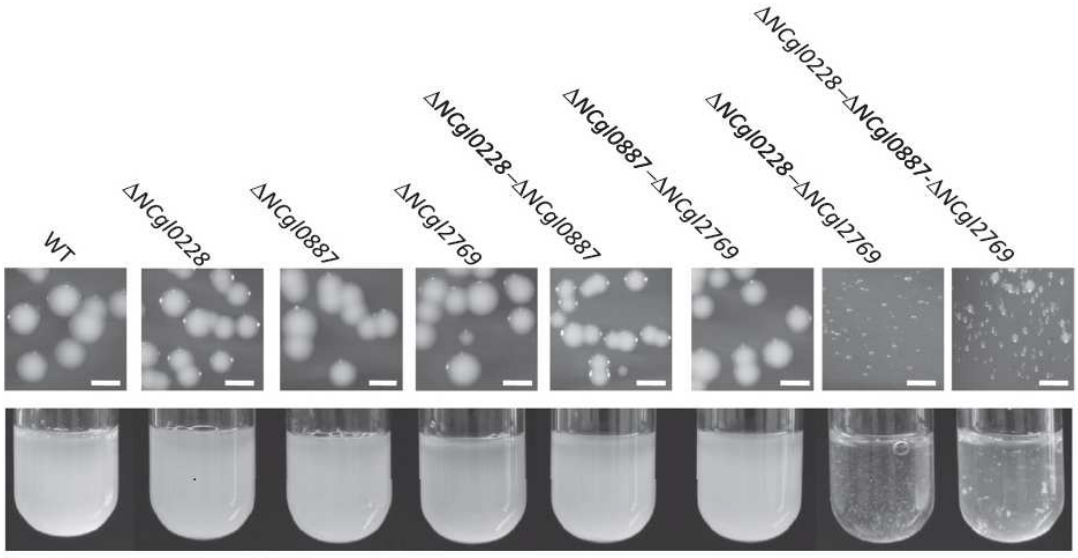

Figure 3.8: Growth characteristics of the *C. glutamicum mmpL*-mutants. Strains were grown at 30ºC using BHI media (agar plates and broth cultures). The pictures show healthy strains when at least one of *NCgl0228* and *NCgl2769* genes is present; on the other hand, the mutation of both genes severely impaires the grown in liquid and solid media as shown in the last two strains on the right. Healthy strains were incubated for 48 h, while the defective ones were incubated for 5 days. Scale bar represents 1 mm. (Varela *et al*., 2012. License Nº 3244880310622).

3.2.5 *NCgl0228* and *NCgl2769* play a role in corynomycolate metabolism

To determine whether the altered growth phenotype observed for some of the *C. glutamicum mmpL* mutants were linked to defects in corynomycolate transport, petroleum ether extracts of surface exposed lipids, and subsequent, remaining total lipids were extracted from [^{14}C]-acetate-labelled cell pellets. TLC analysis showed that the parental

strain and most mutant strains produced TMCM and TDCM, with the latter found predominantly in the petroleum ether extracts containing surface-exposed lipids (Fig.3.9 A-B). Furthermore, levels of AG-bound corynomycolic acids for most mutant strains were the same as the parental, wild-type strain *C. glutamicum*. The two exceptions were the Δ*NCgl0228*-Δ*NCgl2769* and Δ*NCgl0228*-Δ*NCgl0887*-Δ*NCgl2769* mutant strains, in which no TMCM or TDCM were detected in the petroleum ether extracts or in the cell pellets. Additionally, no AG-bound corynomycolic acids were observed in the Δ*NCgl0228*-Δ*NCgl2769* and Δ*NCgl0228*-Δ*NCgl0887*-Δ*NCgl2769* strains (Fig.3.9 C). The absence of any TMCM, TDCM, and AG-bound corynomycolates suggested either that there was a complete cessation of corynomycolic acid biosynthesis in the double and triple mutants or that corynomycolates were being transported in an alternate (carrier-bound) form that was used as substrate for TMCM, TDCM, and AG-bound corynomycolate synthesis. However, the latter seemed less likely as no intermediates were seen to accumulate in the Δ*NCgl0228*-Δ*NCgl2769* and Δ*NCgl0228*-Δ*NCgl0887*-Δ*NCgl2769* mutants. These results also indicated a functional redundancy between *NCgl0228* and *NCgl2769* with regards to corynomycolate metabolism. No additional alterations in lipid profiles were observed in the triple mutant suggesting that *NCgl0887* did not play any apparent role. Complementation of the double mutant with either plasmid-borne *NCgl0228* or *NCgl2769* restored corynomycolate biosynthesis, though in case of the latter gene, the complementation was partial since neither TDCM nor TMCM appear clearly in the TLCs. In order to elucidate the presence of corynomycolates in that strain, the total lipids sample was purified using an anion exchange column which allows collecting apolar lipids fractions. The purification showed the presence of small amounts of both TDCM and TMCM as an effect of the complementation with pVWEx2-*NCgl2769* (Fig.3.10).

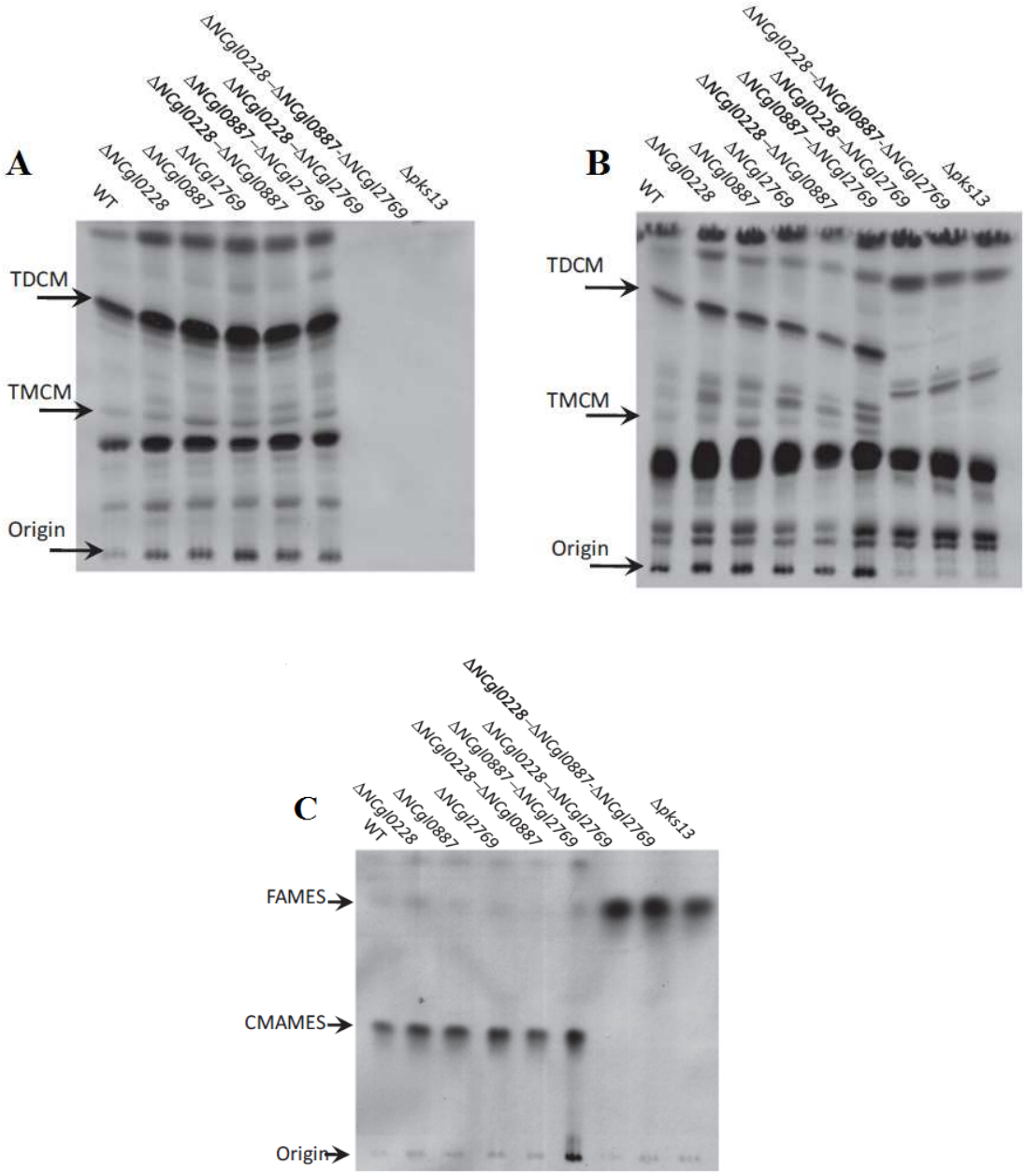

Figure 3.9: Lipid analysis of the *C. glutamicum* mmpL mutant strains.

A and B: TLC analysis of [^{14}C]-labelled lipids extracted from *C. glutamicum* mmpL mutant strains, using $CHCl_3$:CH_3OH:H_2O (60:16:2) as the solvent system. A: petroleum ether extracts, B: total lipids from petroleum ether-treated cells.
C: TLC analysis of [^{14}C]-labelled fatty acid methyl esters (FAMES) and corynomycolic acid methyl esters (CMAMES) extracted from delipidated cells, using petroleum ether:acetone (95:5) as the solvent system; *pks13* null mutant does not produce corynomycolic acids, was used as a control. The trend observed in panels A and B for the TDCM band correspond to an artifact produced by solvent who runs faster through the matrix on the extremes of the silica plate, the effect is increased due to the large width of the plate used (Varela *et al*., 2012. License Nº 3244880310622).

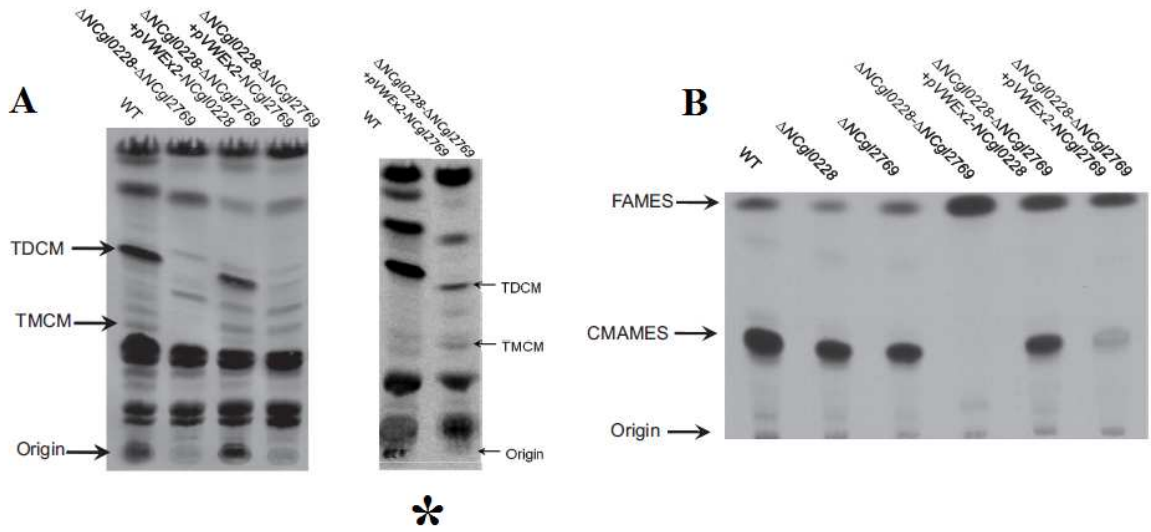

Figure 3.10: Complementation of the *C. glutamicum mmpL* double-mutant strain. TLC analysis of A: total lipids and B: AG-bound corynomycolates, from complemented *C. glutamicum* Δ*NCgl0228*-Δ*NCgl2769* double-mutant strains.
* lanes showing purified apolar lipids samples from wild-type and double mutant complemented with pVWEx2-*NCgl2769* strains (same samples loaded in A), after removing polar lipids, more clear bands appeared as evidence of TDCM and TMCM presence. Conditions as stated in fig. 3.9. (Varela *et al*., 2012. License Nº 3244880310622).

3.3 DISCUSSION

To understand the corynomycolates biosynthetic pathway is paramount to identify the transport step once the trehalose molecule has been transferred to the mature mycolate inside the cell. It has been demonstrated that when the condensation step is impaired, *C. glutamicum* does not produce MA and exhibits an altered cell envelop. Moreover, the same process is vital for survival in *Mycobacterium* (Gande *et al*., 2004; Portevin *et al*., 2005; Gavalda *et al*., 2009). The deletion of both *Rv0206c* homologous *NCgl0228* and *NCgl2769*

in *C. glutamicum* ATCC13032 produced a similar effect, which is lack of both TMCM and TDCM in the cell wall, together with a deficient growth phenotype.

This study has demonstrated that *mmpL3* plays a role in MA transport. The intracellular accumulation of TMM in the Δ*MSMEG_0250* mutant following conditional depletion suggested that TMM was the likely carrier for the MA moiety. The exported TMM is presumably used as substrate by the enzymes of the Ag85-complex for mycolylation of the cell wall AG and the formation of cord factor (TDM). These findings were complemented by the recent studies of La Rosa *et al*. (2012) and Tahlan *et al*. (2012) who used a drug-to-target approach, with the latter demonstrating that treatment with a compound that targeted MmpL3 resulted in a phenotype identical to what we observed with the *M. smegmatis* conditional mutant. Additionally, at the moment this study was performed, Grzegorzewicz *et al*. (2012) reported that AU1235, an adamantyl urea inhibitor of *M. tuberculosis*, also targeted MmpL3. Notably, the authors observed a decrease in the TDM and AG-bound mycolates content in *M. tuberculosis* cells treated with AU1235, and higher levels of TMM inside. Additionally, they were also able to reproduce the effects of AU1235 in a *M. smegmatis* conditional *mmpL3* mutant; showing similar results to that obtained for the Δ*MSMEG_0250* mutant described in this study.

Recent studies have reported that spontaneous resistance observed to the antitubercular compounds BM212 and SQ109 occurs as the result of mutations in *mmpL3* gene. Furthermore, cells exposed to SQ109 have displayed accumulation of intracellular TMM, strongly suggesting that the MmpL3 transporter function should be the efflux of TMM (LaRosa *et al*., 2012; Tahlan *et al*., 2012). Interestingly, in a recent unpublished study, I have observed that the *C. glutamicum* mutant strain Δ*NCgl0228* exhibits a lower MIC to SQ109 even though the strains showed a normal corynomycolates production

suggesting the transporter could be acting as an efflux pump for SQ109 with high specificity (unpublished results).

The complex nature of mycolic acids biosynthesis leads to the idea that the transport mechanism of TMM may not be solely carried out by MmpL3. Previous studies in glycolipids transport of mycobacteria have shown that MmpL proteins may require the concerted action of several proteins forming complexes; in *M. smegmatis*, the biosynthesis of GPL is carried out by a membrane-bound megacomplex where MmpL4a and MmpL4b act as scaffold along with MmpS4, a third transmembrane protein termed Gap, a polyketide synthase and several other proteins (Deshayes *et al*., 2010; Sondén *et al*., 2005). In this context, the existence of a membrane-bound protein complex involved in mycolic acids transport was proposed and blue native polyacrilamide gel electrophoresis (BN-PAGE) technique was performed in order to find protein-protein interactions involving MmpL3. Native membrane fractions from *C. glutamicum* strains where analysed, unfortunately, the isolation of native protein complexes from clumped cell pellets of growth-defective mutants was unsuccessful.

The region downstream of *mmpL3* encodes two TM proteins, *Rv0204c* and *Rv0205*, which may form part of a complex involved in the transport of TMM. Additionally, the biosynthetic clusters for PDIM also contain ABC transporters and thus the role of ABC transporters in mycolates transport (acting in conjunction with MmpL3) remains a possibility. A recent study by Tullius *et al*. (2011) has suggested a role for the *mmpL3-mmpL11* gene cluster in heme transport; interestingly, both *mmpL4* and *mmpL5* have been described as part of siderophore export systems (Wells *et al*., 2013), perhaps the iron-uptake function remains as an ancient role between the paralogs of the mmpL family after the speciation process. A dual function seems also be a fact for MmpL5, as mentioned

before, the protein has been hypothesised to be the efflux-pump for azoles that affect the biosynthesis of sterol in mycobacteria (Milano *et al*., 2009); therefore both iron- and sterol-metabolism appear to be connected via mmpL5 and its transcriptional regulator, a similar situation has also been described in *Cryptococcus neoformans*, where sterols biosynthesis and iron homeostasis are linked via the regulator Sre1p under stress conditions (Chang *et al*., 2007). The authors reported that they were also able to delete a region of the *M. smegmatis* genome that included *MSMEG_0250*. In this study, it was not possible to generate an individual null mutant of *MSMEG_0250* in *M. smegmatis* mc^2155 despite repeated attempts, consistently with results observed for the *M. tuberculosis* homolog by Domenech *et al*., 2005. Specifically for *mmpL11*, previous studies did not report any alteration in the lipid profile of the mutant; nevertheless, a recent study has shown intracellular accumulation of the mycolic acid-precursor MycPL and also the inability to export monomeromycolyl diacylglycerol (MMDAG) and mycolate ester wax in *M. smegmatis* mutant (Pacheco *et al*., 2013), revealing the crucial role of this conserved cluster in the cell wall biogenesis. However, the essentiality of the gene *MSMEG_0250* was demonstrated using CESTET and it was also showed that conditional depletion caused a loss of TDM and of cell wall AG-mycolylation, along the intracellular accumulation of TMM, downstream effects should not have been occurred as result of the disruption of MSMEG_0250 since the orientation of *MSMEG_0249* indicates that the gene is under the control of a different promoter, moreover, the MSMEG_0250 gene was enough to restore the function via CESTET. In contrast to mycobacteria, I observed several differences in the role of *mmpL* genes in corynomycolate transport in *C. glutamicum*. First, there was no equivalent corynebacterial cluster exhibiting synteny with mycobacterial *mmpL3-mmpL11* region. Instead, a functional redundancy was observed between *NCgl0228* and *NCgl2769*

located in two distinct regions of the *C. glutamicum* genome. Individual deletion of either of these *mmpL* genes did not have any effect, but simultaneous deletion of both genes led to complete loss of TMCM, TDCM and AG-bound corynomycolates. This was in contrast to the *M. smegmatis* conditional mutant where conditional depletion of *MSMEG_0250* led to loss of TDM and AG mycolylation, but intracellular accumulation of TMM. As mentioned above, while this result raised the possibility that corynomycolate transport may involve a carrier other than TMCM, this seemed highly unlikely, given the absence of any accumulating intermediate in the *C. glutamicum* Δ*NCgl0228*-Δ*NCgl2769* and Δ*NCgl0228*-Δ*NCgl0887*-Δ*NCgl2769* mutant strains. Instead, variations in the phenotypes of the mycobacterial and corynebacterial mutants may be a reflection of fundamental differences in mycolic acid biosynthesis in the two genera. Mycobacterial mycolic acid biosynthesis requires several components including a multidomain FAS-I, a multienzyme FAS-II complex, modifying enzymes and Pks13 (Radmacher *et al*., 2005; Takayama *et al*., 2005). Corynomycolate biosynthesis on the other hand requires two type-I FAS and Pks13. MmpLs are also envisaged to act as scaffolds for the localized biosynthesis on the cell membrane, facilitating concerted biosynthesis and transport. In mycobacteria, due to the far larger number of components involved, mycolate biosynthesis may be delinked from transport. Instead, MmpL3 could form a complex with other proteins involved in TMM transport. As a result, loss of MmpL3 would not cause a direct cessation of mycolate biosynthesis. In contrast, in *C. glutamicum*, where corynomycolate biosynthesis requires fewer enzymatic components, late-stage enzymes such as Pks13 may depend on interaction with an MmpL complex to ensure that corynomycolate biosynthesis is coupled to transport. Thus, a concurrent loss of *NCgl0228* and *NCgl2769* would lead to not just the loss of a transport complex, but also disrupt the late stages of corynomycolate biosynthesis.

Describing the *mmpL3* gene as essential and involved in mycolate transport confers it vital importance as a target for development of new drugs, fact that it is as well supported by the recently published literature, where MmpL3 has been identified as the target of three different drugs (La Rosa *et al*., 2012; Tahlan *et al*., 2012; Grzegorzewicz *et al*., 2012).

3.4 MATERIALS AND METHODS

3.4.1 Bacterial strains, growth conditions and generation of *C. glutamicum mmpL* mutant strains

Corynebacterium glutamicum ATCC 13032 was grown on the complex medium Brain Heart Infusion at 30ºC. Deletion vectors using the nonreplicable system pK19mobsacB containing inserts synthesized by GeneArt and crossover PCR were used (Schäfer *et al*. 1994). The inserts contained 12 nucleotides of the 30 end of the target gene along with 300 bp of the upstream sequence, and 36 nucleotides of the 50 end together with 300 bp of the downstream sequence. The non-replicative construct was introduced into *C. glutamicum* ATCC 13032 using kanamycin resistance as indicator of the chromosomal integration. Clones displaying sucrose-resistance were selected during a second step of selection in order to indicate loss of the vector-encoded sacB function. After the second recombination event about half of the recombinants contained the desired deletion, as verified by PCR, and one strain each was termed *C. glutamicum* Δ*NCgl0228*, Δ*NCgl0887* and Δ*NCgl2769*, respectively. The double-mutant Δ*NCgl0887*-Δ*NCgl2769* was generated using Δ*NCgl0887* and using the appropriate pK19mobsacB construct. In-

frame deletion of *NCgl0228* in a single or double mutant background was not possible despite repeated attempts. As an alternative, we used pK19mobsacB-*NCgl0228*, containing an internal fragment of *NCgl0228* amplified by primer pairs 5'-CATAGAATTCGTGGCTGTGCTCATTGCGTTGAC-3' and 5'-GTACGTCGACCTCTGCCATCAAATCAGCCGACTG-3'. This vector was used to disrupt *NCgl0228* in *C. glutamicum* Δ*NCgl0887*, Δ*NCgl2769* and in Δ*NCgl0887*-Δ*NCgl2769* to generate the double-mutants *C. glutamicum* Δ*NCgl0228*-Δ*NCgl0887* and Δ*NCgl0228*-Δ*NCgl2769*, and the triple mutant Δ*NCgl0228*-Δ*NCgl0887*-Δ*NCgl2769* respectively. *C. glutamicum* mutants were generated by Dr Eggeling's group at the Institute for Biotechnology 1 of the Research Centre Jülich, Germany (Eggeling and Bott, 2005). Growth of all mutants was characterized on the complex medium brain heart infusion broth at 30ºC, with 25 μg/ml kanamycin when appropriate. Extractions of [^{14}C]-labelled of lipids and corynomycolic acids from all strains were done as described previously (Gande *et al*., 2004, 2007).

3.4.2 Complementation of *C. glutamicum* Δ*NCgl0228*-Δ*NCgl2769*

NCgl0228 was amplified using primer pairs F0228 5'-CTCATTTGTCGACAAGGAGATATAGGTGGCGAAATTGCTATTCAGG-3' and R0228 5'-GGTGGGATCCCTAACGTGCAGCCTGCTTCTCC-3'; and *NCgl2769* using the primer pair F2769 5'ACAATTGTCGACAAGGAGATATAGGTGTTTTCTAAATGGGGCCAC-3' and R2769 5'-TCCTCGCGGATCCTTAATCTAGATCCTCAAGCCTGC-3', using *C. glutamicum* ATCC13032 chromosomal DNA as template. PCR products were cloned in pVWEx2 to yield pVWEx2-*NCgl0228* and pVWEx2-*NCgl2769*, respectively. The inserts

in the plasmids were verified by sequencing, and subsequently used to transform *C. glutamicum* Δ*NCgl0228*-Δ*NCgl0887* to tetracycline resistance 5 μg/ml. Complemented strain were generated by Dr Eggeling's group at the Institute for Biotechnology 1 of the Research Centre Jülich, Germany (Eggeling and Bott, 2005).

3.4.3 Generation and characterization of a *M. smegmatis MSMEG_0250* conditional mutant

The conditional mutant Δ*MSMEG_0250* was generated using CESTET (Bhatt *et al*., 2005). A merodiploid strain was previously generated by introducing an integrating vector pMV306-*mmpL3* by electroporation into *M. smegmatis* mc^2155 (Snapper *et al*., 1990). pMV306-*mmpL3* consists of *mmpL3* cloned downstream of the acetamidase promoter into the integrative vector pMV306 (Stover *et al*., 1991). The merodiploid strain mc^2155::pMV306-*mmpL3* was used to perform specialized transduction (Bardarov *et al*., 2002; Larsen *et al*., 2007) using phΔ*MSMEG_0250* to replace *MSMEG_0250* with a hygromycin resistance cassette. The transductants were selected at 37ºC on plates containing 100 μg/ml hygromycin and the gene replacement of *MSMEG_0250* was confirmed by Southern blot. Conditional depletion of *MSMEG_0250* in the strain Δ*MSMEG_0250* to visualize [^{14}C]-labeled mycolic acids and other lipids was carried out as described before (Bhatt *et al*., 2005).

3.4.4 Extraction and analysis of [^{14}C]-labelled Lipids

Labelled *C. glutamicum* lipids were extracted from 10 ml of BHIS medium cultures grown at 30ºC until OD_{600} 0.4, at which point, 5 μCi/ml [^{14}C] acetate (50 mCi/mmol) were added and the culture incubated overnight.

Free lipids samples were obtained by two consecutive rounds of extraction using 2 ml of $CHCl_3/CH_3OH/H_2O$ (10:10:3, v/v/v) for 3 h at 50 °C. Amounts of 1.75 ml of $CHCl_3$ and 0.75 ml of water were added to the lipid extracts, mixed and centrifuged. The lower organic phase was collected and washed two times using 2 ml of $CHCl_3/CH_3OH/H_2O$ (3:47:48, v/v/v), the organic phase obtained was dried and resuspended later using 200 µl of $CHCl_3/CH_3OH/H_2O$ (10:10:3, v/v/v). An amount of 20,000 cpm was used from each strain to perform the TLC technique using $CHCl_3/CH_3OH/H_2O$ (60:16:2, v/v/v) as mobile phase. Autoradiograms were obtained by 3-day exposure to film to reveal [^{14}C] -labeled lipids (Gande *et al.*, 2004). Supelco LC-SAX anion exchange 3 ml columns were used to separate polar and apolar lipids fractions, a $CHCl_3/CH_3OH$ (2:1, v/v) solution was used as eluent. Firstly, the column was washed with 2 volumes of eluent and then 200 µl of total lipids sample were loaded and the eluate containing the apolar lipids fraction was collected with 3 volumes of eluent. Finally, the polar lipids fraction was collected using 3 ml of ammonium acetate 1 M dissolved in eluent solution. Samples were dried out and analysed by TLCs as mentioned in General Materials and Methods section.

3.4.5 Fatty acid methyl esters (FAMEs) and mycolic acid methyl esters (MAMEs) extraction from delipidated cells and whole cells

The delipidated [^{14}C]-labelled cells were subjected to alkaline hydrolysis reaction with 5% tetrabutylammonium hydroxide at 100°C overnight. CH_2Cl_2 (4 ml), CH_3I (300 µl) and water (2 ml) were added to the reaction and mixed for 30 min. After discarding the upper aqueous phase, the organic phase was washed two times using water and dried out by evaporation. The dried MAMEs were resupended in diethyl ether and centrifuged to sediment insoluble material. The supernatant was collected in a new tube and evaporated to

dryness. The dried extract was dissolved in 200 µl of CH_2Cl_2 and 5 µl were used for liquid scintillation counting. The mixture (10,000 cpm) was subjected to TLC developed in petroleum ether (b.p. 60°C-80°C): acetone (95:5, v/v). [^{14}C]-labelled FAMEs/MAMEs were visualised on an X-ray film following overnight exposure to the TLC plates.

3.4.6 Bioinformatic analysis

MmpL3 homologs were searched using the BLAST function (Altschul *et al*., 1990) from the NCBI database; while the trasmembrane domains were predicted using TopPredII (Claros *et al*., 1994). Cluster analysis was performed using the MycoDB database.

3.4.7 Southern-blot confirmation

The mutant strains obtained were confirmed by PCR and also by Southern-blotting technique using a DIG probe as described in General Materials and Methods section. In this case, probes of the genes *NCgl0228, NCgl0887* and *NCgl2769* were developed using PCR product that later were used to hybridise the genomic DNA of every strain that was previously digested using restriction en enzymes flanking the genes. The following picture shows the hybridasation between the probes and the digested genomic DNA (Fig. 3.11).

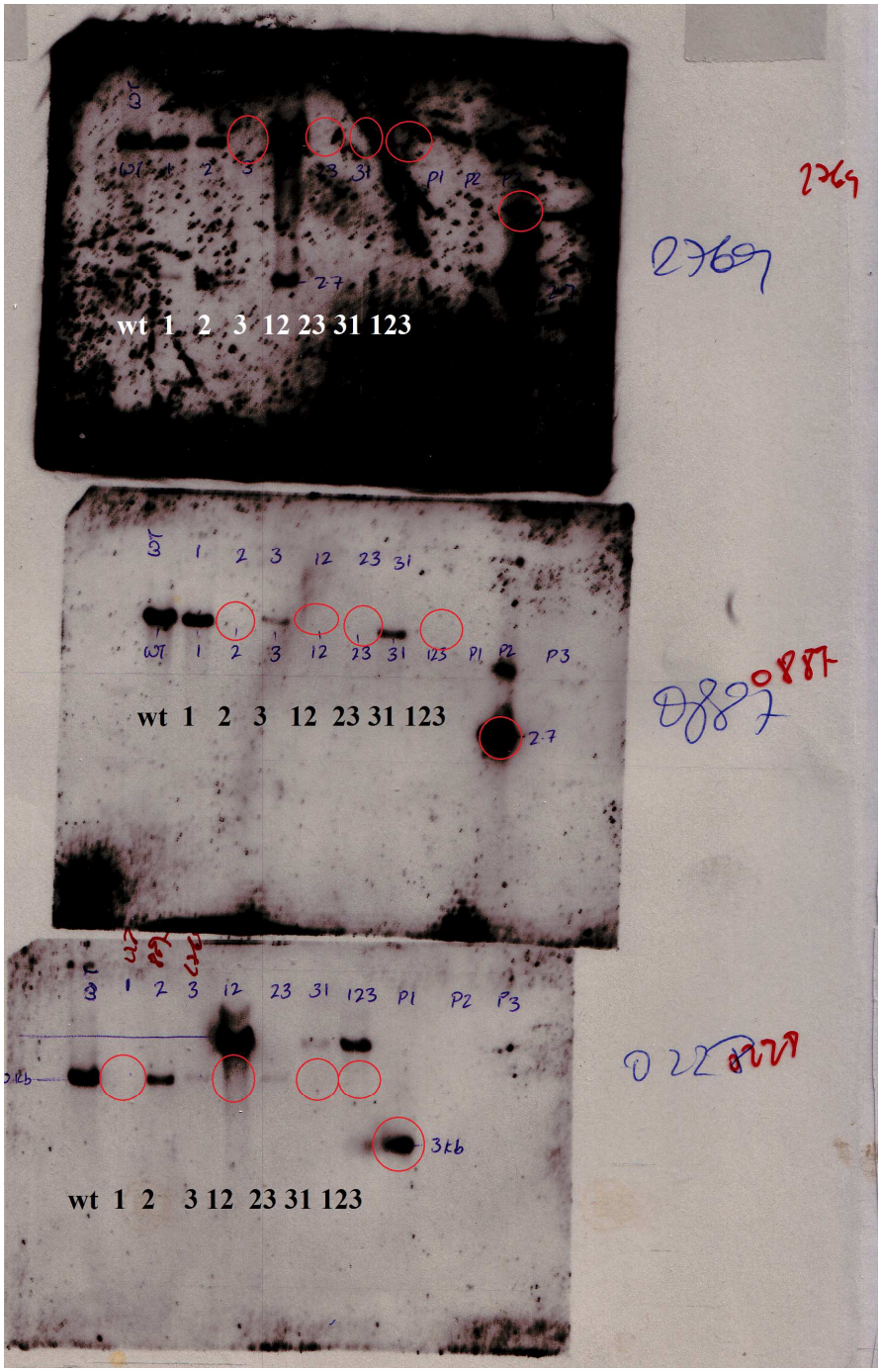

Figure 3.11: Southern-blot confirmation. The picture displays the hybridisation between the digested genomic DNA (from wild-type and mutant strains) and the probes for the genes *NCgl2769*, *NCgl0887* and *NCgl0228* (top, centre and bottom, respectively). First four red circles from the left to the right show the lack of hybridisation in the the mutant and the last red circle on the right side shows the probe.
P1, P2 and P3 indicate the probe used in each case and the numbers indicate the combination used for single (1,2,3), double (12, 23, 31) and triple mutant (123). Southern blot and picture by A. Singh.

CHAPTER 4

ASSESSING THE ROLE OF ABC-TRANSPORTERS IN THE *Mycobacterium smegmatis* CAPSULAR α-GLUCAN TRANSPORT

4.1 INTRODUCTION

As described in the Introduction Chapter, the cell envelope of *Mycobacterium tuberculosis and Mycobacterium smegmatis*, possess three structural components: the plasma membrane, the cell wall containing mycolic acids and the outermost capsule, with the last two structures forming a Gram-negative-like outer membrane (Daffé and Draper, 1998; Sani *et al*., 2010). The capsule appears as an electron transparent region that surrounds the mycobacterial cell envelope in transmission electron microscopy preparations (Chapman *et al*., 1959). It is non-covalently bound and is composed of a small amount of proteins and species or type-specific lipids. However, the major constituent of the mycobacterial capsule is a glycogen-like α-glucan, representing more than 80% of the extracellular polysaccharides, whereas between 10 to 20% of the composition correspond to (lipo)-arabinomannan, PIMs and ESX-1-secreted proteins in some species like *Mycobacterium marinum* (Sani *et al*., 2010; Roy *et al*., 2013).

Mycobacterial α-glucan is made up of repeated elements of either five or six α-D-(1→4)-glucosyl core branched every five or six residues with oligo-glucosyl side chains of glucosides at position 6-OH. Its molecular mass has been estimated to be about 100 kDa and, along the glycogen, is considered a highly branched glucan (Fig. 4.1) (Ortalo-Magne *et al*., 1995; Lemassu *et al*., 1996; Dinadayala *et al*., 2008; Sani *et al*., 2010).

In *Mycobacterium tuberculosis*, like in the majority of bacteria, the capsule is a protective structure; its presence seems to be an adaptive response to stressful conditions and also plays an important role in the successful colonisation of the host, inhibiting the immune response and immunomodulation (Cywes *et al*., 1997; Daffé and Ettiene, 1999; Geurtsen *et al*., 2009, Giovannini *et al*., 2012). Its role in pathogenicity is key since during

the infection process the capsule components are the first to interact with the immune system.

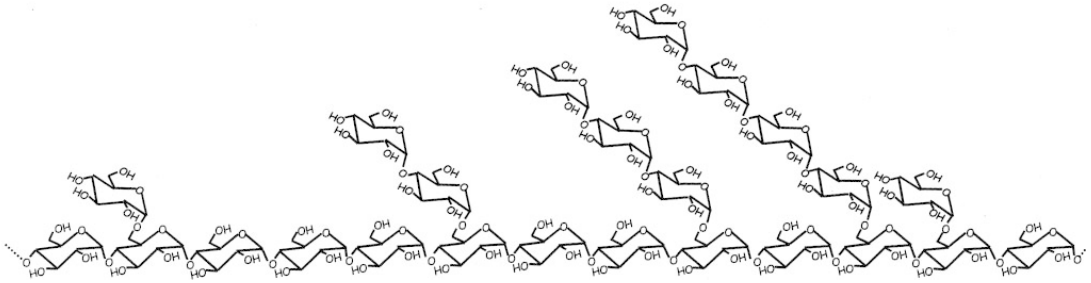

Figure 4.1: Structure of α-glucan. Model for the repeating unit of the α-glucan of *Mycobacterium bovis* BCG based on the data from MALDI-TOF spectrometry. Adapted with permission from Dinadayala *et al*., 2004.

Studies have shown α-glucan induces monocytes to differentiate into an altered form of dendritic cells by blocking CD1 expression and dampening pro-inflammatory cytokine response by suppressing IL-12 production, which allow mycobacteria the evasion of the immune system (Gagliardi *et al*. 2007; Sani *et al*., 2010).

Although the structure and composition of the mycobacterial capsule has been well studied (Daffé and Ettiene, 1999; Dinadayala *et al*., 2008), the genetics and biochemistry of both assembly and transport of its high molecular weight components are not well understood. Due to the structural correspondences shown by capsular α-glucan and glycogen, it is likely that both polymers share common biosynthetic pathways. Different glycogen biosynthesis routes have been described in bacteria: the classical GlgC-GlgA pathway which is glucose dependent, where GlgC activates glucose 1-phosphate to generate glucose nucleotide-diphosphate which is subsequently used by GlgA to polimerise the linear glucan; and the non-classical GlgE pathway that produces glycogen from maltose and also trehalose as precursor. The latter has been hypothesised as the

putative route for capsular glucan biosynthesis (Fig. 4.2) (Chandra *et al*., 2011; Park *et al*., 2011).

In *M. tuberculosis*, the disruption of the *glgA* gene (*Rv1212c*) results in a significant reduction in the amount of capsular α-glucan without affecting the glycogen content. However, capsular glucan production in the *Rv1212c* mutant could be restored not only by complementation with *Rv1212c*, but also the overexpression of *Rv3032*, suggesting functional redundancy between both genes. Moreover, failures to disrupt both genes indicated that the function encoded by these genes was critical for bacteril growth. The presence of more than one functional *glgA* orthologue does not occur in all mycobacterial species but they all need to retain at least one (Sambou *et al*., 2008).

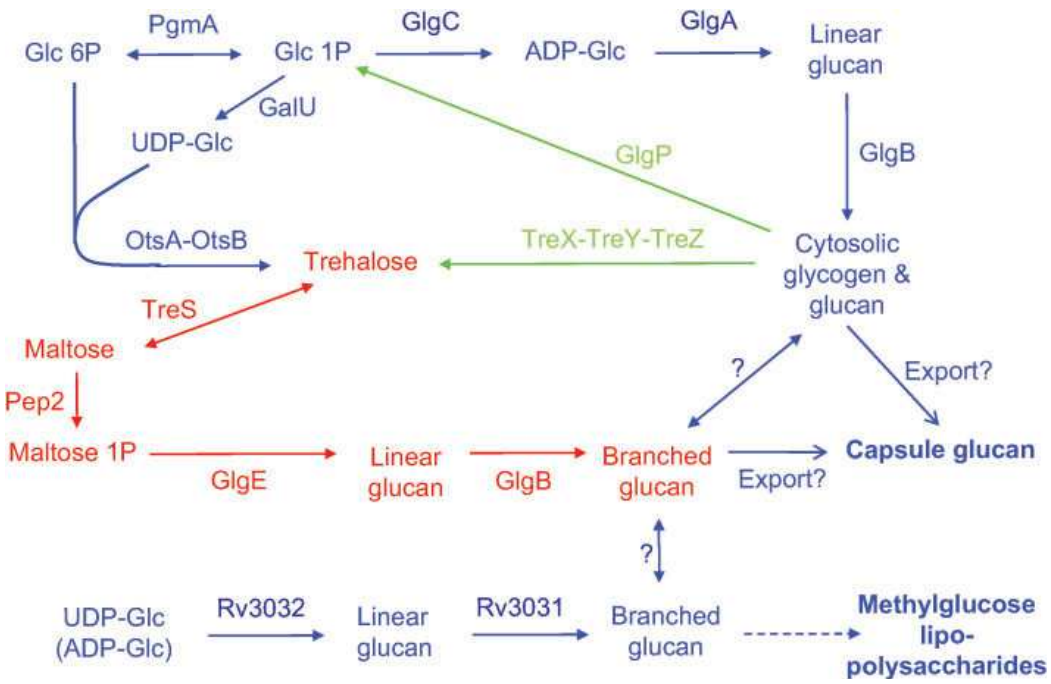

Figure 4.2: Model of mycobacterial α-glucan pathways. The classical glycogen pathway is shown in blue, the *Rv3032* pathway is associated with methylglucose lipopolysaccharide (MGLP) biosynthesis. In red, the GlgE pathway may contribute to cytosolic glycogen, capsular glucan and/or MGLP. Glucans degradation either to glucose-1-P by GlgP or to trehalose by TreX-TreY-TreZ in green, generating potential intermediates for glucan reassembly or other metabolic purposes. Taken from Chandra *et al*., 2011.

Carbohydrate uptake has been a paradox in *M. tuberculosis* because even though there appear to be no exogenous sugars available to transport (and therefore no precursors for capsule biosynthesis), the sugar uptake systems have been shown to be critical during the infection, where transporter systems are necessary for growth in macrophages and mice while facing restricted access to host sugars. For instance, a trehalose-recycling ATP-binding-cassette (ABC) transporter has been found to be required for *M. tuberculosis* to establish infection in mice systems (McKinney *et al*., 2000; Sassetti and Rubin, 2003; Kalscheuer *et al.*, 2010).

In bacteria, operons for carbohydrate-specific ABC-transporters have shown to bear a gene that encodes a sugar-specific periplasmic binding protein or permease (Bertram *et al*., 2004). *In silico* analyses in *Mycobacterium smegmatis* genome sequences revealed twenty eight putative carbohydrate permeases, which consist of nineteen ABC-transporters, three belonging to the phosphotransferase system (PTS) group, one to the major intrinsic protein (MIP) group, four to the major facilitator superfamily (MFS) and one to the sodium solute superfamily, while all the genes encoding for ABC-type sugar binding proteins were adjacent to ABC permease genes. On the other hand, *M. tuberculosis* appears not having the necessary carbohydrate transport systems unlike *M. smegmatis*; only five sugar permeases were present (four associated to the ABC-type group and the other one to the MFS), with only two of them present in *M. smegmatis* and lacking the genes encoding for the PTS group. Since the identity of these four ABC systems to other previously identified transporters not present in mycobacteria is less than 25%, the substrates of these transporters are difficult to predict (Titgemeyer *et al*., 2007).

As it was explained, components of the glycogen biosynthetic pathways that have been already described should be useful in the identification of factors involved in the α-

glucan biosynthesis; additionally, using a combination of comparative genomics and bioinformatics tools, Titgemeyer *et al* (2007) have shown a complete analysis of the carbohydrate-uptake systems of *M. smegmatis* and *M. tuberculosis*. Hypothetically, the systems described for *M. tuberculosis* should contain the sugar-transporters necessaries for the α-glucan biosynthesis; therefore, several genes from the *M. tuberculosis* H37Rv genome were identified and selected as potential candidates involved in α-glucan biosynthesis routes and listed in Table 4.1.

Table 4.1
Candidate genes proposed to be involved in α-glucan transport

***Mycobacterium tuberculosis* H37Rv**	**Description**
Rv2040c	sugar- ABC transporter
Rv2039c	sugar- ABC transporter
Rv1237	sugar- ABC transporter SugB
Rv1236	sugar- ABC transporter SugA
Rv2316	sugar- ABC transporter UspA
Rv2317	sugar- ABC transporter UspB
Rv3783	O-antigen/lipopolysaccharide ABC transporter RfbD

The aim of the study described in this chapter was to investigate pathways involved in the transport of α-glucan in *M. smegmatis*. More specifically, I have looked at the role of predicted sugar specific ABC transporters in this process, using candidate genes from *M. smegmatis* and generating deletion mutants for each of them by specialised transduction (Bardarov *et al*., 2002).

4.2 RESULTS

4.2.1 Selection of candidate ABC-transporters of *M. smegmatis*

Using the list of candidate genes shown above, *M. tuberculosis* homologs were searched in the *M. smegmatis* genome using BLAST (Altschul *et al*., 1990). Due to the

ABC-type nature of all the genes selected, several matches were found and only the highest scores and identity percentages obtained were chosen for further analysis. Additionally, respective genomic regions from the species were analysed in order to find synteny between putative clusters, thus improving the selection criteria of the candidate genes. Only the genes *Rv2039c and Rv2040c* showed low scores and identity through BLAST analysis with the *M. smegmatis* genome; moreover no synteny was found compared to *M. smegmatis* sequences (Fig. 4.3 A), unlike the rest of the query sequences analysed (Fig. 4), which did show high scores and identities, beside the synteny between genomic regions compared. Although no homology was found for *MSMEG_0505* in *the M. tuberculosis* genome, still was chosen to generate a deletion mutant since it was part of a major operon composed by *MSMEG_0506* and *MSMEG_0507* as well. Genes selected are listed on Table 4.2.

Table 4.2
Selected genes from *M. smegmatis* proposed to be involved in α-glucan transport.
In order to identify potential candidate genes in *M. smegmatis* mc^2155, BLAST was performed using the genes from the *M. tuberculosis* H37Rv genome listed in table 4.1 as query sequences. The score and identity values found for each gene are shown as well as the description. Selected genes were deleted by specialised transduction.

***M.tuberculosis* H37Rv**	**Score**	**Identity**	***M. smegmatis* mc^2155**	**Description**
-	-	-	*MSMEG_0505*	Sugar ABC-transporter
Rv2040c	139	33%	*MSMEG_0506*	ABC-transporter, permease protein
Rv2039c	125	33%	*MSMEG_0507*	Probable sugar ABC-transporter
Rv1237	367	85%	*MSMEG_5059*	ABC-transporter, permease protein SugB
Rv1236	412	79%	*MSMEG_5060*	ABC-transporter, permease protein SugA
Rv2316	397	83%	*MSMEG_4466*	ABC-transporter, permease protein UspA
Rv2317	353	79%	*MSMEG_4467*	ABC-transporter permease protein UspE
Rv3783	418	80%	*MSMEG_6369*	O-antigen export system, permease protein

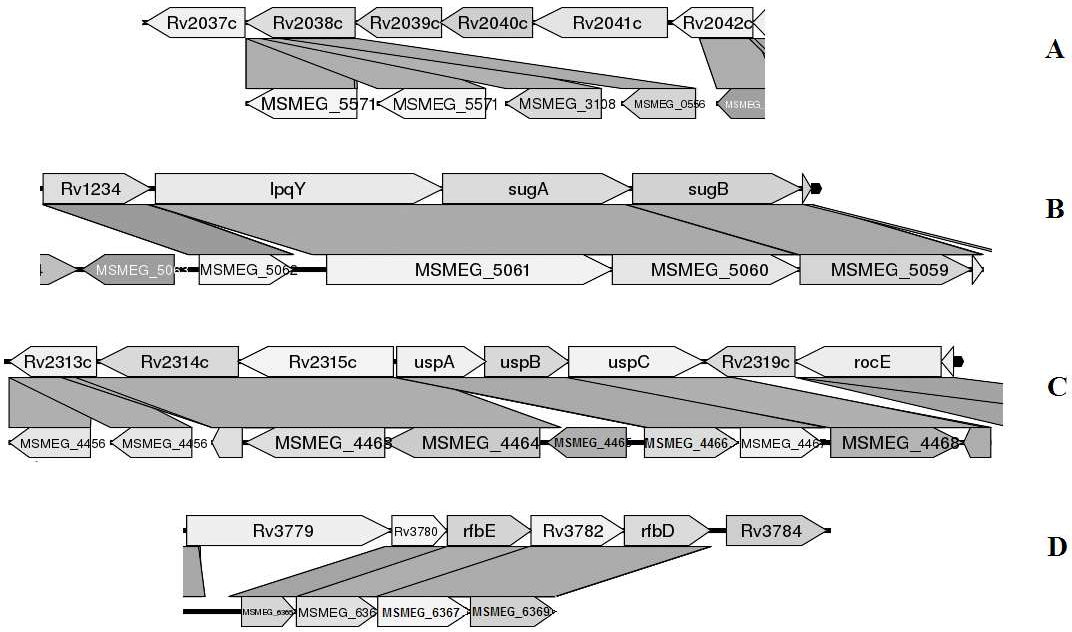

Figure 4.3: Alignment view of the genomic regions of *M. tuberculosis* H37RV (above) and *M. smegmatis* mc^{2}155 (under). Sequences were aligned using the promer algorithm from the xbase database in order to find synteny between selected clusters. A- *Rv2039c-Rv2039c M. tuberculosis* region did not show co-localisation of genetic loci in the *M. smegmatis* genome. B, C and D show, respectively, *Rv1236- Rv1237, Rv2316- Rv2317* and *Rv3783* compared regions showing high level of synteny.

4.2.2 *MSMEG_6369* is an essential gene in *Mycobacterium smegmatis*

The generation of knockout strains by specialised transduction was attempted and all the mutants obtained were confirmed by Southern blot, except for *MSMEG_6369*. In that case, several transduction attempts were carried out but no mutant was observed, suggesting that *MSMEG_6369* was essential. In order to demonstrate that, I used conditional expression–specialized transduction essentiality test (CESTET), a genetic tool designed to prove gene essentiality in *M. smegmatis* (Bhatt *et al*., 2005; Bhatt and Jacobs, 2009). Basically, the native copy of *MSMEG_6369* could be deleted in a merodiploid strain containing a second copy of the gene integrated in the genome under the control of a

promoter inducible by acetamide. The conditional mutant generated was viable only in the presence of 0.2% of acetamide in the media-agar plates (Fig. 4.4 A) demonstrating that *MSMEG_6369* is essential for viability. Furthermore, the strain was unable to grow after three passages in liquid medium without acetamide (Fig 4.4 B).

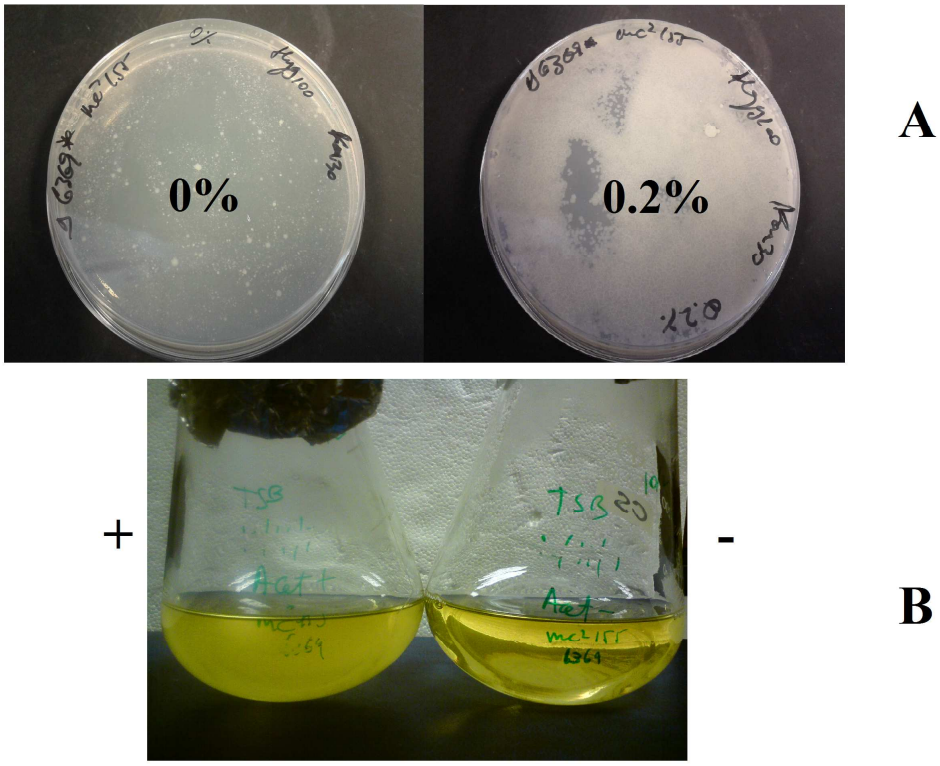

Figure 4.4: Essentiality test for *MSMEG_6369* in *M. smegmatis* mc^{2}155. Growth of the conditional mutant on A- Sauton agar plates with or without acetamide (%), plates incubated at 37ºC for three days, and B- inducing the expression with acetamide in TSB cultures + and – acetamide, incubated at 37ºC for 48h.

4.2.3 Analysis of extracellular α-glucan levels in candidate ABC-transporter mutants

All the ABC-transporter mutants were screened using a spotblot analysis to detect surface-exposed capsule α-glucan. Briefly, the technique allows detection of surface-exposed α-glucan in a colony-blot assay using an antibody-filter-screen, assessing altered production of α-glucan. Interestingly, all the mutants for capsule transporters candidates showed high levels of extracellular α-glucan and normal levels of intracellular glycogen in comparison with the wild-type strain (Fig. 4.5). The positive control used was the Δ*pstS* strain; *pstS* genes encode high-affinity phosphate binding proteins forming the Pst complex which is a membrane-associated complex that belongs to the superfamily of ABC-transporters. The strain is already known for its α-glucan overproduction and the lack of the gene is related to phosphate uptaking deficiency in *M. tuberculosis* (Peirs *et al*., 2005). The negative control results shown correspond to samples from Δ*glgB* strain, known to produce reduced levels of both capsular α-glucan and intracellular glycogen due to the disruption of the biosynthetic pathway (Fig. 4.2). The technique consists in the detection of α-glucan directly on cell samples and also cells treated with 0.5% Tween-80 as a mild detergent in order to remove the capsule material from the outermost layers without disrupting the cells. The results in figure 4.5 show that the wild-type strain produces an amount of capsule exposed outside and also capsule material tightly attached to the mycomembrane structure which can not be removed by a mild detergent as Tween-80; as it was expected the Δ*glgB* strain does not produced capsular material able to interact strongly with the mycomembrane and to organise a capsular structure in the way the wild-type strain did. The α-glucan amounts produced by the mutant strains were similar that the

positive control used and every fraction analysed showed overproduction of capsular material as result of the deletions.

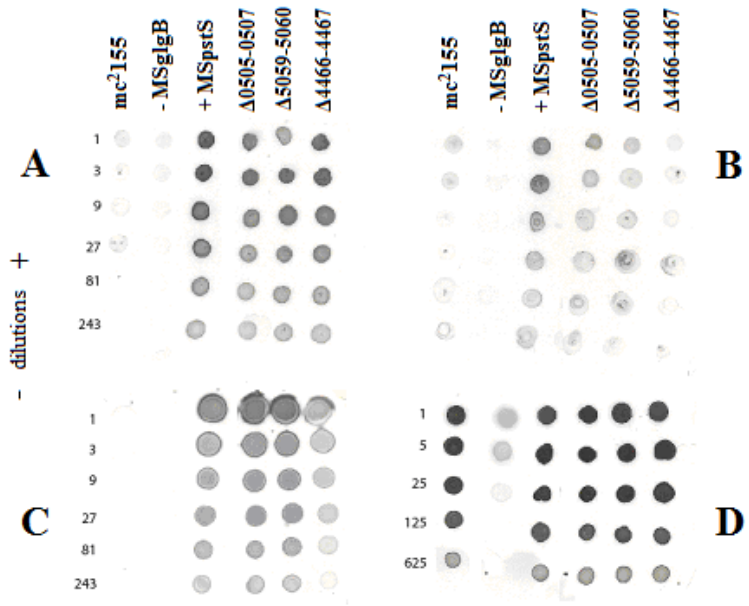

Figure 4.5: Spotblot analysis detecting α-glucan in knockout strains. An antibody-filter-screen was used to detect α-glucan production in samples from: A) Non-treated cells; B) Cells treated with 0.5% Tween-80 as a mild detergent in order to remove the capsule; C) Supernatant from treated cells; D) Intracellular glycogen. MSglgB and MSpstS lanes are positive and negative controls respectively. Numbers indicate the dilution from – to +. Results show overproduction of α-glucan in the mutants tested not as result of an alteration of the production of intracellular glycogen. Assay carried out in collaboration with Dr Jeroen Geurtsen at the VU University Medical Centre in Amsterdam, Netherlands.

4.2.4 Growth of mutant strain in different carbohydrate-based carbon sources

It was likely that the selected ABC-transporter genes could be involved in the uptake of external sugars rather than function as exporters of the capsule or its precursors. Thus, the ability of the strains of growing in fifteen different sugars as the sole carbon source was tested, in order to correlate transporter function and metabolite. As shown in Fig. 4.6 the growth of all mutant strains was similar in every carbon source provided except in 10 mM trehalose, where the mutant *ΔMSMEG_5059-5060* failed to grow.

Although it was not considerable, this strain showed growth ability when using glycogen as carbon source. This fact could be interesting since both trehalose and glycogen pathways share a common metabolic route.

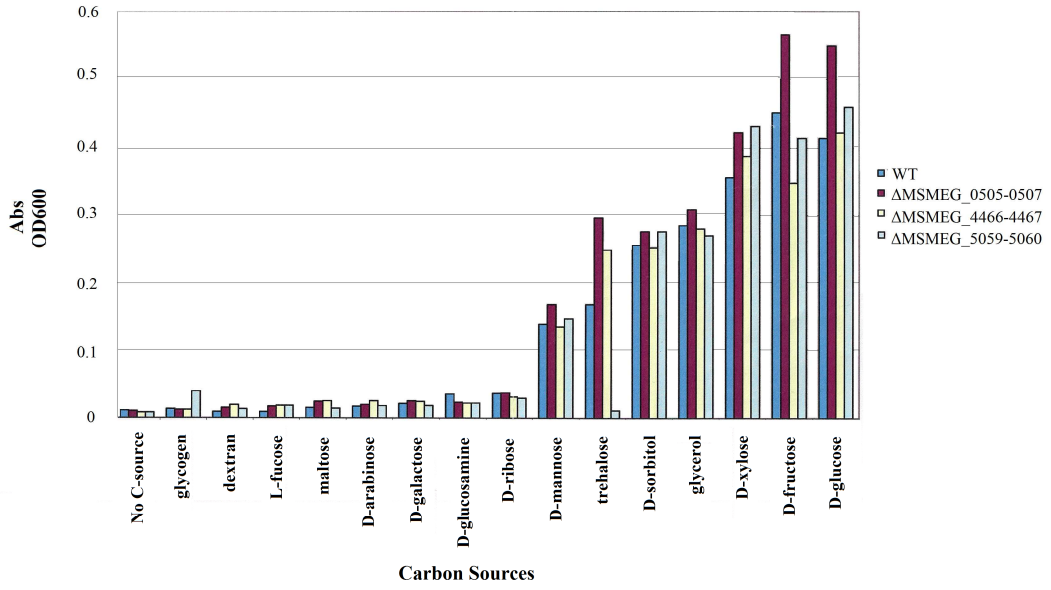

Figure 4.6: *Mycobacterium smegmatis* strains growth in defined media. Every strain was grown in defined Sauton media testing different unique carbon sources and a bar chart was plotted showing the optical density reached by each strain measured at 600nm after 48 hours of incubation at 37ºC. *ΔMSMEG_5059-5060* strain was unable to grow using trehalose as unique carbon source but showed growth in glycogen unlike the rest of the strains. Assay carried out in collaboration with Dr Jeroen Geurtsen at the VU University Medical Centre in Amsterdam, Netherlands.

4.3 DISCUSSION

The analysis of *MSMEG_6369* protein sequence by BLAST showed that the gene is the homolog of *rfbD*, previously reported to be involved in the synthesis of TDP-rhamnose that forms the O-antigen subunit of the lipopolysaccharide (LPS), a major constituent of the outer membrane in several Gram-negative (Burns and Hull, 1998; Cuthbertson *et al*., 2007). Therefore, in mycobacteria, RfbD could have an important role in the biosynthesis of extracellular polysaccharides like arabinomannan or glucan, predominant constituents

on the surface of *M. tuberculosis* (Schwebach *et al*., 2001; 2002). Due to the conditional gene expression in the strain, which depends on the acetamide supply, a different time course experiment needed to be designed to determine the glucan level production under acetamide depletion.

The strain *ΔpstS* was used as positive control for high levels of extracellular capsular α-glucan and perhaps, due to the mutation, the strain encounters a phosphate limiting condition which could trigger a stress response overproducing protection factors like the capsule. Similar results have been found by others with an isocitrate dehydrogenase *Δicd* mutant, who showed high levels of capsular glucan (Chen and Bhatt, unpublished results). In this case a breakdown in the TCA-cycle could induce anaplerotic pathways or glyoxylate cycle in order to re-establishing the homeostasis, ending up on accumulation of capsular material. The high levels of extracellular capsular α-glucan found in the mutant strains could probably be due to two reasons: either an overproduction of the polysaccharide as a result of the stress response or an accumulation because of the breakdown on the sugars recycling system.

While these experiments were carried out, Kalscheuer *et al*. showed the system *MSMEG_5058-MSMEG_5061* to be a high-affinity permease specific for trehalose that plays a major function in the recycling system for cell wall-released trehalose and also confirmed the inability of the mutant to grow using trehalose as sole carbon source (Kalscheuer *et al*., 2010). Any imbalance in sugar metabolism (like the inability to recycle trehalose) could probably have severe consequences on α-glucan levels and considering that mycobacteria use the non-mammalian trehalose as a precursor for essential cell-wall glycolipids and other metabolites (Swarts *et al*., 2012), its high levels could be due to an accumulation rather than an overproduction of capsular material, produced by a broken

recycling pathway. It is interesting that *ΔMSMEG_5059-5060* mutant showed the ability to metabolise glycogen as unique carbon source; perhaps not being able to recycle the trehalose due to the mutation induces and activates the ability to use glycogen which could be used as a sugar storage that need to be activated under specific conditions, perhaps the stringent response or the carbon starvation. On the other hand, a very detailed study is required in order to check the growth dynamic, since in some cases the impaired growth shown may be the effect of a long lag-phase required to adapt the metabolism to that specific carbon source, which is not possible to detect after only 48 hours of incubation. A recycling system of metabolites synthesised by the pathogen appears as an adaptation mechanism to either unfavourable conditions or different types of nutrients. In that context, the determination of changes in gene- and protein- expression profiles via microarrays or proteomics analysis is necessary along with the growth kinetics assays. The growth of the strains in defined media could probably show that the rest of the transporters are either redundant or involved in the uptake of molecules that were not tested in this study. A complete test would require the generation of double, triple or even quadruple mutants.

In summary, while changes in α-glucan production were seen in the mutants, the effects were not likely related to the transport of α-glucan and thus the genes involved in its transport and biosynthesis remain unidentified.

4.4 MATERIALS AND METHODS

4.4.1 Candidate genes, plasmids, phages, bacterial strains and growth conditions

As it was stated in the introduction, ABC-transporter homologs genes from *M. smegmatis* were selected in order to generate knockout strains for the genes

MSMEG_0505-0507, MSMEG_5059-5060, MSMEG_4466-4467 and *MSMEG_6369*. Table 4.1 and 4.2 outline the putative functions and the respective *M. tuberculosis* homologous for candidate genes while vectors and bacterial strains used in this study are listed in Table 4.3. The strains were grown in different liquid media at 37ºC, namely, TSB as culture media and both 7H9 and Sauton as defined media, adding acetamide or different carbon sources when it was required.

4.4.1.1 α-glucan assay

In order to detect α-glucan by colony-blot assay, *M. smegmatis* strains were grown at 37ºC in Middlebrook 7H9 media supplemented with 10% oleic acid-albumin-dextrose catalase (OADC) and 0.05% Tween-80 until an OD_{A600} of ~1, hygromycin was added at 100 μg/ml concentration into mutant strains cultures. Cells were diluted 100 times in 7H9 with neither supplement nor Tween-80 (in order to obtain an intact capsule), adding 0.2% dextrose and grown to exponential phase. Then were harvested by centrifugation and washed thrice and resuspended in phosphate buffered saline solution. Detection of α-glucan was performed before and after an incubation of the cells in the mild detergent Tween-80 (0.5%) by agitation for 30 min at room temperature in order to remove the capsule. Treated cells were collected by centrifugation and separated from the extracted fraction ready to perform blot analysis. These assays were carried out in collaboration with Dr Jeroen Geurtsen at the VU University Medical Centre in Amsterdam, Netherlands.

4.4.1.2 CESTET

A conditional mutant strain was generated by CESTET (Bhatt and Jacobs, 2009) integrating the *MSMEG_6369* gene into the *M. smegmatis* mc^2155 under the control of the

acetamidase promoter (primers used to amplify the gene using *BamHI* and *ClaI* sites: MS_6369F 5'-CATGGATCCATGACGTTCACCGACGCG-3' and MS_6369R 5'-CATATCGATTCAGACCCAGTAGGGCAC-3') and the chromosomal *MSMEG_6369* replaced by a hygromycin resistance cassette afterwards. Cultures were grown either in TSB and Sauton media with 0.2% acetamide and also on 1.5% agar plates using hygromycin at 100 μg/ml and kanamycin at 30 μg/ml to select the conditional mutant strain.

4.4.1.3 Different unique carbon sources test

In order to test growth ability in defined media, 10 mM of different carbon sources were added to Sauton media and the strains grown at 37ºC for 48h. These assays were carried out in collaboration with Dr Jeroen Geurtsen at the VU University Medical Centre in Amsterdam, Netherlands.

4.4.2 Generation of mutant strains

Individual mutants were generated using allelic exchange constructs designed to replace the selected genes from *M. smegmatis* proposed to be involved in α-glucan biosynthesis and transport. Sequences flanking the left and right of the genes were PCR amplified using the primers and restriction sites (*Van91I*) listed on Table 4.4 following the procedure described in General Materials and Methods section to generate knockout phages. Allelic exchange constructs were designed to replace the selected genes with a hygromycin resistance cassette. Each mutant was validated as *bona fide* by Southern blot analysis as described in General Materials and Methods section.

Table 4.3

Phages, plasmid vectors and bacterial strains used and generated in this study. Generation of phages, vectors and strains is fully described in General Material and Methods section.

Vectors and Bacterial Strains	Description	Reference
Phage		
phAE159	Conditionally replicating shuttle phasmid derived from the lytic mycobacteriophage TM4 (TM4ts::pYUB328)	Kriakov *et al.*, 2003
ph*Δ*MSMEG_*4466-4467*	Derivative of phAE159 obtained by cloning p*ΔMSMEG_4466-4467* into its unique *PacI* site.	This work
ph*Δ*MSMEG_*0505-0507*	Derivative of phAE159 obtained by cloning p*ΔMSMEG_0505-0507* into its unique *PacI* site.	This work
ph*Δ*MSMEG_*5059-5060*	Derivative of phAE159 obtained by cloning p*ΔMSMEG_5059-5060* into its unique *PacI* site.	This work
ph*Δ*MSMEG_6369	Derivative of phAE159 obtained by cloning p*ΔMSMEG_6369* into its unique *PacI* site.	This work
Vector		
p0004s	Cosmid for cloning allelic-exchange substrates. Used for specialized transduction. Contains λphage *cos* site and *Hyg*^{R}-*sacB* cassette.	Bardarov *et al*., 2002
pSD26	*Escherichia coli*-mycobacterial shuttle plasmid with acetamidase promoter Kan^R	Parish and Brown, 2008
pMV306	Single-copy-integrating vector; inserts into the phage L5 chromosomal integrating site *attB* in many mycobacteria Kan^R,	Stover *et al*., 1991
pMV306-*6369*	*MSMEG_6369* cloned into pMV306 . Kan^R.	This work
Bacteria		
M. smegmatis mc^{2}155	Parental strain, *ept-1* mutation conferring high efficiency of plasmid transformation	Snapper *et al*., 1990
ΔMSMEG_4466-4467	Chromosomal copy of *MSMEG_4466-4467* in mc2155 was replaced by a Hyg^R cassette	This work
ΔMSMEG_0505-0507	Chromosomal copy of *MSMEG_0505-0507* in mc2155 was replaced by a Hyg^R cassette	This work
ΔMSMEG_5059-5060	Chromosomal copy of *MSMEG_5059-5060* in mc2155 was replaced by a Hyg^R cassette	This work
mc^{2}155::6369	*MSMEG_6369* under the control of the acetamidase promoter was integrated using pMV306	This work
ΔMSMEG_6369	Chromosomal copy of MSMEG_6369 in mc^{2}155::6369 was replaced by a Hyg^R cassette	This work

Table 4.4
Primers used for generation of allelic exchange substrates and sequencing
Sequences flanking the left and right sides of the genes were amplified using the following primers and restriction sites (*Van91I*) to generate allelic exchange constructs

Name	Sequences
HL	5' AGGATCCAGGACCTGCCAAT 3'
HR	5' CTTCACCGATCCGGAGGAAC 3'
OL	5' CGGCCGATAATACGACTCA 3'
OR	5' CTGACGCTCAGTCGAACGAA 3'
MS0505-0507-LL	5' TTTTTTTTCCATAAATTGGGCTGAGGCTCGCCAGCGCCTGC 3'
MS0505-0507-LR	5' TTTTTTTTCCATTTCTTGGATCTGCTGTGCGGCTTTGAGCGAC 3'
MS0505-0507-RL	5' TTTTTTTTCCATAGATTGGACCGAGGCGTTCATCATCCC 3'
MS0505-0507-RR	5' TTTTTTTTCCATCTTTTGGGGGTCTGCACACGCATCTTG 3'
MS4466-4467-LL	5' TTTTTTTTCCATAAATTGGAAGTCCAGCGACGCCGGATAGTTC 3'
MS4466-4467-LR	5' TTTTTTTTCCATTTCTTGGGAAGGATCGGTGAGCCACTCGATG 3'
MS4466-4467-RL	5' TTTTTTTTCCATAGATTGGTGACCGTGGTGCCGCTGTATCTG 3'
MS4466-4467-RR	5' TTTTTTTTCCATCTTTTGGTCCGGCGAAGTATCCGTTGGAG 3'
MS5059-5060-LL	5' TTTTTTTTCCATAAATTGGAGCGGCTCGTCCATGAGAAAC 3'
MS5059-5060-LR	5' TTTTTTTTCCATTTCTTGGGCTGGTCACACCGATCTTCAAC 3'
MS5059-5060-RL	5' TTTTTTTTCCATAGATTGGCATGAACGGCGTGGTCTTCC 3'
MS5059-5060-RR	5' TTTTTTTTCCATCTTTTGGGTTCGACGCGAGCAAGAAGG 3'
MS6369-LL	5' TTTTTTTTCCATAAATTGGTCGTCGTCGACAACGACAAC 3'
MS6369-LR	5' TTTTTTTTCCATTTCTTGGTGGCGATGGTGATCCAGAAC 3'
MS6369-RL	5' TTTTTTTTCCATAGATTGGATCAGGAACTTCGGCACTGG 3'
MS6369-RR	5' TTTTTTTTCCATCTTTTGGTCCGCGCATCGCAGATCAAC 3'

LL forward primer for left flank, LR reverse primer for left flank, RL forward primer for right flank, RR reverse primer for right flank.
HL, HR, OL and OR: sequencing primers used to check flanks cloned into p0004s.

4.4.3 α-glucan detection by colony-blot assay

Serial dilutions of the samples (5 µl) were spotted on nitrocellulose membrane, the membrane was dried for 1 h at 80ºC, blocked, immuno-labelled using an anti-α-glucan monoclonal antibody overnight (1:5) and washed with PBS plus 0.05% Tween-80. Then, incubated with peroxidase-labelled goat anti-mouse IgM (1:1000) and developed using 3,3-diaminobenzidine tetrahydrochloride (Baba, 1993). The *M. smegmatis* Δ*glgB* and Δ*pstS* mutant strains were chosen as negative and positive control for α-glucan production,

respectively. These assays were carried out in collaboration with Dr Jeroen Geurtsen at the VU University Medical Centre in Amsterdam, Netherlands.

4.4.4 Southern-blot confirmation

The mutant strains obtained were confirmed by Southern-blotting technique using a DIG probe as described in General Materials and Methods section. The following pictures show a diagram representing the digestion pattern of genomic DNA from wild-type and mutant strains on the left side. The right side of the pictures display the films obtained by hybridisation between the probes and the digested genomic DNA.

A

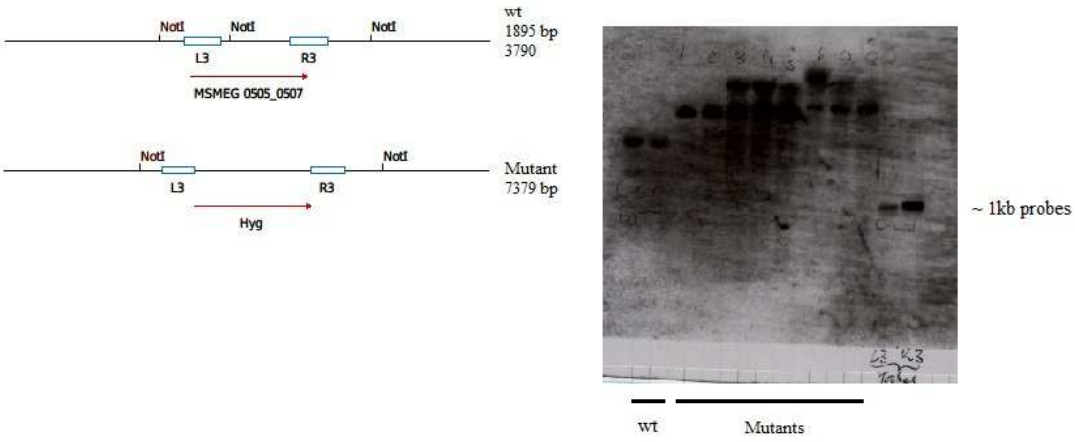

B

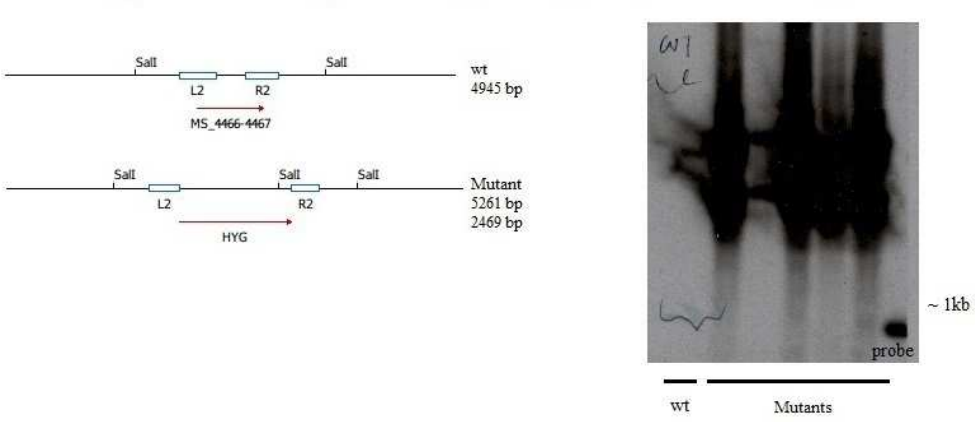

C

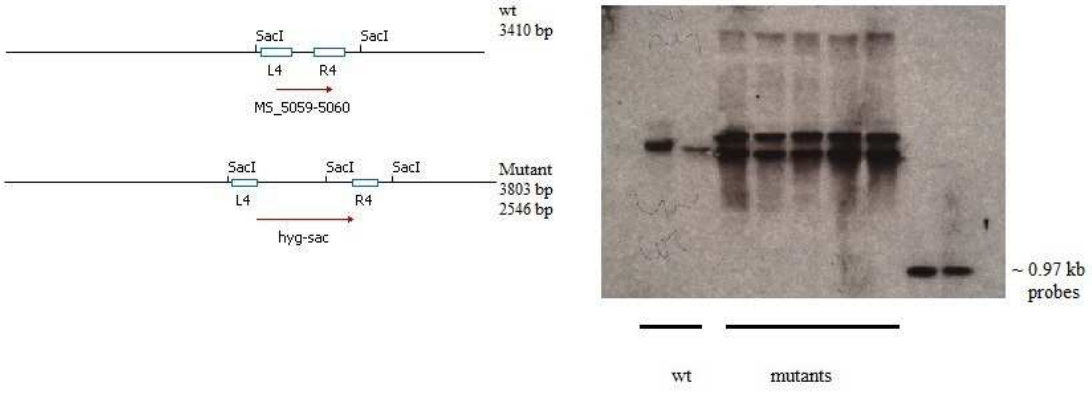

D

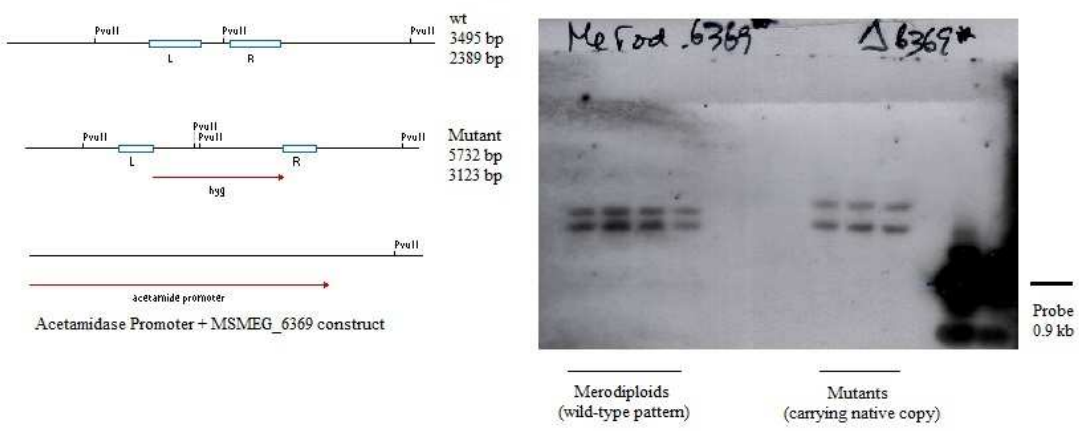

Figure 4.7: Southern-blot confirmation. The left sides of the pictures display the digestion pattern diagrams of genomic DNA from wild-type and mutant strains. Right sides display the films obtained by hybridisation between the probes and the digested genomic DNA. The diagrams include the restriction enzyme used and the expected sizes for each strain after the digestion; the films display the digestion pattern obtained for each strain tested and the probe was also used as molecular-weight size reference. The strains that showed the expected pattern were choosen to perform the experiments described in this chapter. L and R indicate the flanking regions, hyg: hygromycin resistance cassette. A- *ΔMSMEG_0505-0507,* B- *ΔMSMEG_4466-4467,* C- *ΔMSMEG_5059-5060,* D- *ΔMSMEG_6369.*

CHAPTER 5

DECIPHERING THE ROLE OF EXOPOLYPHOSPHATASES IN MYCOBACTERIAL BIOLOGY

5.1 INTRODUCTION

Inorganic polyphosphate (polyP) is an ubiquitous long polymer of tens or hundreds of orthophosphate (Pi) units linked by phosphoanhydride bonds, widespread in every single organism: bacteria, archaea and eukaryotes (Fig. 5.1) (Kulaev *et al*., 1999). The molecule has several functions e.g., phosphate and energy storage, role regulating the levels of nucleotides like ATP, maintenance of cell homeostasis, regulation of gene expression, storage of inorganic cations, membrane transport, etc (Kornberg *et al*., 1999). In prokaryotes, it has been demonstrated that polyP metabolism is involved in bacterial virulence, sporulation, motility, cell division and response to both stress and stringency (Rao *et al*., 1998; Brown and Kornberg, 2004; Zhang *et al*., 2005a, Sureka *et al*., 2009; Varela *et al*., 2010).

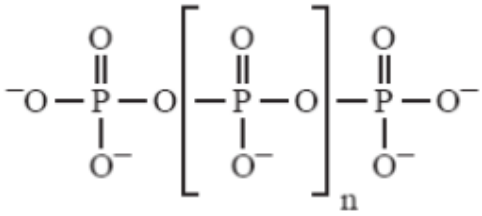

Figure 5.1: Schematic diagram of inorganic polyphosphate molecule. polyP molecule made up of tens to hundreds of phosphate residues linked by phosphoanhydride bonds. (Adapted with permission from Kornberg *et al*., 1999. Confirmation Nº 11129104).

The polymer is synthesised reversibly by the enzyme Polyphosphate kinase 1 (Ppk1) that adds the γ-phosphate of an ATP molecule to the polyP chain extreme (Ahn and Kornberg, 1990). This enzyme is highly conserved in several bacteria and archaea, including some main pathogens, whilst in eukaryotes only *Dictyostelium discoideum*

(DdPPK1) has been demonstrated to have a Ppk1 homologue (Zhang *et al*., 2005b). PolyP biosynthesis can also be produced by other enzymes such as Polyphosphate kinase 2 (Ppk2), a nucleoside diphosphate kinase (NDK) which syntesises polyP from GTP and is responsible for the 20% of the normal polyP cellular amount shown by *ppk1 Pseudomonas aeruginosa* mutants strains, despite the fact the NDK-activity is 75-fold greater (Rashid *et al*., 2000; Ishige *et al*., 2002; Zhang *et al*., 2002); additionally, Polyphosphate kinase 3 (Ppk3) reversibly utilises inorganic polyP as a donor to produce CTP from CDP. Activity assays have shown that while Ppk2 and Ppk3 are able to utilise 100% of the polyP amount, but Ppk1 only utilises 30%, leading to the idea that Ppk1 function is mainly the polyP synthesis for phosphate and energy storage, while the other two enzymes consume polyP (Nahalka *et al*., 2009).

Studies in prokaryotes have demonstrated that *ppk1* is an important factor in bacterial survival, stringency, long-term cell survival, nutrient limitation and virulence including pathogenic bacteria, moreover is an interesting candidate for drug development since is not present in humans (Rao *et al*., 1998; Kuroda and Kornberg, 1997; Hengge-Aronis, 2002; Zhang *et al*., 2005b; Brown and Kornberg, 2004). Specifically, in *Mycobacterium tuberculosis*, results show that downregulation of either *ppk1* or *ppk2* causes the failure of survival in macrophages, proving its role as key factor in the intracellular life (Sureka *et al*., 2007; Sureka *et al*., 2009).

PolyP degradation is accomplished by an exopolyphosphatase, designated Ppx that belongs to the Ppx/GppA family. The enzyme acts by breaking down the polymer from the end of the chain into inorganic phosphate units and contributes to maintain the dynamic balance of polyP and phosphate levels in the cell (Akiyama *et al*., 1993; Miyake *et al*., 1999). Interestingly, bacteria lacking Ppx exhibited increased resistance to complement-

mediated killing in *Neisseria meningitidis* (Zhang *et al*., 2010). Ppx is also required for survival inside the necrotic lung lesions produced by *M. tuberculosis* (Thayil *et al*., 2011). The genome of *Corynebacterium glutamicum* ATCC13032, encodes two *ppx* genes: *NCgl0396* (*ppx1*) and *NCgl0938* (*ppx2*), but Ppx2 is the major exopolyphophatase with substrate specificity toward short-chain polyP (Lindner *et al*., 2009). In the case of *M. tuberculosis* H37Rv, the genome also contains two genes encoding putative Ppxs, namely *Rv0496* and *Rv1026*. While the *Rv0496* encoded protein has shown to possess Ppx activity, the role of *Rv1026* remains unknown since its product has not been able to degrade polyp in vitro, although both proteins have low ATPase and ADPase activities that can be inhibited by the hyperphosphorylated guanine nucleotide alarmone (p)ppGpp (Thayil *et al*., 2011; Choi *et al*., 2012). Previous studies suggested that *Rv1026* may be involved in an adaptive response to amino acid starvation and its up-regulation might reflect the adaptive response to stress within the macrophage (Srivastava *et al*., 2007). It has been classified as an essential gene by Himar1-based transposon mutagenesis of *M. tuberculosis* (Sassetti *et al*., 2003). The main reactions involved in polyP metabolism can be summarised as follows:

PolyP synthesis

Polyphosphate kinase (PPK1)

$$nATP \leftrightarrow polyPn + nADP$$

PolyP degradation

Polyphosphate kinase (PPK2)

$$polyPn + GDP \leftrightarrow GTP + polyPn\text{-}1$$

Exopolyphosphatase (PPX)

$$polyPn \rightarrow polyPn\text{-}1 + Pi \rightarrow nPi$$

In *Escherichia coli*, polyP plays an important role in cell physiology during the stringent response which is regulated principally by (p)ppGpp, the effector, synthesized by RelA and SpoT in response to limiting conditions (Magnusson *et al*., 2005; Braeken *et al*., 2006). In several species of the genus *Mycobacterium*, polyP accumulation results in the appearance of visible granules under certain stress conditions (Ward *et al*., 2012). In *M. tuberculosis*, which is able to survive and replicate within the hostile environment inside macrophages and can lie dormant in humans for years, polyP has been implicated in the persistence. It has also been demonstrated that the Rel protein catalyzes the synthesis and hydrolysis of (p)ppGpp, regulating its intracellular levels and consequently the ability to survive long-term starvation in culture (Primm *et al*., 2000; Avarbock *et al*., 2005).

In *E. coli*, the amount of polyP is regulated by a coordinated activity between Ppx and Ppk and increments of polyP levels following stress, as a result of the suppression of Ppx activity by the effect of the alarmone (p)ppGpp and the expression of *ppk1* in stationary phase. This leads to an accumulation of the polymer due to a boost in its biosynthetic rate (Kuroda and Kornberg, 1997; Manganelli, 2007; Achbergerová and Nahálka, 2011; Choi *et al*., 2012). On the other hand, in mycobacteria, polyP acts on a signalling path way where polyP is key for the induction of *rel* and the biosynthesis (p)ppGpp during stationary phase, acting upstream of (p)ppGpp, unlike other bacteria such as *E. coli* and *Streptomyces lividans* where it occurs downstream and the deletion of *ppk1* does not provoke variations in either the expression of *rel* gene or the biosynthesis (p)ppGpp (Chouayekh and Virolle, 2002; Sureka *et al*., 2007). Thus, in *M. tuberculosis*, the induction of *rel* gene during the stationary phase is regulated by the sigma factor σ^E, which is related to the response under stress conditions, growth in macrophages and pathogenesis (Rodrigue *et al*., 2006; Donà *et al*., 2008). Moreover, it has been shown that

the two-component system MprAB modulates the transcription of *sigE* during stress where MprB phosphorylates MprA using polyP as phosphate donor, activating *mprAB* and *sigE* expression (Fig. 5.2). Interestingly, the activation does not occur in *ppk* mutants but only in wild-type strains, and down-regulation of *ppk1* impairs the ability of growing inside the cytoplasm of the macrophage which is a phosphate-lacking environment (Manganelli *et al*., 2001; He *et al*., 2006; Pang *et al*., 2007; Sureka *et al*., 2007). Recent studies have demonstrated that low levels of phosphate activate the *ppk1* transcription via two different regulator factors that could bind its promoter: the phosphorilated response regulator RegX3 (from another two-components system, the SenX3-RegX3) and SigE; forming a regulated network where *ppk1* connects a pair of two-components systems during phosphate scarcity (Sanyal *et al*., 2013).

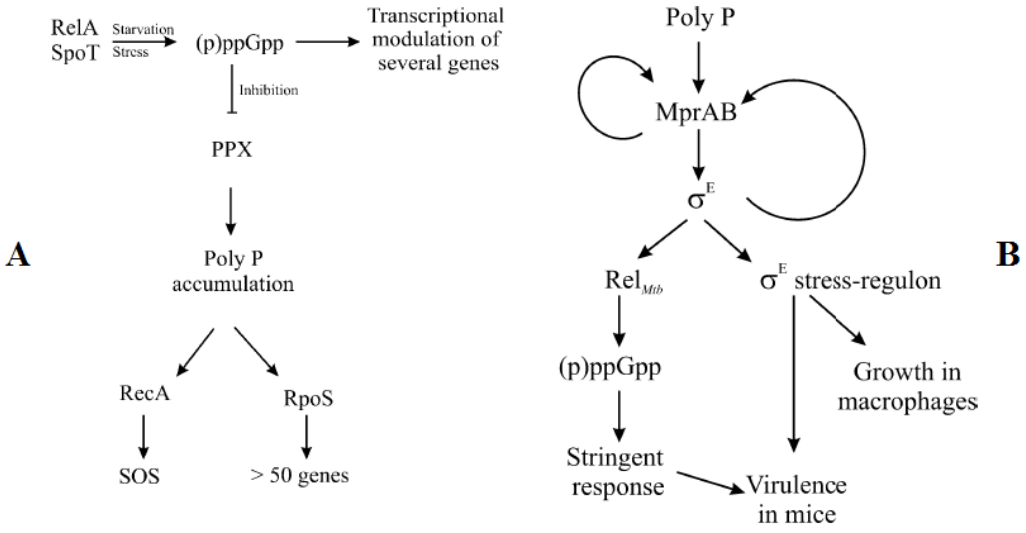

Figure 5.2: Schematic representations of the signalling cascades where polyP is involved in bacteria. A.- Pathway of stringent response development in *E. coli* showing polyP role. B.- Stress-induced signalling pathway in mycobacteria starting from polyP. (Adapted with permission from Manganelli, 2007 and Sureka *et al*., 2007. Licence Nº3244860716435).

Understanding the basis of *M. tuberculosis* persistence is an important step in tackling latent tuberculosis infection, where polyP should play a crucial role. The majority

of the studies available in polyP metabolism have been focused in the biosynthesis of the polyP, and therefore the role of polyphosphate kinases, rather than the degradation of polyP by the exopolyphosphatases. So far, studies have shown pleiotropic effects as result of the lack of Ppk function, which is perhaps not strongly relevant on phosphate usage during active growth of the cell because, as it has been said, the organisms are still able to overcome the condition and accumulate polyP regardless the mutation, therefore focusing in polyphosphate kinases role might not be the right strategy. On the other hand, exopolyphosphatases and its importance in persistence have not been studied, and then little is known about the cellular and molecular functions of mycobacterial Ppxs. Considering that *M. tuberculosis* faces a harsh intracellular environment in macrophages where the essential phosphate supply is extremely poor, the role of the exopolyphosphatase activity in persistence and infection appears as an interesting topic to be studied.

The study described in this chapter aimed to determine the potential role played by exopolyphosphatases and polyP in phosphate metabolism during phosphate starvation in mycobacteria. Two exopolyphosphatases homologs were found in the genome of *Mycobacterium smegmatis* mc^2155, namely *MSMEG_0939* and *MSMEG_5413*; deletion mutants of each gene were generated by specialised transduction and the strains were tested on the ability to survive under phosphate limiting conditions.

5.2 RESULTS

5.2.1 Identification of putative *M. smegmatis* exopolyphosphatases

Using BLAST, two putative exopolyphosphatases homologous genes were identified in *Mycobacterium* species genomes. The Ppx protein sequence from *Escherichia*

coli K-12 (NCBI Reference sequence NP_416997.1) was used as a query. In *M. tuberculosis* H37Rv, *Rv0496* (score 57.8, Id 23%, E-value $6e^{-10}$) and *Rv1026* (score 70.5, Id 27%, E-value $4e^{-14}$) were predicted to encode exopolyphosphatases; meanwhile, in *M. smegmatis* mc^2155, *MSMEG_0939* (score 70.9, Id 24%, E-value $5e^{-14}$) and *MSMEG_5413* (score 70.1, Id 28%, E-value $1e^{-13}$) showed to be, respectively, the identified homologs.

5.2.2 Deletion of both *MSMEG_0939* and *MSMEG_5413* genes produces slower growth rate in *M. smegmatis*

Using allelic exchange substrates, the apramycin and hygromycin antibiotic resistance cassettes were transduced into *M. smegmatis* mc^2155 strain in order to replace regions of the exopolyphosphatase genes, *MSMEG_0939* and *MSMEG_5413*, respectively. Three mutant strains were generated, namely *ΔMSMEG_0939*, *ΔMSMEG_5413* and *ΔMSMEG_0939-5413* depending either on the single or double gene disruption caused. Each deletion was checked by Southern blot analysis, also confirming the introduction of the resistance cassettes and discarding any possible leaking RNA transcription. As it is mentioned in the methods, serial dilutions were spotted on both TSB and Sauton agar plates in order to check colony morphology alterations, the deletions of the genes did not produce alterations in any of the mutants grown on the media mentioned above compared to the wild-type strain used as control (Fig. 5.3 A). No clumping effect was observed in liquid media either, although, the double mutant strain showed a slower growth rate and reached lower OD value at stationary phase compared to the wild-type and single mutants strains (Fig. 5.3 B). Since the morphology does not show any change between the strains, the OD values shown by the strains are reliable in terms of the growth rate, which is also consistent with the data obtained by cell-counting (Fig. 5.4).

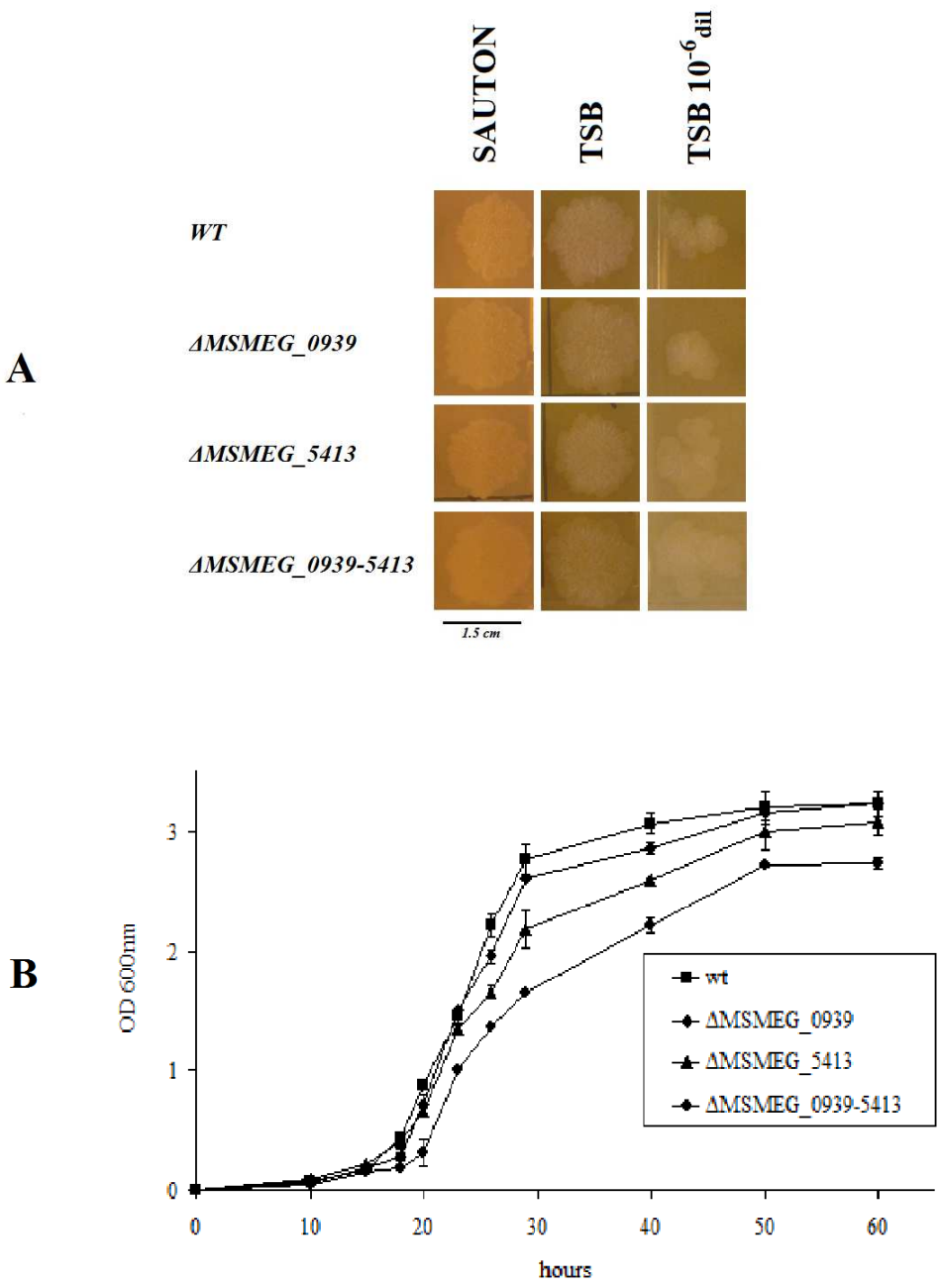

Figure 5.3: Growth characteristics of *ppx* mutants of *M. smegmatis* mc^{2}155. A- Colony pictures from 10 µl of culture spots on different media, left and centre columns: 10^{-1} dilutions on Sauton and TSB-agar, respectively, right column: 10^{-6} dilution on TSB-agar. Cultures were grown in Sauton and TSB liquid media at 37ºC until stationary phase, spotted on respective solid media and incubated for 3 days until colonies were visible. B- Growth curves for control and mutant strains grown in 50 ml of TSB media at 37ºC and 180 rpm of agitation. Values and error bars shown were obtained from experiments performed in duplicates.

5.2.3 *MSMEG_0939* and *MSMEG_5413* genes have a crucial role in phosphate supply from intracellular polyP during phosphate starvation

As it was mentioned in the introduction, polyP metabolism is involved in stress and stringency response. Several studies carried out in *E. coli* and *Pseudomonas aeruginosa* have been focused in the function of *ppk1* in bacterial survival within harsh environments (Rao and Kornberg, 1996; Kuroda *et al*., 1999) and, specifically, nutrients starvation and oxidative stress (Sureka *et al*., 2007); although, the role of the exopolyphosphatase activity in phosphate metabolism has not been carefully studied. In order to decipher the effect of *ppx* genes deletion in phosphate metabolism, mutant strains were subjected to phosphate starvation assays. The strains were grown until stationary phase in rich TSB media and later transferred into a defined minimal Sauton were phosphate was not added. Details are described in materials and methods section.

In order to test the growth dynamic, optical density (OD) measurements and cell-counting were carried out. During phosphate starvation treatments, the single mutant strains *ΔMSMEG_0939* and *ΔMSMEG_5413* did not seem to suffer major effects in the growth dynamic due to the lack of one of the exopolyphosphatases. The OD values demonstrated that the the single mutants were able to grow in the absence of phosphate showing a similar growing pattern than the wild-type strain under the same conditions. A slighty reduced growth was shown by single mutants in the absence of phosphate, which was not larger than one order of magnitude in terms of cell viability, and their growth seemed to be only limited by the amount of phosphate available. On the other hand, the lack of both putative exopolyphosphatases produced a negative effect under the conditions tested, the OD values obtained showed that cells were not able to grow when phosphate

was removed from the environment; surprisingly, the same effect was observed even when the double mutant strain was grown in the presence of phosphate (3 mM KH_2PO_4 in Sauton medium), where apparently the uptake or the utilisation of the extracellular phosphate available was impaired. Moreover, while the OD measurements showed no growth for the strain (Fig. 5.4), the viability tests demonstrated that the lack of both genes produced a lethal effect undergoing growth in Sauton minimal media (Fig. 5.5). The presence of at least one of the putative exopolyphosphatases genes suffices to survive under phosphate scarcity, strongly suggesting that intracellular polyP was degraded and used by the wild-type and single mutant strains to overcome the starvation, while the double mutant was not able to use polyP via another pathway.

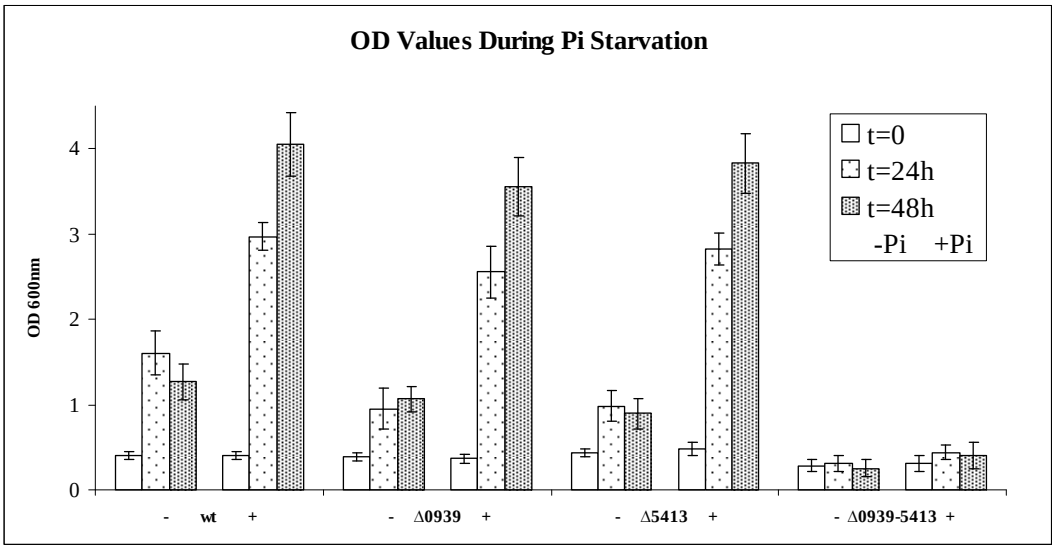

Figure 5.4: Optical density measurements for *ppx* mutant strains of *M. smegmatis* mc²155 during phosphate starvation. Cells previously grown in TSB medium until stationary phase were washed two times with Sauton medium without phosphate and diluted until OD_{600nm}=0.4 where the starvation experiment started. Strains were grown in Sauton media with (control +Pi) and without (-Pi) phosphate supply during 48 hours at 37ºC in agitation and growth was monitored by optical density. OD was measured every 24 hours in order to test the effect of gene deletions. The lack of both exopolyphosphatases produced a lethal effect in Sauton medium even in the presence of Pi. Values and error bars taken from three experiments carried out independently.

A

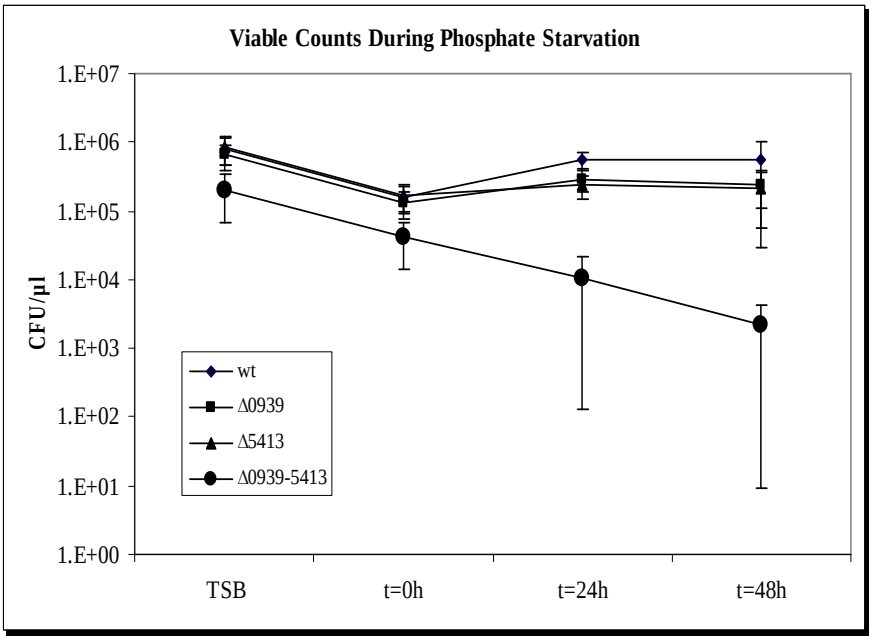

B

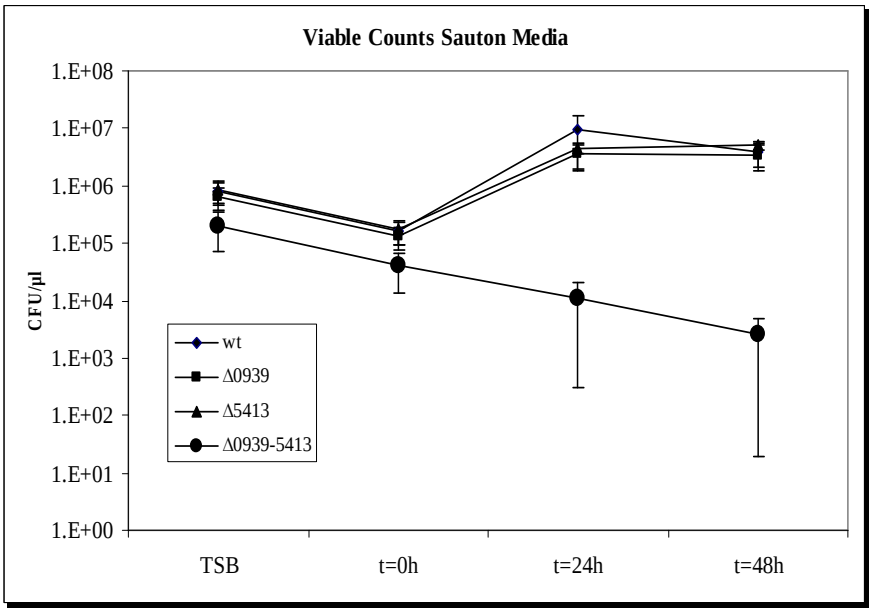

Figure 5.5: Viability test for *ppx* mutant strains of *M. smegmatis* mc^{2}155 during phosphate starvation. Cells previously grown in TSB medium until stationary phase were washed two times with Sauton medium without phosphate and diluted until OD_{600nm}=0.4 where the starvation experiment started. Strains were grown in Sauton media without (A) and with (B) phosphate supply during 48 hours at 37ºC in agitation and viability was monitored by cell counting on TSB plates by plating 25 µl of -3, -4, -5 and -6 dilutions. Viable cell counting was performed at the end of the incubation in TSB, the beginning of the starvation and every 24 hours in order to test the effect of gene deletions. Wild-type and single mutant strains were able to survive while undergoing Pi starvation and showed similar growth patterns. The lack of both exopolyphosphatases produced a lethal effect in Sauton medium even in the presence of Pi. Values and error bars taken from three experiments carried out independently.

5.2.4 Deletion of *MSMEG_0939* and *MSMEG_5413* genes induce polyP accumulation during phosphate starvation

Inasmuch as intracellular levels of free phosphate are limited and must be maintained at a concentration close to 10 mM (Rao *et al*., 2009), the results shown in section 5.2.3 suggested that the phosphate consumption and usage during the starvation should be dependent on polyP, thereby the double mutant strain should exhibit high levels of polyP as result of the inability to degrade the polymer; on the other hand, wild-type and single mutant strains should exhibit similar levels of polyP due to the usage of polyP as phosphate source. In order to test this hypothesis and to determine whether the genes *MSMEG_0939* and *MSMEG_5413* play a role in the utilisation of polyP, the cellular polyP contents of every strain were measured by a DAPI-based assay. Levels were quantified at each stage were growth and viability was tested, the amounts of polyP quantified were normalised in terms of the protein content, as a ratio between polyP and protein amounts.
The results showed that deletions did not seem to have a significant effect in the amounts of polyP displayed by the strains when they were incubated in a rich-media as TSB and abnormal polyP accumulation or depletion were not observed (Fig. 5.6 A).

As it was mentioned, polyP levels were quantified during the incubation in Sauton medium with and without phosphate (0, 24 and 48 hours). The results showed that whereas the wild-type and the single mutant strains exhibited similar levels of polyP, the lack of both exopolyphosphatases produced an accumulation of approximately 5-fold at the end of the incubation (Fig. 5.6 B); those polyP values compared to the ones found at the beginning of the starvation suggested that the phosphate used by the wild-type and single mutants must come from the degradation of polyP, since the strains were actively growing and dividing without any other source of phosphate available rather than the polyP. On the

other hand, the double mutant strain showed similar levels of polyP than the initial condition, indicating that the cells did not use polyP as a source of phosphate and, as it has been shown by cell counting, they underwent cellular death.

The wild-type and single mutant strains tested under control conditions (Sauton media with phosphate) contained similar amounts of polyP than after growing in TSB, since these strains were actively growing and dividing it is valid to assert that new polyP was synthesised from the polyP available in the medium, keeping the ratio polyP/mass on a relatively constant level. Interestingly, the double mutant strain displayed a higher content of polyP even though cell-death was observed.

These results demonstrate that the uptaken phosphate from the medium has been directed to the synthesis of polyP but without the ability to be degraded and used in the case of the double mutant strain, which is likely the cause of the lethal effect observed (Fig. 5.6 C); moreover, the experiments also showed differences in the polyP levels between the single mutant strains. While the *ΔMSMEG_5413* content was similar to the wild-type strain one in every condition tested, the levels shown by *ΔMSMEG_0939* strain where approximately 1.5-fold higher, confirming previously published results where different activities and/or functions were ascribed and hypothesised to each exopolyphosphatase (Thayil *et al*., 2011; Choi *et al*., 2012). Although, these results suggested a redundant effect for the genes, since the presence of one of them suffices for the survival of the organism and the use of phosphate units from the polyP during the starvation, where the metabolism relies totally in polyP.

A

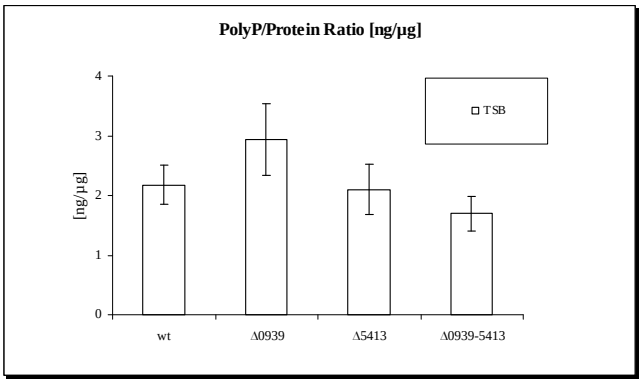

B

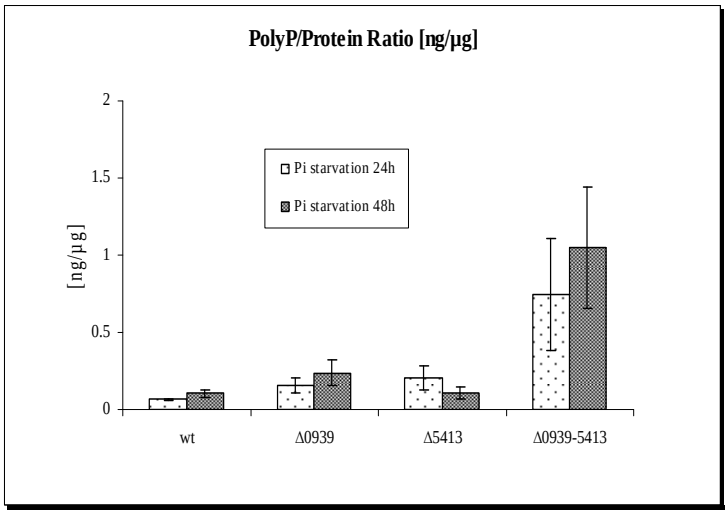

C

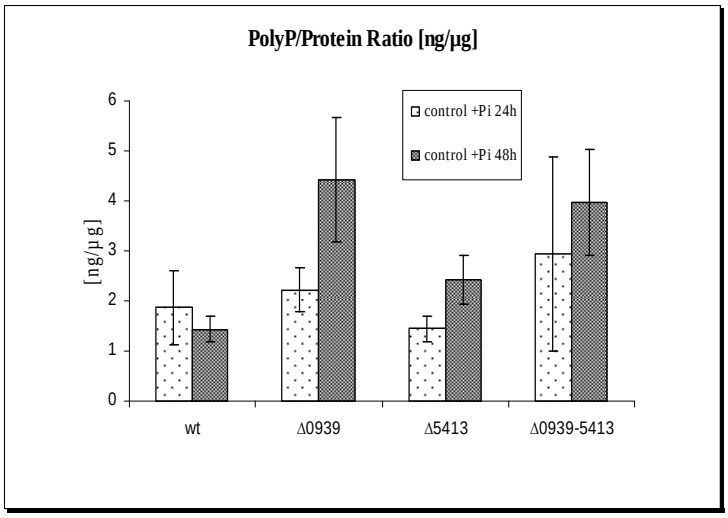

Figure 5.6: Effect of *ppx* genes deletions in polyP content during Pi starvation in *M. smegmatis* strains. Bar chart showing polyP levels of wild-type, *ΔMSMEG_0939*, *ΔMSMEG_5413* and *ΔMSMEG_0939-5413* strains during incubation in TSB (A) and Sauton media without (B) and with phosphate (C). Cells previously grown in TSB were washed and incubated in fresh Sauton media –Pi and +Pi during 48 hours at 37ºC. Samples were taken at 0, 24 and 48 hours of the incubation and polyP levels were measured using a DAPI-based fluorescence method. Data collected from three independent experiments.

In order to avoid the lethal effect of the double mutation, gene complementation attempts were carried out by introducing the multicopy-replicating plasmid pMV261, carrying either *MSMEG_0939*, *MSMEG_5413*, *Rv0496* or *Rv1096* into the double knockout mutant; additionally, a control recombinant strain was developed carrying only the vector without any of the genes. The double mutant strains bearing the constructs were incubated under the conditions already described, but the initial incubation in TSB was extended up to sixty hours due to the slow-growth pattern shown by complemented strains. OD values were measured during the experiment in the same way described above and the polyP levels were quantified after 48 hours of starvation. Surprinsingly, the polyP levels shown by the double mutant after 48 hours of incubation in Sauton medium were approximately 10-folder and 5-folder (Sauton without and with phosphate, respectively) higher compared to the levels found in the previous experiment, while the complemented strains showed similar or even higher levels of polyP than the double knockout mutant (Fig. 5.7). Moreover, the complementation assays were not successful, since the OD measurements showed that the complemented strains were not able to survive the incubation in Sauton media (Fig. 5.8).

5.3 DISCUSSION

Using the *E. coli* K-12 exopolyphosphatase sequence already described as query (Akiyama *et al*., 1993; Zago *et al*., 1999), I identified two putative exopolyphosphatases in the *M. tuberculosis* HRv37 genome, namely *Rv0496* and *Rv1026*, as it was predicted by previous studies (Lindner *et al*., 2009). At the time when this work was carried out, Thayil *et al*. and Choi *et al*. attempted to determine exopolyphosphatase functions in these two putative exopolyphosphatases and showed each as having distinct biochemical activities:

only *Rv0496* was found able to degrade polyP (preferable short chains) but *Rv1026* had no detectable exopolyphosphatase activity *in vitro*. The *M. smegmatis* mc^2155 homologues, *MSMEG_0939* and *MSMEG_5413*, were chosen in order to check their roles in bacterial survival under phosphate starvation and the *in vivo* polyP degradation by generating single mutants and a double mutant strain. Surprisingly, even though *Rv1026* was predicted to be essential in *M. tuberculosis*, I was able to generate a *MSMEG_5413* knockout in *M. smegmatis*. My results showed a high degree of redundancy between both *M. smegmatis* putative exopolyphosphates since the presence of either gene was enough to rescue the double mutant strain from cell death while growing in Sauton medium. Additionally, these data strongly suggested that polyP is the only source of inorganic phosphate while growing in minimal medium like Sauton, which is available by the action of exopolyphosphatases.

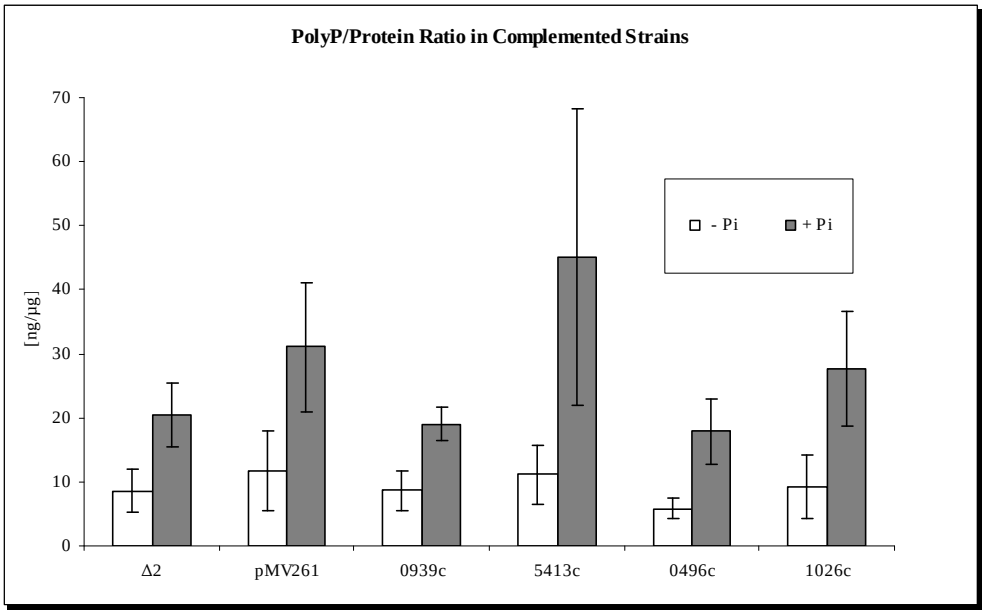

Figure 5.7: polyP content during Pi starvation in complemented *ΔMSMEG_0939-5413* strains. Bar chart showing polyP levels during incubation in Sauton media without (-Pi) and with phosphate (+Pi). Cells previously grown during 60 hours in TSB were washed and incubated in fresh Sauton media during 48 hours at 37ºC. Samples were taken at the end of the incubation (48 hours) and polyP levels were measured using a DAPI-based fluorescence method. Complementation was carried out using the vector pMV261, where the genes *MSMEG_0939, MSMEG_0939, Rv0496 and Rv1026* were cloned. Δ2: double mutant, pMV261: only vector control, c: complemented strains. Data shown collected from three independent experiments.

A

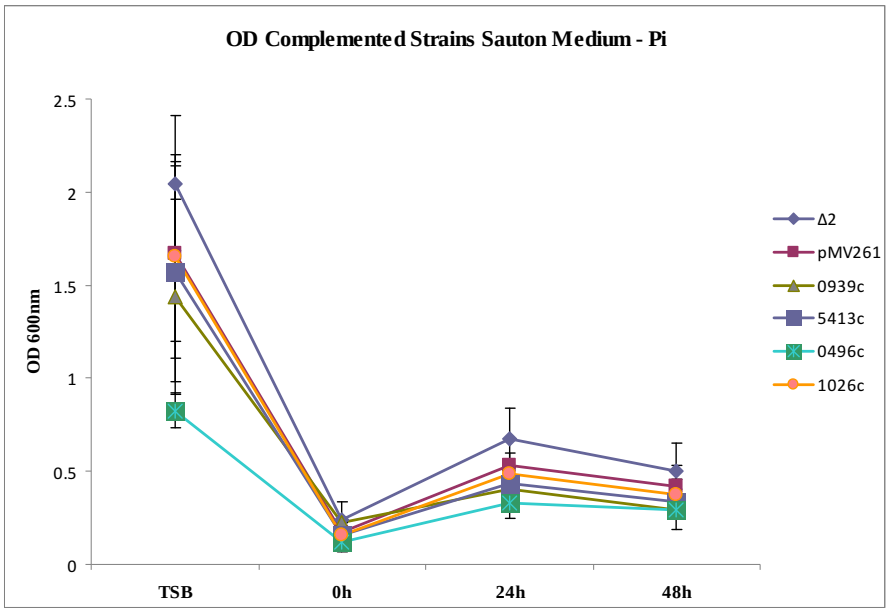

B

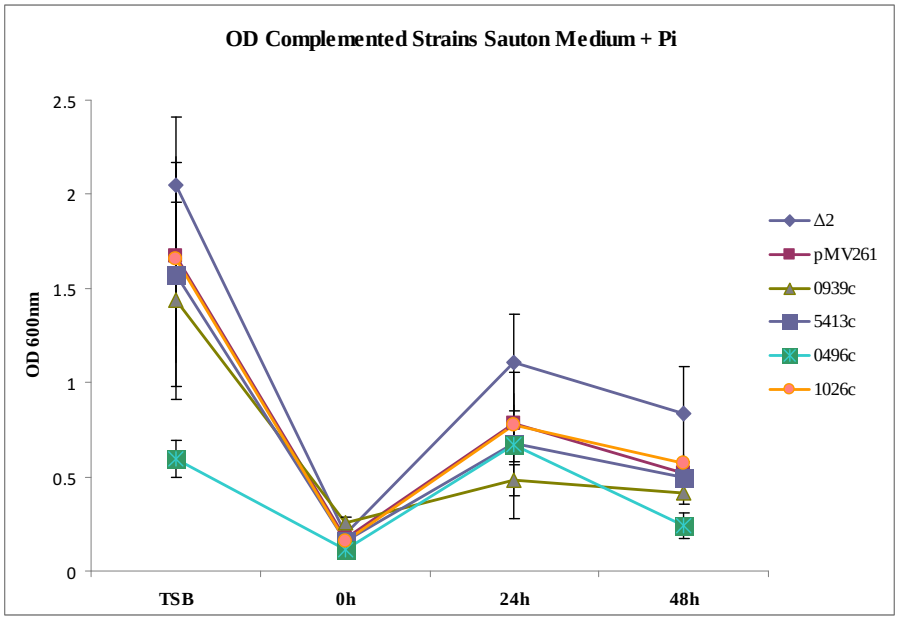

Figure 5.8: OD values for the growth of complemented *ΔMSMEG_0939-5413* strains during phosphate starvation. Cells previously grown in TSB medium during 60 hours were washed two times with Sauton medium without phosphate and diluted until OD_{600nm}=0.4. Later, the strains were grown in Sauton media with (+Pi) and without (-Pi) phosphate during 48 hours at 37ºC in agitation and growth was monitored by optical density. OD was measured every 24 hours in order to test the effect of the complementation which was carried out using the vector pMV261 where the genes *MSMEG_0939, MSMEG_0939, Rv0496 and Rv1026* were cloned. Δ2: double mutant, pMV261: only vector control, c: complemented strains. Data shown collected from three independent experiments.

Nevertheless, single mutants clearly exhibited different physiological roles for each gene, judging by the difference in polyP content described. The data support the idea that each gene has a different function but still retaining exopolyphosphatase activity *in vivo* since the double mutant was not able to survive in Sauton medium even in the presence of phosphate. The strains present no colony morphology alterations and parallel analysis of capsule α-glucan and total lipid profile in the *ΔMSMEG_5413* strain did not show, at least, any change attributable to the cell envelope (data not shown). In the case of *MSMEG_5413*, the genetic context shows that the gene is downstream *MSMEG*_5414, both forming part of the same operon. This gene encodes for a septum formation initiator protein DivIC, whose function and link with the exopolyphosphatase encoded by *MSMEG_5413* need to be elucidated, due to the nature of DivIC it is likely that the function of this exopolyphosphatase could be related to cell division, perhaps doning phosphate groups. On the other hand, the genetic context of the gene *MSMEG*_0939 reveals a close distance to the genes that encode for the two component system SenX3-RegX3, *MSMEG_0936* and *MSMEG_0937*, respectively. Therefore, a function directly related to the regulation of phosphate-uptake, -use and -store could be hypothesised for *MSMEG_0939*, where the degradation of polyP should be the most important one, and now supported by the activity described in the literature (Thayil *et al*., 2011; Choi *et al*., 2012). In this case, it is likely that the exopolyphosphatases are under the strict regulation of the SenX3-RegX3 system, perhaps a minimal medium like Sauton triggers a stringent response where the phosphate uptake is completely directed to the synthesis of polyP and the phosphate supply relies exclusively on the exopolyphosphatase activity (not present in the double mutant), independently of the phosphate available in the media, which the double mutant used in this study was not able to use. If the regulation of the exopolyphosphatase

activity was simple, a normal complementation assay should rescue the double mutant from the death while growing in Sauton medium; since the expression using the pMV261 vector is constitutive, a stress condition could be generated that either prevents the activity of the exopolyphosphatases via (p)ppGpp or the organism undergoes a general metabolic dysregulation.

Due to the diversity of metabolic processes in which polyP is involved (Brown and Kornberg, 2008) and considering that representative genomes of the Actinomycetales in general contain both *ppx* genes, it seems very likely that their functions had reached a high level of specialisation where each exopolyphosphatase could have a specific role at different stages, under different conditions or having substrate specificity as it has been said for polyP-length and Ppx2 (Lindner *et al*., 2009). For instance, a BLAST analysis showed a high degree of identity between *Rv1026* and *NCgl0938* (52% of identity, E=2e-102), but functionally the enzymes have not shown to possess similar exopolyphosphatase behaviour *in vitro* (Lindner *et al*., 2009; Choi *et al*., 2012), likely suggesting that the activity *in vivo* is regulated by additional factors and under different environmental conditions or stages that could be biasing the results and might have not been considered when *in vitro* reaction are performed, like protein complexes or reaction involving several proteins. This study has shown that in *M. smegmatis* the polyP degradation by Ppxs consists in the only source of inorganic phosphate during starvation, an interesting point, since that could also be the scenario that *M. tuberculosis* could face as an intracellular pathogen and during dormancy as well. Additionally, it supports the idea of both homologous exopolyphosphatases having different biological functions, but showing signs of redundancy under certain conditions that must be studied in great detail since gene expression is highly regulated and critical in this pathway (Manganelli, 2007). Then, the

next goal in this context must be to determine substrate specificity, expression conditions and gene regulation for each exopolyphosphatase.

5.4 MATERIALS AND METHODS

5.4.1 Bacterial strains and growth conditions

M. smegmatis mc^2155 strain was used in all experiments as wild-type control and to generate mutant strains for the exopolyphosphatase homologous genes *MSMEG_0939* and *MSMEG_5413*. Using specialised transduction, three strains were generated, namely individual single mutants and double mutant strain (Table 5.1). Antibiotics concentrations used for selection in each case were hygromycin 100 μg/ml, apramycin 50 μg/ml and kanamycin 30 μg/ml. Colony morphology of the mutant strains was observed on both TSB and Sauton 1.5%-agar plates by spotting 10 μl of 10^{-1} to 10^{-6} dilutions from *M. smegmatis* cultures previously grown in TSB and Sauton media, respectively, until stationary phase. Plates were incubated at 37ºC until colonies were visible (3-6 days). The growth of the strains was measured in duplicates by optical density at 600 nm, 50 ml of TSB liquid cultures were grown at 37ºC, 180 rpm of agitation, and started using 1/1000 dilutions of previously grown cultures adding antibiotics according to the concentrations mentioned above. Sauton medium contains 0.05% (3.7 mM) KH_2PO_4, 2% glycerol, 0.4% L-asparagine, 0.2% glucose, 0.2% citric acid, 0.05% magnesium sulfate, 0.005% ferric ammonium citrate, at pH 7.0. Phosphate starvation assays were performed using Sauton medium prepared using Milli-Q water with no monopotassium phosphate added; in order to avoid traces of phosphate, the flasks were previously washed with acetic acid and all the

chemicals used were analytical grade, with no levels of phosphate detected. Liquid media were prepared adding 0.05% Tween-80 as surfactant agent.

5.4.2 Generation of mutant strains

Individual mutants were generated using allelic exchange constructs designed to replace the *MSMEG_0939* and *MSMEG_5413* genes with apramycin and hygromycin resistance cassettes, respectively. Sequences flanking the left and right of the genes were PCR amplified using the primers listed on Table 5.2 and *Van91I* restriction sites, following the procedure described in General Materials and Methods chapter to generate knockout phages. The double mutant strain was generated from the *ΔMSMEG_5413* mutant, using the phage designed to delete *MSMEG_0939*, to obtain *ΔMSMEG_0939-5413*, a double Apra-Hyg resistant strain. Each mutant was validated as *bona fide* by Southern blot analysis as described in General Materials and Methods section.

5.4.3 Phosphate starvation

Phosphate starvation assays were performed as it follows. Firstly, the strains were grown during 30 hours until stationary phase in 50 ml of TSB culture in aeration at 37ºC and 180 rpm. Each culture was split into two similar volumes and the cells collected by centrifugation and washed twice with Sauton media without phosphate. Cells were transferred into 20 ml of Sauton media with and without phosphate, diluting the cells until approximately an OD=0.4 and continuing the incubation for 48 hours in the same conditions. Samples of 1 ml were collected at the end of the incubation in TSB and every 24 hours during incubation in Sauton media in order to determine polyphosphate content. In addition, at the same stages, cell couting was carried out by plating 25 ul of cell

dilutions 10^{-3}, 10^{-4}, 10^{-5} and 10^{-6} on TSB-agar plates in duplicates. Phosphate starvation assay was carried out in triplicates, starting from independent cultures.

5.4.4 Complementation of mutant strains

The open reading frames for *MSMEG_0939, MSMEG_5413, Rv0496 and Rv1026* were PCR-amplified from *M. smegmatis* mc^2155 and *M. tuberculosis* H37Rv genomic-DNA, respectively, using the primers pairs Ms0939F/Ms0939R, Ms5413F/Ms5413R, pMV261-Rv0496F/pMV261-Rv0496R, pMV261-Rv1026F/pMV261-Rv1026R (Table 5.2). Amplified genes were cloned into the pMV261 vector using the primer-incoporated *BamHI* and *HindIII* cloning sites and the constructs generated were used to transform Top10 chemically competent *E. coli* cells using kanamycin for selection. Recombinant plasmids were purified, checked by DNA-sequencing and used to transform *M. smegmatis* strains by electroporation.

5.4.5 Polyphosphate extraction

PolyP extraction was performed using the method described by Ault-Riché *et al*., (1998). Samples of 1 or 2 ml of culture were taken and cell pellets collected by centrifugation for 3 min at 13,000xg and discarding the supernatant. Each pellet was resuspended in 0.3 ml of the a mix solution containing 4 M guanidinium thiocyanate (GITC), 50 mM Tris/Cl, pH 7 (or QG buffer, QIAGEN) and 50 µl of the suspension were used for protein amount determination using the BCA Protein Assay by Pierce (Biuret's method-based) as an indicator of amount of bacterial mass per sample. The suspension was incubated at 95ºC for 3 min, and 30 µl of 10% SDS was added. The mix was incubated at

95ºC for 2 min. Next, 300 µl of 100% ethanol and 5 µl of Glassmilk suspension were added to the tubes, which were then mixed by vortexing and incubated for 30 s at 95ºC. The mix was centrifuged at 13,000xg for 2 min and the supernatant was discarded. The pellet was resuspended in 200 µl of cold New Wash solution (5 mM Tris/Cl, pH 7.5, 50 mM NaCl, 5 mM EDTA, 50% ethanol) and centrifuged at 13,000xg for 30 s. The pellet was resuspended in 100 µl of a solution containing 50 mM Tris/Cl, pH 7, 5 mM $MgCl_2$, 5 µg/ml DNAase and 5 µg/ml RNAase and incubated at 37ºC for 30 min. The suspension was centrifuged and the supernatant discarded. The pellet containing the polyP was washed twice with 200 µl of cold New Wash solution, centrifuged and supernatant discarded.

Finally, the polyP was collected two times by resuspending the pellet by vortex in 50 µl of water, incubating the sample for 2 min at 95ºC, centrifuging at 13,000xg, and saving the supernatant containing the polyP. The polyP samples were stored at -20Cº for no longer than 10 days.

5.4.6 Polyphosphate quantification assay

A DAPI (4',6-diamidino-2-phenylindole)-based assay was carried out for polyP quantification doing modifications to a protocol previously described by Aschar-Sobbi *et al*. (2008) and Díaz and Ingall (2010). Reactions of 250 µl volume were prepared in 96-well black microplates containing 125 µl HEPES (20mM final concentration), 1 µl DAPI (10 µM final concentration), 119 H_2O and 5 µl of each sample of polyP on triplicates. In order to standarise the quatification, each plate that was read included wells with known amounts of commercial polyphosphate (KeraFast, High MW P700) from 0-20 µM and these readings were used to plot standard curves. The amounts of polyphosphate were finally expressed as weight [µg], assuming that 1 µg of polyP in a volume of 2 ml

corresponds to 6.3 μM of orthophosphate, using the -PO_3 group as a monomeric unit (Aschar-Sobbi *et al*., 2008). The shift in fluorescence was measured using a PHERAstar*FS* microplate reader (BMG LABTECH) at 415 nm (excitation) and 525 nm (emission) wavelengths. Blank reactions were prepared using 5 μl of water instead of polyP. Diluted polyP samples 1/10 and 1/20 were also measured using the same method when signals were saturated. The amount of polyP obtained in μg from each sample was divided by the amount of proteins present in the same sample, and a ratio between amount of polyP and protein per sample was calculated.

Table 5.1
Plasmids, Phages and Bacterial Strains used in this study

Plasmid, Bacterial Strains and Phages	Description	Reference
Plasmids		
p0004s	Cosmid for cloning allelic-exchange substrates. Used for specialized transduction. Contains λphage *cos* site and *Hyg^R-sacB* cassette.	Bardarov *et al*., 2002
p*ΔMSMEG_0939*	Derivative of p0004s designed for allelic exchange of *M. smegmatis MSMEG_0939.*	This work
p*ΔMSMEG_5413*	Derivative of p0004s designed for allelic exchange of *M. smegmatis MSMEG_5413.*	This work
pMV261	*Escherichia coli*-mycobacterial shuttle vector, *aph* from Tn903, *hsp60* gene promoter from *M. tuberculosis.* Kan^R.	Stover *et al*., 1991
pMV261-*MSMEG_0939*	*MSMEG_0939* cloned into pMV261. Kan^R.	This work
pMV261-*MSMEG_5413*	*MSMEG_5413* cloned into pMV261. Kan^R.	This work
pMV261-*Rv0496*	*Rv0496* cloned into pMV261. Kan^R	This work
pMV261-*Rv1026*	*Rv1026* cloned into pMV261. Kan^R	This work
Phages		
phAE159	Conditionally replicating shuttle phasmid derived from the lytic mycobacteriophage TM4.	Bardarov *et al*., 2002
ph*Δ*MSMEG_0939	Derivative of phAE159 obtained by cloning pΔ*MSMEG_0939* into its unique *PacI* site.	This work
ph*Δ*MSMEG_*5413*	Derivative of phAE159 obtained by cloning pΔ*MSMEG_5413* into its unique *PacI* site.	This work
Bacteria		
M. smegmatis mc^{2}155	Parental strain, *ept-1* mutation conferring high efficiency of plasmid transformation.	Snapper *et al*., 1990
ΔMSMEG_0939	Null mutant of *MSMEG_0939* in mc^{2}155 (replaced by a Apra^R cassette).	This work
ΔMSMEG_5413	Null mutant of *MSMEG_5413* in mc^{2}155 (replaced by a Hyg^R cassette).	This work
ΔMSMEG_0939-5413	Double mutant of mc^{2}155 in which chromosomal copies of *MSMEG_0939* and *MSMEG_5413* were replaced by Apra^R and Hyg^R cassettes, respectively.	This work

Table 5.2
List of primers used in this study

Primers for generation of allelic exchange substrates	
MSMEG_0939-LL	5' TTTTTTTTCCATAAATTGGCTCGAGGTAGCCCTTCTTGCCC 3'
MSMEG_0939-LR	5' TTTTTTTTCCATTTCTTGG GGACAGCTCCAGCGAACCGCCG 3'
MSMEG_0939-RL	5' TTTTTTTTCCATAGATTGGCTGGCTCGCCACCGAGCTCGCCG 3'
MSMEG_0939-RR	5' TTTTTTTTCCATCTTTTGGCGGCATCCCTGGCCGCGCCGGC 3'
MSMEG_5413-LL	5' TTTTTTTTCCATAAATTGGCGACGGCACCAACTACCGCGCACTG 3'
MSMEG_5413-LR	5' TTTTTTTTCCATTTCTTGGCGAATACGATCCCGAGCAGATCCAC 3'
MSMEG_5413-RL	5' TTTTTTTTCCATAGATTGGCGATCATCAACGCGACGTAG 3'
MSMEG_5413-RR	5' TTTTTTTTCCATCTTTTGGACGGCTGGGTTTCGTGATGC 3'
	LL forward primer for left flank, LR reverse primer for left flank, RL forward primer for right flank, RR reverse primer for right flank
Primers for generating plasmids for complementation (*BamHI* and *HindIII* sites underlined)	
Ms0939F	5' GACCCGTGCGGGATCCTGTGCTCGATGTGG 3'
Ms0939R	5' GGCTAGAAGCTTCTTATCGTCCGGCGTCGC 3'
Ms5413F	5' CTGGAGCGGATCCCATGGGTGTGAACGACC 3'
Ms5413R	5' CCGTTCGCTTTAAGCTTTCAGCTGATCG 3'
pMV261-Rv0496F	5' CACGGTCCAGGATCCGGTGGTCGATG 3'
pMV261-Rv0496R	5' GGTGTGAAGCTTTCATGGTTTGCTGCC 3'
pMV261-Rv1026F	5' CTGGTGGGGATCCAGTGGCGCTAACCCG 3'
pMV261-Rv1026R	5' TGTGGCAGAAGCTTCTTATCCGGCCAG 3'
Primers used for sequencing reactions	
pMV261-F	5' CCAGTGGCAGCGAGGACAAC 3'
pMV261-R	5' TGTGCAATGTAACATCAGAG 3’

5.4.7 Southern-blot confirmation

The mutant strains obtained were confirmed by Southern-blotting technique using a DIG probe as described in General Materials and Methods section. The following pictures show a diagram representing the digestion pattern of genomic DNA from wild-type and mutant strains on the left side. The right side of the pictures display the films obtained by hybridisation between the probes and the digested genomic DNA.

A

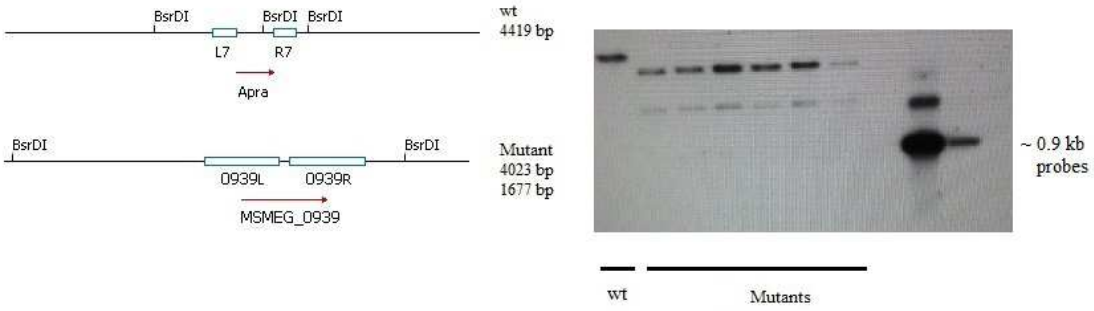

B

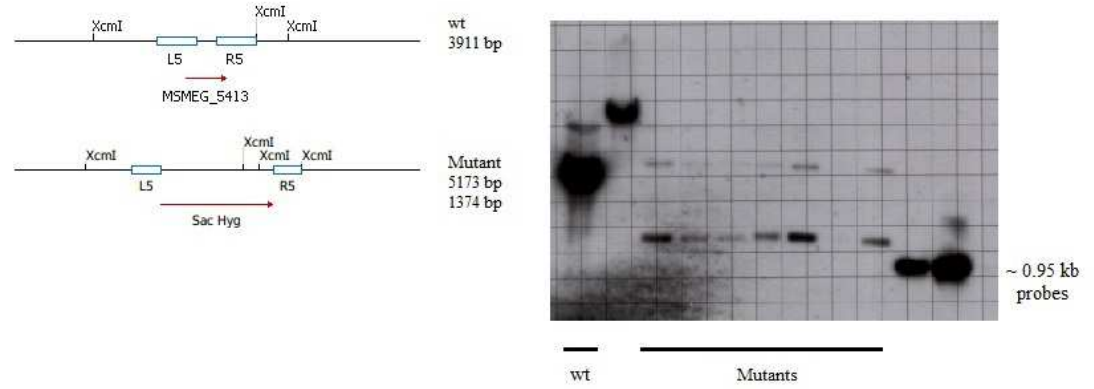

Figure 5.9: Southern-blot confirmation. The left sides of the pictures display the digestion pattern diagrams of genomic DNA from wild-type and mutant strains. Right sides display the films obtained by hybridisation between the probes and the digested genomic DNA. The diagrams include the restriction enzyme used and the expected sizes for each strain after the digestion; the films display the digestion pattern obtained for each strain tested and the probe was also used as molecular-weight size reference. The strains that showed the expected pattern were choosen to perform the experiments described in this chapter. L and R indicate the flanking regions, hyg-apra: hygromycin and apramycin resistance cassette, respectively. A- Includes three *ΔMSMEG_0939* lanes and three *ΔMSMEG_0939-5413* lanes. *B- ΔMSMEG_5413.*

CHAPTER 6

GENERAL DISCUSSION

Despite the major progresses achieved in the care and control of Tuberculosis (TB) since the mid-1990s, the development and identification of new diagnostics, drugs and vaccines is still a priority against the disease as well as better, shorter and cheaper treatments for all forms of TB, especially due to drug resistance and persistence. In this context, the efforts of molecular microbiology must be focused, firstly, on a good understanding of the molecular basis involved in the structure and biosynthesis of the cell envelope, and also on decipher the molecular mechanisms of bacterial survival in harsh conditions and dormancy.

The main objective of this study was to explore novel areas inside the proposed fields by using different strategies, in order to tackle topics mainly unexplored, "forgotten" or unproductive during the previous years. Surprisingly, during the course of my project, several publications appeared in the topics chosen, complementing my results and also supporting the criteria behind the choice taken. Summarising, four projects were carried out: three regarding the mycobacterial cell envelope and one regarding the survival in order to find new genetic determinants (*i.e.*, transposon mutant library) and to study topics not yet fully explored (*i.e.*, capsular α-glucan biosynthesis, mycolic acid transport and the role of exopolyphosphatases). In this project, searching for defective cell-cell interactions (as the lack of biofilm formation) or the selection of strains with visual defective morphologies have demonstrated to be an effective tool to use in order to look for key genes related to cell wall metabolism. The selected or "randomly"-discovered genes studied in this project were related to functions as different as transport or division, and also to metabolites as different as lipids, sugars or phosphate; but finally all of them genetically or metabolically related to cell wall biosynthesis, a key structure in the survival of mycobacteria.

The first strategy chosen to tackle the objectives proposed was based on random transposon mutagenesis, using *Mycobacterium smegmatis* as surrogate model for generating a Tn-mutant library, looking for colony morphology alterations and antibiotic resistance and using them as selection parameters of the screening. Although the lipid analysis performed did not display evidences of alteration in chemical composition in the strains as it was expected, since no changes regarding noncovalently bound glycoconjugates like PDIMs, PGLs, free mycolic acids, PIMs or SL were found by TLC analysis. Nevertheless, structural changes and increased sensitivity to rifampicin were associated to several diferent genes, for instance, *MSMEG_6387* (arabinosyltransferase A) and *MSMEG_0408* (type I modular polyketidesynthase), which are involved in lipid metabolism and whose homologous genes in *Mycobacterium tuberculosis* have been related to cell wall components (Escuyer *et al*., 2001; Alderwick *et al*., 2011), validating the technique used at the same time. Therefore, further projects should focused in elucidating, accurately, what are the chemical changes occurred and the factors involved in the alterations. In the specific case of the disruption of *MSMEG_3743*, previously describe to be part of a group of genes related to cell cycle and DNA segregation (Jakimowicz *et al*., 2007; Maloney *et al*., 2009), new structural changes were discovered in terms of DNA distribution and cell partitioning, adding precious information in a field which is still no deeply investigated. Moreover, a recently published study has shown similar results involving its homologs in *M. smegmatis* (Ginda *et al*., 2013), and also started to speculate about how the genes involved in cell division could be related to persistency, which is the other field that I tried to focus this project on and also showing that is a field which needs to be explored. Nevertheless, the mutant strains obtained in this project yet need to be used

to perform a sugar analysis in order to find a correlation between the chemical composition and the structural/functional defects found.

Regarding mycolic acid biosynthesis, at the beginning of this project its transport remained completely unclear and only hypothetical pathways were proposed (Takayama *et al*., 2005). Based on the known functions of a group of proteins belonging to the RND family called MmpL, the gene *mmpL3* was predicted to encode a glycolipid transporter and it was chosen as a candidate to transport trehalose monomycolate. As it was previously described by Domenech *et al*. (2005), in this project the gene was confirmed to be essential in *M. smegmatis* by developing a conditional expression system. Additionally, trying to obtain stronger results and a broader panorama of its function, the role of *mmpL3* in mycolic acid biosynthesis was addressed using two organisms who present mycolic acid as component of the cell wall, both belonging to the order *Actinomycetales*, namely *M. smegmatis* and *Corynebacterium glutamicum*. Using the conditional mutant and a set of *mmpL* mutants for the three orthologs present in *C. glutamicum*, the results showed *mmpL* to be involved in mycolic acid transport in both organisms. In the conditional *M. smegmatis* mutant, loss of the MmpL3 function produced a decrease of trehalose dimycolate (TDM) levels and also reduced mycolylation of arabinogalactan (AG); on the other hand, the complete loss of trehalose monocorynomycolates (TMCM), trehalose dicorynomycolates (TDCM) and AG-bound corynomycolates was observed in one of the *C. glutamicum* double mutants (Δ*NCgl0228-NCgl276)*. These results were published (Chemistry and Biology, 2012; 19(4):498-506) and surprisingly, while the paper was under revision, three new studies were published regarding MmpL3 functions, identifying it as the target of three drugs and one of them showing similar results (La Rosa *et al*., 2012; Tahlan *et al*., 2012; Grzegorzewicz *et al*., 2012). This is remarkable, due to the fact that

eleven out of twelve publications related to MmpL3 have been published only in the last twenty months, proving that the topic has become important and this project has been part of that process. Regarding the different publications, the characterisation of *mmpL3* as a gene involved in heme group transport in *M. tuberculosis* (Tullius *et al*., 2011) opened another door in order to delucidate the real function of the transporter, since it could be involved in more than one vital function and displaying two completely different roles with a high degree of promiscuity. That fact does not seem to be completely well understood and still need to be elucidated, since some results seemed to be contradictory. Therefore, MmpL3 remains as a key transporter and it keeps adding reasons to be consider as a good drug target candidate since several changes in the ratios of mycolic acids species occur during infection and also because it connects the metabolisms of two important virulence factor as TMM/TDM and trehalose, a key sugar during infection and nutrient scarcity, topic which has also been tackled in this project.

The project related to the capsule α-glucan transport did not accomplish its main objective, since the candidate genes selected did not show to be involved in the transport of α-glucan in *M. smegmatis* under the conditions tested. Nevertheless, the essentiality of *MSMEG_6369* was demonstrated by generating a conditional expression system for the gene, and also the mutant *ΔMSMEG_5059-5060* showed not to be able to grow using trehalose as a unique sole carbon, as it was proved by Kalscheuer *et al*. (2010) while these experiments were carried out, validating the methods and techniques used as strong tools to obtain new data, despite the fact that the main objectives were not accomplished. In the case of the *ΔMSMEG_5059-5060* strain, an interesting fact was observed, since the mutation seemed to activate the route to metabolise glycogen as unique carbon source when it was unable to recycle trehalose; it is known that some organisms accumulate

glycogen (glycogen accumulating organisms, GAO) in order to use it under certain conditions (*e.g*., anaerobic), even though mycobacteria do not belong to that group (in fact they accumulate polyphosphate) the metabolic repertoire could include the ability to induce the use of glycogen under stress conditions. Perhaps a genetic comparison between mycobacteria and GAO organisms could open a door to a better understanding of glycogen metabolism in the *Mycobacterium* genus. This topic yet have to be expanded due to the role that capsule plays in pathogenicity via the facilitation of the interaction with macrophages, the modulation of the induction of cytokines or its components acting as major polysaccharides antigens. The genetic and molecular bases underlying those processes need to be described and elucidated in order to find more drug targets.

Finally, considering the survival and dormancy as crucial processes in mycobacterial virulence, the role of inorganic polyphosphate (polyP) in survival under harsh condition was tested using a point of view not considered before. The majority of the publications and studies available at the beginning of this project were focused on the role and on the function of the enzyme polyphosphate kinase (Ppk) in virulence and stringent response (Brown and Kornberg, 2008), obtaining pleiotropic effects when generating knockout mutants. In this project, I decided to address the role of polyP in survival when the cells face absence of phosphate, but focusing in the two exopolyphosphatases (Ppx) present in mycobacteria instead of Ppk. The role of exopolyphosphatases in mycobacteria has also started to become an important area and a couple of publications appeared during the progress of this project, showing different in vitro activity for each Ppx among other functions (Thayil *et al*., 2011; Choi *et al*., 2012), supporting the data obtained and showing that further analysis are necessary in a nascent research topic.

The results obtained have shown that the polyP is the unique source of inorganic phosphate during phosphate starvation and it is supplied by the activity of the exopolyphosphatases, which seems to have a protective role during stress and likely having different physiological functions. As it was explained, the polyP and exopolyphosphatases are involved in complex signalling pathways related to the transcription of several genes and, undoubtedly, needing a very accurate regulation in terms of the levels of metabolites and depending on the stage of expression. The genetic context of both genes reveal interesting information about their potential functions; as it was stated, the gene *MSMEG_0939* must be related directly to the use of phosphate groups as a result of the degradation of polyP by removing the last phosphate residue. On the other hand, a very careful insight of the genetic context of *MSMEG_5413* reveals that downstream effects were likely to happen since it forms part of an operon and it must be transcribed as a polycistronic mRNA unit, since the gene overlapped with *MSMEG_5414*, involved in cell division and sporulation processes (Katis and Wake, 1999; Bennett *et al*., 2007), thus, analysis by fluorescence microscopy is needed in order to determine changes in the division function. The alignment of its genomic region with the equivalent one in the genome of *M. tuberculosis* reveals high level of synteny, and also shows that a nucleoside triphosphate pyrophosphohydrolase (encoded by *Rv1021*) seems to be transcribed as part of the same operon. In this case, the function is likely to be related to the synthesis (or degradation) of signalling molecules using the exopolyphosphatase as a phosphate donor and probably related to the stringent response. Moreover, the genome of *M. tuberculosis* shows a very close distance between *Rv1026* and genes related to the donation of phosphate groups to sugar and that could be related to the biosynthesis teichoic acids, where phosphate is a major component (Schneewind and Missiakas, 2014). Therefore,

even though no morphology alterations were found, a complete analysis of peptidoglycan, arabinogalactan and lypoglycans must be perform in the *ΔMSMEG_5413* strain in order to reveal the function of the gene, where the effect of the deletion could have not resulted in structural changes, but maybe in an impaired regulation of other genes. In this sense, *MSMEG_5413* is possible to be related to the cell wall biosythesis as a phosphate-donor to molecules involved in cell-shaping and cell wall composition; membrane-staining assays like the one performed with the *ΔMSMEG_3743* (Chapter 2) strain would also be suitable in order to find alteration in the shape or the septum formation at cellular level. As it has been explained, the exopolyphosphatases transcription and activities seem to be tighly regulated, and also forming part of operons susceptible to suffer polar effects as result of their deletions. A similar situation occurs with the gene *MSMEG_3743* that is upstream of an operon composed by six genes; thus, successful complementation assays necessarily require the use of an integrative vector that allows the transcription of the genes under native conditions, reducing the effect of gene overexpression and plasmid replication. The deletion of genes without disrupting the open reading frames of the other members of the operon does also appear as an effective tool to avoid polar effects as result of the deletions.

This summary shows that the strategies chosen in order to achieve the objectives proposed at the beginning of this study were appropriate, since each project carried out was prolific in terms of the amount and quality of the data obtained, and also opening the possibilities to continue future experiments in order to discover new drug targets and a better understanding of the metabolism of mycobacteria.

CHAPTER 7

GENERAL MATERIALS AND METHODS

7.1 Genomic DNA extraction

Cells from a 10 ml bacterial culture were collected by centrifugation and resuspended in 450 µl of resuspension buffer (50 mM Tris/Cl pH 8.0, 10 mM EDTA,100 µl/ml RNaseA), 10 mg/ml lysozyme were added and incubated overnight at 37ºC. After the incubation, 100 µl of 10% SDS and 50 µl of 10mg/ml Proteinase K were added, the suspension was mixed gently and incubated for 4 hours at 55ºC. 200 µl of 5 M NaCl were added and the mix was incubated at 65ºC for 15 min. Later 500 µl $CHCl_3$ were added mixing for 5 min and centrifuged at 13,000 rpm for 5 min. The aqueous layer was transferred to a new clean tube and 350 µl isopropanol (~0.7x of the volume obtained) were added and the tube gently mixed by inversion until DNA precipitated out of the solution. The reaction was centrifuged at 13,000 rpm for 10 min (or more if necessary). Supernatant was aspired and 1 ml 70% ethanol was added, the tube was gently inverted and spun in microfuge for 5 min. Supernatant was removed and the DNA dried out for 15 min. Finally, 50 µl of water or TE buffer (10 mM Tris/Cl, 1 mM EDTA, pH 8) were added, the DNA sample was quantified by absorbance at 260 nm and stored at -20ºC.

7.2 PCR, DNA-ligation and DNA-digestion

Polymerase chain reactions were carried out using Phusion® HF PCR kit from NEB, DNA-ligation reaction using T4-DNA ligase kit from NEB and DNA-digestion using NEB restriction enzymes. Every reaction was performed according to protocols established by the manufacturer.

7.3 Preparation of competent cells

Chemically competent cells were prepared starting from an overnight culture of *Escherichia coli* that was used to inoculate 100 ml of LB medium with 20 mM $MgSO_4$. Cells were grown until OD_{600} of 0.6 at 37ºC and then centrifuged at 4,500xg for 5 min at 4ºC. The pellet was gently resuspended in 0.4 ml of ice-cold TFB1 solution (30 mM potassium acetate, 10 mM $CaCl_2$, 50 mM $MnCl_2$, 100 mM RbCl, 15% glycerol) and incubated on ice for 5 min. The cells were centrifuged at 4,500xg for 5 min at 4ºC and the pellet gently resuspended in 2.5 ml of TFB2 solution (10 mM MOPS, 75 mM CaCl2, 10 mM RbCl, 15% glycerol, pH 6.5). Finally the cells were incubated on ice for 15-60 min and 200 µl aliquots were stored at -80ºC.

Mycobacterium smegmatis electrocompetent cells were prepared from 50 ml of 7H9+OADC+0.05% Tween-80 culture grown until OD_{600} ~ 0.5-1.0 at 37ºC. The culture was incubated on ice for 90 min and then centrifuged at 2,000xg for 10 min at 4ºC. The pellet was washed two times with 40 ml of sterile ice cold 10% glycerol. Finally the cells were resuspended in 5 ml of ice cold 10% glycerol and aliquots of 200 ul stored at -80ºC.

7.4 Transformation of competent cells

E. coli top10 competent cells were thawed on ice and 5µl of plasmid DNA were added (< 5% of cell volume or < 50 ng in 10 µl or less). The tube was gently swirl and mix by finger flicking. The reaction was incubated on ice for 20 min, then placed at 42°C for 45 sec and back on ice for 5 min. Later 1 ml of LB was added and incubated for 60 min at 37°C with agitation 150 rpm. Finally, 50, 100 and 200 µl of reaction were spread on different LB-agar plates containing the selection marker and incubated overnight at 37ºC.

M. smegmatis competent cells were transformed by electroporation. Aliquots of 200 µl of cells were thawed on ice and poured in a 1 mm gap electroporation cuvette previously frozen, 5-10 µl of plasmid DNA were added and the mix was subjected to a single pulse using an Eppendorf Electroporator 2510 (2.5kV), 1 ml of TSB was added and cells were recovered at 37ºC for 4 hours. Finally, cells were plated on TSB-agar solid media adding the selection marker.

7.5 Generation of mutants strains by specialised transduction

7.5.1 Construction of the allelic exchange substrate (AES) plasmid

Approximately 1 kb of upstream (left) and downstream (right) flanking sequences of each gene were PCR amplified from *M. smegmatis* mc^2155 genomic DNA using the primers listed on each chapter (LL-LR and RL-RR, respectively). Amplified fragments did not have restriction sites for the enzymes used to ligate and included between 100 to 400 bp of the 5' end of the gene in the left flank and 100 to 400 bp of the 3' end of the gene in the right flank.

Then, 10 µl of purified PCR product were digested with the appropriate restriction enzyme while 50 µg of plasmid p0004s were digested with *Van91I*. The top two vector fragments of size 3.68 kb and 1.60 kb (containing both the *hyg*/*sacB* and *oriE* fragments) were cut out from agarose gel. The digested vector fragments from p0004s were mixed with the digestions from the left and right flanking sequences and purified using the Qiagen gel extraction kit following the user guide protocol. Then, 30 µl of mixed fragments were collected and ligated using T4 DNA ligase from NEB using 5 µl of ligation mix and 100 µl *E. coli* Top10 chemically competent cells. Transformants were selected

and the plasmids obtained were checked by digestion with the previous enzymes and *PacI* and sequenced using the primers HL, HR, OL, and OR. This protocol describes the exchange between the target gene and the hygromycin cassette, but in this study the apramycin cassette was also used as selection marker.

7.5.2 Phasmid Construction

Sequence-confirmed plasmids and the phAE159 DNA where digested with *PacI*, using 1 µg each in 20µl of reaction. Approximately 2-4 µl of the phage and 4-6 µl of the plasmid were used for a T4 ligase reaction of 10 µl. An *in vitro* packaging was carried out by adding 5 µl of ligation mixture directly to the MaxPlax™ packaging extract tube and incubated for 1.5 h. The reaction was stopped with 200 µl MP buffer (50 mM Tris/HCl pH 7.6, 150 mM NaCl, 10 mM $MgCl_2$ and 2 mM $CaCl_2$) and incubated at room temperature for 30 min, 100 µl of HB101 host cell suspension were added directly to the packaging tube and incubated at 37ºC for 1 h. The cells were collected by centrifugation, the supernatant removed and the pellet resuspended with 1 ml of fresh LB media. The cells were plated on LB-hyg 150 µg/ml and incubated at 37ºC overnight. The hygromycin resistant colonies were selected to look for potential phasmids, which were purified and checked by digestion with *PacI* enzyme. The right digestion pattern consists in a phage genomic ~40kb band and a linearised band of allelic exchange plasmid of ~7kb.

E. coli HB101 was previously prepared for transduction from a 50 ml LB culture supplemented with 10 mM $MgSO_4$ and 0.2% maltose incubated at 37°C until OD_{600} 0.8-1.0. Cells were collected by centrifugation at 3000 rpm, 4°C for 10 min and resuspended in 500 µL of MP buffer and stored for no longer than a week at 4°C.

7.5.3 Generation of knockout phage

An amount of 5-10 µl phasmid DNA was electroporated into 200 µl electrocompetent *M. smegmatis* cells, 1 ml of LB media was added and the mix incubated at 30ºC (not 37ºC) for 1 h. Aliquots of 100, 200 and 400 µl were mixed with 500 µl of actively growing culture of *M. smegmatis*. The dilutions were mixed separated and added to 4 ml of molten top agar (at 50°C) in a snap cap tube and mixed gently by inverting the tube and poured onto pre-warmed 7H9 basal agar plates. The plates were incubated at 30ºC until plaques were observed. Plaques were picked and soaked in 200 µl of MP buffer to recover the phage.

7.5.4 High titre phage lysate

Firstly, plates containing 7H9 basal agar were overlaid with 4 ml of top agar containing 500 µl actively growing *M. smegmatis* culture. 10-fold dilutions of the phage were prepared using MP buffer. 10 µl of each dilution were spotted on the above overlaid plate and the plate incubated at 30ºC for 3 days until plaques were observed in the spot zones. The plaques on every spot were counted and the amount of plaque forming units (PFU) per ml of phage suspension was calculated. Phages were overlaid in triplicate on 7H9 agar basal plates with top agar containing 500 µl actively growing *M. smegmatis* culture giving approximately 1000 plaques per plate, incubation at 30ºC until plaques displayed the typical lysis pattern. Each plate was soaked with 4ml of MP buffer and incubated at room temperature for 5 h (or overnight at 4°C). The suspension containing the bacterial debris and phages was taken, filtered using a 0.22 µm PVDF filter, the filtrate containing a high density of phage particles was stored at 4°C until further use. Ideal titre for transduction should have at least 10^{10} PFU per ml.

7.5.5 Specialized transduction

A 50 ml *M. smegmatis* culture was grown in TSB + 0.05% Tween-80 at 37ºC until OD A_{600} of 0.8 to 1. The culture was collected and cells were span down for 15 min at 4,000 rpm. The pellet was resuspended in 5 ml of MP buffer obtaining an even consistency and 45 ml of buffer were added and mixed well. Cells were washed twice following the same way. Finally, the cells were resuspended in 5 ml of MP buffer and 1 ml of cell suspension was mixed with 1 ml high titre knockout-phage lysate. A negative control reaction was set using only 1 ml of MP buffer and cells suspension. Reactions were incubated at 37ºC (non-permissive temperature for phage replication) for 1 h to allow infection. Tubes were centrifuged for 15 min at 4,000 rpm, supernatants were decanted, and the pellet resuspended in 3 ml of TSB + 0.05% Tween-80 and incubated for 3 h at 37ºC. After incubation, the pellet was collected and resuspended in 400 µl of TSB + 0.05% Tween-80 and 100 µl spread on each TSB-agar plate containing 100 µg/ml hygromycin and incubated at 37ºC until transductants colonies appeared. Selected colonies were verified by Southern blot.

7.6 Southern blot analysis

Gene knock-out mutant strains were confirmed by Southern blot analysis using digested genomic DNA, appropriate restriction enzymes and DIG-High Prime (ROCHE) labelled probes. Basically, a selected restriction enzyme was used to digest genomic DNA from wild-type and mutant *M. smegmatis* strains and the digested DNA was separated by agarose gel electrophoresis producing a laddering effect. Each mutant showed a different digestion pattern compared to the wild-type (due to the hygromycin cassette incorporated) and PCR products of approximately 1 kb of the flanking regions were used as probes.

The agarose gel containing digested DNA was depurinated with 0.25 M HCl, for 15min, denatured with a solution containing 1.5 M NaCl and 0.5 M NaOH for 15 min and finally neutralised with 0.5 Tris/Cl, 1 M NaCl, pH 7.2. The DNA contained by the gel was transferred to positively charged nitrocellulose membrane via capillary action with 20 x SSC (3 M NaCl, 0.3 M sodium citrate, pH 7.0), the DNA on membrane was then covalently bound by UV-crosslinking for 3 min. The membrane was finally rinsed with distilled water.

The probe was prepared by boiling, snap chilling and labelled with digoxigenin-dUTP, using the DIG High Prime DNA labelling and Detection Start Kit (Roche), as described in the manual. Meanwhile, the membrane was washed at 42ºC in 10 ml of DIG Easy Hyb granules solution for 30 min, the probe was added into the hybridisation bottle and then incubated overnight at 65ºC. After the hibridisation, the membrane was washed, the probe immunodetected with the antibody and visualized with the chemiluminescence as follows:

- 50 ml (2xSSC + 0.1% SDS). 5 min at 25ºC. Two times
- 50 ml (0.5 xSSC + 0.1% SDS). 15 min at 65ºC. Two times
- 50 ml Washing Buffer: Maleic Acid Buffer (0.1 M maleic acid, 0.15 M NaCl, pH 7.5) + 0.3% v/v Tween-20. 5 min at 25ºC
- 10 ml Blocking Buffer: 9 ml MAB + 1 ml Blocking Solution. 30 min at 25ºC
- 10 ml Antibody Solution: 10 ml Blocking Buffer + 1 µl Anti-DIG-AP. 30 min at 25ºC
- 50 ml Washing Buffer. 15 min at 25ºC. Two times
- 20 ml Detection Buffer: 0.1 M Tris/Cl, 0.1 M NaCl, pH 9.5. 5 min at 25ºC

Finally, the membrane was exposed to CSPD ready-to-use reagent, incubated for 15 min at 37ºC and exposed to Kodak X-Omat film for 5-10 min.

7.7 *M. smegmatis* lipid extraction

M. smegmatis [^{14}C]-labelled polar and non-polar lipids were extracted using the methods described by Dobson *et al* (1985), 10 ml of *M. smegmatis* cultures were labelled during mid-log phase with 50 μCi/ml [14C] acetate, followed by overnight incubation. Firstly, the [^{14}C]-labelled cells were collected by centrifugation, and dried by aeration; later cells were mixed with 2 ml of CH_3OH/0.3% NaCl (100:10, v/v) and 1ml of petroleum ether (b.p. 60-80°C) for 15 min. The mix was centrifuged and the upper layer was collected to add 1 ml of petroleum ether to the lower fraction, the suspension was mixed and centrifuged again as previously indicated and the upper layer collected again.

Both upper layers containing the non-polar lipids were combined, dried and dissolved in 200 μl of $CHCl_3$/CH_3OH (2:1, v/v), then 5 μl sample were collected in a scintillation vial, dried and then mixed with 5 ml scintillation liquid for radioactivity measurement.

The polar lipids were extracted by adding 2.3 ml of $CHCl_3$/CH_3OH/0.3% NaCl (90:100:30, v/v/v) to the lower aqueous fraction remaining, the mixture was mixed for 1 h, centrifuged and stored after removing the supernatant. The step was repeated by adding 0.75 ml of $CHCl_3$/CH_3OH/0·3% NaCl (50: 100: 40, v/v/v) and mixing for 30 min. Delipidated cells were kept for further analysis.

A volume of 26 ml of $CHCl_3$/0.3 % NaCl (1:1, v/v) was added to the collected supernatants, mixed for 5 min, centrifuged, the lower fraction recovered and dried out. The polar lipids were dissolved in 200 μl of $CHCl_3$/CH_3OH (2:1, v/v), a 5 μl sample was dried in a scintillation vial and then mixed with 5 ml scintillation liquid for radioactivity measurement.

7.8 Thin layer chromatography (TLC) analysis for *M. smegmatis* lipids

Apolar and polar *M. smegmatis* lipid extracts were analysed by two-dimensional thin layer chromatography (2D-TLC). Apolar lipids were analysed using four different solvent systems (A–D) and polar lipids by two different systems (D and E) according to Dobson *et al*. (1985). Equal amounts of radioactive counts (20,000 cpm) of each lipid sample were spotted on TLC plates (5554 silica gel 60F524, Merck) for consecutive 1D- and 2D-TLC analysis using following solution systems and allowing plates to dry between each run. Finally, [^{14}C]-labelled lipids were revealed by overnight exposure to Kodak X-Omat AR film.

Table 7.1: Solvent systems for 2D-TLC lipid analysis

System	Direction 1	Runs
A	Petroleum ether 60-80 / Ethyl acetate (98:2)	3
B	Petroleum ether 60-80 / Acetone (92:8)	3
C	Chloroform / Methanol (96:4)	1
D	Chloroform / Methanol / Water (100:14:0.8)	1
E	Chloroform / Methanol / Water (60:30:6)	1

System	Direction 2	Runs
A	Petroleum ether 60-80 / Acetone (98:2)	1
B	Toluene / Acetone (95:5)	1
C	Toluene / Acetone (80:20)	1
D	Chloroform / Acetone/ Methanol / Water (50:60:2.5:3)	1
E	Chloroform / Acetic acid (glacial) / Methanol / Water (40:25:3:6)	1

7.9 Generation of *M. smegmatis* conditional mutants by CESTET (conditional expression–specialized transduction essentiality test)

CESTET consists in obtain a merodiploid strain which contains a second copy of a putative essential gene (*peg*) controlled by the acetamidase promoter (Bhatt and Jacobs, 2009). The general protocol used in this study was cloning the acetamidase promoter and the selected gene into a single-copy integrating vector, namely pMV306, which contains a gene encoding the mycobacteriophage L5 integrase (*int*), an attachment site (*attP*), a

kanamycin resistance cassette and that replicates as a plasmid in *E. coli*. When electroporated into mycobacteria, pMV306 integrates in the bacterial chromosome integration site (*attB*) as a single copy.

At the same time, a specialized transducing phage (ph∆*peg*) containing an allelic exchange substrate was designed to replace the target gene by infecting the merodiploid strain. If the gene was essential, the ability to obtain transductants was dependent on the acetamidase-driven expression of the gene, obtaining transductants only on plates with acetamide.

In first place, *peg* was cloned downstream of the acetamidase promoter in the mycobacterial expression plasmid pSD26, the continuous fragment containing the acetamidase promoter and *peg* was then cloned into pMV306. The open reading frame (ORF) for *peg* was possible to be cloned into the corresponding sites of pSD26. The entire fragment was then cloned in pMV306.

Secondly, pMV306-P_{ac}*peg* was then introduced into *M. smegmatis* mc^2155 by electroporation and the transformants were selected with 20 μg/mL kanamycin. The resistant merodiploid colonies were inoculated into 5 mL TSB cultures containing 0.05% Tween-80 and 20 μg/mL kanamycin, grown by shaking at 37ºC until OD_{600} reaches between 0.8 to 1, mixed with 1:1 (v/v) sterile 50% glycerol and stored at -80ºC.

Finally, the merodiploids were used for generating a knock-out mutant by specialised transduction using the ph∆*peg*. Once finished, bacterial suspensions were split into equal parts and spread each on TSB-agar plates containing kanamycin and hygromycin and TSB-agar plates containing kanamycin, hygromycin, and acetamide. Plates were incubated the plates at 37ºC for 3 days before scoring for colonies. The

criterion behind the technique is: if hyg^R and kan^R colonies are obtained only in the presence of acetamide in the plates, then the targeted gene is essential for growth.

CHAPTER 8

REFERENCES

Achbergerová L, Nahálka J. (2011). Polyphosphate - an ancient energy source and active metabolic regulator. Microb Cell Fact 10:63.

Adam A, Petit JF, Weitzerbin-Falszpan J, Sinay P, Thomas DW, Lederer E. (1969). Mass spectrometric identification of N-glycolymuramic acid, a constituent of *Mycobacterium smegmatis* walls. FEBS Lett 4(2):87–92.

Ahn K, Kornberg A. (1990). Polyphosphate kinase from *Escherichia coli*. J Biol Chem 265:11734-11739.

Akiyama M, Crooke E, Kornberg A. (1993). An exopolyphosphatase of *Escherichia coli*. The enzyme and its *ppx* gene in a polyphosphate operon. J Biol Chem 268:633-639.

Alderwick LJ, Birch HL, Mishra AK, Eggeling L, Besra GS. (2007). Structure, function and biosynthesis of the *Mycobacterium tuberculosis* cell wall: arabinogalactan and lipoarabinomannan assembly with a view to discovering new drug targets. Biochem Soc Trans 35:1325-1328.

Alderwick LJ, Lloyd GS, Ghadbane H, May JW, Bhatt A, Eggeling L, Fütterer K, Besra GS. (2011). The C-terminal domain of the arabinosyltransferase *Mycobacterium tuberculosis* EmbC is a lectin-like carbohydrate binding module. PLoS Pathog 7(2):e1001299.

Alonso-Hearn M, Eckstein TM, Sommer S, Bermudez LE. (2010). A *Mycobacterium avium subsp. paratuberculosis* LuxR regulates cell envelope and virulence. Innate Immun 16(4):235-47.

Altaf M, Miller CH, Bellows DS, O'Toole R. (2010). Evaluation of the *Mycobacterium smegmatis* and BCG models for the discovery of *Mycobacterium tuberculosis* inhibitors. Tuberculosis (Edinb) 90(6):333-7.

Altschul SF, Gish W, Miller W, Myers EW, Lipman DJ. (1990). Basic local alignment search tool. J Mol Biol 215:403-410.

Amin AG, Goude R, Shi L, Zhang J, Chatterjee D, Parish T. (2008). EmbA is an essential arabinosyltransferase in *Mycobacterium tuberculosis*. Microbiology 154(Pt 1):240-8.

Andersen CS, Agger EM, Rosenkrands I, Gomes JM, Bhowruth V, Gibson KJ, Petersen RV, Minnikin DE, Besra GS, Andersen, P. (2009). A simple mycobacterial monomycolated glycerol lipid has potent immunostimulatory activity. J Immunol 182(1):424-32.

Andersen CA, Rosenkrands I, Olsen AW, Nordly P, Christensen D, Lang R, Kirschning C, Gomes JM, Bhowruth V, Minnikin DE, Besra GS, Follmann F,Andersen P, Agger EM. (2009). Novel generation mycobacterial adjuvant based on liposome-encapsulated monomycoloyl glycerol from *Mycobacterium bovis* bacillus Calmette-Guérin. J Immunol 183(4):2294-302.

Anes E, Peyron P, Staali L, Jordao L, Gutierrez MG, Kress H, Hagedorn M, Maridonneau-Parini I, Skinner MA, Wildeman AG, Kalamidas SA, Kuehnel M, Griffiths G. (2006). Dynamic life and death interactions between *Mycobacterium smegmatis* and J774 macrophages. Cell Microbiol 8(6):939-60.

Aschar-Sobbi R, Abramov AY, Diao C, Kargacin ME, Kargacin GJ, French RJ, Pavlov E. (2008). High sensitivity, quantitative measurements of polyphosphate using a new DAPI-based approach. J Fluoresc 18(5):859-66.

Asselineau, J, Lederer E. (1950). Structure of the mycolic acids of mycobacteria. Nature 166:782–783.

Astarie-Dequeker C, Le Guyader L, Malaga W, Seaphanh FK, Chalut C, Lopez A, Guilhot C. (2009). Phthiocerol dimycocerosates of *M. tuberculosis* participate in macrophage invasion by inducing changes in the organization of plasma membrane lipids. PLoS Pathog 5(2):e1000289.

Ault-Riché D, Fraley CD, Tzeng C, Kornberg A. (1998). Novel assay reveals multiple pathways regulating stress-induced accumulations of inorganic polyphosphate in *Escherichia coli*. J Bacteriol 180:1841-1847.

Avarbock A, Avarbock D, Teh JS, Buckstein M, Wang ZM, Rubin H. (2005). Functional regulation of the opposing (p)ppGpp synthetase/hydrolase activities of Rel_{Mtb} from *Mycobacterium tuberculosis*. Biochemistry 44(29):9913-23.

Azuma I, Yamamoto Y. (1963). Studies on the firmly bound lipids of human tubercle bacillus. II. Isolation of arabinose mycolate and identification of its chemical structure. J Biochem (Tokyo) 53:274–281.

Baba O. (1993). Production of monoclonal antibody that recognizes glycogen and its application for immunohistochemistry. Kokubyo Gakkai Zasshi 60(2):264-87.

Bafica A, Scanga CA, Feng CG, Leifer C, Cheever A, Sher A. (2005). TLR9 regulates Th1 responses and cooperates with TLR2 in mediating optimal resistance to *Mycobacterium tuberculosis*. J Exp Med 202(12):1715-24.

Bange FC, Collins FM, Jacobs WR Jr. (1999). Survival of mice infected with *Mycobacterium smegmatis* containing large DNA fragments from *Mycobacterium tuberculosis*. Tuber Lung Dis 79(3):171-80.

Bardarov S, Kriakov J, Carriere C, Yu S, Vaamonde C, McAdam RA, Bloom BR, Hatfull GF, Jacobs WR Jr. (1997). Conditionally replicating mycobacteriophages: a system for transposon delivery to *Mycobacterium tuberculosis*. PNAS 30;94(20):10961-6.

Bardarov S, Bardarov S Jr., Pavelka MS, Jr., Sambandamurthy V, Larsen M, Tufariello J, Chan J, Hatfull G, Jacobs WR Jr. (2002). Specialized transduction: an efficient method for generating marked and unmarked targeted gene disruptions in *Mycobacterium tuberculosis, M. bovis* BCG and *M. smegmatis*. Microbiology 148, 3007–3017.

Barry CE 3rd, Lee RE, Mdluli K, Sampson AE, Schroeder BG, Slayden RA, Yuan Y. (1998). Mycolic acids: structure, biosynthesis and physiological functions. Prog Lipid Res 37(2-3):143-79.

Barry CE 3rd. (2001a). *Mycobacterium smegmatis*: an absurd model for tuberculosis?. Trends Microbiol 9(10):473-4.

Barry CE 3rd. (2001b). Interpreting cell wall 'virulence factors' of *Mycobacterium tuberculosis*. Trends Microbiol 9(5):237-41.

Barry CE 3rd, Boshoff HI, Dartois V, Dick T, Ehrt S, Flynn J, Schnappinger D, Wilkinson RJ, Young D. (2009). The spectrum of latent tuberculosis: rethinking the biology and intervention strategies. Nat Rev Microbiol 7: 845–855.

Bayle, GL. (1810). Recherches sur la phthisie pulmonaire. Paris: Gabon. p. 439.

Bedard K, Krause KH. (2007). The NOX family of ROS generating NADPH oxidases: physiology and pathophysiology. Physiol Rev 87: 245–313.

Behar SM, Divangahi M, Remold HG. (2010). Evasion of innate immunity by *Mycobacterium tuberculosis*: is death an exit strategy?. Nat Rev Microbiol 8(9):668-74.

Belisle JT, Vissa VD, Sievert T, Takayama K, Brennan PJ, Besra GS. (1997) Role of the major antigen of *Mycobacterium tuberculosis* in cell wall biogenesis. Science 276: 1420-1422.

Bennett JA, Aimino RM, McCormick JR. (2007). *Streptomyces coelicolor* genes *ftsL* and *divIC* play a role in cell division but are dispensable for colony formation. J Bacteriol 189(24):8982-92.

Bertram R, Schlicht M, Mahr K, Nothaft H, Saier MH Jr, Titgemeyer F. (2004). In silico and transcriptional analysis of carbohydrate uptake systems of *Streptomyces coelicolor* A3(2). J Bacteriol 186:1362–1373.

Besra GS, Sievert T, Lee RE, Slayden RA, Brennan PJ, Takayama K. (1994). Identification of the apparent carrier in mycolic acid synthesis. PNAS 91(26):12735-9.

Besra GS, Khoo KH, McNeil MR, Del A, Morris HR, Brennan PJ. (1995). A new interpretation of the structure of the mycolyl-arabinogalactan complex of *Mycobacterium tuberculosis* as revealed through characterization of oligoglycosylalditol fragments by fast-atom bombardment mass spectrometry and 1H nuclear magnetic resonance spectroscopy. Biochemistry 34:4257-4266.

Besra GS, Morehouse CB, Rittner CM, Waechter CJ, Brennan PJ. (1997). Biosynthesis of mycobacterial lipoarabinomannan. J Biol Chem 272:18460-18466.

Beste DJ, Bonde B, Hawkins N, Ward JL, Beale MH, Noack S, Noh K, Kruger NJ, Ratcliffe RG, McFadden J. (2011). ^{13}C metabolic flux analysis identifies an unusual route for pyruvate dissimilation in mycobacteria which requires isocitrate lyase and carbon dioxide fixation. PLoS Pathog 7:e1002091.

Betts JC, Lukey PT, Robb LC, McAdam RA, Duncan K. (2002). Evaluation of a nutrient starvation model of *Mycobacterium tuberculosis* persistence by gene and protein expression profiling. Mol Microbiol 43: 717–731.

Bhamidi S, Scherman MS, Rithner CD, Prenni JE, Chatterjee D, Khoo K-H, McNeil MR. (2008). The identification and location of succinyl residues and the charcaterization of the interior arabinan region allows for a model of the complete primary structure of *Mycobacterium tuberculosis* mycolyl arabinogalactan. J Biol Chem 283:12992–13000.

Bhatt A, Kremer L, Dai AZ, Sacchettini JC, Jacobs WR Jr. (2005). Conditional depletion of KasA, a key enzyme of mycolic acid biosynthesis, leads to mycobacterial cell lysis. J Bacteriol 187(22):7596-606.

Bhatt A, Fujiwara N, Bhatt K, Gurcha SS, Laurent K, Chen B, Chan J, Porcelli SA, Kobayashi K, Besra GS, Jacobs WR. (2007). Deletion of *kasB* in *Mycobacterium tuberculosis* causes loss of acid-fastness and subclinical latent tuberculosis in immunocompetent mice. PNAS 104(12):5157-5162.

Bhatt A, Brown AK, Singh A, Minnikin DE, Besra GS. (2008). Loss of a mycobacterial gene encoding a reductase leads to an altered cell wall containing beta-oxo-mycolic acid analogs and accumulation of ketones. Chem Biol 22;15(9):930-9.

Bhatt A, Jacobs WR Jr. (2009). Gene essentiality testing in *Mycobacterium smegmatis* using specialized transduction. Methods Mol Biol 465:325-36.

Bignell C, Thomas CM. (2001). The bacterial ParA-ParB partitioning proteins. J Biotechnol 91:1–34.

Billman-Jacobe H, McConville MJ, Haites RE, Kovacevic S, Coppel RL. (1999). Identification of a peptide synthetase involved in the biosynthesis of glycopeptidolipids of *Mycobacterium smegmatis*. Mol Microbiol 33(6):1244-53.

Birch HL, Alderwick LJ, Bhatt A, Rittmann D, Krumbach K, Singh A, Bai Y, Lowary TL, Eggeling L, Besra GS. (2008). Biosynthesis of mycobacterial arabinogalactan: identification of a novel alpha (1-->3) arabinofuranosyltransferase. Mol Microbiol 69(5):1191-206.

Birch HL, Alderwick LJ, Appelmelk BJ, Maaskant J, Bhatt A, Singh A, Nigou J, Eggeling L, Geurtsen J, Besra GS. (2010). A truncated lipoglycan from mycobacteria with altered immunological properties. PNAS 107(6):2634-9.

Blomgran R, Ernst JD. (2011). Lung neutrophils facilitate activation of naive antigen-specific CD4+ T cells during *Mycobacterium tuberculosis* infection. J Immunol 186, 7110–7119.

Botella H, Peyron P, Levillain F, Poincloux R, Poquet Y, Brandli I, Wang C, Tailleux L, Tilleul S, Charrière GM, Waddell SJ, Foti M, Lugo-Villarino G, Gao Q, Maridonneau-Parini I, Butcher PD, Castagnoli PR, Gicquel B, de Chastellier C, Neyrolles O. (2011). Mycobacterial P(1)-type ATPases mediate resistance to zinc poisoning in human macrophages. Cell Host Microbe 10: 248–259.

Botella H, Stadthagen G, Lugo-Villarino G, de Chastellier C, Neyrolles O. (2012). Metallobiology of host-pathogen interactions: an intoxicating new insight. Trends Microbiol. 20(3):106-12.

Braeken K, Moris M, Daniels R, Vanderleyden J, Michiels J. (2006). New horizons for (p)ppGpp in bacterial and plant physiology. Trends Microbiol 14: 45–54.

Brennan, PJ, Nikaido H. (1995). The envelope of mycobacteria. Annu Rev Biochem 64: 29-63.

Brennan PJ. (2003). Structure, function, and biogenesis of the cell wall of *Mycobacterium tuberculosis*. Tuberculosis (Edinb). 83(1-3):91-7.

Brennan PJ, Crick DC. (2007). The cell-wall core of *Mycobacterium tuberculosis* in the context of drug discovery. Curr Top Med Chem 7(5):475-88.

Brennan MJ, Stone MR, Evans T. (2012). A rational vaccine pipeline for tuberculosis. Int J Tuberc Lung Dis. 16(12):1566-73.

Brewer, TF. (2000). Preventing tuberculosis with bacillus Calmette-Guerin vaccine: a meta-analysis of the literature. Clin Infect Dis 31 Suppl 3, S64-67.

Briken V, Porcelli SA, Besra GS, Kremer L. (2004). Mycobacterial lipoarabinomannan and related lipoglycans: from biogenesis to modulation of the immune response. Mol Microbiol 53:391–403.

Brosch R, Gordon SV, Marmiesse M, Brodin P, Buchrieser C, Eiglmeier K, Garnier T, Gutiérrez C, Hewinson G, Kremer K, Parsons LM, Pym AS, Samper S, van Soolingen D, Cole ST. (2002). A new evolutionary scenario for the *Mycobacterium tuberculosis* complex. PNAS 99:3684-3689.

Brown MR, Kornberg A. (2004). Inorganic polyphosphate in the origin and survival of species. PNAS 101(46):16085-7.

Brown AK, Sridharan S, Kremer L, Lindenberg S, Dover LG, Sacchettini JC, Besra GS. (2005). Probing the mechanism of the *Mycobacterium tuberculosis* beta-ketoacyl-acyl carrier protein synthase III mtFabH: factors influencing catalysis and substrate specificity. J Biol Chem 280: 32539–32547.

Brown AK, Bhatt A, Singh A, Saparia E, Evans AF, Besra GS. (2007). Identification of the dehydratase component of the mycobacterial mycolic acid-synthesizing fatty acid synthase-II complex. Microbiology 153: 4166–4173.

Brown MR, Kornberg A. (2008). The long and short of it - polyphosphate, PPK and bacterial survival. Trends Biochem Sci 33:284–290.

Brülle JK, Grau T, Tschumi A, Auchli Y, Burri R, Polsfuss S, Keller PM, Hunziker P, Sander P. (2010). Cloning, expression and characterization of *Mycobacterium tuberculosis* lipoprotein LprF. Biochem Biophys Res Commun 1;391(1):679-84.

Brumfield KM, Moroney JV, Moore TS, Simms TA, Donze D. (2010). Functional characterization of the *Chlamydomonas reinhardtii* ERG3 ortholog, a gene involved in the biosynthesis of ergosterol. PLoS One 11;5(1):e8659.

Brzostek A, Dziadek B, Rumijowska-Galewicz A, Pawelczyk J, Dziadek J. (2007). Cholesterol oxidase is required for virulence of *Mycobacterium tuberculosis*. FEMS Microbiol Lett 275: 106–112.

Calmette, A. (1928). On preventative vaccination of the new-born against tuberculosis by BCG. Br J Tuberc 22, 161-165.

Canaday DH, Wilkinson RJ, Li Q, Harding CV, Silver RF, Boom WH. (2001). CD4(+) and CD8(+) T cells kill intracellular *Mycobacterium tuberculosis* by a perforin and Fas/Fas ligand-independent mechanism. J Immunol 167(5):2734-42.

Carranza C, Juárez E, Torres M, Ellner JJ, Sada E, Schwander SK. (2006). *Mycobacterium tuberculosis* growth control by lung macrophages and CD8 cells from patient contacts. Am J Respir Crit Care Med 173(2):238-45.

Chakravarty SD, Xu J, Lu B, Gerard C, Flynn J, Chan J. (2007). The chemokine receptor CXCR3 attenuates the control of chronic *Mycobacterium tuberculosis* infection in BALB/c mice. J Immunol 178(3):1723-35.

Chakravorty S, Aladegbami B, Motiwala AS, Dai Y, Safi H, Brimacombe M, Helb D, Alland D. (2008). Rifampin resistance, Beijing-W clade-single nucleotide polymorphism cluster group 2 phylogeny, and the Rv2629 191-C allele in *Mycobacterium tuberculosis* Strains. J Clin Microbiol 46(8): 2555–2560.

Chang YC, Bien CM, Lee H, Espenshade PJ, Kwon-Chung KJ. (2007). Sre1p, a regulator of oxygen sensing and sterol homeostasis, is required for virulence in *Cryptococcus neoformans*. Mol Microbiol 64(3):614-29.

Chapman GB, Hanks JH, Wallace JH. (1959). An electron microscope study of the disposition and fine structure of *Mycobacterium lepraemurium* in mouse spleen. J Bacteriol 77: 205–211.

Chatterjee D, Khoo KH. (2001). The surface glycopeptidolipids of mycobacteria: structures and biological properties. Cell Mol Life Sci 58:2018-2042.

Chaturvedi V, Dwivedi N, Tripathi RP, Sinha S. (2007). Evaluation of *Mycobacterium smegmatis* as a possible surrogate screen for selecting molecules active against multi-drug resistant *Mycobacterium tuberculosis*. J Gen Appl Microbiol 53(6):333-7.

Chen M, Divangahi M, Gan H, Shin DS, Hong S, Lee DM, Serhan CN, Behar SM, Remold HG. (2008). Lipid mediators in innate immunity against tuberculosis: opposing roles of PGE2 and LXA4 in the induction of macrophage death. J Exp Med 205(12):2791-801.

Chen J, Kriakov J, Singh A, Jacobs WR Jr, Besra GS, Bhatt A. (2009). Defects in glycopeptidolipid biosynthesis confer phage I3 resistance in *Mycobacterium smegmatis*. Microbiol 155(Pt 12):4050-7.

Chen J. (2010.) Identifying biosynthetic pathways for mycobacterial cell wall components using transposon mutagenesis. School of Biosciences. University of Birmingham. PhD Thesis.

Choi KH, Kremer L, Besra GS, Rock CO. (2000). Identification and substrate specificity of beta-ketoacyl (acyl carrier protein) synthase III (mtFabH) from *Mycobacterium tuberculosis*. J Biol Chem 275: 28201–28207.

Choi MY, Wang Y, Wong LL, Lu BT, Chen WY, Huang JD, Tanner JA, Watt RM. (2012). The two PPX-GppA homologues from *Mycobacterium tuberculosis* have distinct biochemical activities. PLoS One 7(8):e42561.

Chouayekh H, Virolle MJ. (2002). The polyphosphate kinase plays a negative role in the control of antibiotic production in *Streptomyces lividans*. Mol Microbiol 43(4):919-30.

Chung GA, Aktar Z, Jackson S, Duncan K. (1995). High-throughput screen for detecting antimycobacterial agents. Antimicrob Agents Chemother 39(10):2235-8.

Claros MG, von Heijne G. (1994). TopPred II: An Improved Software For Membrane Protein Structure Predictions. CABIOS 10: 685-686.

Coar T. (1982) The aphorisms of Hippocrates with a translation into Latin, and English. Birmingham, AB: Gryphon Editions.

Cohen-Gonsaud M, Barthe P, Bagneris C, Henderson B, Ward J, Roumestand C, Keep NH. (2005). The structure of a resuscitation-promoting factor domain from *Mycobacterium tuberculosis* shows homology to lysozymes. Nat Struct Mol Biol 12: 270–273.

Cole ST, Brosch R, Parkhill J, Garnier T, Churcher C, Harris D, Gordon, SV, Eiglmeier K, Gas S, Barry CE 3rd., et al. (1998). Deciphering the biology of Mycobacterium tuberculosis from the complete genome sequence. Nature 393, 537–544.

Constant P, Pérez E, Malaga W, Lanéelle M-A, Saurel O, Daffé M, Guilhot C. (2002). Role of the *pks15/1* gene in the biosynthesis of phenolglycolipids in the *Mycobacterium tuberculosis* complex. J Biol Chem 277:38148–38158.

Converse SE, Mougous JD, Leavell MD, Leary JA, Bertozzi CR, Cox JS. (2003). MmpL8 is required for sulfolipid-1 biosynthesis and *Mycobacterium tuberculosis* virulence. PNAS 100(10):6121-6.

Cooper AM, Magram J, Ferrante J, Orme IM. (1997a). Interleukin 12 (IL-12) is crucial to the development of protective immunity in mice intravenously infected with *Mycobacterium tuberculosis*. J Exp Med 186, 39-45.

Cooper AM, D'Souza C, Frank AA, Orme IM. (1997b). The course of *Mycobacterium tuberculosis* infection in the lungs of mice lacking expression of either perforin- or granzyme-mediated cytolytic mechanisms. Infect Immun 65:1317-1320.

Cooper AM. (2009). Cell-mediated immune responses in tuberculosis. Annu Rev Immunol 27:393-422.

Cooper AM, Mayer-Barber KD, Sher A. (2011). Role of innate cytokines in mycobacterial infection. Mucosal Immunol 4(3):252-60.

Court N, Vasseur V, Vacher R, Frémond C, Shebzukhov Y, Yeremeev VV, Maillet I, Nedospasov SA, Gordon S, Fallon PG, Suzuki H, Ryffel B, Quesniaux VF. (2010). Partial redundancy of the pattern recognition receptors, scavenger receptors, and C-type lectins for the long-term control of *Mycobacterium tuberculosis* infection. J Immunol 184(12):7057-70.

Cox JS, Chen B, McNeil M, Jacobs WR Jr. (1999). Complex lipid determines tissue-specific replication of *Mycobacterium tuberculosis* in mice. Nature 402, 79-83.

Crellin PK, Kovacevic S, Martin KL, Brammananth R, Morita YS, Billman-Jacobe H, McConville MJ, Coppel RL. (2008). Mutations in *pimE* restore lipoarabinomannan synthesis and growth in a *Mycobacterium smegmatis lpqW* mutant. J Bacteriol 190(10):3690-9.

Crubézy É, Ludes B, Poveda J-D, Clayton J, Crouau-Roy B, Montagnon D. (1998) Identification of *Mycobacterium* DNA in an Egyptian Pott's disease of 5400 years old. C R Acad Sci Paris (Sciences de la vie) 321:941–51.

Cywes C, Hoppe HC, Daffé M, Ehlers MRW. (1997). Nonopsonic binding of *Mycobacterium tuberculosis* to human complement receptor type 3 is mediated by capsular polysaccharides and is strain dependent. Infect Immun 65:4258–4266.

Daffé M, Brennan PJ, McNeil M. (1990). Predominant structural features of the cell wall arabinogalactan of *Mycobacterium tuberculosis* as revealed through characterization of oligoglycosyl alditol fragments by gas chromatography/mass spectrometry and by ^{1}H and ^{13}C NMR analyses. J Biol Chem 265:6734-6743.

Daffé M, Draper P. (1998). The envelope layers of mycobacteria with reference to their pathogenicity. Adv Microb Physiol 39:131–203.

Daniel TM. (2005). Robert Koch and the pathogenesis of tuberculosis. Int J Tuberc Lung Dis 9(11):1181-2.

Daniel TM. (2006). The history of tuberculosis. Respir Med 100, 1862-1870.

Daniel J, Maamar H, Deb C, Sirakova TD, Kolattukudy PE. (2011). *Mycobacterium tuberculosis* uses host triacylglycerol to accumulate lipid droplets and acquires a dormancy-like phenotype in lipid-loaded macrophages. PLoS Pathog 7:e1002093.

Davis JM, Ramakrishnan L. (2009). The role of the granuloma in expansion and dissemination of early tuberculous infection. Cell 136(1):37-49.

Deshayes C, Bach H, Euphrasie D, Attarian R, Coureuil M, Sougakoff W, Laval F, Av-Gay Y, Daffé M, Etienne G, Reyrat JM. (2010). MmpS4 promotes glycopeptidolipids biosynthesis and export in *Mycobacterium smegmatis*. Mol Microbiol 78: 989–1003.

Diaz JM, Ingall ED. (2010). Fluorometric quantification of natural inorganic polyphosphate. Environ Sci Technol 44(12):4665-71.

Dinadayala P, Lemassu A, Granovski P, Cérantola S, Winter N, Daffé M. (2004). Revisiting the structure of the anti-neoplastic glucans of *Mycobacterium bovis* Bacille Calmette-Guerin. Structural analysis of the extracellular and boiling water extract-derived glucans of the vaccine substrains. J Biol Chem 279(13):12369-78.

Dinadayala P, Sambou T, Daffé M, Lemassu A. (2008). Comparative structural analyses of the α-glucan and glycogen from *Mycobacterium bovis*. Glycobiology 18(7):502–508.

Dmitriev BA, Ehlers S, Rietschel ET, Brennan PJ. (2000). Molecular mechanics of the mycobacterial cell wall: from horizontal layers to vertical scaffolds. Int J Med Microbiol 290: 251-258.

Dobson G, Minnikin D E, Minnikin S M, Parlett M, Goodfellow M, Ridell M, Magnusson M. (1985). Systematic analysis of complex mycobacterial lipids. In chemical methods in bacterial systematics. Edited by M. Goodfellow & D. E. Minnikin. London: Academic. pp. 237-265.

Domenech P, Reed MB, Dowd CS, Manca C, Kaplan G, Barry CE 3rd. (2004). The role of MmpL8 in sulfatide biogenesis and virulence of *Mycobacterium tuberculosis*. J Biol Chem 279: 21257–21265.

Domenech P, Reed MB, Barry CE. (2005). Contribution of the *Mycobacterium tuberculosis* MmpL protein family to virulence and drug resistance. Infect Immun 73:3492-3501.

Donà V, Rodrigue S, Dainese E, Palù G, Gaudreau L, Manganelli R, Provvedi R. (2008). Evidence of complex transcriptional, translational, and posttranslational regulation of the extracytoplasmic function sigma factor sigmaE in *Mycobacterium tuberculosis*. J Bacteriol 190(17):5963-71.

Dorhoi A, Desel C, Yeremeev V, Pradl L, Brinkmann V, Mollenkopf HJ, Hanke K, Gross O, Ruland J, Kaufmann SH. (2010). The adaptor molecule CARD9 is essential for tuberculosis control. J Exp Med 207(4):777-92.

Dubnau E, Chan J, Raynaud C, Mohan V P, Lanéelle MA, Yu K, Quémard A, Smith, I, Daffe M. (2000). Oxygenated mycolic acids are necessary for virulence of *Mycobacterium tuberculosis* in mice. Mol Microbiol 36(3):630-637.

Dunn MF, Ramírez-Trujillo JA, Hernández-Lucas I. (2009). Major roles of isocitrate lyase and malate synthase in bacterial and fungal pathogenesis. Microbiology 155(Pt 10):3166-75.

Ehlers MR, Daffé M. (1998). Interactions between *Mycobacterium tuberculosis* and host cells: are mycobacterial sugars the key?. Trends Microbiol 6(8):328-35.

Eggeling L, Bott M. (2005). Handbook of *Corynebacterium glutamicum* (Boca Raton, FL: CRC Press).

Engelhardt H, Heinz C, Niederweis M. (2002). A tetrameric porin limits the cell wall permeability of *Mycobacterium smegmatis.* J Biol Chem 4;277(40):37567-72.

Ernst JD. (1998). Macrophage Receptors for *Mycobacterium tuberculosis*. Infect Immun 66(4): 1277–1281.

Ernst JD. (2012). The immunological life cycle of tuberculosis. Nat Rev Immunol 12(8):581-91.

Errington J, Daniel RA, Scheffers DJ. (2003). Cytokinesis in bacteria. Microbiol Mol Biol Rev 67:52–65.

Escuyer VE, Lety MA, Torrelles JB, Khoo KH, Tang JB, Rithner CD, Frehel C, McNeil MR, Brennan PJ, Chatterjee D. (2001). The role of the *embA* and *embB* gene products in the biosynthesis of the terminal hexaarabinofuranosyl motif of *Mycobacterium smegmatis* arabinogalactan. J Biol Chem 276(52):48854-62.

Etienne G, Laval F, Villeneuve C, Dinadayala P, Abouwarda A, Zerbib D, Galamba A, Daffé M. (2005). The cell envelope structure and properties of *Mycobacterium smegmatis* mc^2155: is there a clue for the unique transformability of the strain? Microbiology. 151(Pt 6):2075-86.

Fang H, Yu D, Hong Y, Zhou X, Li C, Sun B. (2013). The LuxR family regulator *Rv0195* modulates *Mycobacterium tuberculosis* dormancy and virulence. Tuberculosis (Edinb) 93(4):425-31.

Flores-Villanueva PO, Ruiz-Morales JA, Song CH, Flores LM, Jo EK, Montaño M, Barnes PF, Selman M, Granados J. (2005). A functional promoter polymorphism in monocyte chemoattractant protein-1 is associated with increased susceptibility to pulmonary tuberculosis. J Exp Med 202(12):1649-58.

Gagliardi MC, Lemassu A, Teloni R, Mariotti S, Sargentini V, Pardini M, Daffé M, Nisini R. (2007). Cell wall-associated alpha-glucan is instrumental for *Mycobacterium tuberculosis* to block CD1 molecule expression and disable the function of dendritic cell derived from infected monocyte. Cell Microbiol 9: 2081–2092.

Gagneux S, DeRiemer K, Van T, Kato-Maeda M, de Jong BC, Narayanan S, Nicol M, Niemann S, Kremer K, Gutiérrez MC, Hilty M, Hopewell PC, Small PM. (2006). Variable host-pathogen compatibility in Mycobacterium tuberculosis. PNAS 103(8):2869-73.

Gallegos AM, Pamer EG, Glickman MS. (2008). Delayed protection by ESAT-6-specific effector CD4+ T cells after airborne *M. tuberculosis* infection. J Exp Med 205(10):2359-68.

Gande R, Gibson KJC, Brown AK, Krumbach K, Dover LG, Sahm H, Shioyama S, Oikawa T, Besra GS, Eggeling L. (2004). Acyl-CoA carboxylases (*accD2* and *accD3*), together with a unique polyketide synthase (Cg-*pks*), are key to mycolic acid biosynthesis in *Corynebacterianeae* such as *Corynebacterium glutamicum* and *Mycobacterium tuberculosis*. J Biol Chem 279:44847–44857.

Gande R, Dover LG, Krumbach K, Besra GS, Sahm H, Oikawa T, Eggeling L. (2007). The two carboxylases of *Corynebacterium glutamicum* essential for fatty acid and mycolic acid synthesis. J Bacteriol 189: 5257–5264.

Gao LY, Laval F, Lawson EH, Groger RK, Woodruff A, Morisaki JH, Cox JS, Daffe M, Brown EJ. (2003a). Requirement for *kasB* in *Mycobacterium* mycolic acid biosynthesis, cell wall impermeability and intracellular survival: implications for therapy. Mol Microbiol 49(6):1547-63.

Gao LY, Groger R, Cox JS, Beverley SM, Lawson EH, Brown EJ. (2003b). Transposon mutagenesis of *Mycobacterium marinum* identifies a locus linking pigmentation and intracellular survival. Infect Immun 71(2):922-9.

Garg A, Barnes PF, Porgador A, Roy S, Wu S, Nanda JS, Griffith DE, Girard WM, Rawal N, Shetty S, Vankayalapati R. (2006). Vimentin expressed *on Mycobacterium tuberculosis*-infected human monocytes is involved in binding to the NKp46 receptor. J Immunol 177(9):6192-8.

Gavalda S, Léger M, van der Rest B, Stella A, Bardou F, Montrozier H, Chalut C, Burlet-Schiltz O, Marrakchi H, Daffé M, Quémard A. (2009). The Pks13/FadD32 crosstalk for the biosynthesis of mycolic acids in *Mycobacterium tuberculosis*. J Biol Chem 284(29):19255-19264.

Gebhardt H, Meniche X, Tropis M, Krämer R, Daffé M, Morbach S. (2007). The key role of the mycolic acid content in the functionality of the cell wall permeability barrier in *Corynebacterineae*. Microbiology 153:1424–34.

Gengenbacher M, Kaufmann SH. (2012). *Mycobacterium tuberculosis*: success through dormancy. FEMS Microbiol Rev 36(3):514-32.

Geurtsen J, Chedammi S, Mesters J, Cot M, Driessen NN, Sambou T, Kakutani R, Ummels R, Maaskant J, Takata H, Baba O, Terashima T, Bovin N, Vandenbroucke-Grauls CM, Nigou J, Puzo G, Lemassu A, Daffé M, Appelmelk BJ. (2009). Identification of mycobacterial alpha-glucan as a novel ligand for DC-SIGN: involvement of mycobacterial capsular polysaccharides in host immune modulation. J Immunol 183(8):5221-31.

Giebel JD, Carr KA, Anderson EC, Hanna PC. (2009). The germination-specific lytic enzymes SleB, CwlJ1, and CwlJ2 each contribute to *Bacillus anthracis* spore germination and virulence. J Bacteriol 191: 5569–5576.

Ginda K, Bezulska M, Ziółkiewicz M, Dziadek J, Zakrzewska-Czerwińska J, Jakimowicz D. (2013). ParA of *Mycobacterium smegmatis* co-ordinates chromosome segregation with the cell cycle and interacts with the polar growth determinant DivIVA. Mol Microbiol 87(5):998-1012.

Giovannini D, Cappelli G, Jiang L, Castilletti C, Colone A, Serafino A, Wannenes F, Giacò L, Quintiliani G, Fraziano M, Nepravishta R, Colizzi V, Mariani F. (2012). A new *Mycobacterium tuberculosis* smooth colony reduces growth inside human macrophages and represses PDIM Operon gene expression. Does an heterogeneous population exist in intracellular mycobacteria?. Microb Pathog 53(3-4):135-46.

Glickman MS, Cox JS, Jacobs WR Jr. (2000). A novel mycolic acid cyclopropane synthetase is required for cording, persistence, and virulence of *Mycobacterium tuberculosis*. Mol Cell 5: 717–727.

Goren MB, Brokl O, Das BC , Lederer E. (1971). Sulfolipid I of *Mycobacterium tuberculosis*, strain H37Rv. Nature of the acyl substituents. Biochemistry 10: 72 – 81.

Goren MB, Brennan PJ. (1980). Mycobacterial lipids: chemistry and biological activities. In: Youmans GP, editor. Tuberculosis. Philadelphia: W. B. Saunders, p. 63–193.

Goude R, Amin AG, Chatterjee D, Parish T. (2008). The critical role of *embC* in *Mycobacterium tuberculosis*. J Bacteriol 190:4335–4341.

Grzegorzewicz AE, Pham H, Gundi VA, Scherman MS, North EJ, Hess T, Jones V, Gruppo V, Born SE, Kordulakova J, *et al*. (2012). Inhibition of mycolic acid transport across the *Mycobacterium tuberculosis* plasma membrane. Nat Chem Biol 8, 334–341.

Guérardel Y, Maes E, Elass E, Leroy Y, Timmerman P, Besra GS, Locht C, Strecker G, Kremer, L. (2002). Structural study of lipomannan and lipoarabinomannan from *Mycobacterium chelonae*. Presence of unusual components with alpha 1,3-mannopyranose side chains. J Biol Chem 277:30635-30648.

Guilhot C, Otal I, Van Rompaey I, Martìn C, Gicquel B. (1994). Efficient transposition in mycobacteria: construction of *Mycobacterium smegmatis* insertional mutant libraries. J Bacteriol 176(2):535-9.

Gutiérrez MC, Brisse S, Brosch R, Fabre M, Omaïs B, Marmiesse M, Supply P, Vincent V. (2005). Ancient origin and gene mosaicism of the progenitor of *Mycobacterium tuberculosis*. PLoS Pathog 1(1):e5.

Hartkoorn RC, Uplekar S, Cole ST. (2014). Cross-resistance between Clofazimine and Bedaquiline through upregulation of MmpL5 in *Mycobacterium tuberculosis*. Antimicrob Agents Chemother 58(5):2979-2981.

He H, Hovey R, Kane J, Singh V, Zahrt TC. (2006). MprAB is a stress-responsive two-component system that directly regulates expression of sigma factors SigB and SigE in *Mycobacterium tuberculosis*. J Bacteriol 188:2134–2143.

Hengge-Aronis R. (2002). Signal transduction and regulatory mechanisms involved in control of the sigma(S) (RpoS) subunit of RNA polymerase. Microbiol Mol Biol Rev 66(3):373-395.

Herrero M, de Lorenzo V, Timmis KN. (1990). Transposon vectors containing non-antibiotic resistance selection markers for cloning and stable chromosomal insertion of foreign genes in Gram-negative bacteria. J Bacteriol 172(11):6557-67.

Hinshaw HV, Feldman WH. (1945). Streptomycin in the treatment of clinical tuberculosis: a preliminary report. Proc Staff Meetings Mayo Clinic 20:313–8.

Hirasawa T, Wachi M, Nagai K. (2000). A mutation in the *Corynebacterium glutamicum ltsA* gene causes susceptibility to lysozyme, temperature-sensitive growth, and L-glutamate production. J Bacteriol 182(10):2696-701.

Hirsh AE, Tsolaki AG, DeReimer K, Feldman MW, Small PM. (2004). Stable association between strains of *Mycobacterium tuberculosis* and their human populations. PNAS 101:4871–6.

Holt PG, Strickland DH, Wikström ME, Jahnsen FL. (2008). Regulation of immunological homeostasis in the respiratory tract. Nat Rev Immunol 8(2):142-52.

Hsu FF, Turk J, Owens RM, Rhoades ER, Russell DG. (2007). Structural characterization of phosphatidyl-myo-inositol mannosides from *Mycobacterium bovis* Bacillus Calmette Guerin by multiple-stage quadrupole ion-trap mass spectrometry with electrospray ionization. II. Monoacyl- and diacyl-PIMs. J Am Soc Mass Spectrom 18: 479-492.

Hunter SW, Brennan PJ. (1990). Evidence for the presence of a phosphatidylinositol anchor on the lipoarabinomannan and lipomannan of *Mycobacterium tuberculosis*. J Biol Chem 265: 9272-9279.

Ishige K, Zhang H, Kornberg A. (2002). Polyphosphate kinase (PPK2), a potent, polyphosphate-driven generator of GTP. PNAS 99(26):16684-8.

Jain M, Cox JS. (2005). Interaction between polyketide synthase and transporter suggests coupled synthesis and export of virulence lipid in *M. tuberculosis*. PLoS Pathog 1(1):e2.

Jakimowicz D, Brzostek A, Rumijowska-Galewicz A, Zydek P, Dołzbłasz A, Smulczyk-Krawczyszyn A, Zimniak T, Wojtasz L, Zawilak-Pawlik A, Kois A, Dziadek J,Zakrzewska-Czerwińska J. (2007). Characterization of the mycobacterial chromosome segregation protein ParB and identification of its target in *Mycobacterium smegmatis*. Microbiol 153(Pt 12):4050-60.

Jordao L, Bleck CK, Mayorga L, Griffiths G, Anes E. (2008). On the killing of mycobacteria by macrophages. Cell Microbiol 10(2):529-48.

Kan-Sutton C, Jagannath C, Hunter RL Jr. (2009). Trehalose 6,6'-dimycolate on the surface of *Mycobacterium tuberculosis* modulates surface marker expression for antigen presentation and costimulation in murine macrophages. Microbes Infect 11: 40-48.

Kana BD, Gordhan BG, Downing KJ, Sung N, Vostroktunova G, Machowski EE, Tsenova L, Young M, Kaprelyants A, Kaplan G, Mizrahi V. (2008). The resuscitation-promoting factors of *Mycobacterium tuberculosis* are required for virulence and resuscitation from dormancy but are collectively dispensable for growth in vitro. Mol Microbiol 67: 672–684.

Kaplan G, Post FA, Moreira AL, Wainwright H, Kreiswirth BN, Tanverdi M, Mathema B, Ramaswamy SV, Walther G, Steyn LM, Barry CE 3rd, Bekker LG. (2003). *Mycobacterium tuberculosis* growth at the cavity surface: a microenvironment with failed immunity. Infect Immun 71(12):7099-108.

Katis VL, Wake RG. (1999). Membrane-bound division proteins DivIB and DivIC of *Bacillus subtilis* function solely through their external domains in both vegetative and sporulation division. J Bacteriol 181(9):2710-8.

Kaufmann, SH. (2001). How can immunology contribute to the control of tuberculosis? Nat Rev Immunol 1, 20-30.

Kaur D, Guerin ME, Škovierová H, Brennan PJ, Jackson M. (2009). Biogenesis of the cell wall and other glycoconjugates of *Mycobacterium tuberculosis*. Adv Appl Microbiol 69: 23–78.

Keane J, Balcewicz-Sablinska MK, Remold HG, Chupp GL, Meek BB, Fenton MJ, Kornfeld H. (1997). Infection by *Mycobacterium tuberculosis* promotes human alveolar macrophage apoptosis. Infect Immun 65(1):298-304.

Koch R. (1882). Die Aetiologie der Tuberkulose. Berliner klinische Wochenschrift 19: 221–230.

Kordulakova J, Gilleron M, Puzo G, Brennan PJ, Gicquel B, Mikusova K, Jackson M. (2003). Identification of the required acyltransferase step in the biosynthesis of the phosphatidylinositol mannosides of *Mycobacterium* species. J Biol Chem 278, 36285-36295.

Kornberg A, Rao N, Ault-Riché D. (1999). Inorganic polyphosphate: a molecule of many functions. Annu Rev Biochem 68:89-125.

Koul A, Arnoult E, Lounis N, Guillemont J, Andries K. (2011). The challenge of new drug discovery for tuberculosis. Nature 469(7331):483-90.

Kovacevic S, Anderson D, Morita YS, Patterson J, Haites R, McMillan BN, Coppel R, McConville MJ, Billman-Jacobe H. (2006). Identification of a novel protein with a role in lipoarabinomannan biosynthesis in mycobacteria. J Biol Chem 281(14):9011-7.

Kremer L, Dover LG, Carrere S, Nampoothiri KM, Lesjean S, Brown AK, *et al*. (2002). Mycolic acid biosynthesis and enzymic characterization of the beta-ketoacyl-ACP synthase A-condensing enzyme from *Mycobacterium tuberculosis*. Biochem J 364: 423–430.

Kriakov J, Lee Sh, Jacobs WR Jr. (2003). Identification of a regulated alkaline phosphatase, a cell surface-associated lipoprotein, in *Mycobacterium smegmatis*. J Bacteriol 185(16):4983-91.

Krubasik P, Kobayashi M, Sandmann G. (2001). Expression and functional analysis of a gene cluster involved in the synthesis of decaprenoxanthin reveals the mechanisms for C50 carotenoid formation. Eur J Biochem 268: 3702–3708.

Kulaev I, Vagabov V, Kulakovskaya T. (1999). New aspects of inorganic polyphosphate metabolism and function. J Biosci Bioeng 88:111-129.

Kumar A, Toledo JC, Patel RP, Lancaster JR Jr, Steyn AJ. (2007). *Mycobacterium tuberculosis* DosS is a redox sensor and DosT is a hypoxia sensor. PNAS 104:11568–11573.

Kuroda A, Kornberg A. (1997). Polyphosphate kinase as a nucleoside diphosphate kinase in *Escherichia coli* and *Pseudomonas aeruginosa*. PNAS 94:439-442.

Kuroda A, Tanaka S, Ikeda T, Kato J, Takiguchi N, Ohtake H. (1999). Inorganic polyphosphate kinase is required to stimulate protein degradation and for adaptation to amino acid starvation in *Escherichia coli*. PNAS 96(25):14264-9.

Lamichhane G, Zignol M, Blades NJ, Geiman DE, Dougherty A, Grosset J, Broman KW, Bishai WR. (2003). A postgenomic method for predicting essential genes at subsaturation levels of mutagenesis: application to *Mycobacterium tuberculosis*. PNAS 100(12):7213-8.

La Rosa V, Poce G, Canseco JO, Buroni S, Pasca MR, Biava M, Raju RM, Porretta GC, Alfonso S, Battilocchio C, *et al*. (2012). MmpL3 is the cellular target of the antitubercular pyrrole derivative BM212. Antimicrob Agents Chemother 56: 324–331.

Larsen MH, Biermann K, Tandberg S, Hsu T, Jacobs WR Jr. (2007). Genetic manipulation of *Mycobacterium tuberculosis*. Curr Protoc Microbiol. Chapter 10, Unit 10A, 12.

Layre E, Paepe DC, Larrouy-Maumus G, Vaubourgeix J, Mundayoor S, Lindner B, Puzo G, Gilleron M. (2011). Deciphering sulfoglycolipids of *Mycobacterium tuberculosis*. J Lipid Res 52(6):1098-110.

Lazarevic V, Flynn J. (2002). CD8-T cells in tuberculosis. Am J Respir Crit Care Med 166:1116–1121.

Lederer E, Adam A, Ciorbaru R, Petit J-F, Wietzerbin J. (1975). Cell walls of mycobacteria and related organisms: chemistry and immunological stimulant properties. Mol Cell Biochem 7:87–104.

Lee A, Wu S-W, Scherman MS, Torrelles JB, Chatterjee C, McNeil MR, Khoo K-H. (2006). Sequencing of the oligoarabinosyl units released from mycobacterial arabinogalactan by endogenous arabinanase: Identification of distinctive and novel structural motifs. Biochemistry 45:15817–15828.

Lee OY, Wu HH, Donoghue HD, Spigelman M, Greenblatt CL, Bull ID, Rothschild BM, Martin LD, Minnikin DE, Besra GS. (2012). *Mycobacterium tuberculosis* complex lipid virulence factors preserved in the 17,000-year-old skeleton of an extinct bison, *Bison antiquus*. PLoS One. 7(7):e41923.

Lemassu A, Ortalo-Magné A, Bardou F, Silve G, Laneélle MA, Daffé M. (1996). Extracellular and surfaceexposed polysaccharides of non-tuberculous mycobacteria. Microbiology 142:1513–1520.

Li XZ, Zhang L, Nikaido H. (2004). Efflux pump-mediated intrinsic drug resistance in *Mycobacterium smegmatis*. Antimicrob Agents Chemother 48(7):2415-23.

Lin YG, Zhang M, Hofman FM, Gong JH, Barnes PF. (1996). Absence of a prominent Th2 cytokine response in human tuberculosis. Infect Immun 64, 1351–1356.

Lindner SN, Knebel S, Wesseling H, Schoberth SM, Wendisch VF. (2009). Exopolyphosphatases PPX1 and PPX2 from *Corynebacterium glutamicum*. Appl Environ Microbiol 75: 3161–3170.

Liu J, Takiff HE, Nikaido H. (1996). Active efflux of fluoroquinolones *in Mycobacterium smegmatis* mediated by LfrA, a multidrug efflux pump. J Bacteriol 178(13): 3791–3795.

Low KL, Rao PS, Shui G, Bendt AK, Pethe K, Dick T, Wenk MR. (2009). Triacylglycerol utilization is required for regrowth of in vitro hypoxic nonreplicating *Mycobacterium bovis* bacillus Calmette-Guerin. J Bacteriol 191:5037–5043.

Magnusson LU, Farewell A, Nystrom T. (2005). ppGpp: a global regulator in *Escherichia coli*. Trends Microbiol 13: 236–242.

Mahapatra S, Crick DC, McNeil MR, Brennan PJ. (2008). Unique structural features of the peptidoglycan of *Mycobacterium leprae*. J Bacteriol 190(2):655-61.

Málaga W, Constant P, Euphrasie D, Cataldi A, Daffé M, Reyrat J-M, Guilhot C. (2008). Deciphering the genetic bases of the structural diversity of phenolic glycolipids in strains of the *Mycobacterium tuberculosis* complex. J Biol Chem 283:15177–15184.

Maloney E, Madiraju M, Rajagopalan M. (2009). Overproduction and localization of *Mycobacterium tuberculosis* ParA and ParB proteins. Tuberculosis (Edinb) 89 Suppl 1:S65-9.

Manganelli R, Voskuil MI, Schoolnik GK, Smith I. (2001). The *Mycobacterium tuberculosis* ECF sigma factor SigE: role in global gene expression and survival in macrophages. Mol Microbiol 41: 423–437.

Manganelli R. (2007). Polyphosphate and stress response in mycobacteria. MicroCommentary. Mol Microbiol 65(2):258–260.

Manna D, Breier AM, Higgins NP. (2004). Microarray analysis of transposition targets in *Escherichia coli*: the impact of transcription. PNAS 29;101(26):9780-5.

Manoil C, Beckwith J. (1985). Tnpho A: a transposon probe for protein export signals. PNAS 82:8129-8133.

Marrero J, Rhee KY, Schnappinger D, Pethe K, Ehrt S. (2010). Gluconeogenic carbon flow of tricarboxylic acid cycle intermediates is critical for *Mycobacterium tuberculosis* to establish and maintain infection. PNAS 107:9819–9824.

Matsunaga I, Bhatt A, Young DC, Cheng TY, Eyles SJ, Besra GS, Briken V, Porcelli SA, Costello CE, Jacobs WR Jr, Moody DB. (2004). *Mycobacterium tuberculosis pks12* produces a novel polyketide presented by CD1c to T cells. J Exp Med 20;200(12):1559-69.

McAdam RA, Quan S, Smith DA, Bardarov S, Betts JC, Cook FC, Hooker EU, Lewis AP, Woollard P, Everett MJ, Lukey PT, Bancroft GJ, Jacobs Jr WR Jr, Duncan K. (2002). Characterization of a *Mycobacterium tuberculosis* H37Rv transposon library reveals insertions in 351 ORFs and mutants with altered virulence. Microbiology 148(Pt 10):2975-86.

McNeil M, Daffé M, Brennan PJ. (1990). Evidence for the nature of the link between the arabinogalactan and peptidoglycan of mycobacterial cell walls. J Biol Chem 265: 18200-18206.

McNeil MR, Daffé M, Brennan PJ. (1991). Location of the mycolyl ester substituents in the cell walls of mycobacteria. J Biol Chem 266:13217–13223.

McKinney JD, zu Bentrup KH, Muñoz-Elias EJ, Miczak A, Chen B, Chan WT, Swenson D, Sacchettini JC, Jacobs WR, Russell DG. (2000). Persistence of *Mycobacterium tuberculosis* in macrophages and mice requires the glyoxylate shunt enzyme isocitrate lyase. Nature 406: 735–738.

Milano A, Pasca MR, Provvedi R, Lucarelli AP, Manina G, Ribeiro AL, Manganelli R, Riccardi G. (2009). Azole resistance in *Mycobacterium tuberculosis* is mediated by the MmpS5–MmpL5 efflux system. Tuberculosis 89(1):84-90.

Minnikin DE. (1982). Lipids: complex lipids, their chemistry, biosynthesis and roles. In The Biology of the Mycobacteria pp. 95-184. Edited by C. Ratledge & J. Stanford. London: Academic Press Inc Ltd.

Minnikin DE, Kremer L, Dover LG, Besra GS. (2002). The methyl-branched fortifications of *Mycobacterium tuberculosis*. Chem Biol 9(5):545-53.

Mishra AK, Alderwick LJ, Rittmann D, Wang C, Bhatt A., Jacobs WR, Jr., Takayama, K., Eggeling, L., and Besra, G.S. (2008). Identification of a novel alpha (1—>6) mannopyranosyltransferase MptB from *Corynebacterium glutamicum* by deletion of a conserved gene, *NCgl1505*, affords a lipomannan- and lipoarabinomannan-deficient mutant. Mol Microbiol 68: 1595–1613.

Mishra AK, Alves JE, Krumbach K, Nigou J, Castro AG, Geurtsen J, Eggeling L, Saraiva M, Besra GS. (2012). Differential arabinan capping of lipoarabinomannan modulates innate immune responses and impacts T-helper cell differentiation. J Biol Chem 287(53):44173-83.

Miyake T, Shiba T, Kameda A, Ihara Y, Munekata M, Ishige K, Noguchi T. (1999). The gene for an exopolyphosphatase of *Pseudomonas aeruginosa*. DNA Res 6:103-108.

Miyamoto Y, Mukai T, Maeda Y, Kai M, Naka T, Yano I, Makino M. (2008). The *Mycobacterium avium* complex *gtfTB* gene encodes a glucosyltransferase required for the biosynthesis of serovar 8-specific glycopeptidolipid. J Bacteriol 190(24):7918-24.

Mougous JD, Petzold CJ, Senaratne RH, Lee DH, Akey DL, Lin FL, Munchel SE, Pratt MR, Riley LW, Leary JA, Berger JM, Bertozzi CR. (2004). Identification, function and structure of the mycobacterial sulfotransferase that initiates sulfolipid-1 biosynthesis. Nat Struct Mol Biol 11(8):721-9.

Mostowy S, Cousins D, Brinkman J, Aranaz A, Behr MA. (2002). Genomic deletions suggest a phylogeny for the Mycobacterium tuberculosis complex. J Infect Dis 186(1):74-80.

Muñoz-Elias EJ, McKinney J D. (2005). *Mycobacterium tuberculosis* isocitrate lyases 1 and 2 are jointly required for in vivo growth and virulence. Nat Med 11:638-644.

Nagata S. (1999). Fas ligand-induced apoptosis. Annu Rev Genet 33:29.

Nahalka J, Patoprsty V. (2009). Enzymatic synthesis of sialylation substrates powered by a novel polyphosphate kinase (PPK3). Org Biomol Chem 7:1778-1780.

Nanninga N. (1998). Morphogenesis of *Escherichia coli*. Microbiol Mol Biol Rev 62: 110–129.

Nathan C, Shiloh MU. (2000). Reactive oxygen and nitrogen intermediates in the relationship between mammalian hosts and microbial pathogens. PNAS 97:8841–8848.

Nerlich AG, Haas CJ, Zink A, Szeimies U, Hagedorn HG. (1997). Molecular evidence for tuberculosis in an ancient Egyptian mummy. Lancet 1997;350:1404.

Nigou J, Gilleron M, Puzo G. (2003). Lipoarabinomannans: from structure to biosynthesis. Biochimie 85(1-2):153-66.

Nishiuchi Y, Baba T, Hotta HH, Yano I. (1999). Mycolic acid analysis in *Nocardia* species: The mycolic acid compositions of *Nocardia asteroides,N. farcinica,* and *N. nova*. J Microbiol Methods 37:111–22.

Noll H, Bloch H. (1955). Studies on the chemistry of the cord factor of *Mycobacterium tuberculosis*. J Biol Chem. 224:149–163.

Noll H, Asselineau J, Lederer E. (1956). The chemical structure of the cord factor of *Mycobacterium tuberculosis*. Biochim Biophys Acta 20:299–309.

Ojha A, Anand M, Bhatt A, Kremer L, Jacobs WR Jr., Hatfull GF. (2005). GroEL1: a dedicated chaperone involved in mycolic acid biosynthesis during biofilm formation in mycobacteria. Cell 123: 861–873.

Ojha AK, Trivelli X, Guerardel Y, Kremer L, Hatfull GF. (2010). Enzymatic hydrolysis of trehalose dimycolate releases free mycolic acids during mycobacterial growth in biofilms. J Biol Chem. 285(23):17380-9.

O'Toole R, Smeulders MJ, Blokpoel MC, Kay EJ, Lougheed K, Williams HD. (2003). A two-component regulator of universal stress protein expression and adaptation to oxygen starvation in *Mycobacterium smegmatis*. J Bacteriol 185(5): 1543-54.

Pacheco SA, Hsu FF, Powers KM, Purdy GE. (2013). MmpL11 protein transports mycolic acid-containing lipids to the mycobacterial cell wall and contributes to biofilm formation in *Mycobacterium smegmatis*. J Biol Chem 288(33): 24213-24222.

Pandey AK, Sassetti CM. (2008). Mycobacterial persistence requires the utilization of host cholesterol. PNAS 105: 4376–4380.

Pang X, Vu P, Byrd TF, Ghanny S, Soteropoulos P, Mukamolova GV, Wu S, Samten B, Howard ST. (2007). Evidence for complex interactions of stress-associated regulons in an *mprAB* deletion mutant of *Mycobacterium tuberculosis*. Microbiol 153: 1229–1242.

Parish T, Roberts G, Laval F, Schaeffer M, Daffé M, Duncan K. (2007). Functional complementation of the essential gene *fabG1* of *Mycobacterium tuberculosis* by *Mycobacterium smegmatis fabG* but not *Escherichia coli fabG*. J Bacteriol 189Ñ 3721–3728.

Parish T and Brown AC. (2008). Mycobacteria protocols, 2nd ed. edn. New York: Humana Press.

Park JT, Shim JH, Tran PL, Hong IH, Yong HU, Oktavina EF, Nguyen HD, Kim JW, Lee TS, Park SH, Boos W, Park KH. (2011). Role of maltose enzymes in glycogen synthesis by *Escherichia coli*. J Bacteriol 193(10):2517-26.

Pasca MR, Guglierame P, De Rossi E, Zara F, Riccardi G. (2005). *mmpL7* gene of *Mycobacterium tuberculosis* is responsible for isoniazid efflux in *Mycobacterium smegmatis*. Antimicrob Agents Chemother 49: 4775–4777.

Pathan AA, Minassian AM, Sander CR, Rowland R, Porter DW, Poulton ID, Hill AV, Fletcher HA, McShane H. (2012). Effect of vaccine dose on the safety and immunogenicity of a candidate TB vaccine, MVA85A, in BCG vaccinated UK adults. Vaccine. 30(38):5616-24.

Patterson JH, McConville MJ, Haites RE, Coppel RL, Billman-Jacobe H. (2000). Identification of a methyltransferase from *Mycobacterium smegmatis* involved in glycopeptidolipid synthesis. J Biol Chem 275: 24900-24906.

Peirs P, Lefèvre P, Boarbi S, Wang XM, Denis O, Braibant M, Pethe K, Locht C, Huygen K, Content J. (2005) *Mycobacterium tuberculosis* with disruption in genes encoding the phosphate binding proteins PstS1 and PstS2 is deficient in phosphate uptake and demonstrates reduced in vivo virulence. Infect Immun 73(3):1898-902.

Petit JF, Adam A, Weitzerbin-Falszpan J, Lederer E, Ghuysen JM. (1969). Chemical structure of the cell wall of *Mycobacterium smegmatis*. I. Isolation and partial characterization of peptidoglycan. Biochim Biophys Res Commun 35: 478–83.

Pitarque S, Larrouy-Maumus G, Payré B, Jackson M, Puzo G, Nigou J. (2008). The immunomodulatory lipoglycans, lipoarabinomannan and lipomannan, are exposed at the mycobacterial cell surface. Tuberculosis (Edinb) 88(6):560-5.

Portevin D, De Sousa-D'Auria C, Houssin C, Grimaldi C, Chami M, Daffé M, Guilhot C. (2004). A polyketide synthase catalyzes the last condensation step of mycolic acid biosynthesis in mycobacteria and related organisms. PNAS 101:314–9.

Portevin D, de Sousa-D'Auria C, Montrozier H, Houssin C, Stella A, Lanéelle MA, Bardou F, Guilhot C, Daffé M. (2005). The acyl-AMP ligase FadD32 and AccD4-containing acyl-CoA carboxylase are required for the synthesis of mycolic acids and essential for mycobacterial growth: identification of the carboxylation product and determination of the acyl-CoA carboxylase components. J Biol Chem 280: 8862-8874.

Primm TP, Andersen SJ, Mizrahi V, Avarbock D, Rubin H, Barry CE. (2000). The stringent response of *Mycobacterium tuberculosis* is required for long-term survival. J Bacteriol 182:4889-4898.

Puech V, Guilhot C, Perez E, Tropis M, Armitige LY, Gicquel B, Daffé M. (2002). Evidence for a partial redundancy of the fibronectin-binding proteins for the transfer of mycoloyl residues onto the cell wall arabinogalactan termini of *Mycobacterium tuberculosis*. Mol Microbiol 44: 1109–1122.

Purdy GE, Niederweis M, Russell DG. (2009). Decreased outer membrane permeability protects mycobacteria from killing by ubiquitin-derived peptides. Mol Microbiol 73, 844–857.

Quan S, Venter H, Dabbs ER. (1997). Ribosylative inactivation of rifampin by *Mycobacterium smegmatis* is a principal contributor to its low susceptibility to this antibiotic. Antimicrob Agents Chemother 41(11):2456-60.

Quartararo CE, Blanchard JS. (2011). Kinetic and chemical mechanism of malate synthase from *Mycobacterium tuberculosis*. Biochemistry 50(32):6879-87.

Quemard A, Sacchettini JC, Dessen A, Vilcheze C, Bittman R, Jacobs WR Jr., Blanchard JS. (1995). Enzymatic characterization of the target for isoniazid in *Mycobacterium tuberculosis*. Biochemistry 34: 8235–8241.

Qureshi N, Takayama K, Jordi HC, Schnoes HK. (1978). Characterization of the purified components of a homologous series of alpha-mycolic acids from *Mycobacterium tuberculosis* H37Ra. J Biol Chem 253:5411–5417.

Radhakrishnan A, Kumar N, Wright CC, Chou TH, Tringides ML, Bolla JR, Lei HT, Rajashankar K, Su CC, Purdy GE, Yu EW. (2014). Crystal structure of the transcriptional regulator *Rv0678* of *Mycobacterium tuberculosis*. J Biol Chem [Epub ahead of print].

Radmacher E, Alderwick LJ, Besra GS, Brown AK, Gibson KJ, Sahm H, Eggeling L. (2005). Two functional FAS-I type fatty acid synthases in *Corynebacterium glutamicum*. Microbiol 151, 2421–2427.

Rao NN, Kornberg A. (1996). Inorganic polyphosphate supports resistance and survival of stationary-phase *Escherichia coli*. J Bacteriol 178(5):1394-400.

Rao NN, Liu S, Kornberg A. (1998). Inorganic polyphosphate in *Escherichia coli*: the phosphate regulon and the stringent response. J Bacteriol. 180:2186-2193.

Rao V, Fujiwara N, Porcelli SA, Glickman, MS. (2005). *Mycobacterium tuberculosis* controls host innate immune activation through cyclopropane modification of a glycolipid effector molecule. J Exp Med 201(4):535-543.

Rao V, Gao F, Chen B, Jacobs WR, Glickman MS. (2006). Trans-cyclopropanation of mycolic acids on trehalose dimycolate suppresses *Mycobacterium tuberculosis* induced inflammation and virulence. J Clin Invest 116(6): 1660–1667.

Rao NN, Gómez-García MR, Kornberg A. 2009. Inorganic polyphosphate: Essential for growth and survival. Annu. Rev. Biochem. 78:35.1-35.43.

Rashid MH, Rao NN, Kornberg A. (2000). Inorganic polyphosphate is required for motility of bacterial pathogens. J Bacteriol 182:225–227.

Recht J, Kolter R. (2001). Glycopeptidolipid acetylation affects sliding motility and biofilm formation in *Mycobacterium smegmatis*. J Bacteriol 183(19):5718-24.

Reece ST, Kaufmann SHE. (2011). Floating between the poles of pathology and protection: can we pin down the granuloma in tuberculosis? Curr Opin Microbiol 15: 63–70.

Ren H, Liu J. (2006). AsnB is involved in natural resistance *of Mycobacterium smegmatis* to multiple drugs. Antimicrob Agents Chemother 50(1):250-5.

Ren H, Dover LG, Islam ST, Alexander DC, Chen JM, Besra GS, Liu J. (2007). Identification of the lipooligosaccharide biosynthetic gene cluster from *Mycobacterium marinum*. Mol Microbiol 63(5):1345-59.

Reyrat JM, Berthet FX, Gicquel B. (1995). The urease locus of *Mycobacterium tuberculosis* and its utilization for the demonstration of allelic exchange in *Mycobacterium bovis* bacillus Calmette-Guerin. PNAS USA 92: 8768–8772.

Reyrat JM, Kahn D. (2001). *Mycobacterium smegmatis*: an absurd model for tuberculosis? Trends Microbiol 9(10):472-4.

Rifat D, Bishai WR, Karakousis PC. (2009). Phosphate depletion: a novel trigger for *Mycobacterium tuberculosis* persistence. J Infect Dis 200(7):1126-35.

Rodrigue S, Provvedi R, Jacques PE, Gaudreau L, Manganelli R. (2006). The sigma factors of *Mycobacterium tuberculosis*. FEMS Microbiol Rev 30: 926–941.

Rodrígues L, Ramos J, Couto I, Amaral L, Viveiros M. (2011). Ethidium bromide transport across *Mycobacterium smegmatis* cell-wall: correlation with antibiotic resistance. BMC Microbiol 11:35.

Rodríguez JE, Ramírez AS, Salas LP, Helguera-Repetto C, Gonzalez-y-Merchand J, Soto CY, Hernández-Pando R. (2013). Transcription of genes involved in sulfolipid and polyacyltrehalose biosynthesis of *Mycobacterium tuberculosis* in experimental latent tuberculosis infection. PLoS One 8(3):e58378.

Rombouts Y, Alibaud L, Carrère-Kremer S, Maes E, Tokarski C, Elass E, Kremer L, Guérardel Y. (2011). Fatty acyl chains of *Mycobacterium marinum* lipooligosaccharides: structure, localization and acylation by PapA4 (*MMAR_2343*) protein. J Biol Chem 286(38):33678-88.

Rothfuchs AG, Bafica A, Feng CG, Egen JG, Williams DL, Brown GD, Sher A. (2007). Dectin-1 interaction with *Mycobacterium tuberculosis* leads to enhanced IL-12p40 production by splenic dendritic cells. J Immunol 179(6):3463-71.

Rousseau C, Sirakova TD, Dubey VS, Bordat Y, Kolattukudy PE, Gicquel B, Jackson M. (2003). Virulence attenuation of two Mas-like polyketide synthase mutants of *Mycobacterium tuberculosis*. Microbiology 149(Pt 7):1837-47.

Roy R, Veeraraghavan U, Kermani A, Scott DJ, Hyde EI, Besra GS, Alderwick LJ, Fütterer K. (2013). Synthesis of α-glucan in mycobacteria involves a hetero-octameric complex of trehalose synthase TreS and Maltokinase Pep2. ACS Chem Biol 8(10):2245-55.

Rubin EJ, Akerley BJ, Novik VN, Lampe DJ, Husson RN, Mekalanos JJ. (1999). In vivo transposition of mariner-based elements in enteric bacteria and mycobacteria. PNAS 96(4):1645-50.

Russell DG. (2007). Who puts the tubercle in tuberculosis? Nat Rev Microbiol 5, 39-47.

Russell DG, Cardona PJ, Kim MJ, Allain S, Altare, F. (2009). Foamy macrophages and the progression of the human tuberculosis granuloma. Nat Immunol 10, 943-948.

Rybniker J, Wolke M, Haefs C, Plum G. (2003). Transposition of Tn5367 in *Mycobacterium marinum*, using a conditionally recombinant mycobacteriophage. J Bacteriol 185(5):1745-8.

Sacchettini JC, Rubin EJ, Freundlich JS. (2008). Drugs versus bugs: in pursuit of the persistent predator *Mycobacterium tuberculosis*. Nat Rev Microbiol 6(1):41-52.

Sambou T, Dinadayala P, Stadthagen G, Barilone N, Bordat Y, Constant P, Levillain F, Neyrolles O, Gicquel B, Lemassu A, Daffé M, Jackson M. (2008). Capsular glucan and intracellular glycogen of *Mycobacterium tuberculosis*: biosynthesis and impact on the persistence in mice. Mol Microbiol 70(3):762–774.

Sani M, Houben EN, Geurtsen J, Pierson J, de Punder K, van Zon M, Wever B, Piersma SR, Jiménez CR, Daffé M, Appelmelk BJ, Bitter W, van der Wel N, Peters PJ. (2010). Direct visualization by cryo-EM of the mycobacterial capsular layer: a labile structure containing ESX-1-secreted proteins. PLoS Pathog 6(3):e1000794.

Sanyal S, Banerjee SK, Banerjee R, Mukhopadhyay J, Kundu M. (2013). Polyphosphate kinase 1, a central node in the stress response network of *Mycobacterium tuberculosis*, connects the two-component systems MprAB and SenX3-RegX3 and the extracytoplasmic function sigma factor, sigma E. Microbiology. 159:2074-86.

Sassetti CM, Boyd DH, Rubin EJ. (2001). Comprehensive identification of conditionally essential genes in mycobacteria. PNAS 98(22):12712-7.

Sassetti CM, Boyd DH, Rubin EJ. (2003). Genes required for mycobacterial growth defined by high density mutagenesis. Mol Microbiol 48(1):77-84.

Sassetti CM, Rubin EJ. (2003). Genetic requirements for mycobacterial survival during infection. PNAS 100(22):12989-94.

Schafer A, Tauch A, Jager W, Kalinowski J, Thierbach G, Puhler A. (1994). Small mobilizable multi-purpose cloning vectors derived from the *Escherichia coli* plasmids pK18 and pK19: selection of defined deletions in the chromosome of *Corynebacterium glutamicum*. Gene 145:69–73.

Schaeffer ML, Agnihotri G, Volker C, Kallender H, Brennan PJ, Lonsdale JT. (2001) Purification and biochemical characterization of the *Mycobacterium tuberculosis* beta-ketoacyl-acyl carrier protein synthases KasA and KasB. J Biol Chem 276: 47029–47037

Schatz A, Bugie E, Waksman SA. (1944). Streptomycin, a substance exhibiting antibiotic activity against Gram-positive and Gram-negative bacteria. Proc Exp Biol Med 55:66–9.

Schleifer KH, Kandler O. (1972). Peptidoglycan types of bacterial cell walls and their taxonomic implications. Bacteriol Rev 36:407–477.

Schnappinger D, Ehrt S, Voskuil MI, Liu Y, Mangan JA, Monahan IM, Dolganov G, Efron B, Butcher PD, Nathan C, Schoolnik GK. (2003). Transcriptional Adaptation of *Mycobacterium tuberculosis* within Macrophages: Insights into the Phagosomal Environment. J Exp Med 198(5):693-704.

Schneewind O, Missiakas D. (2014). Lipoteichoic acids, phosphate-containing polymers in the envelope of gram-positive bacteria. J Bacteriol 196(6):1133-42.

Schoenen H, Bodendorfer B, Hitchens K, Manzanero S, Werninghaus K, Nimmerjahn F, Agger EM, Stenger S, Andersen P, Ruland J, Brown GD, Wells C, Lang R. (2010). Cutting edge: Mincle is essential for recognition and adjuvanticity of the mycobacterial cord factor and its synthetic analog trehalose-dibehenate. J Immunol 184(6):2756-60.

Schönlein JL. (1839). “Zur Pathogenie der Impetigines. Auszug aus einer brieflichen Mitteilung an den Herausgeber. Johannes Müllers Archiv für Anatomie, Physiologie und wissenschaftliche Medicin” p. 82.

Schorey JS, Sweet L. (2008). The mycobacterial glycopeptidolipids: structure, function, and their role in pathogenesis. Glycobiology 18(11):832-41.

Schreiber HA, Hulseberg PD, Lee J, Prechl J, Barta P, Szlavik N, Harding JS, Fabry Z, Sandor M. (2010). Dendritic cells in chronic mycobacterial granulomas restrict local anti-bacterial T cell response in a murine model. PLoS One 5(7):e11453.

Schwander S, Dheda K. (2011). Human lung immunity against *Mycobacterium tuberculosis*: insights into pathogenesis and protection. Am J Respir Crit Care Med. 183(6):696-707.

Scott HM, Flynn JL. (2002). *Mycobacterium tuberculosis* in chemokine receptor 2-deficient mice: influence of dose on disease progression. Infect Immun 70(11):5946-54.

Serbina NV, Flynn JL. (2001). CD8(+) T cells participate in the memory immune response to *Mycobacterium tuberculosis*. Infect Immun 69:4320–4328.

Shah IM, Laaberki MH, Popham DL, Dworkin J. (2008) A eukaryotic-like Ser/Thr kinase signals bacteria to exit dormancy in response to peptidoglycan fragments. Cell 135: 486–496.

Sirakova TD, Thirumala AK, Dubey VS, Sprecher H, Kolattukudy PE. (2001). The *Mycobacterium tuberculosis pks2* gene encodes the synthase for the hepta- and octa-methylbranched fatty acids required for sulfolipid synthesis. J Biol Chem 276:16833–9.

Smith SJ, Parks LW. (1993). The ERG3 gene in *Saccharomyces cerevisiae* is required for the utilization of respiratory substrates and in heme-deficient cells. Yeast 9(11):1177-87.

Smith NH, Kremer K, Inwald J, Dale J, Driscoll JR, Gordon SV, van Soolingen D, Hewinson RG, Smith JM. (2006a). Ecotypes of the *Mycobacterium tuberculosis* complex. J Theor Biol1 239(2):220-5.

Smith NH, Gordon SV, de la Rua-Domenech R, Clifton-Hadley RS, Hewinson RG. (2006b). Bottlenecks and broomsticks: the molecular evolution of *Mycobacterium bovis*. Nature Rev Microbiol 4, 670–681.

Smith NH, Hewinson RG, Kremer K, Brosch R, Gordon SV. (2009). Myths and misconceptions: the origin and evolution of *Mycobacterium tuberculosis*. Nat Rev Microbiol 7(7):537-44.

Snapper SB, Melton RE, Mustafa S, Kieser T, Jacobs WR Jr. (1990). Isolation and characterization of efficient plasmid transformation mutants of *Mycobacterium smegmatis*. Mol Microbiol 4(11):1911-1919.

Sondén B, Kocıncova D, Deshayes C, Euphrasie D, Rhayat L, Laval F, Frehel C, Daffé M, Etienne G, Reyrat, JM. (2005). Gap, a mycobacterial specific integral membrane protein, is required for glycolipid transport to the cell surface. Mol Microbiol 58: 426–440.

Sreevatsan S, Pan X, Stockbauer KE, Connell ND, Kreiswirth BN, Whittam TS, Musser JM. (1997). Restricted structural gene polymorphism in the *Mycobacterium tuberculosis* complex indicates evolutionarily recent global dissemination. PNAS 94(18): 9869–9874.

Srivastava V, Rouanet C, Srivastava R, Ramalingam B, Locht C, Srivastava BS. (2007). Macrophage-specific *Mycobacterium tuberculosis* genes: identification by green fluorescent protein and kanamycin resistance selection. Microbiol 153(Pt 3):659-66.

Stenger S. (2005). Immunological control of tuberculosis: role of tumour necrosis factor and more. Ann Rheum Dis 64 Suppl 4:iv24-8.

Stewart GR, Robertson BD, Young DB. (2003). Tuberculosis: a problem with persistence. Nat Rev Microbiol 1(2):97-105.

Stover CK, de la Cruz VF, Fuerst TR, Burlein JE, Benson LA, Bennett LT, Bansal GP, Young JF, Lee MH, Hatfull GF, Snapper SB, Barletta RG, Jacobs WR Jr, Bloom BR. (1991). New use of BCG for recombinant vaccines. Nature 351: 456–460.

Sturgill-Koszycki S, Schlesinger PH, Chakraborty P, Haddix PL, Collins HL, Fok AK, Allen RD, Gluck SL, Heuser J, Russell DG. (1994). Lack of acidification in *Mycobacterium* phagosomes produced by exclusion of the vesicular proton-ATPase. Science 263: 678–681.

Sureka K, Dey S, Datta P, Kumar SA, Dasgupta A, Rodrigue S, Basu J, Kundu M. (2007). Polyphosphate kinase is involved in stress-induced *mprAB-sigE-rel* signalling in mycobacteria. Mol Microbiol 65:261-276.

Sureka K, Sanyal S, Basu J, Kundu M. (2009). Polyphosphate kinase 2: a modulator of nucleoside diphosphate kinase activity in mycobacteria. Mol Microbiol 74(5):1187-97.

Sutcliffe IC. (1998). Cell envelope composition and organisation in the genus *Rhodococcus*. Antonie Van Leeuwenhoek 74:49–58.

Tahlan K, Wilson R, Kastrinsky DB, Arora K, Nair V, Fischer E, Barnes, SW, Walker, J.R., Alland, D., Barry, C.E., 3rd, and Boshoff, H.I. (2012). SQ109 targets MmpL3, a membrane transporter of trehalose monomycolate involved in mycolic acid donation to the cell wall core of *Mycobacterium tuberculosis*. Antimicrob Agents Chemother 56(4):1797-809.

Tailleux L, Neyrolles O, Honoré-Bouakline S, Perret E, Sanchez F, Abastado JP, Lagrange PH, Gluckman JC, Rosenzwajg M, Herrmann JL. (2003). Constrained intracellular survival of *Mycobacterium tuberculosis* in human dendritic cells. J Immunol 170, 1939-1948.

Takayama K, Wang C, Besra GS. (2005). Pathway to synthesis and processing of mycolic acids in *Mycobacterium tuberculosis*. Clin Microbiol Rev 18(1):81-101.

Tameris MD, Hatherill M, Landry BS, Scriba TJ, Snowden MA, Lockhart S, Shea JE, McClain JB, Hussey GD, Hanekom WA, Mahomed H, McShane H; MVA85A 020 Trial Study Team. (2013). Safety and efficacy of MVA85A, a new tuberculosis vaccine, in infants previously vaccinated with BCG: a randomised, placebo-controlled phase 2b trial. Lancet 381(9871):1021-8.

Tan JS, Canaday DH, Boom WH, Balaji KN, Schwander SK, Rich EA. (1997). Human alveolar T lymphocyte responses to *Mycobacterium tuberculosis* antigens: role for CD4 and CD8 cytotoxic cells and relative resistance of alveolar macrophage to lysis. J Immunol 159:290.

Tanne A, Ma B, Boudou F, Tailleux L, Botella H, Badell E, Levillain F, Taylor ME, Drickamer K, Nigou J, Dobos KM, Puzo G, Vestweber D, Wild MK, Marcinko M,Sobieszczuk P, Stewart L, Lebus D, Gicquel B, Neyrolles O. (2009). A murine DC-SIGN homologue contributes to early host defense against *Mycobacterium tuberculosis*. J Exp Med 206(10):2205-20.

Tatham E, Sundaram Chavadi S, Mohandas P, Edupuganti UR, Angala SK, Chatterjee D, Quadri LE. (2012). Production of mycobacterial cell wall glycopeptidolipids requires a member of the MbtH-like protein family. BMC Microbiol 12:118.

Telenti A, Philipp WJ, Sreevatsan S, Bernasconi C, Stockbauer KE, Wieles B, Musser JM, Jacobs WR Jr. (1997). The *emb* operon, a gene cluster of *Mycobacterium tuberculosis* involved in resistance to ethambutol. Nat Med 3(5):567-70.

Thayil SM, Morrison N, Schechter N, Rubin H, Karakousis PC. (2011). The role of the novel exopolyphosphatase *MT0516 in Mycobacterium tuberculosis* drug tolerance and persistence. PLoS One 6(11):e28076.

Titgemeyer F, Amon J, Parche S, Mahfoud M, Bail J, Schlicht M, Rehm N, Hillmann D, Stephan J, Walter B, Burkovski A, Niederweis M. (2007). A genomic view of sugar transport *in Mycobacterium smegmatis* and *Mycobacterium tuberculosis*. J Bacteriol 189(16):5903-15.

Trunz BB, Fine P, Dye C. (2006). Effect of BCG vaccination on childhood tuberculous meningitis and miliary tuberculosis worldwide: a meta-analysis and assessment of cost-effectiveness. Lancet 367, 1173-1180.

Tsolaki AG, Hirsh AE, DeRiemer K, Enciso JA, Wong MZ, Hannan M, Goguet de la Salmoniere YO, Aman K, Kato-Maeda M, Small PM. (2004). Functional and evolutionary genomics of *Mycobacterium tuberculosis*: insights from genomic deletions in 100 strains. PNAS 101(14):4865-70.

Tullius MV, Harmston CA, Owens CP, Chim N, Morse RP, McMath LM, Iniguez A, Kimmey JM, Sawaya MR, Whitelegge JP, *et al*. (2011). Discovery and characterization of a unique mycobacterial heme acquisition system. PNAS 108: 5051–5056.

Tyagi JS, Sharma D. (2002). *Mycobacterium smegmatis* and *tuberculosis*. Trends Microbiol 10(2):68-9.

van Heijenoort J. (2001). Formation of the glycan chains in the synthesis of bacterial peptidoglycan. Glycobiology 11(3):25R-36R.

Vandal OH, Pierini LM, Schnappinger D, Nathan CF, Ehrt S. (2008). A membrane protein preserves intrabacterial pH in intraphagosomal *Mycobacterium tuberculosis*. Nat Med 14:849–854.

Vandal OH, Roberts JA, Odaira T, Schnappinger D, Nathan CF, Ehrt S. (2009). Acid-susceptible mutants of *Mycobacterium tuberculosis* share hypersusceptibility to cell wall and oxidative stress and to the host environment. J Bacteriol 191: 625–631.

Varela C, Mauriaca C, Paradela A, Albar JP, Jerez CA, Chávez FP. (2010). New structural and functional defects in polyphosphate deficient bacteria: a cellular and proteomic study. BMC Microbiol 12;10:7.

Ventura M, Canchaya C, Tauch A, Chandra G, Fitzgerald GF, Chater KF, van Sinderen D. (2007). Genomics of *Actinobacteria*: tracing the evolutionary history of an ancient phylum. Microbiol Mol Biol Rev 71(3):495-548.

Verschoor JA, Baird MS, Grooten J. (2012). Towards understanding the functional diversity of cell wall mycolic acids of *Mycobacterium tuberculosis*. Prog Lipid Res 51(4):325-39.

Vilchèze C, Morbidoni HR, Weisbrod TR, Iwamoto H, Kuo M, Sacchettini JC, Jacobs WR Jr. (2000). Inactivation of the *inhA*-encoded fatty acid synthase II (FASII) enoyl-acyl carrier protein reductase induces accumulation of the FASI end products and cell lysis of *Mycobacterium smegmatis*. J Bacteriol 182(14):4059-67.

Wada K, Arita M, Nakajima A, Katayama K, Kudo C, Kamisaki Y, Serhan CN. (2006). Leukotriene B4 and lipoxin A4 are regulatory signals for neural stem cell proliferation and differentiation. FASEB J 20(11):1785-92.

Wang L, Slayden RA, Barry CE 3rd, Liu J. (2000). Cell wall structure of a mutant of *Mycobacterium smegmatis* defective in the biosynthesis of mycolic acids. J Biol Chem 275:7224-7229.

Wang C, Hayes B, Vestling MM, Takayama K. (2006). Transposome mutagenesis of an integral membrane transporter in *Corynebacterium matruchotii*. Biochem Biophys Res Commun 340: 953–960.

Ward SK, Heintz JA, Albrecht RM, Talaat AM. (2012). Single-cell elemental analysis of bacteria: quantitative analysis of polyphosphates in *Mycobacterium tuberculosis*. Front Cell Infect Microbiol 2012;2:63.

Wells RM, Jones CM, Xi Z, Speer A, Danilchanka O, Doornbos KS, Sun P, Wu F, Tian C, Niederweis M. (2013). Discovery of a siderophore export system essential for virulence of *Mycobacterium tuberculosis*. PLoS Pathog 9(1):e1003120.

WHO. (2009). Bull World Health Organ 87(7): 505–511.

WHO. (2012).World Health Organisation. Global Tuberculosis Report.

Woese CR. (1987). Bacterial evolution. Microbiol Rev 51(2):221-71.

Wolf AJ, Desvignes L, Linas B, Banaiee N, Tamura T, Takatsu K, Ernst JD. (2008). Initiation of the adaptive immune response to *Mycobacterium tuberculosis* depends on antigen production in the local lymph node, not the lungs. J Exp Med 205(1):105-15.

Woodworth JS, Wu Y, Behar SM. (2008). *Mycobacterium tuberculosis*-specific CD8+ T cells require perforin to kill target cells and provide protection invivo. J Immunol 181(12):8595-603.

Yassin AF, Brzezinka H, Schaal KP, Trüper HG, Pulverer G. (1998). Menaquinone composition in the classification and identification of aerobic actinomycetes. Source Instituten für Medizinische Mikrobiologie und Immunologie, Universität zu Köln. Zentralbl Bakteriol Mikrobiol Hyg A. 267(3):339-56.

Yu J, Tran V, Li M, Huang X, Niu C, Wang D, Zhu J, Wang J, Gao Q, Liu J. (2012). Both phthiocerol dimycocerosates and phenolic glycolipids are required for virulence of *Mycobacterium marinum*. Infect Immun 80(4):1381-9.

Yuan Y, Zhu Y, Crane DD, Barry CE, 3rd. (1998). The effect of oxygenated mycolic acid composition on cell wall function and macrophage growth in *Mycobacterium tuberculosis*. Mol Microbiol 29: 1449–1458.

Zago A, Chugani S, Chakrabarty AM (1999). Cloning and characterization of polyphosphate kinase and exopolyphosphatase genes from *Pseudomonas aeruginosa* 8830. Appl Environ Microbiol 65:2065-2071.

Zahrt TC, Song J, Siple J, Deretic V. (2001). Mycobacterial FurA is a negative regulator of catalase-peroxidase gene *katG*. Mol Microbiol 39(5):1174-85.

Zhang H, Ishige K, Kornberg A. (2002). A polyphosphate kinase (PPK2) widely conserved in bacteria. PNAS 99(26):16678-83.

Zhang N, Torrelles JB, McNeil MR, Escuyer VE, Khoo KH, Brennan PJ, Chatterjee D. (2003). The Emb proteins of mycobacteria direct arabinosylation of lipoarabinomannan and arabinogalactan via an N-terminal recognition region and a C-terminal synthetic region. Mol Microbiol 50(1):69-76.

Zhang H, Rao NN, Shiba T, Kornberg A. (2005a). Inorganic polyphosphate in the social life of *Myxococcus xanthus*: motility, development, and predation. PNAS. 102:13416-13420.

Zhang H, Gómez-García MR, Brown MR, Kornberg A. (2005b). Inorganic polyphosphate in *Dictyostelium discoideum*: influence on development, sporulation, and predation. PNAS 102:2731-2735.

Zhang Q, Li Y, Tang CM. (2010). The role of the exopolyphosphatase PPX in avoidance by *Neisseria meningitidis* of complement-mediated killing. J Biol Chem. 285(44):34259-68.